IEEE
Std 149-1979

(Revision of
IEEE Std 149-1965)

IEEE Standard
Test Procedures for Antennas

Sponsor

Antenna Standards Committee

ISBN 0-471-08032-2

Library of Congress Catalog Number 79-92425

December 19. 1979 *SH07682*

Approved December 15, 1977

IEEE Standards Board

William R. Kruesi, *Chairman* *Irvin N.* Howell, Jr, *Vice Chairman*

Ivan G. Easton, *Secretary*

William E. Andrus
Jean Jacques Archambault
Mark Barber
Edward J. Cohen
Warren H. Cook
Louis Costrell
R. L. Curtis
David B. Dobson
R. 0. Duncan
Charles W. Flint
Jay Forster
Ralph I. Hauser
Joseph L. Koepfinger
Irving Kolodny
Benjamin J. Leon
Thomas J. Martin
Donald T. Michael
Voss A. Moore
William S. Morgan
William J. Neiswender
Ralph M. Showers
Robert A. Souderman
Leonard W. Thomas, Sr
B. W. Whittington

Foreword

(This Foreword is not a part of IEEE Std 149-1979, IEEE Standard Test Procedures for Antennas.)

This document is a major revision of IEEE Std 149-1965 which it supersedes. It represents the second revision of the standard since the original issuance in 1948 of 48IRE2S2, Standards on Antennas – Methods of Testing. Practically every topic contained in the previous standard has been expanded to reflect the great changes that have taken place, since 1965, in metrology and instrumentation technology as applied to antenna measurements.

This document contains sections on the design, evaluation, and operation of antenna ranges, electromagnetic radiation hazards, and environmental factors which did not appear in the preceding standard. The section on the determination of scattering cross-section, which appeared previously, has been omitted since it will appear as a separate standard at a later date.

Suggestions for the improvement of this standard will be welcome. They should be sent to:

Secretary
IEEE Standards Board
The Institute of Electrical and Electronics Engineers, Inc
345 East 47th Street
New York, NY 10017

This standard was prepared by the Subcommittee 2.11 on Methods of Testing Antennas of the IEEE Antenna Standards Committee. The Subcommittee preparing this revision had the following membership :

W. H. Kummer, ***Chairman***

J. D. Dyson
E. S. Gillespie
T. Mukaihara
A. C. Newell
A. F. Seaton
G. P. Tricoles
A. T. Villeneuve

Members of the IEEE Antenna Standards Committee who contributed to this standard document were:

E. S. Gillespie, ***Chairman***

C. C. Allen
K. G. Balmain
P. L. Burgmyer
H. V. Cottony*
G. A. Deschamps
J. D. Dyson
E. S. Gillespie
P. W. Hannan
H. Jasik
W. K. Kahn
E. M. Kennaugh
W. H. Kummer
D. J. LeVine
T. Mukaihata
A. C. Newell
D. C. Ports
L. J. Ricardi
A. C. Schell
A. F. Seaton
C. J. Sletten*
P. H. Smith
W. T. Tilston
G. P. Tricoles
A. T. Villeneuve
M. S. Wheeler

*Past chairmen

Contents

SECTION PAGE

SECTION PAGE

FIGURES PAGE

FIGURES

TABLES

APPENDIXES

APPENDIX FIGURE

IEEE Standard
Test Procedures for Antennas

1. Scope

This document comprises test procedures for the measurement of antenna properties. It is a cornprehensive revision and extension of the previous test procedure ANSI/IEEE Std 149-1965 (Reaff 1971).

Throughout this standard it is assumed that the antenna to be measured can be treated as a passive, linear, and reciprocal device. Therefore its radiation properties can be measured in either the transmitting or the receiving mode. Many of the test procedures decribed can, however, be adapted for use in the measurement of antenna systems containing circuit elements that may be active, nonlinear, or nonreciprocal. For these cases there is no simple relationship between the antenna system's transmitting and receiving properties. Therefore measurements shall be performed for the mode or modes in which the antenna system has been designed to be used.

A fundamental property of any antenna is its radiation pattern. The measurement of radiation patterns on an antenna range is discussed in Section 3, with the emphasis placed on ampli tude patterns. The design of antenna ranges, or antenna test facilities, is described in Sec tion 4.

The instrumentation required for the antenna range, directions for the evaluation of an (existing) range, and the operation of ranges are discussed in Sections 5, 6, and 8, respectively. A variety of special measurement techniques are included in Section 7.

The working environment in which an antenna is installed may substantially modify the intrinsic pattern of an antenna. Consequently measurements *in situ are* frequently required. These are discussed in Section 9.

For each direction of space, the radiation pattern is characterized by amplitude, phase, and polarization. The latter characteristics are taken up in Sections 10 and 11, respectively.

The relative amplitude-pattern information may be converted into absolute intensities through information derived from the measurement of antenna gain. The determination of gain and closely related directivity is described in Section 12. Errors in conventional gain calibration measurements are discussed particularly in 12.5. Losses in the antenna itself can be of importance in some types of antennas, These losses can be accounted for by the radiation efficiency. Procedures for their determination are treated in Section 13.

Section 14 deals with boresight measurements, which are concerned with the precise determination of the direction of the beam or tracking axis of an antenna system. The sensitive components of the antenna frequently require protection from harsh influences of the environment. The electrically transmissive shield or radome which provides this protection shall frequently be evaluated so that its effect on the radiation pattern is understood. This topic is treated in Section 15.

Power transfer from generator to antenna is controlled by the input impedance to the

antenna. This important parameter frequently limits the useful bandwidth of the antenna. Measurement procedures and network descriptions appropriate from low to microwave frequencies are presented in Section 16.

An important class of antennas relies on ground to enhance the received signal. In this case the ground_ shall be considered as an integral part of the antenna. The modification of antenna concepts and additional data on the ground-wave propagation are presented in Section 17.

The antenna and its associated circuits rather than the capacity of the transmitter generator may limit the amount of power, either average power or peak power, that can be effectively radiated. It is desirable therefore to determine these limitations as well as the environmental factors that may modify them independently of the system context. Procedures for testing power-handling capacity are outlined in Section 18.

Another concern to the antenna engineer is that of radiation hazards. It is well known that radio-frequency (rf) fields of sufficient intensity can cause damage to biological tissue. Therefore it is usually necessary to determine the level of the radiation intensity in the vicinity of antennas radiating high radio-frequency power so that appropriate safety precautions can be taken before personnel enter the area. This important aspect of antenna measurements is discussed in Section 19.

Mechanical or structural properties along with environmental factors are described in Section 20. Because these properties are so varied and specialized in nature, no attempt has been made to include descriptions of actual measurements in this test procedure. The environmental impact of an antenna is also an important consideration for the antenna engineer. One aspect of environmental impact is that of aesthetics. Large antenna structures are necessarily conspicuous, and their appearance is of concern to those who live in their vicinity. This is particularly true in an urban setting. Since the aesthetic quality of the antenna structure is highly subjective, it is beyond the scope of this document to suggest any evaluation procedure.

Throughout this test procedure an attempt has been made to discuss measurement techniques as thoroughly as is practicable. However, in general step-by-step procedural descriptions have been avoided. References are provided which are illustrative of measurement techniques and in which details may be found. Because measurement techniques undergo continuing refinement, the reader should be alert to references on the subject of antenna measurement that will have appeared after this test procedure was prepared.

Many commonly used terms used in this test procedure are defined in ANSI/IEEE Std 145-1973, Definitions of Terms for Antennas. Commonly used terms that do not appear in that standard are italicized in this test procedure.

2. Standards References

When the following standard documents referenced in the text are superseded by an approved revision, the revision shall apply.

ANSI C95.1-1974, Safety Level of Electromagnetic Radiation with Respect to Personnel.

ANSI C95.3-1973, Techniques and Instrumentation for the Measurement of Potentially Hazardous Electromagnetic Radiation at Microwave Frequencies.

ANSI/IEEE Std 100-1977, Dictionary of Electrical and Electronics Terms.

ANSI/IEEE Std 145-1973, Definitions of Terms for Antennas.

ANSI/IEEE Std 148-1959 (Reaff 1971), Measurement of Waveguides and Components.

IEEE Std 211-1977, Standard Definitions of Terms for Radio Wave Propagation.

IEEE Std 291-1969, Standards Report on Measuring Field Strength in Radio Wave Propagation.

3. Antenna-Range Measurements of Radiation Patterns

3.1 General. Associated with the antenna under test is an operational coordinate system

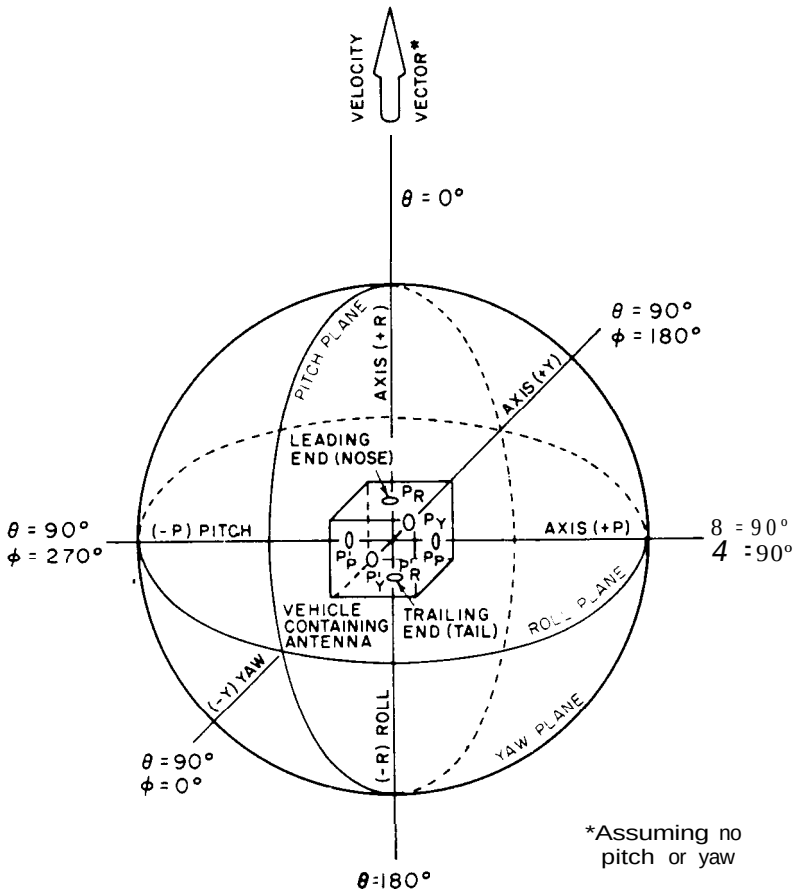

Fig 1
Coordinate System of Inter-Range Instrumentation Group

[1, pp 5.4-5.71],[1] usually a spherical one. Generally this coordinate system is defined by the system in which the antenna is used, although at times, for testing a specific antenna, it may be necessary to define a different coordinate system. The Inter-Range Instrumentation Group of the Range Commanders Council [2, p 1201, for example, has defined a coordinate system specifically for use with rockets, missiles, and space vehicles (Fig 1).

The antenna's coordinate system is typically defined with respect to a mechanical reference on the antenna. A means of establishing the mechanical reference should be provided. The standard spherical coordinate system used in antenna measurements is shown in Fig 2.

To completely characterize the radiation field of an antenna, one shall measure its relative amplitude, relative phase, polarization, and the power gain on the surface of a sphere the center of which is located at the antenna under test. A representation of any of these radiation properties as a function of space coordinates is defined as a radiation pattern, or antenna pattern, of the test antenna. Since the distance R from the antenna under test to the measuring point is fixed, only the two angular coordinates are variables in a given radiation pattern. Usually the radio frequency of opera-

[1] Numbers in brackets correspond to those of the Bibliography, Section 21 of this standard.

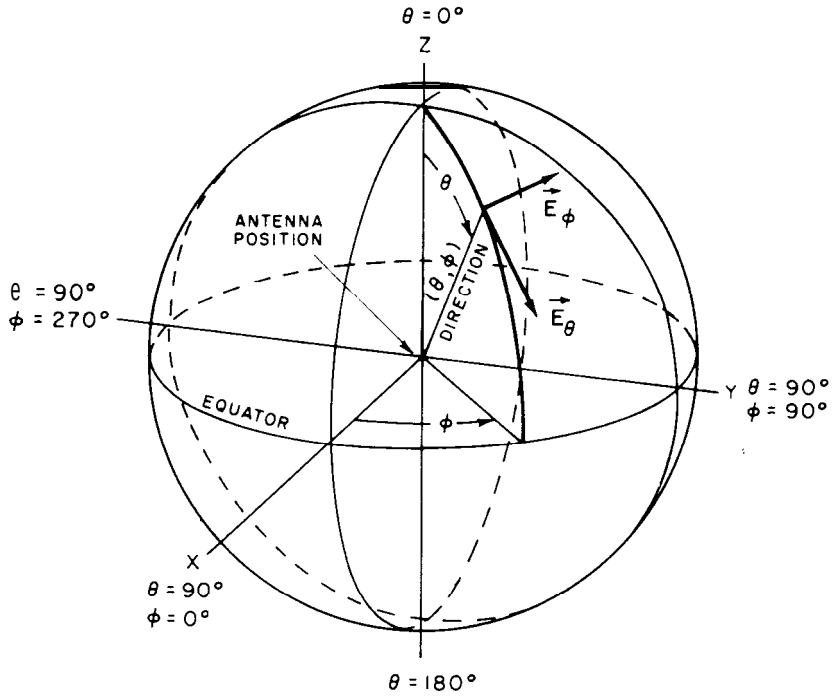

Fig 2
Standard Spherical Coordinate System Used in Antenna Measurements

tion is treated as a parameter, with the radiation pattern being measured at specified frequencies. For some antenna applications it is necessary to make frequency a variable. If frequency is varied continuously, such a procedure is called a swept-frequency technique; it is discussed in 7.4. It is impractical to measure the radiation pattern of an antenna completely, and therefore it is necessary to resort to sampling techniques. For example, with the frequency of operation and polarization fixed, the θ coordinate can be varied incrementally, and for each increment the desired antenna property can be measured continuously over the range of ϕ. If the increments are small enough, then for all practical purposes the complete antenna pattern is obtained. The resulting patterns taken for all increments of θ are usually referred to as a set of radiation patterns.

There are situations in which the operational antenna illuminates structures in its immediate vicinity which alter the radiation field of the isolated antenna. In these cases it may be necessary for measurements of the radiation field to include with the antenna those relevant parts of the nearby structures. The use of scale models is quite common for such cases (see 7.1). Throughout this standard the expression "test antenna" or, alternately, "antenna under test" shall mean the antenna itself plus any structure included with it. This means that the test antenna can be physically larger than the antenna alone.

3.2 Pattern Cuts. A direct method of measuring the radiation pattern of a test antenna is to employ a suitable source antenna, which can be positioned in such a manner that it moves relative to the test antenna along lines of constant θ and constant ϕ (see Fig 2). The loci of constant θ directions describe cones;

hence measurements made with 4 as the variable and 8 as a parameter are called *conical cuts* or 4 cuts Those made with 8 as the variable and 4 as a parameter are called *great-circle cuts* or 8 cuts Note, however, that the conical cut for 8 = 90" is also a great-circle cut.

Though rarely done, it is possible to position the antenna in such a manner that the loci of directions describe a spiral. For this case both 0 and @ are variables, and the resultant motion is called a *spiral cut.* When spiral cuts are being made, it is usual for the motion in θ to be slowly varying with respect to that in ϕ; hence for each 360" rotation in ϕ the resulting pattern is approximately a conical cut.

Principal-plane cuts refer to orthogonal great-circle cuts which are through the axis of the test antenna's major lobe. For this definition to hold, the beam axis shall lie either in the equator of the spherical coordinate system ($\theta = 90^\circ$) or at one of the poles ($\theta = 0^\circ$ or $\theta = 180$").

If the positioner system is designed to provide θ and ϕ cuts, then the alignment of the axis of a pencil-beam antenna along the poles is usually avoided. This is because the ϕ cut for the $\theta = 0^\circ$ orientation yields only a polarization pattern (see 11.2.2). When near the poles θ cuts involve radical changes in the direction of polarization of the incident field relative to the test antenna's polarization, except when the incident field is identically circularly polarized. For these reasons if the test antenna is of a pencil-beam type, it is usually oriented with its beam axis in any desired direction in the equator (most often in the $\phi = 0$" or $\phi = 180$" direction).

3.3 Basic Antenna-RangeConfigurations. There are two basic range configurations that accomplish the position requirement for θ and ϕ cuts [1, pp 5.12-5.24]. One is *the fixed-line-of-sight* configuration. Here the test antenna and its associated coordinate system are rotated about a suitable axis (usually one passing through the phase center (see 10.3) of the test antenna). If the test antenna is operating in the receive mode, then the signal that it receives from an appropriately located fixed source antenna is recorded. The other one is called the *movable-line-of-sight* configuration. For this case the source antenna is moved incrementally or continuously along the circumference of a circle centered approximately at the phase center of the antenna under test. If it is moved incrementally, then for each position of the source antenna the test antenna is rotated and the received signal is recorded. Alternately the test antenna can be rotated incrementally, and for each of its positions the source antenna is moved continuously along its circumferential path.

If the test antenna and the source antenna are both reciprocal devices, the functions of receive and transmit may be interchanged. The measured patterns should be identical. This means that the test antenna may be used in either the receive or the transmit mode; most often it is used in the receive mode. In the following, unless otherwise stated, the test antenna shall be considered as the receiving antenna, and it will be illuminated by the field of the transmitting source antenna.

4. Antenna-Range Design

4.1 General. *Antenna ranges* have been developed for the purpose of measuring the radiation patterns of antennas independent of their operational environment. The antenna range consists of the appropriate instrumentation and the physical space required for the measurements. In this section the design is discussed. Evaluation and use of antenna ranges are described in Sections 6 and 8. Emphasis is placed on the measurement of the relative amplitude patterns. The measurement of relative phase, polarization, and power gain is discussed in Sections 10, 11, and 12, respectively. It should be pointed out that the various criteria for antenna-range design presented here, as well as the methods of evaluation, apply equally well to other types of ranges usually found at antenna testing facilities, such as *radome ranges* and *scattering ranges.* Radome measurements are discussed in Section 15, and

scattering ranges are beyond the scope of this standard.

The ideal incident field for measuring the radiation characteristics of the test antenna is that of a uniform plane wave. In practice it is only possible to approximate such a field. Attempts to do this have led to the development of two basic types of ranges:

(1) *Free-space ranges.* This type of range is designed in such a manner that all the effects of the surroundings are suppressed to acceptable levels.

(2) *Reflection ranges.* This type of range is designed to judiciously use reflections in order to produce an approximated plane wave.

Typical ranges that come under the free-space-range classification are: the elevated range, the slant range, the compact range, and most anechoic chambers.

The *elevated range [3]* includes those ranges in which the test and source antennas are located on towers, on adjacent mountain peaks, on the roofs of adjacent buildings or on diagonally opposing sides of abandoned quarries. Generally, however, it is designed over an approximately flat area, and the effects of the surroundings are suppressed :

(1) by careful choice of the source antenna with regard to directivity and side-lobe level

(2) by clearance of the line of sight along the range surface

(3) by redirection or absorption of energy reaching the range surface or obstacles that cannot be removed

(4) by special signal-processing techniques such as modulation tagging of the desired signal

(5) by use of short pulses

The *ground-reflection range [4]* is designed to make use of the energy that is specularly reflected from the range surface to create a constructive interference with the direct-path energy in the region of the test antenna. With proper design the illuminating field will have a small, essentially symmetric amplitude taper. This is usually achieved by adjusting the height of the source antenna above the range surface with the test antenna at a fixed height.

Since the elevated range over a flat surface and the ground-reflection range are so basic to antenna-pattern measurements, their design will be discussed in detail in 4.3 and 4.4, respectively. Other range types will be discussed in 4.5.

4.2 Antenna-Range Design Criteria

4.2.1 General. To establish the design criteria for either basic range type, one must consider the following:

(1) the coupling between source and test antennas

(2) the transverse and longitudinal amplitude taper of the illuminating wave front

(3) the phase curvature of the illuminating wave front

(4) spatial variations in the illuminating wave front caused by reflections

(5) interference from spurious radiating sources

Items *(l)-(3)* are discussed in this section. The problems associated with reflections from the range surface and other obstacles are discussed in 4.3 and Section 6.

Outdoor ranges are usually subjected to interference from signal sources -outside the range area. These sources can be mobile communications, radar, or telemetry systems. The use of filters can often suppress the effect of these interfering signals.

4.2.2 *Effect of Mutual Coupling Between Source and Test Antennas.* The total field of any antenna consists of a radiation part and a reactive part. The radiation field decays as the reciprocal of the distance from the antenna, whereas the reactive field decays at least as rapidly as the reciprocal of the square of the distance from the antenna. Usually the spacing between source and test antennas is large enough so that the level of the reactive field of the source antenna is negligible. However, practical situations do arise for which this may not be the case. In these cases the test antenna will couple to the reactive field, and for some types of measurements this produces an error. Such effects are considered negligible when the spacing is greater than about 10 wavelengths. Based upon calculations made for a very short dipole antenna at 10 wavelengths

from the antenna, the level of the inductive field (which is the part of the reactive field that would couple) will be 36 dB below that of the radiation field.

In addition to the reactive field coupling, the reradiative coupling or mutual coupling between source and test antennas is also of concern [5]. For this case, part of the energy received by the test antenna is reradiated toward the source antenna. In turn, part of the energy received by the *source* antenna is again reradiated toward the test antenna. While this level is quite low, it can cause a measurable error in the level of the signal observed near the peak of the test antenna's major lobe. The effect on the side-lobe levels is usually negligible. A careful analysis [1, pp 14.3-14.5] was performed; it was based upon identical source and test antennas, each with a (sin x)/x antenna pattern, a 50 percent aperture efficiency, and an equivalent power reflection coefficient of 0.25. The level of the reradiated signal reaching the test antenna was at least 45 dB below that of the original received signal when the ratio of the plane angle subtended at the source antenna by the diameter of the test antenna, to the 3 dB beamwidth of the source antenna was made equal to or less than 0.3. This ratio corresponds to a subtended angle that is approximately equal to the source antenna's beamwidth at the 0.25 dB level. It is generally considered good practice to adhere to a 0.25 dB criterion for the amplitude taper of the direct illuminating field [1, pp 14.13-14.15], [4].

4.2.3 ***Effect of a Transverse Amplitude Taper over the Test Aperture.*** An amplitude taper of the illuminating field can produce an error in the measured antenna pattern of the test antenna. This effect is dependent upon the aperture excitation function of the test antenna. For typical excitation functions the effect of the amplitude taper of the incident field is a reduction in measured gain with a slight modification to the close-in side lobes. This effect can be evaluated by recognizing that the variation of the amplitude of the incident field over the aperture of the test antenna on receive is analogous to a modification of the aperture illumination from its feed on transmit. Suppose that the test antenna has an aperture illumination from its feed on transmit given by $f(x, y)$. If it is used *on* receive and is illuminated by an incident field with an amplitude variation given by g(x, y), then the measured radiation pattern is essentially the same as that for the transmitting case, with the feed modified to produce a distribution over the test antenna aperture given by $f(x, y)\text{-}g(x, y)$. For example, consider a test antenna having a circular aperture with a 10 dB *cosine-on-pedestal* distribution the far-field radiation pattern of which is to be measured with the use of a source antenna that produces a circularly symmetric amplitude taper over the aperture of the test antenna. The taper is assumed to have a (sin x)\x form. One can now compute the directivity of the equivalent distribution, which is the product of the cosine-on-pedestal and (sin x)/x functions for various tapers. If the amplitude taper varies to -0.5 dB at the periphery of the aperture, an apparent directivity reduction of approximately 0.15 dB will result as compared to the case without taper. If the amplitude taper varies to -0.25 dB at the periphery of the aperture, one obtains a reduction in directivity of about 0.10 dB.

Generally it is better to choose a source antenna that yields a 0.25 dB taper, rather than one with a broader beamwidth which would produce a smaller amplitude taper. This is because the use of broader beamwidth source antennas usually results in an increased error due to the reflections (see Section 6). Conversely, there are situations in which it may be necessary to use a source antenna with a narrower beam in order to reduce the effect of reflections. If a more directive source antenna is used, the alignment of the source antenna becomes more critical. Care shall be exercised in orienting the source antenna so that the peak of its beam is centered on the test antenna to prevent an excessive and asymmetrical illumination taper with a resultant increase in measurement error.

4.2.4 ***Effect of a Longitudinal Amplitude Taper at the Test Antenna.*** To achieve a given accuracy in the measurement of the radiation pattern of a test antenna, the illuminating

field shall be sufficiently constant in amplitude along the range axis, as well as in planes normal to the range axis. Consider an end-fire antenna under test with an active region having a maximum dimension ***L*** along the range axis. If the separation between the source antenna and the center of the active region is R_0, then the ratio ρ_p, of the power density at the forward extreme of the active region to that at the rear is given by [7]

$$10 \log (\rho_p) = 20 \log \frac{R_0 + L/2}{R_0 - L/2} \quad [\text{dBl}$$

Severe axial variations of the illuminating field can cause a measurement error, particularly in the minor lobe structure of radiation patterns. For most antenna types that have a significant depth to their active regions, such an error is usually considered to be negligible when the power density over the region is constant to within 1 dB. This condition corresponds to an approximate restraint on R_0 of

$$R_0 \geq 10L$$

The criterion for such structures as high-gain end-fire antennas often is more restrictive than the greater of the previously discussed range-length criteria that were based on the suppression of reactive-field coupling and phase curvature.

4.2.5 ***Effect of Phase Variation over the Test Aperture.*** A criterion has to be established for the phase variation of the illuminating field over the test antenna. For most practical situations the phase variation is a function solely of the separation between the source antenna and the antenna under test. If, in the absence of reflections, the 0.25 dB criterion for amplitude variation is adhered to, then the corresponding phase variation will be very close to that of a spherical wave emanating from the phase center of the source antenna. This is true for spacings considerably less than $2d^2/\lambda$, where d is the diameter of the source antenna. For example, calculations [1, pp 14.5-l4.11] made for a source antenna with a 30 dB Taylor distribution revealed that its phase pattern differed from that of a spherical wave by at most 2° between the 1 dB points of its amplitude pattern at a spacing of d^2/λ. Thus the expected phase variation can be determined by assuming that the phase front at the test antenna is a sphere. It can readily be shown [4] that for a test-antenna diameter D and a separation ***R,*** a phase deviation $\Delta\phi$ will be given by

$$\Delta\phi \approx \frac{\pi D^2}{4\lambda R}$$

A commonly employed criterion for determining the minimum allowable separation between source and test antennas is to restrict A+ to n/8 rad. This results in the restriction that $R \geq 2D^2/\lambda$.

The effect of phase variation is that the nulls of the pattern are partially filled, and the amplitudes of the side lobes are changed. An example is shown in Fig 3 which depicts calculated patterns of a circular aperture with a 30 dB Taylor distribution at separations of $2D^2/\lambda, 4D^2/\lambda$, and approaching infinity. It is possible to correct for phase deviations by changing the focus of the test antenna, a technique that is discussed in 7.2.

4.3 Design of Elevated Ranges

4.3.1 ***Elevated Ranges over Flat Surfaces.*** In view of the interdependence between the diameter of the test antenna and the range or separation between source and test antennas, it is convenient to specify the separation as $R = KD^2/\lambda$, where ***K*** is a number to be chosen for a particular measurement (see Fig 3). It can be shown [1, pp 14.15-14.28] that for elevated ranges the 0.25 dB criterion for amplitude taper leads to a criterion for the diameter of the source antenna, namely, that

$$d \leq 0.37KD$$

This assumes that the main lobe of the source antenna has a (sin x)/x amplitude characteristic.

If the elevated range is designed over a flat surface as shown in Fig 4, then steps shall be taken to suppress the reflections from the range surface in the region near the range axis.

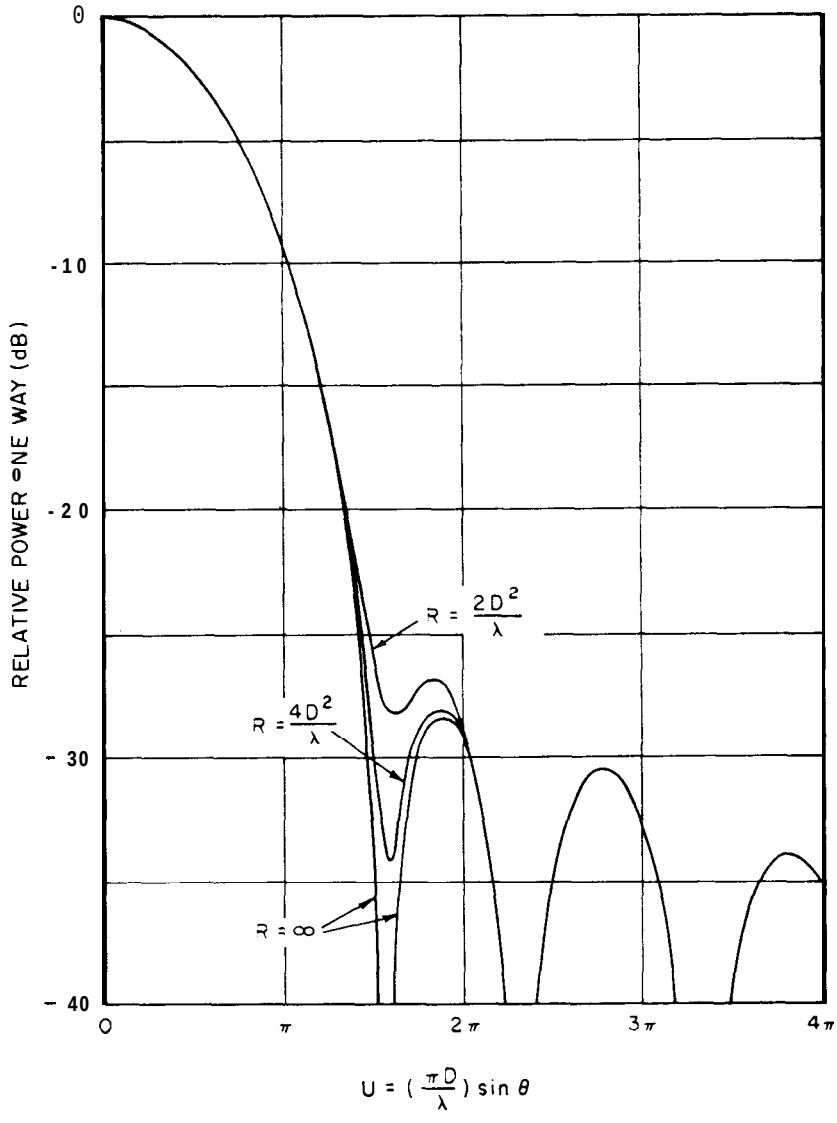

Fig 3
Calculated Radiation Patterns Illustrating the Effect of Quadratic Phase Errors Encountered in Measuring Patterns at the Ranges Indicated.
A 30 dB Taylor Distribution Is Assumed

As a basic design goal, the range surface in front of the test antenna should not intercept any energy contained in the main lobe of the source antenna. It is suggested that the first null in the radiation pattern of the source antenna be directed toward the base of the test antenna tower. This leads to the imposition of a minimum-size restriction on the source antenna, namely,

$$d \geq 1.5KD^2/h_r$$

where h_r is the height of the receiving antenna. This result is based upon the fact that typical source antennas have a main-lobe width of approximately $3X/d$ rad. A comparison of the

two criteria for the diameter of the source antenna shows that the height of the test antenna should satisfy the inequality

$$h_r \geq 4D$$

where D is the diameter of the antenna under test. The source antenna should be elevated to the same height as the test antenna. For physically small antennas this requirement is easily met. However, as the antenna's size is increased, it becomes more difficult, and in some cases impractical, to satisfy.

4.32 ***Elevated Ranges over Irregular Surfaces.*** Elevated ranges are often designed over irregular terrain, for example, between two adjacent mountain peaks or perhaps between two hilltops. Such ranges are useful for the testing of physically large antennas. For these ranges the location of the points of specular reflection, which reflect energy toward the test antenna, may not be immediately obvious. When designing these ranges it is usually necessary to construct a scaled drawing of the vertical profile of the range, showing the exact ground contour [8] from data obtained from the U.S. Geological Survey map of the area. These maps give detailed information on the topography of the ground by means of contour lines plotted every 20 ft in elevation above sea level, which sould be adequate for ranges operating as high in frequency as UHF. For microwave frequencies it may be necessary to locate the points experimentally using directive antennas (see Section 6). Once the points of specular reflection are determined, the level of the reflected energy at the test antenna can be estimated [8], and corrective measures can be taken if the level of reflected energy is excessive. For these ranges the restriction on the height of the test antenna is removed, since the mountain itself is part of the test-antenna tower.

4.3.3 ***Estimation of Errors Due to Reflections.*** To illustrate the effect of reflections on the measured radiation patterns of a test antenna, consider the following examples. Suppose that the nominal side lobe levels of both source and test antennas are 25 dB below their respective maximum levels and the range surface produces a 10 dB attenuation of the reflected wave. Then the extraneous signal level will be approximately 60 dB below the direct-path signal level for the case where the main lobe of the test antenna is pointing toward the source antenna. The graph of Fig 5 can be used

Fig 4
Elevated-Range Geometry

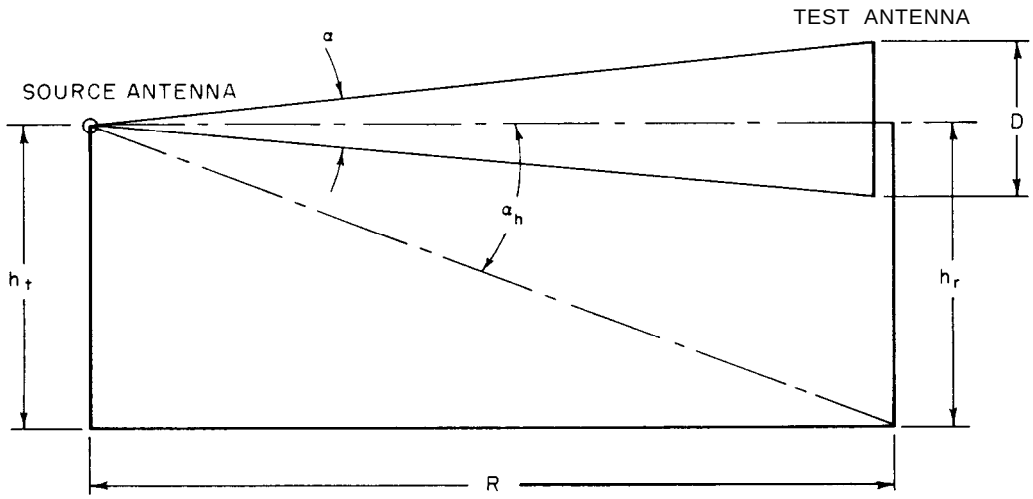

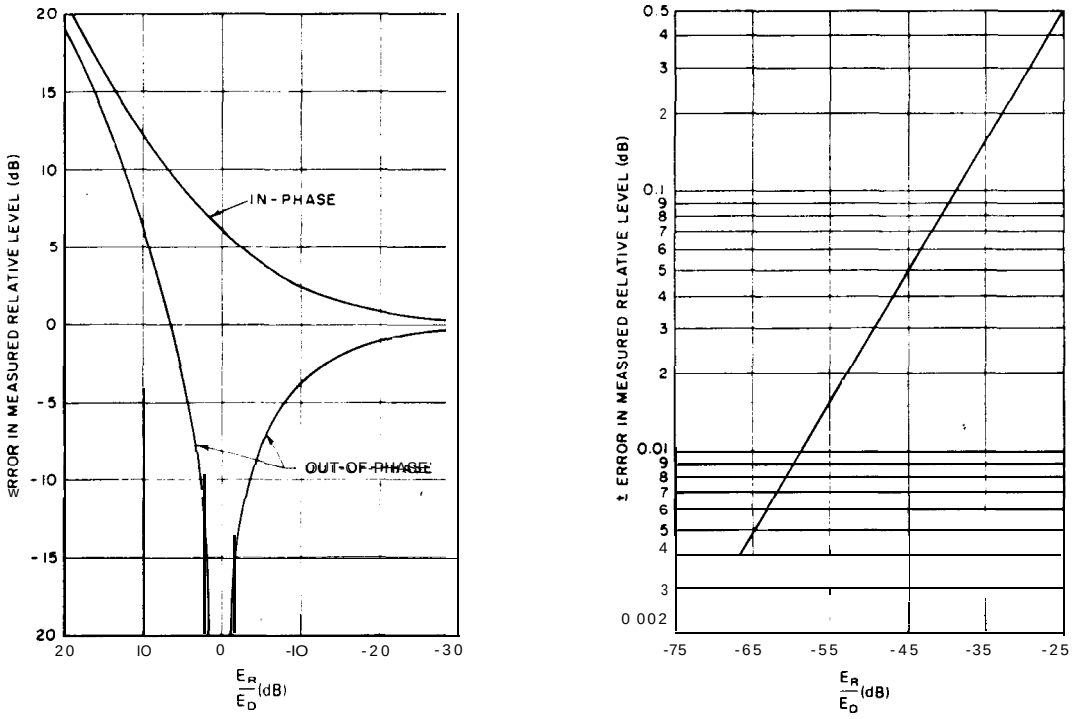

Fig 5
Possible Error in Measured Relative Pattern Level Due to Coherent Extraneous Signals
Linear Scales Are Employed for Signal Ratios of + 20 to -30 dB; the Plus-or-Minus Errors Are Essentially Equal for Ratios of – 25 dB or Less, as Indicated in the Logarithmic Plot for Ratios down to – 75 dB

to determine the possible error in the relative amplitude pattern of the test antenna due to this reflected signal. Fig 5 shows that the measured value of the peak of the beam will be in error by less than 0.01 dB. However, if the peak of the main lobe of the test antenna is pointed toward the range surface and a -25 dB side lobe is directed toward the source antenna, the relative level of the extraneous signal will be only 10 dB below the level of the direct-path signal, and the measurement error is -3.3 to +2.4 dB.

This example illustrates the fact that it is never advisable to direct the main beam of the test antenna toward the ground when measuring side lobes. The operational procedure for the range should be planned in such a way as to ensure that this does not happen. A means of rotating the test antenna through 180° about the axis of the main lobe should be provided for this purpose.

4.3.4 Use of ***Diffraction Fences and Longitudinal Ramps to Redirect Reflected Energy.*** When the antenna under test is essentially omnidirectional or when the required measurement calls for extremely small errors, then other means of suppressing the reflected signal will be required. Two methods which have found wide usage are diffraction fences and longitudinal ramps [1, pp 14.28-14.37].

Diffraction fences are metallic screens which are strategically located on the range in such a manner as to redirect, from the antenna under test, a portion of the energy that would, in the absence of the fence, be reflected from the range surface toward the test antenna. Diffraction fences can be of simple wooden frame construction covered with an ordinary conduct-

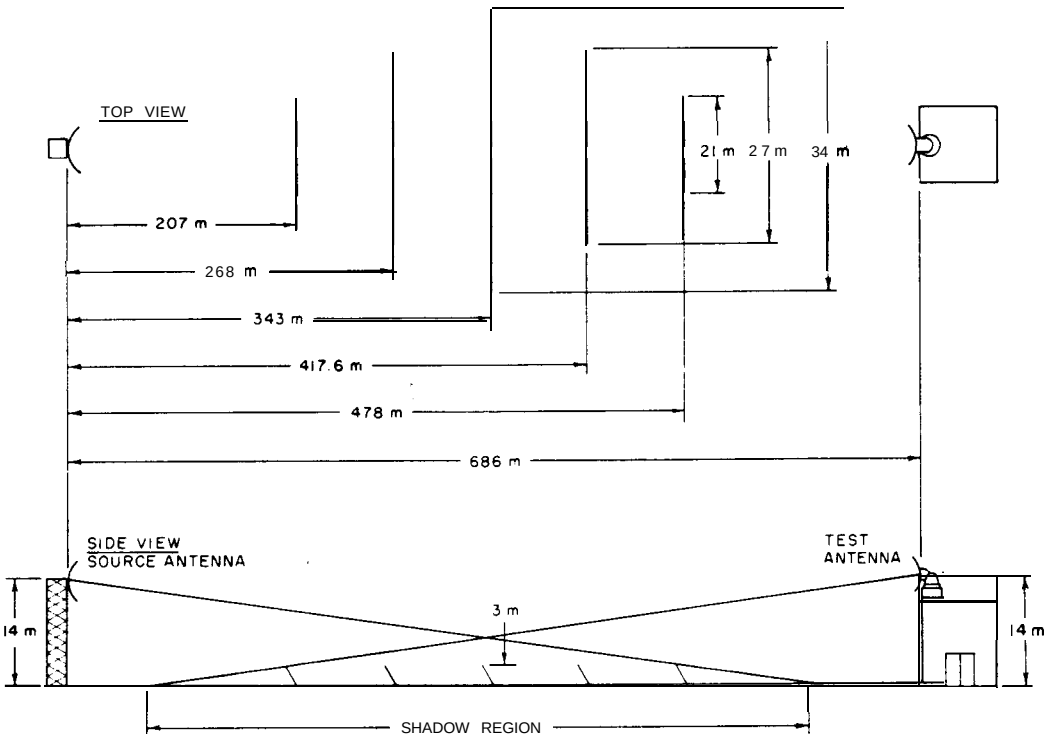

Fig 6
Example Configurations of a 686 Meter Elevated Range with Diffraction Fences

ing screen that has a mesh size of approximately 0.1 wavelength or less. When designing diffraction fences care shall be exercised to reduce the diffraction by their top edges. The effect of this diffracted field can be estimated by means of the theory of Fresnel diffraction by a half-plane. This leads to a result given in terms of Fresnel integrals, which are usually presented in graphical form as Cornu's spiral. The fences should be designed and located in such a way that they will not be illuminated by the main lobe of the source antenna. Thus it might be desirable to use several fences, each with a lower height than if a single fence were used. Additional suppression of the diffracted field can be achieved by installing either tuned slots or serratidns on the top edge of the fence. Tuned slots are more effective; however, they are frequency sensitive. The fences should also be tilted, especially if multiple fences are used, to suppress multiple reflections.

The necessary width of the fences has been empirically determined to span approximately 20 Fresnel zones constructed on the range surface. A possible diffraction-fence configuration for the 686 meter elevated antenna range is shown in Fig 6, and a sketch of a typical diffraction fence with serrations is shown in Fig 7. To save in cost, all fences are usually made identical in shape. The actual number of fences required and their positions and orientation should be determined experimentally (see 6.2).

A ***longitudinal ramp*** is a wedge-shaped reflecting surface symmetrically placed on the ground with its apex parallel to the range axis. Its purpose is to scatter the incident energy away from the test antenna. It can provide a moderate suppression of reflected energy at the test antenna; but generally it is less effective than a diffraction fence. Ideally the width of the base of the ramp should be such

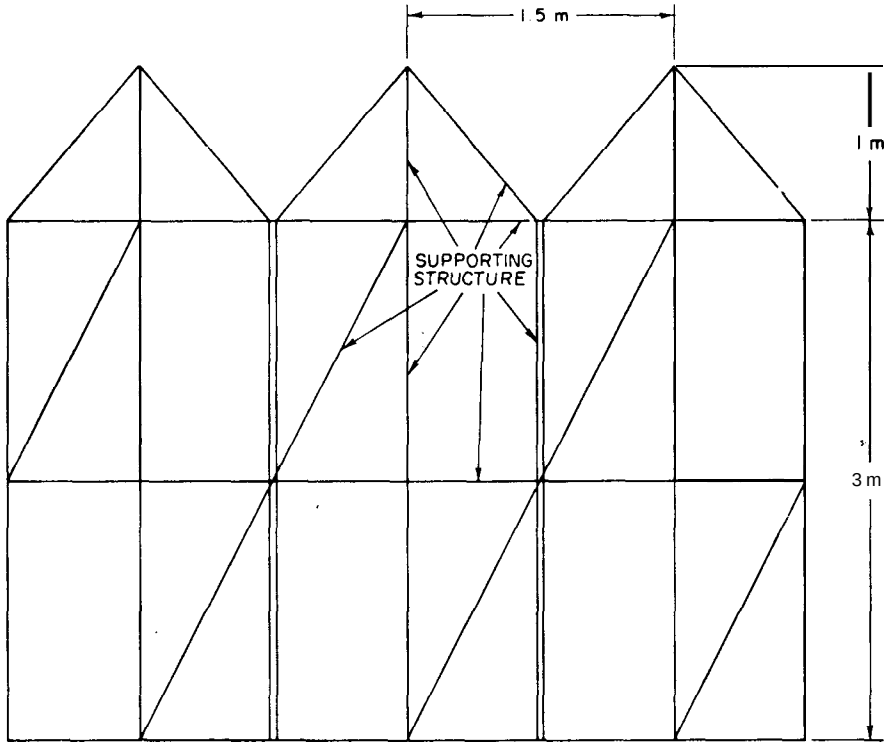

Fig 7
Example Configuration of a Diffraction Fence with Serrations
All Lines Indicate Supporting Structure; Not Shown Is the Wire-Mesh Covering

that it spans about 20 Fresnel zones as laid out on the ground surface between source and test antennas. The apex angle is usually chosen to be about 120°. For many situations these dimensions yield a prohibitively large structure, and a compromise is required, thus reducing the effectiveness of the ramp. For those ranges where the grazing angles of the incident energy are very small, more Fresnel zones are spanned by a ramp of a given size. Hence for these ranges one would expect the ramp to be more effective. Another design factor is the construction of the apex itself. Generally it is necessary to round it off rather than having it as a sharp edge. This results in a degradation at the higher frequencies. An obvious disadvantage of the ramp is that it fixes the range axis. If either the source antenna or the test antenna is moved in the transverse direction, the symmetry of the range is destroyed, and the unwanted reflected energy level at the test antenna increases. If the range has permanent tracks installed for the longitudinal motion of the antenna towers, then this is of little concern.

4.4 Design of Ground-Reflection Ranges. For the *ground-reflection range* the amplitude taper of the illuminating field at the test antenna in the horizontal direction will be the same as for the elevated range, and the criterion for the source-antenna size applies. In the vertical direction the reflected signal from the surface between the antennas combines with the direct signal to form an interference pattern (see Fig 8). By an adjustment of the height of the

source antenna, the first interference lobe can be peaked at the center of the test antenna [4]. For a given frequency the height of the source antenna h_t is given approximately by

$$h_t \approx \frac{\lambda R}{4h_r}$$

where h_r is the height of the test antenna. The expected field at the test antenna will be dependent upon the complex reflection coefficient of the reflecting surface. Attempts are made, in the design of these ranges, to make the magnitude of the reflection coefficient approximately equal to 1.

The vertical amplitude taper of the illuminating field is determined by the height of the test antenna. In particular if the 0.25 dB criterion is applied, the height of the test antenna should be

$$h_r \geq 3.30$$

where D is the diameter of the test antenna [4], [9]. Usually it is recommended that the criterion be

$$h_r \geq 4D$$

It is not always practical to position physically large test antennas at this height. For example, if it is necessary that the height of the test antenna be only $2D$, then the amplitude taper will be about 1 dB. This yields less accurate results but might be satisfactory for some applications. As previously discussed, the effect of amplitude taper is usually a reduction in measured gain and a slight modification in the side lobes. Also if the excitation of the test antenna is known, the error in gain produced by a known amplitude taper can be estimated.

Thus far it has been assumed that the magnitude of the reflection coefficient of the ground is equal to 1. Since this is not exactly true, the virtual center of radiation will not be midway between the source antenna and its image, but rather it will be some distance h_t' above that point, as shown in Fig 8. It has been found that for any range length greater than $2D^2/\lambda$ the apparent phase center is located directly beneath the source antenna at an approximate height above the range surface given by

$$h_t' \approx \frac{1 - |\Gamma|}{1 + |\Gamma|} h_t$$

Fig 8
Ground-Reflection-Range Geometry

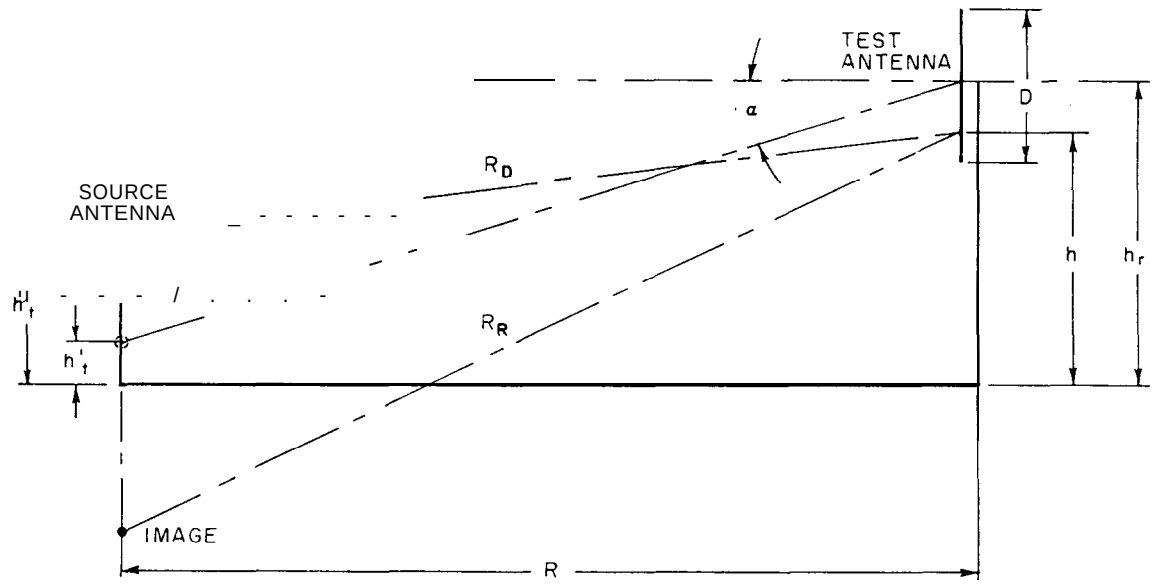

where $|\Gamma|$ is the magnitude of the reflection coefficient of the range surface for the polarization used at the angle of incidence determined from the range geometry. It is therefore necessary to calculate the direction from the test antenna to the virtual center of radiation and to orient the test antenna accordingly by providing the test antenna positioner with a tilt axis so that the entire positioner can be appropriately tilted.

It is crucial to the operation of a ground-reflection range that the surface of the range be prepared in such a manner that the energy incident upon it is specularly reflected [10]. This necessitates the specification of the "smoothness" of the surface. The Rayleigh criterion for smoothness is usually employed [1, pp 14.37–14.39], [3]. A useful form of it is given by

$$\Delta h < \frac{\lambda}{M \sin \psi}$$

where Ah is the root-mean-square deviation of the irregularities relative to the median surface, λ is the wavelength, ψ is the angle an incident ray makes with the horizontal (the grazing angle), and M is the smoothness factor. Smoothness factors ranging from 8 to 32 or greater are commonly used. This range of values corresponds to surfaces that are tolerable to very smooth. Of course Δh shall be computed for the highest operating frequency to be used.

The grazing angle ψ shall be kept small in order to avoid operating at the Brewster angle, which occurs at approximately 14" (measured from the horizontal) over land [11]. As the Brewster angle is approached, the magnitude of the reflection coefficient of the flat range surface decreases to a low value for waves that are vertically polarized, whereas the reflection coefficient for horizontal polarization is unaffected. This is undesirable if the range is to be used for both polarizations (see 6.4). It should be noted that the Brewster angle is dependent upon the electric properties of the material used in the construction of the range surface (and subsurface). For example, if the range surface were water, then the Brewster angle would decrease to approximately 4° [12]. In order for the polarization characteristics to be about the same as those for a range over land, the grazing angle shall be correspondingly smaller. This usually means that the length of the range would have to be increased.

Obviously the region directly between test and source antennas is the most critical, and as one moves from the centerline of the range, the requirement for surface smoothness becomes less demanding. A possible ground-reflection-range layout is depicted in Fig 9 [1, pp 14.39–14.41]. Notice that the range is divided into three areas: the primary area which is a nominally rectangular region located directly between source and test antennas, a secondary surface extending beyond the primary area, and a cleared area beyond that. The width of the primary surface is determined by constructing Fresnel zones over the range surface centered upon the specular reflection point that had been determined by the use of geometrical optics (ray tracing). The width of the primary surface should be such that about 20 Fresnel zones are contained within its boundaries. The surface tolerance of the secondary region can be reduced by a factor of 2 or 3. Its overall width should be about twice that of the primary region, but it should extend past the position of the test antenna by an amount of at least one quarter of the range length. In the actual design there would be no abrupt change in surface tolerance, but rather a gradual change from the primary to the secondary regions. The cleared area should be maintained by range personnel and kept free of all major reflecting obstacles. If practicable, it should extend from the edge of the secondary region at the source end of the range to points defined by the width of the first nulls in the horizontal plane of the source antenna's radiation pattern at the test-site end of the range. The cleared region should then continue as a rectangular area beyond the test site to a distance approximately equal to one half the range length.

In an alternate form of the ground-reflection range, the test antenna is mounted with its positioner on a nonconducting tower of suf-

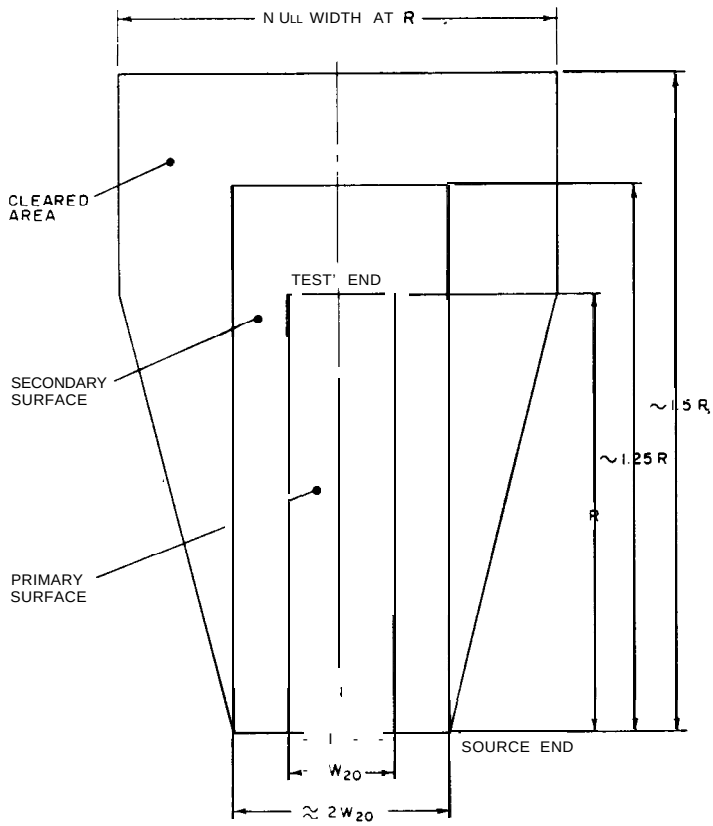

Fig 9
Possible Layout for a Ground-Reflection Range

ficient height so that the source antenna is placed within a few wavelengths of the ground and the test antenna is centered upon the first interference lobe. This type of range is a variation of the slant range discussed in 4.5 [9], [13]. It is common practice to cover the reflection region of the ground in front of the source antenna with a smooth conducting surface. Since the source antenna is close to the ground, the extent of the conducting surface is relatively small so that it becomes economically feasible.

Ground-reflection ranges find their greatest use at lower frequencies, especially in the VHF region of the spectrum, because of the difficulty of suppressing reflections in equivalent free-space ranges. However, ground-reflection ranges have been designed to operate at frequencies as high as about 35 GHz.

4.5 Other Ranges

4.5.1 ***Slant Range.*** The *slant range* [9], as the name implies, is designed with the source antenna near the ground and the test antenna along with its positioner mounted on a nonconducting tower at a fixed height, as depicted in Fig 10. The source antenna is located and oriented so that its free-space radiation-pattern maximum points toward the center of the test region and its first null is pointing toward the specular reflection point on the ground. In this way the reflected signal is suppressed. Alternate forms of the slant range are classed as reflection ranges in as much as reflections

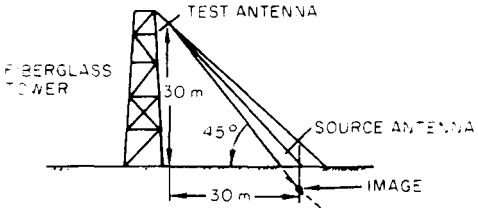

Fig 10
Slant-Range Geometry

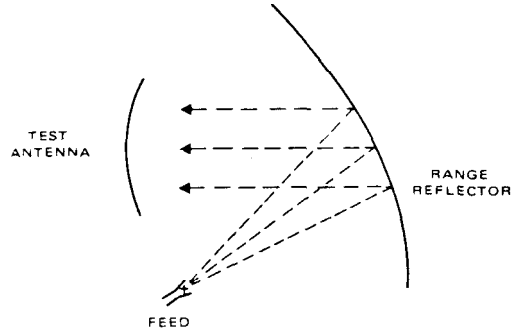

Fig 11
Schematic Representation of a Compact Range Using a Reflector and Feed

from the ground are used in order to approximate a plane wave at the test region [13],[14]. This type of slant range is a variation of the ground-reflection range and is discussed in 4.4. Slant ranges have been designed with towers where the height can be changed so that the spacing between source and test antennas can be varied. In general a slant range requires less land for a given spacing than an elevated range.

4.5.2 ***Compact Range.*** The *compact range* [15], is one in which the test antenna is illuminated by the collimated energy in the aperture of a larger point or line focus antenna. For example, a precision paraboloidal antenna can be used to collimate the energy as shown schematically in Fig 11. The linear dimensions of the reflector is usually chosen to be at least three times that of the test antenna so that the illumination at the test antenna sufficiently approximates a plane wave. An offset feed for the reflector is recommended to prevent aperture blockage and to reduce the diffracted energy from the feed structure which may contaminate the field in the test region. To further reduce the effects of the diffraction from the feed structure and also to suppress any direct radiation from the feed antenna in the direction of the test region, the reflector can be designed with a focal length long enough that the feed antenna can be mounted directly below the test antenna. If this is done, then high-quality absorbing material can be placed between test and feed antennas to absorb the unwanted radiation. The use of a relatively long-focal-length reflector has the additional advantage that for a given size reflector the depolarization effect associated with curved reflectors is lessened. Diffraction from the edges of the reflector can be reduced by designing the reflector with serrations about the edges.

In order to obtain good results with a compact range, the reflector shall be constructed with sufficient accuracy. Small deviations in the fabricated reflector surface can result in significant variations in the amplitude and phase distribution of the incident field at the test antenna. To assess the effect of surface deviations not only their shapes and maximum deviations shall be specified but, also very importantly, their areas. For example, if the reflector has small deviations that do not exceed $\lambda/100$ and their individual sizes are also small (less than one square wavelength), then the integrated effect of all the deviations over the entire reflector will be quite small, and hence a fairly uniform amplitude distribution of the incident field over the test antenna will be obtained. On the other hand, suppose the reflector had a single surface

deviation near the center of the reflector, extending over an area comparable to 1 Fresnel zone. Then a very significant change in the incident field would be expected [16]. As indicated by this example, the range reflector shah be fabricated with great care.

The compact range can be evaluated in the same manner as conventional ranges by the use of field-probing techniques (see 6.2). Since the illuminating field is obtained by the reflection from a curved surface, some depolarization is to be expected. The field probing should, therefore, include measurements of polarization as well as amplitude and phase, especially if the measurements to be made depend upon the polarization characteristics in the illuminating field.

4.5.3 ***Image-Plane Range.*** The *image-plane range* consists of a precision ground plane surrounded by absorbing material or with serrations along its edges which reduce the edge effects due to its finite size. The antenna under test is cut into two parts along its image plane, and the part above the image plane is mounted onto the ground plane.

NOTE: The image plane of an antenna refers to an imaginary plane through the antenna over which the tangential electric field is zero.

The radiation pattern of the resulting configuration in the half-space above the ground plane IS equivalent to that of the entire antenna radiating into free space. (This is not true for the input impedance.) That this is so can be shown by evoking image theory, hence the name image-plane range. The radiation pattern above the ground plane is measured by moving a source antenna in such a manner as to appropriately sample the field. This type of range has the obvious disadvantage that its use is restricted to those antennas that have an image plane, that is, antennas that exhibit linear polarization over a plane with excitations having even symmetry for polarizations normal to the plane (sum mode) or odd symmetry for polarizations parallel to the plane (difference mode). Perhaps even more restrictive is the fact that if the antenna is not designed to operate as an image-plane antenna, it shall be cut along its image plane. This means that this range is generally relegated to developmental and research work.

4.5.4 ***Anechoic Chambers.*** There are two basic types of anechoic chambers, the rectangular and the tapered types [17].

(1) The *rectangular anechoic chamber* is usually designed to simulate free-space conditions. High-quality absorbing material is used on surfaces that reflect energy directly toward the test region in order to reduce the reflected energy level. Even though the sidewalls, floor, and ceiling are covered with absorbing material, significant specular reflections can occur from these surfaces, especially for the case of large angles of incidence. One precaution that can be taken is to limit the angles of incidence to those for which the reflected energy is below the level consistent with the accuracy required for the measurements to be made in the chamber. Often, for high-quality absorbers, this limit is taken to be a range of incidence angles of 0" to 70" (as measured from the normal to the wall). For the rectangular chamber this leads to a restriction of the overall width or height of the chamber such that

$$W \geq \frac{R}{2.75}$$

where R is the separation between source and test antennas and W is the overall width or height of the chamber. The actual width and height chosen shall depend upon the magnitude of the errors that can be tolerated and upon the measured characteristics of the absorbing material used to line the walls. Additionally the room width and the size of the source antenna should be chosen such that no part of the main lobe of the source antenna is incident upon the sidewalls, ceiling, and floor.

(2) The *tapered anechoic chamber* is designed in the shape of a pyramidal horn that tapers from the small source end to a large rectangular test region, as shown in Fig 12. This type of anechoic chamber has two modes of operation. At the lower end of the frequency band for which the chamber is designed it is possible to place the source antenna close

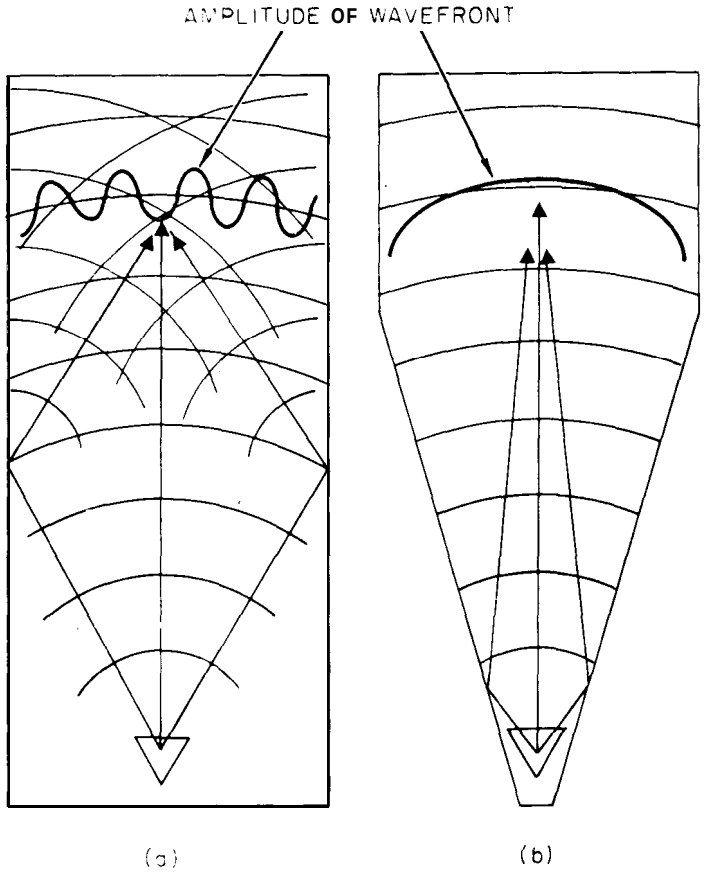

Fig 12
Specular Reflections from Sidewalls in Anechoic Chamber
(a) Rectangular Chamber. (b) Tapered Chamber

enough to the apex of the **tapered** section so that the reflections from the sidewalls, which contribute directly to the field at the test antenna, occur fairly close to the source antenna. Using ray-tracing techniques, one can show that for a properly located source antenna there is little change in the phase difference between the direct-path and the reflected-path rays at any point in the test region of the tapered chamber. The net effect is that these rays add vectorially in such a manner as to produce a slowly varying spatial interference pattern and hence a relatively smooth illumination amplitude in the test region of the chamber. It should be emphasized that the **source** antenna shall be positioned close enough to the apex for this condition to exist. The position is best determined experimentally, although a useful way of estimating its required position can be obtained by drawing an analogy between the tapered anechoic chamber and the ground-reflection range (see 4.4). By use of this analogy the perpendicular distance h_t from the source antenna to the chamber wall should satisfy the inequality

$$h_t < \frac{AR}{4h_r}$$

where λ is the wavelength, ***R*** is the separation

between source and test antennas, and h_r is the perpendicular distance from the fixed test antenna to the chamber wall. If the source antenna is moved forward in the chamber, then the interference pattern becomes more pronounced, with deep nulls appearing in the region of the test antenna.

As the frequency of operation is increased, it becomes increasingly difficult to place the source antenna near enough to the apex. When this occurs, a higher gain source antenna is used in order to suppress reflections. It is moved away from the apex, and the chamber is then used in the free-space mode similar to the rectangular chamber.

The field does not spread in the manner of a spherical wave, hence the tapered chamber cannot be used for any gain measurement based directly upon the Friis transmission formula, such as the two-antenna or three-antenna gain-transfer methods [6].

5. Antenna-Range Instrumentation

5.1 General. The instrumentation required for an antenna test range can be classified into five subsystems:

(1) source antenna and transmitting system
(2) receiving system
(3) positioning system
(4) recording system
(5) data-processing system

The extent of the instrumentation required depends upon the functional requirements imposed by the measurements to be made. The instrumentation may range from very simple systems designed for making only principal-plane patterns of simple antennas to highly automated systems in which computers are programmed to control all aspects of the measurement, including the data processing for the complete characterization of highly complex antennas.

A block diagram of the basic instrumentation elements of an antenna test range is shown in Fig 13. The control units, indicators, receiver, recorders, and tuning units for the transmitters are usually located in a master-control console. The signal source itself is usually located at a remote antenna tower.

5.2 Source Antennas for Antenna Ranges. With the exception of a few highly specialized installations, antenna test ranges are designed to operate over a wide band of frequencies. This means that they shall be equipped with a family of source antennas and transmitters covering the entire band. The antennas shall, of course, have the beamwidths and polarization properties consistent with the measurements to be performed on the range.

For frequencies below 1.0 GHz, log-periodic arrays are often used, and for frequencies above 400 MHz families of parabolas with broad-band feeds are most often used. In some cases large horn antennas have been utilized. A means for controlling the polarization is usually required. As will be discussed in 5.5, this can be accomplished by mounting a linearly polarized source antenna on a polarization positioner. Then the direction of polarization can be continuously rotated. This feature is required for some types of measurements. Some other types of measurements require circular polarization so that a well-equipped antenna test range usually has families of both linear and circularly polarized source antennas. The circularly polarized antennas can be designed so that they can produce right-hand or left-hand circular polarization, as well as orthogonal linear polarizations. Crossed log-periodic arrays are examples of such antennas. In addition, a set of gain-standard antennas is necessary if power-gain measurements are to be made using the gain-transfer method (see 12.3).

5.3 Transmitting Systems. The selection of the transmitter depends upon several system considerations [1, pp 15.11–15.37]. There are a number of types of signal sources available such as triode cavity oscillators, klystrons, magnetrons, backward wave oscillators, and various solid-state oscillators.

Whatever type of signal source is chosen, the following performance requirements apply:

(1) *Frequency control.* A means shall be available to tune the signal source to the

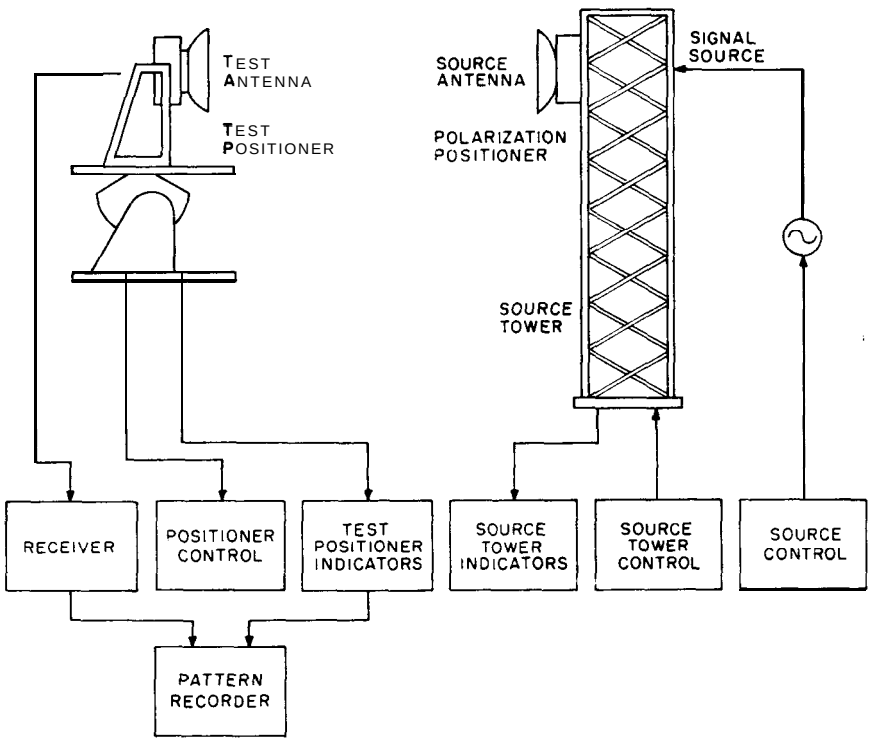

Fig 13
Block Diagram of Typical Antenna-Measurement System

desired frequency. Depending upon the type of signal source used, mechanical, electromechanical, or electrical means may be employed. If the transmitter is remote, a means of remote control is highly desirable. A calibrated position servo loop or a rate servo loop can be used to control a motor that mechanically tunes the oscillator. For the case of oscillators that can be electrically tuned, an adjustable, regulated power supply is required.

(2) *Frequency stability.* Since the antennas and their associated radio-frequency circuitry are highly frequency sensitive, it is necessary that the signal-source frequency remain constant over the measurement period, which may be in excess of 30 minutes. Frequency variations of the order of 0.01 to 0.1 percent are usually acceptable. But for more precise measurements, a frequency stability of one part in 10^6 or better may be required.

The following are several methods of frequency stabilization in common use:

(a) control of the operating environment, such as by immersion of the oscillator in a temperature-controlled oil-bath

(b) coupling of the oscillator to a high-Q cavity

(c) electronically referencing the oscillator to a microwave cavity (the Pound system) [18]

(d) electronically referencing the frequency to a stable source (automatic frequency control)

(e) phase locking the frequency to a stable source (automatic phase control)

The particular scheme used depends upon the type of oscillator used.

(3) *Spectral purity*. Some types of oscillators are rich in harmonics which, if transmitted, would contaminate the desired signal. In some cases spurious or nonharmonically related signals are generated. To eliminate these unwanted signals one can either use filters or employ a receiver that will discriminate between desired and undesired signals.

(4) *Power level*. The required power output of the signal source for a particular measurement is dependent upon the source and test antenna gains, the receiver sensitivity, the transmission loss between the two antennas, and the dynamic range required for the measurement. Typical detectors used in antenna instrumentation systems have sensitivities on the order of -50 to -65 dBm. If a receiver is used, this figure may be improved as much as 30 to 60 dB. Power levels provided by typical antenna-range signal sources range from 0 to 33 dBm. Since most antenna tests are amplitude measurements, it is important that the output of the signal source be relatively constant. For most measurements a variation of ± 0.05 dB, which is easy to obtain, is not significant; but for some cases, such as insertion-loss or gain-transfer measurements, variations of ± 0.01 to ± 0.02 dB for short periods of time may be required. For these cases an automatic power-level control shall be provided.

(5) *Modulation*. For some systems amplitude modulation is required; hence the signal sources should have that capability. There are cases where special pulse shaping is required to reduce the distortion of the pulse spectrum.

5.4 Receiving Systems. The receiving subsystem used in the *antennaamplitude-pattern measurement system* may be simply a bolometer detector (usually mounted directly on the test antenna or, in the case of a scale model, inside the model) and its associated amplifier, the output of which supplies the signal to the recorder. With this system the transmitter is usually modulated. Also the dynamic range of the system is limited to the range over which the bolometer has a square-law characteristic, usually about 40 dB. The simple *detector–amplifier receivingsystem* finds wide application for antenna ranges where extensive scale-model work is done or where quasi-isotropic antennas are tested. With this system the detected signal can be fed to an amplifier by means of a high-impedance cable, thus reducing the reflections from the cable connecting the test antenna to the console (see 7.1).

The simple bolometer-amplifier system lacks the dynamic range, sensitivity, and frequency discrimination for most antenna measurements. This has led to the development of superheterodyne receivers specifically for use in antenna measurements. These receivers are typically designed to operate over an extremely wide range of frequencies, from a few megahertz to above 100 GHz. The harmonics of the local oscillator are used for operation in the millimeter and submillimeter range and, for the case of low-frequency reception, the received signal is upconverted to a frequency within the range of the receiver [1, pp 15.38–15.49].

It is desirable that the receiver be physically located in the master console, whereas the antenna under test may be remotely located. To avoid the degradation of excessive cable attenuation at lower frequencies and the inconvenience of long runs of waveguide at higher frequencies, the first mixer is usually mounted directly on the terminals of the antenna under test. A single coaxial cable carries the local oscillator power to the mixer and provides the return of the intermediate-frequency signal from the mixer to the receiver. This places a limitation on the allowable cable attenuation for proper mixing, usually about 15 dB.

The receivers are often equipped for both manual and motor-driven tuning. The motor control can be used for a mechanical automatic frequency control and can be designed in such

a manner that the receiver can be used for swept-frequency measurements.

Antenna-pattern recorders are typically designed to operate at a fixed 1 kHz audio carrier frequency; for these cases the output of the receiver shall be 1 kHz. Antenna-pattern-range receivers are usually designed for continuous-wave reception, and the 1 kHz amplitude modulation is introduced in the receiver. The need for remote adjustment of the modulation frequency of the signal source is thus eliminated.

A bolometer is most often used for detecting the 1 kHz modulation of the intermediate-frequency carrier. The dynamic range of the receiving system is limited by the square-law range of the bolometer (about 40 dB), unless some means of compensation is provided. Compensation can be accomplished by the introduction of a bias voltage in the intermediate-frequency amplifier to vary its gain by the use of an auxiliary potentiometer connected to the pen drive. The bias voltage can be controlled so that the receiver gain increases as the recorder pen moves downscale. The system does require a set of adjustments for proper operation, with which the dynamic range can be increased to about 60 dB.

If the signal source is not sufficiently frequency stabilized to eliminate all significant frequency drift, then an automatic frequency control must be employed. The automatic frequency control may also be needed to compensate for local oscillator drift. It shall be capable of operation over the dynamic range of the input signal, that is, more than 40 dB.

A useful circuit which is sometimes incorporated into measurement receivers is one that compensates for small transmitter power-level variations. This circuit requires that the signal from the transmitter be monitored continuously during the measurement.

If greater sensitivity, precision, and dynamic range are required, the *double-conversion phase-locked receiver* may be employed. This type of receiver produces the required 1 kHz output signal by conversion rather than by square-law detection. Heterodyning to such a low second intermediate frequency is made possible by the use of phase-lock techniques. A block diagram of a single-channel double-conversion heterodyne circuit is shown in Fig 14 [1, pp 9.9–9.13]. The phase-lock circuit causes the first intermediate frequency to be synchronous (locked) to the frequency of a highly stable crystal oscillator. Because of the purity of the crystal-oscillator spectrum, the intermediate-frequency contains almost no frequency-modulation components within the passband of the phase-lock loop. This permits the intermediate-frequency signal to be converted to 1 kHz by means of a second crystal oscillator, which is in turn phase-locked so that its frequency differs from the intermediate frequency by precisely 1 kHz. The bandwidth of the first intermediate-frequency amplifier is typically of the order of 10 MHz, while that of the second intermediate-frequency amplifier is of the order of 100 Hz.

The noise bandwidth of the double-conversion system is approximately equal to twice that of the output bandwidth of the receiver, that is, usually 200 Hz. This is in contrast to that of the conventional receiver employing square-law detection. The noise bandwidth of the latter is approximately $\sqrt{2B_1 \cdot B_2}$, where B_1 is the bandwidth of the intermediate-frequency amplifier and B_2, the bandwidth of the postdetection amplifier. Typically B_1 and B_2 are chosen to be 1 MHz and 100 Hz, respectively. A considerable improvement in sensitivity is obtained by using the double-conversion phase-locked receiver rather than the conventional receiver.

An additional advantage of the double-conversion phase-locked receiver is the fact that the change in output voltage is linearly proportional to the change in input voltage rather than input power. In receivers with square-law detectors a 10 000:1 change in output voltage is required to represent a 100:1 change in input voltage. The double-conversion phase-locked receiver requires only a 100:1 output ratio to represent a 100:1 input ratio. It is quite easy to achieve a 1000:1 output ratio, giving a 60 dB dynamic range. Although dynamic ranges of 80 dB can be achieved with extreme care in design, a 60 dB dynamic range appears to satisfy most measurement problems.

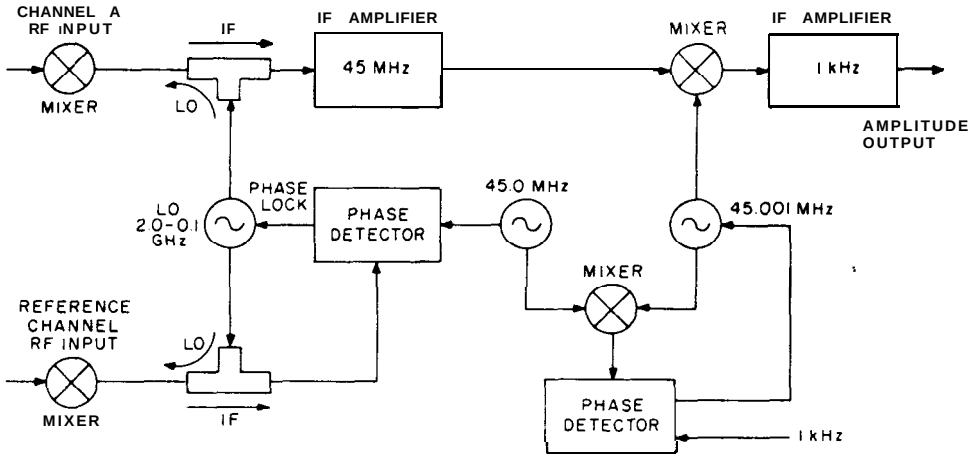

Fig 14
Basic Heterodyne Receiving System Using Double Conversion and Phase Locking

For some antenna-measurement applications the rate al which data can be taken is of importance. While often the data rate is limited by the rate at which the antenna under test (or the source antenna in the case of a movable line-of-sight range) can be physically moved, there are situations where the data rate is limited by the bandwidth of the output circuit of the receiver. For these cases, in order to increase the data rate, the output bandwidth has to be increased. This will also reduce the sensitivity, and hence the dynamic range, of the system so that there is a trade-off between increased data rate and system sensitivity. Usually in order to increase the output bandwidth the output frequency shall also be increased. Since the sensitivity of bolometer detectors decreases rapidly with increased modulation frequency, it is impractical to increase the output frequency of a conventional receiver. With the double-conversion phase-locked receiver a detector is not used, so one has a choice of output frequencies. For example, if the output frequency is such that the output bandwidth can be increased by a factor of 10, then for this receiver the data rate will increase by a factor of 10 with a corresponding decrease in system sensitivity of 10 dB.

The phase-locked receiver requires a reference signal that can be obtained either from a reference antenna or, where distances are short, by a direct sample from the signal source.

If phase measurements are also required, then a dual-channel double-conversion phased-locked receiver may be used [1, pp 9.9–9.13],[19]. A block diagram is shown in Fig 15. The circuit is similar to that shown in Fig 14 except that it has two signal channels, designated A and B, which are fed by the same first and second local oscillators. The output voltage of each channel is directly proportional to the input microwave voltage of that channel, and the signal level in each channel can vary independently over the dynamic range of the system.

One of the primary areas of concern in a sys-

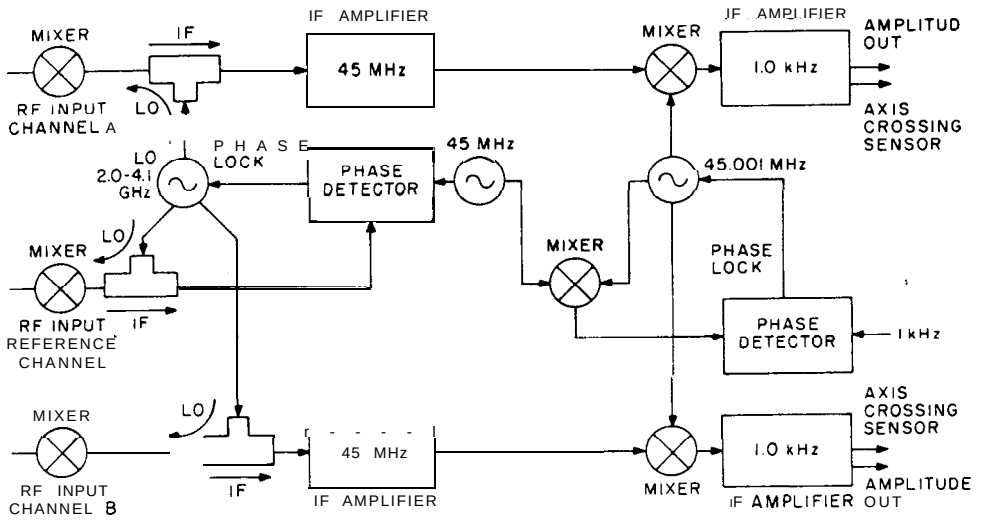

Fig 15
Dual-Channel Heterodyne Receiving System for Phase Measurements

tern of this nature is that of eliminating interchannel interference. By the use of isolators, proper shielding, and careful design, the interchannel isolation can be maintained greater than 90 dB. An interchannel isolation of this magnitude results in linearity errors over a 60 dB dynamic range of less than ± 0.25 dB.

After the heterodyning of the two input signals to a final frequency of 1 kHz, phase measurement becomes essentially a time measurement. Fig 15 shows a second output from each of the 1 kHz intermediate-frequency amplifiers feeding an axis-crossing sensor. As the name implies, each axis-crossing sensor senses the time of the axis crossover of the 1 kHz signal. Specifically it senses each positive axis crossing. At that instant each axis-crossing sensor provides a narrow pulse output. Measurement of the time between axis crossings of the signal in channel A and that in channel B can be directly translated to degrees at 1 kHz, and consequently to the input radio-frequency signal. With a system of this type, amplitude variations of the signals in the two signal channels and the phase difference between them can be measured simultaneously. Amplitude and phase readouts can be provided in either analog or digital form as required.

If the receiver is to be used in an automated system, it is highly desirable that it be computer compatible, that is, its output should be such that the receiver can be interfaced directly with a computer. Also, an agile local oscillator is required if the operating frequency has to be changed during the course of the measurement.

5.5 Positioning Systems

5.5.1 ***Antenna Positioners.*** For either the fixed- or the movable-line-of-sight methods (see 3.3) two orthogonal axes are required if true θ and ϕ cuts are to be made. These axes axe designated as the θ rotational axis and the ϕ rotational axis and are depicted in Fig 16. The

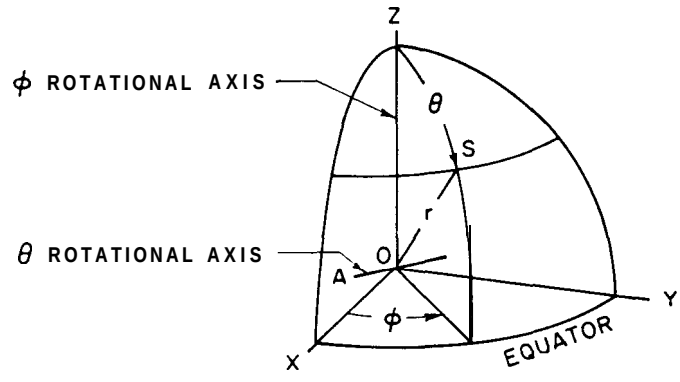

Fig 16
The Two Orthogonal Axes of Rotation Required by an Antenna Positioner Using Spherical Coordinates

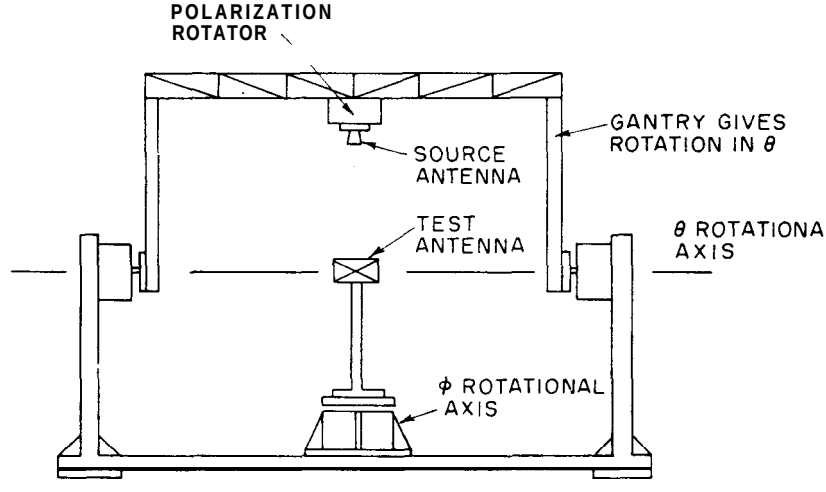

Fig 17
Positioner Configuration in which the Source Antenna Is Supported by a Gantry that Provides the θ Rotation

ϕ axis, which permits cuts in ϕ with θ as the parameter, is the $0Z$ axis of the coordinate system. The θ axis, which provides for θ cuts with ϕ as the parameter, is coincident with the line $0A$ drawn through the origin normal to the line OS, where OS defines the direction to the source antenna. These axes are employed in all spherical-coordinate positioner configurations [1, pp 5.12–5.24].

A possible positioner configuration for the movable-line-of-sight system is shown in Fig 17. It consists of a gantry which provides the θ rotation and an azimuth positioner which provides the ϕ rotation. This scheme is of restricted utility, since the distance between the two antennas is limited. It is useful for testing small antennas such as primary feeds for reflector antennas. An alternate approach to the use of a gantry is to mount the source antenna on a carriage that moves along a fixed semicircular arch centered upon a turntable on which the test antenna is mounted. By control of the movements of the carriage and the turntable both θ and ϕ cuts can be obtained. Arches with radii as large as 19.8 meters have been constructed [20]. This type of range is primarily used for testing vehicle-mounted VHF and UHF antennas, as well as scaled models of high-frequency antennas (see 7.1) [20].

In the case of the fixed-line-of-sight system the θ and ϕ rotations are provided completely by the positioner for the test antenna. Two positioners which meet the requirements for this system are the azimuth-over-elevation and the elevation-over-azimuth types. These positioners and their associated coordinate systems are shown in Fig 18. An alternate example of an elevation-over-azimuth positioner is the model tower (see Fig 19). Greater flexibility can be obtained by the use of additional axes; for example, azimuth-over-elevation-over-azimuth positioners are frequently employed.

It is desirable that the operational coordinate system of the test antenna be coincident with that of the positioner. Otherwise the interpretation of the measured data and the evaluation of errors become difficult. Moreover, the physical characteristics of the test antenna and the general shape of its radiation pattern are important considerations in the selection of a positioner. Indeed it is often necessary that a positioner be designed explicitly to satisfy a specific measurement requirement where nonstandard motions are required [3].

Specially designed positioners may be required when the radiation pattern of the test antenna is essentially isotropic. For this case the positioner has to be designed so that it does not significantly alter the radiation pattern of the antenna under test. One method is to suspend the antenna on the end of a long nonmetallic boom. Another method is to mount the antenna on a plastic foam tower. For either of these methods, obtaining the motions required for a complete set of radiation patterns is difficult.

If the measurement requires the use of orthogonal polarizations, then the source antenna should be provided with a means to change its polarization. Source antennas can be designed in such a manner that their polarization can be electrically switched between two orthogonal linear or circular polarizations. For the case of orthogonal linear polarizations, a more common method is to use a source antenna positioner that is capable of rotating a linearly polarized source antenna through at least 180°, although for some methods of polarization measurement the direction of polarization shall be rotated continuously through 360° during the measurement (see 11.2).

5.5.2 ***Antenna-Positioner Errors.*** The errors introduced in the measurement of radiation patterns by positioners are angle errors or pointing errors. The following is an outline of errors associated with positioners [1, pp. 5.32-5.411:

(1) *Geometric error*

(a) *Coordinate-axis-alignment error.* Improper alignment of the coordinate system of the test antenna with that of the antenna positioner.

(b) *Orthogonality error.* Nonorthogonality of the two rotation axes of the antenna positioner.

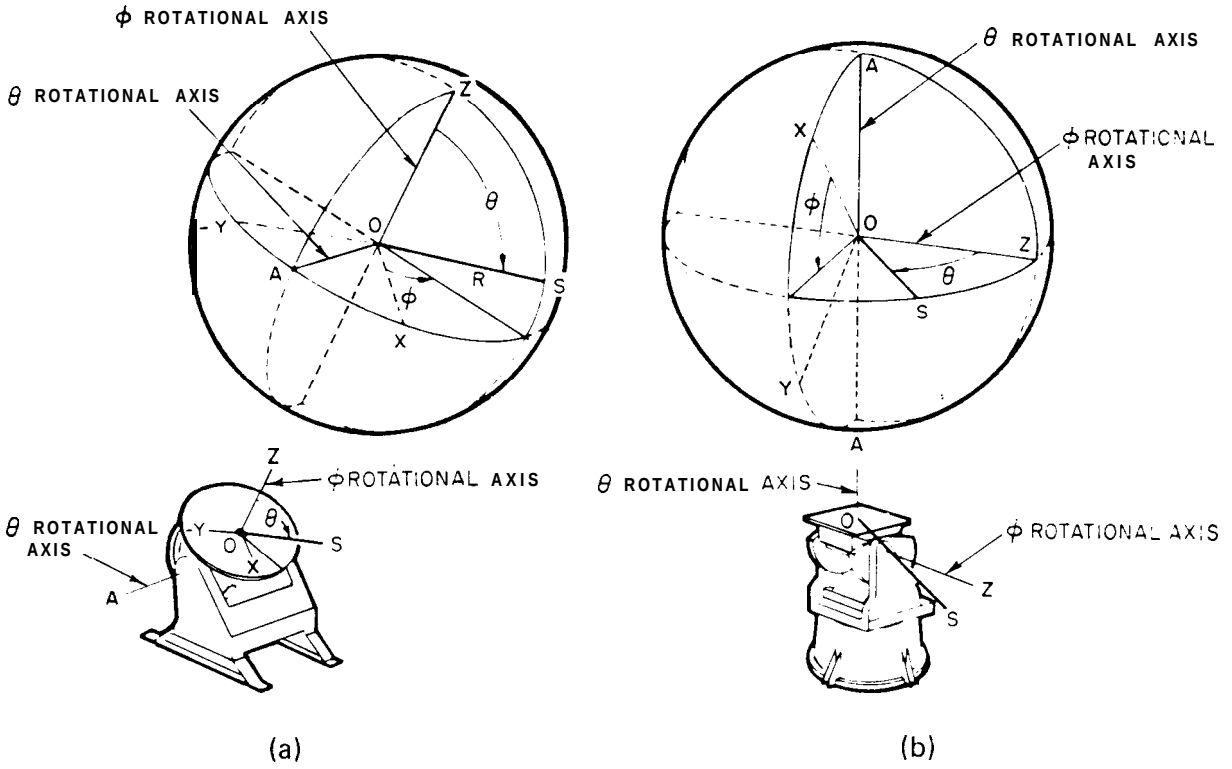

Azimuth-over-Elevation Positioner.

Elevation-over-Azimuth Positioner

Fig 18
Two Standard Positioner Configurations and their Associated Spherical Coordinate Systems

(c) Collimation error. Nonorthogonality of the θ axis with the line from the origin of the positioner coordinate system to the source antenna (line OS in Fig 16)

(d) *Axis runout and axis wobble*

(2) Shaft-position error. Errors in the determination of the shaft-position angle

(3) *Deflection errors.* Structural changes in the positioner because of thermal expansion and contraction and changes in the forces applied to the positioner

Some of the geometric errors are inherent in the design and construction of the positioner. However, for well-designed positioners these errors are generally very small, and their magnitudes can usually be determined from the manufacturer's information. For errors due to the installation of the positioner and the mounting of the test antenna, range personnel do have some control. This is especially true in the case of mounting the test antenna onto the positioner. Care should be exercised in the design of the mount so that the test antenna's coordinate system coincides with that of the positioner.

Shaft-position-angle information can be ob-

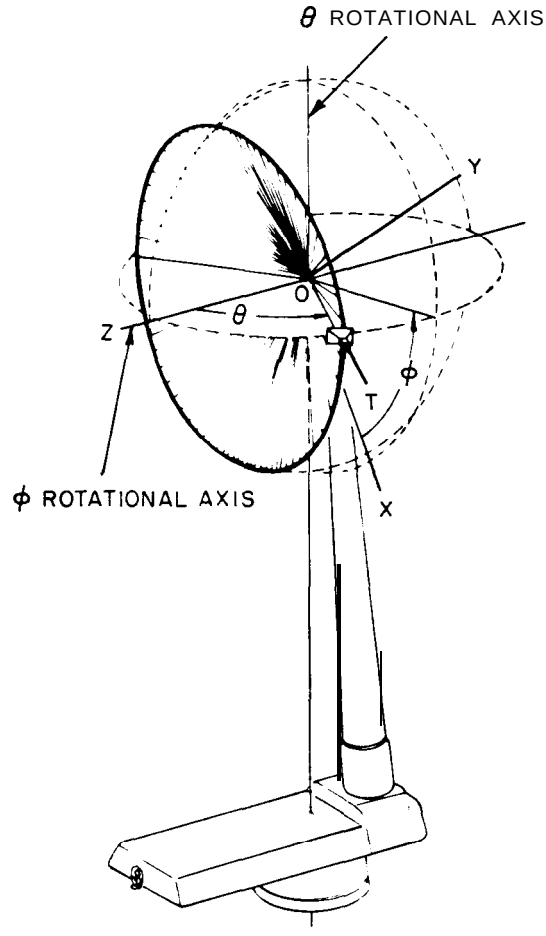

Fig 19
Model Tower and Its Associated Spherical Coordinate System

tained by the use of synchro systems, potentiometers, or digital encoders. Typically commercial positioners use dual synchro systems with the transmitters geared at ratios of 1:1 and 36:1 with respect to each axis. The readout system may be of either an analog type or a digital type. The analog type consists of a synchro receiver indicator, whereas the digital type requires an analog-to-digital converter. Readout errors of approximately 0.05' to less than 0.01" are typical, depending upon the unit considered. Direct-drive digital encoders are more accurate than the geared synchro system and are used where high precision is required. High-accuracy digital encoders may either be of the multipole-resolver type or of the optical type.

Deflection errors due to solar heating can be reduced by solar reflectors, insulating shields, reflecting paint, and barriers. Those due to changes in bending moments applied at the antenna mounting surfaces can frequently be reduced by incorporating counter balance weights in the design of the antenna mount in such a way that the change in bending moment is reduced.

5.6 Antenna-Pattern Recorder. The *antenna-pattern recorder* provides a means of obtaining

a visual display of the antenna pattern. It is used to plot the relative signal strength received by the test antenna as a function of the angular position of the antenna. The signal to be plotted is obtained from the output of a receiver or directly from a microwave detector, depending upon the type of receiving system used. The position information is normally obtained from synchro transmitters or digital encoders geared to the positioner axes. In addition to the measurement of signal strength, the relative phase angle between two signals can be recorded if the receiving system provides a dc output with an amplitude in proportion to the radio-frequency phase angle.

Typical antenna-pattern recorders are electromechanical devices employing servo systems to drive the recorder axes. A chart servo system usually positions the recording paper as a function of the angular position of the antenna. A pen servo system positions a recording pen in response to the amplitude of the input signal. Ink-writing systems are mostly used in preference to electric, thermal, pressure-sensitive, or photographic systems because of the high quality, high writing speed, reproducibility, economy, and simplicity of an ink system.

The antenna pattern may be recorded in either polar or rectangular form. The polar form is often preferred for plotting patterns of antennas that are not highly directional. The polar format is particularly useful for visualizing the power distribution in space. Such a plot is illustrated in Fig 20(a).

In the rectangular format [Fig 20(b)] the signal amplitude is the y axis (ordinate) and the position angle is the x axis (abscissa). The rectangular format permits narrow beam patterns to be recorded in finer detail because the pattern does not become crowded in regions of relatively low gain as it does in a polar graph. To provide adequate resolution in a rectangular display of patterns of different beamwidths, selectable chart scales are required.

An expanded rectangular-coordinate chart scale is obtained by deriving the angle information from a synchro transmitter geared to the positioner axis, so that the synchro shaft rotates a number of times for one revolution of the positioner turntable. A 36:1 synchro ratio is commonly employed, resulting in one turn of the synchro shaft corresponding to 10° of positioner rotation. This ratio is especially convenient for a readout of the positioner angles with devices such as dual-pointer synchro indicators, since the 36:1 ratio is compatible with the decimal numbering system.

NOTE: A ratio such as 16:1 or 32:1 is used in dual-speed synchro systems in which position angles are read as binary numbers.

With dual-speed 1: 1 and 36:1 synchro transmitters the recorder chart scale (or one chart cycle) is 10° of 360". An intermediate 60° chart cycle can also be provided by gearing a synchro to the chart axis of the recorder at a 6:1 ratio. Thus six rotations of the 36:1 synchro transmitter are required for one chart cycle.

A rectangular-coordinate recorder in which the chart paper is driven by the chart servo is referred to as a strip-chart recorder. If the pen is driven in both the x and the y coordinates, the recorder is referred to as an x-y recorder. Usually polar recordings are obtained by driving a turntable with the chart servo. However, an x-y recorder can be used to generate polar plots by electronically performing the coordinate conversion. For practical reasons the transformation is made using 1 :1 synchro information only.

Antenna pattern recorders usually provide for a selection of amplitude functions. The pen deflection may be directly proportional to the amplitude of the input signal to the recorder, or the response may be proportional to the square, square root, or logarithm of the input. If the proper pen function is selected for the particular type of detector used, either a linear or a square-law detector, the recording may be presented as a function of the power, radio-frequency voltage, or relative signal level in decibels. This leads to the following pattern formats.

Relative power patterns illustrate the variation of power density at a fixed distance from the antenna as a function of angular coordinates [Fig 21(a)]. Power patterns are most useful in assessing small power variations be-

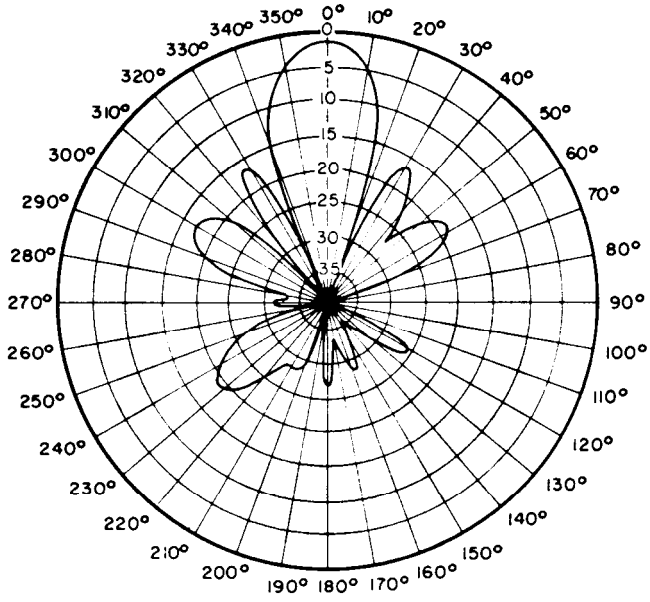

(a)

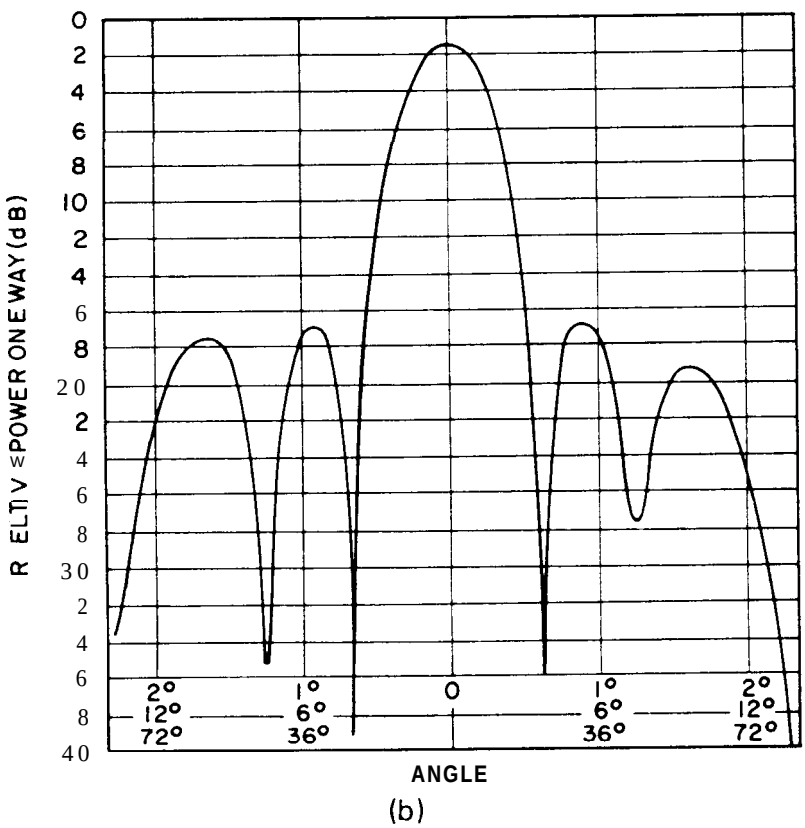

(b)

Fig 20
Polar and Rectangular Logarithmic Plots of a Normalized Radiation Pattern
(a) Polar Plot. (b) Rectangular Plot

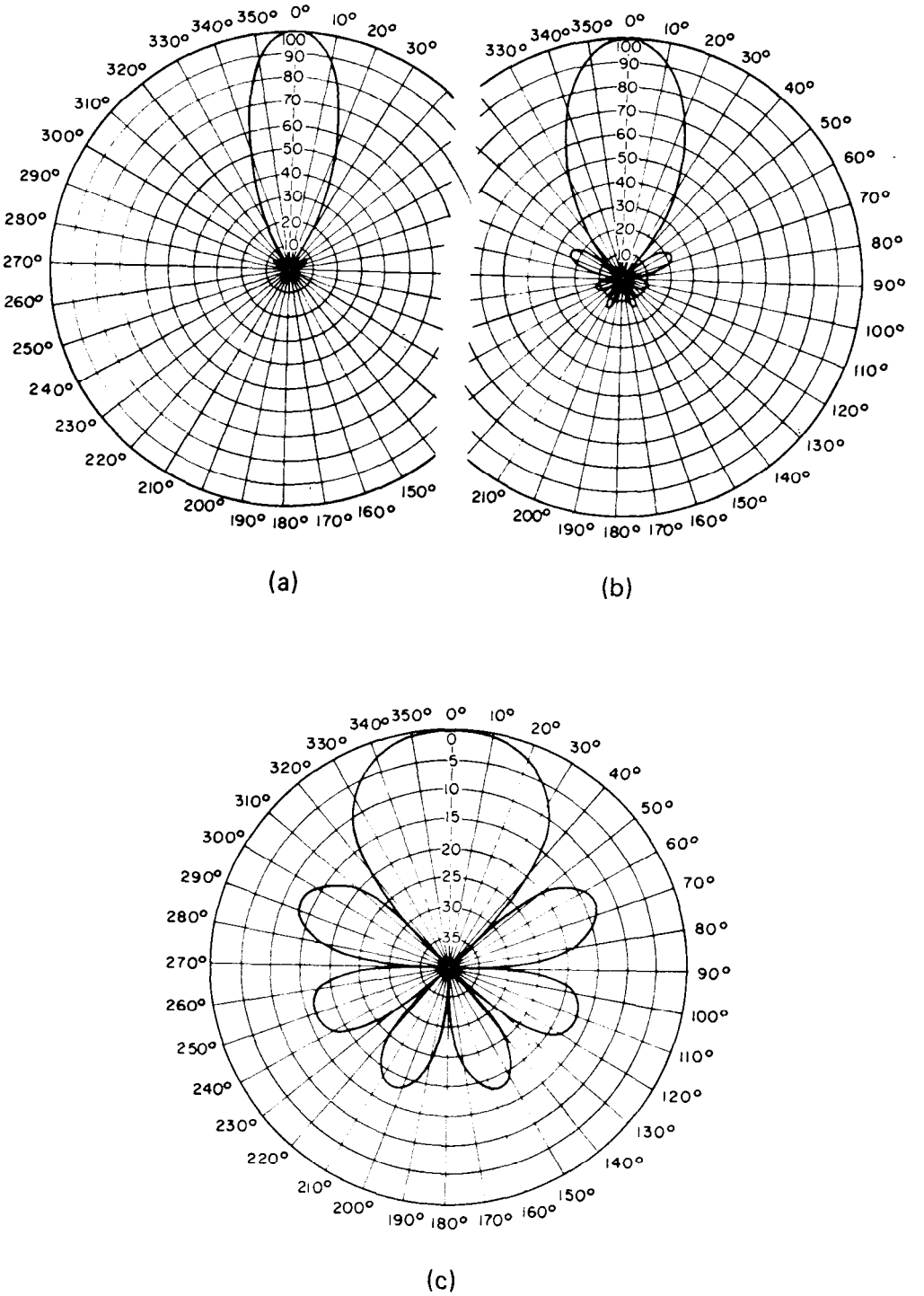

Fig 21
Power, Field, and Decibel Plots of the Same Antenna Pattern
(a) Relative Power Pattern. (b) Relative Field Pattern. (c) Decibel Pattern.

tween 100 and 10 percent of the peak value. Power variations in the range below 10 percent of full scale are difficult to resolve without changing gain levels. Power patterns are used in calculating directivity, and sometimes in making measurements to determine half-power beamwidths of antennas because of the increased resolution afforded at the higher signal levels. They would not be useful in measurement problems where low side lobe levels and high front-to-back ratios are of interest.

Relative field patterns show the variation of the electric field intensity at a fixed distance from the antenna as a function of angular coordinates [Fig 21(b)]. Field patterns provide greater side lobe resolution while still displaying small variations in field level near the maximum. The half-power level on this format is 0.707 times the full-scale value.

If the recorder scales are linearly calibrated in decibels, a *logarithmic relative gain pattern* results. This format is particularly useful since antenna gain is usually specified in decibels. The decibel scale provides constant resolution over the entire display range, and a wider dynamic range can be displayed than with other formats. Comparison of patterns is also easier with a decibel scale, since a difference in system gain is equivalent to a constant offset of the recorded data. A recording range of 40 dB is most often used, because this range is usually sufficient to show the side lobe levels of interest, and it generally provides sufficient resolution for an examination of the main lobe structure [Fig 21(c)]. However, to achieve a 40 dB dynamic range when operating from a square-law detector, the recorder shall have an *80* dB usable dynamic range. In order for the recorder noise to be small relative to the minimum input signal level, the noise level should be approximately 110 to 120 dB below the full-scale input.

There are other formats for the presentation of antenna patterns which have found wide use. A complete radiation pattern can be presented on a single page as a *contour plot* by connecting points of equal signal levels with lines to form isolevel contours in the manner employed for topographic contour maps. Key levels are numerically identified to permit interpretation of the graph. One such system employs different colors to highlight the contours. These approaches usually require the use of computer graphics.

An alternate approach, which has found wide acceptance, is the *radiation distribution table* which provides the same basic information as the contour plot, but accomplishes it in a simpler manner. A portion of a radiation distribution table is shown in Fig 22. Signal levels are printed numerically in decibels at preselected intervals of θ and ϕ. The graph shown was made by scanning in ϕ and stepping in θ after each ϕ cut. In the figure the angular increments are 0.5° in θ and ϕ, and the dynamic range is 40 dB. Signal levels are sensed by an encoder coupled to the servo-driven logarithmic potentiometer in an antenna-pattern recorder and printed on the data form.

The contour effect is obtained by printing the even values of signal level and omitting the odd values or by underlining either the odd or the even numbers.

5.7 Data-Processing and Control Computers. Although not shown in the block diagram of Fig 13, an on-line instrumentation minicomputer provides a natural solution to the data-gathering, control, and data-processing requirements of an automatic antenna-measurement system. Instrumentation computers can be equipped with a variety of input-output devices, depending on the requirements of the particular measurement program. Magnetic tape, teletype, and paper-tape input-output units are commonly employed for programming the computer and recording and storing data. The computer also becomes a source of stored routines that can be called up to meet the basic demands of the system.

In addition to solving the on-line data-processing and control requirements, the computer can be programmed for analysis and reduction of the measured data. For example, the polarization properties of the antenna can

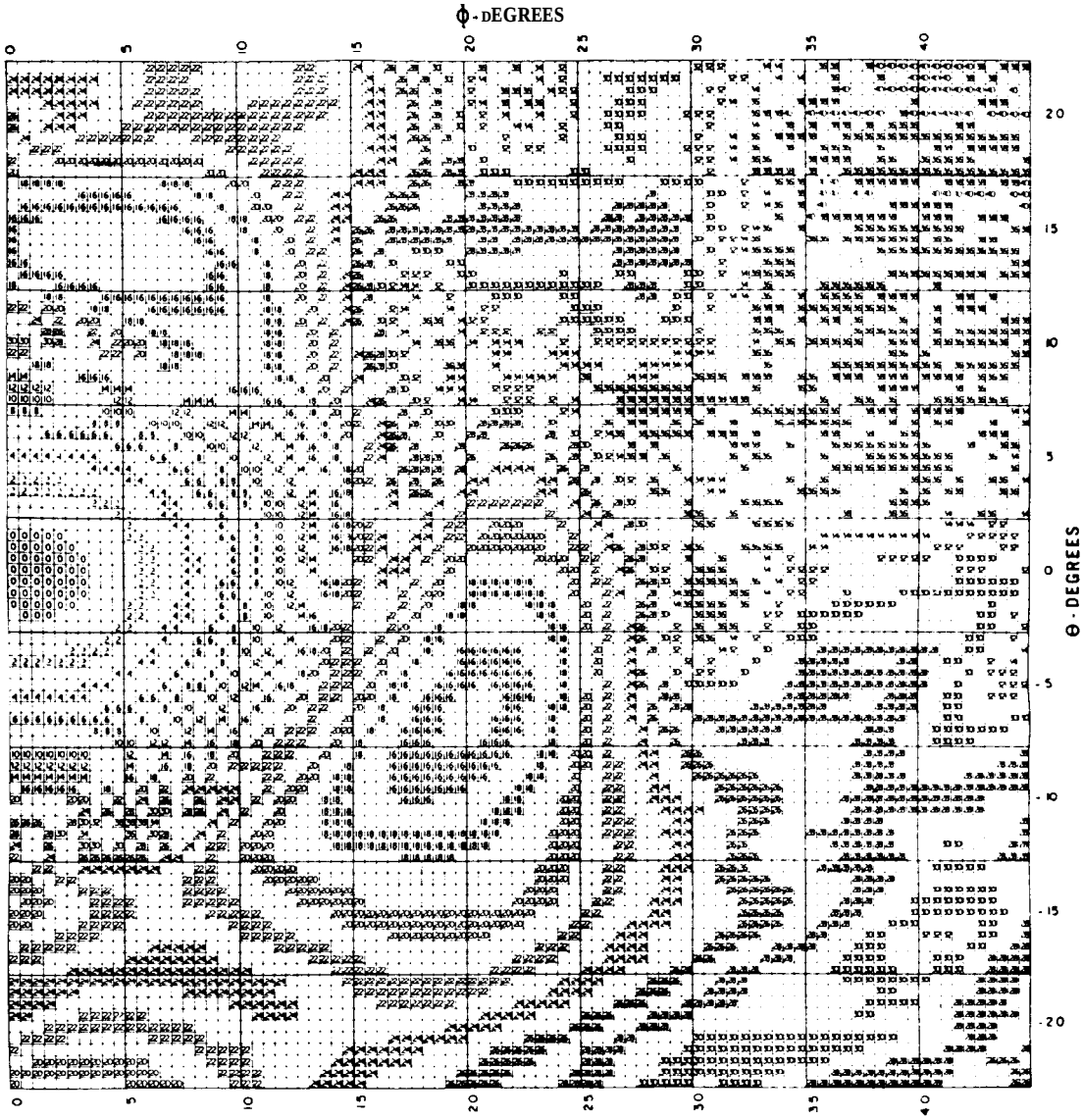

Fig 22
Radiation Distribution Table Recorded by Scanning in ϕ and Stepping in θ
Data Are Presented at 0.5' Increments over a 40 dB Dynamic Range

be calculated as well as its directivity. Computer plotters can be employed to provide a variety of visual displays of antenna patterns. Not only can contour plots be produced, but also three-dimensional presentations. For lengthy programs or for programming convenience, the recorded data can be processed by a larger central computer at the user's facility.

6. Antenna-Range Evaluation

6.1 General. Once an antenna-pattern range has been designed, constructed, and instrumented, it is necessary to experimentally determine the state of the illuminating electromagnetic field over the *test region,* that is, the region where the test antenna is to be mounted. Indeed, a continuing program of experimental evaluation is usually required to determine whether or not the errors experienced will be less than those required for the measurements to be performed using the range. The extent of the experimental evaluation depends upon the desired accuracies of the measurements to be made on the range and the possible need for official documentation of these accuracies.

The illuminating field over the test region will deviate from that predicted from calculations based upon a highly ideal range geometry because of reflections from various mounting structures, cables, obstacles on or near the range surface, and from irregularities in the range surface itself. In addition radio-frequency interference is often a cause of difficulty.

It is convenient to investigate separately that part of the field which is incident from the general direction of the source antenna and that which arrives from wide angles with respect to a line drawn from the center of the test region toward the phase center of the source antenna. The former is often referred to as the near-axis *incident field,* and the latter as the *wideangle incident field.* The near-axis incident field may be determined from a field-probe measurement over a plane perpendicular to the range axis and coincident with the expected location of the test antenna. This plane is called the *test aperture.*

6.2 Field-Probe Measurements over Test Aperture. Prior to making field-probe measurements, it is necessary to align the axes of the positioner. For example, the vertical axis (ϕ axis in the case of an azimuth-over-elevation positioner, or the θ axis for an elevation-over-azimuth positioner, including the model tower, can be aligned by use of a clinometer or a precision level. In the case of the model tower a plumb bob can also be used. The horizontal axis can be aligned optically. For the model tower a scope can be mounted in the tower head. In this way the scope's optical line of sight corresponds to the horizontal axis (ϕ axis) of the model tower, and thus alignment can be checked. Once the axes have been aligned, the field probe can be mounted. The field probe consists of an antenna, usually a pyramidal horn or a log periodic dipole antenna, mounted upon a carriage or track such that it can be moved along an I-beam support. The entire unit is mounted on an appropriate positioner in such a manner that the incident field may be sampled as a function of position over the test aperture. A sketch of a typical field probe is shown in Fig 23 [1, pp 14.42–14.63]. The motion of the probe antenna is remotely controlled, and by the use of a synchro system or potentiometers, which indicate the instantaneous position of the probe antenna, a continuous automatic plot of the received field amplitude as a function of position can be made. These data are usually presented as decibel plots.

The probe antenna should be moderately directive in order to discriminate against wide-angle reflections and also reflections from the probe-mounting structure. As an added precaution an absorbing baffle should be placed behind the probe antenna. The *E*- and H-plane beamwidths of the probe antenna should be such that a major portion of the range surface is contained within its half-power beamwidth. A useful criterion which ensures that this condition is met is given by

$$\theta_3 \geq 2 \tan^{-1} \left(\frac{4h_r}{R} \right)$$

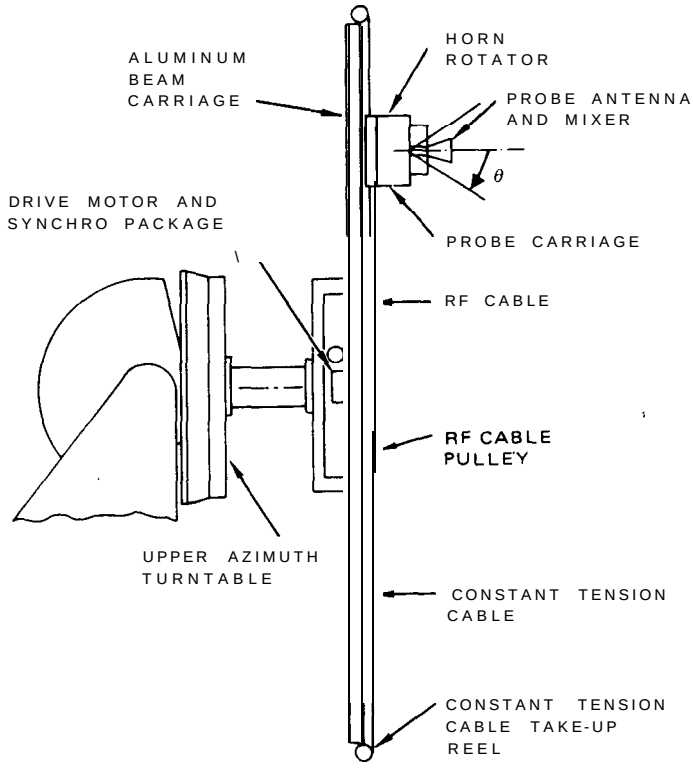

Fig 23
Typical Field-Probe Mechanism

where h_r is the height of the test antenna, R is the range length, and θ_3 is the 3 dB beamwidth of the probe antenna.

A means of rotating the probe antenna about its axis shall also be provided so that two orthogonal polarizations, vertical and horizontal, may be measured. This is necessary because the range might be used with either polarization, and hence the incident field should be probed for both cases. It is good practice to measure also the cross-polarized components for both orientations of polarization of the source antenna, because not only may the source antenna itself generate a cross-polarized component, but some depolarization usually accompanies the reflection of waves from irregular or curved objects.

One of the principal objectives of the probe measurement is to determine the source of the reflections so that remedial action can be taken. If there is only one principal source of reflection contributing to the incident field, it is a rather simple matter to locate it from the measured data. Suppose that the direct wave is incident upon the aperture from a direction perpendicular to the plane of the aperture and the reflected wave arrives at an angle θ with respect to that direction. From Fig 24 it is seen that an interference pattern over the test aperture results. The spatial period P of the resultant waveform is given by

$$P = \frac{\lambda}{\sin \theta}$$

If the probe antenna were moved along a line in the test aperture which is formed by the intersection of a plane containing the directions of propagation of both the direct and the reflected waves and the plane containing the test aperture, then the measured field should be that depicted in Fig 24. However, if the

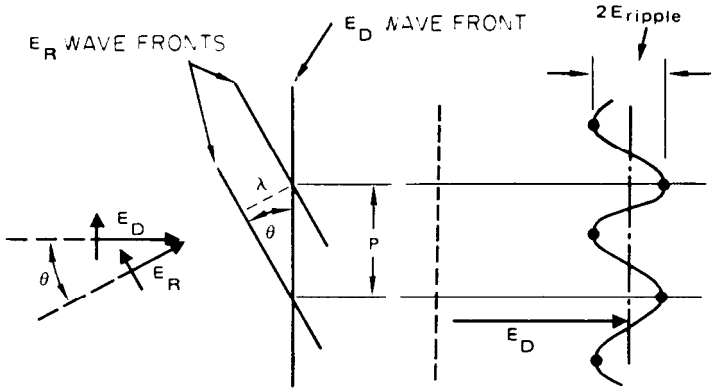

Fig 24
Spatial Interference Pattern Due to a Reflected Wave

probe were rotated to any other orientation in the test aperture, then the spatial period would increase and have a value given by

$$P' = \frac{\lambda}{\sin\theta\cos\alpha}$$

where α is the angle between the probe path which yielded the result shown in Fig 24 and the new orientation. From these results it is seen that by probing the field over radial lines centered on the test aperture the direction from which the reflected signal arrives can be determined. Furthermore the peak-to-peak amplitude of the interference pattern yields a measure of the relative amplitude of the reflected wave E_R to the direct wave E_D. This ratio, expressed in decibels, is given by

$$\frac{E_R}{E_D}(\text{dB}) = 20\log\left[\frac{-1 + \text{antilog}\ (a/20)}{1 + \text{antilog}\ (a/20)}\right]$$

where σ is the difference in decibels between the maxima and minima of the measured pattern. The ratio $E_R/E_D(\text{dB})$ is plotted as a function of σ in Fig 25. Generally there are several reflected waves, with the reflected wave from the ground being the predominant one. For this case the measured field is a composite spatial distribution. Usually, however, the Principal sources of reflection can be located from the data.

6.3 Incident-Field Measurements Near the Range Axis on an Elevated Range. For elevated ranges, if the amplitude distribution has excessive variations, then some means of either absorbing the reflected energy or redirecting it from the test aperture shall be employed. In the case of reflection from the range, surface diffraction fences usually are very effective. The field probe can be used in the adjustment of the position, size, and orientation of the fences.

Another important use of the field probe is in the alignment of the source antenna. Since the source antenna is directive, any misalignment might yield an excessive asymmetrical amplitude taper in the illumination field over the test aperture. The alignment procedure shall be performed in both the azimuthal and the elevation planes, which corresponds to horizontal and vertical motions of the field-probe antennas, respectively. A convenient method of alignment is as follows. First, from a horizontal traverse of the probe antenna two equal power points are located for reference. The source antenna is then adjusted until the geometrical mean of these two equal-power points coincides with the center of the test aperture. Next the source antenna is rotated 180" about its axis and again checked for alignment. If the source antenna is still aligned, it indicates that the beam axis of the source antenna is coincident with the roll axis of the source antenna's positioner. If it is not, then

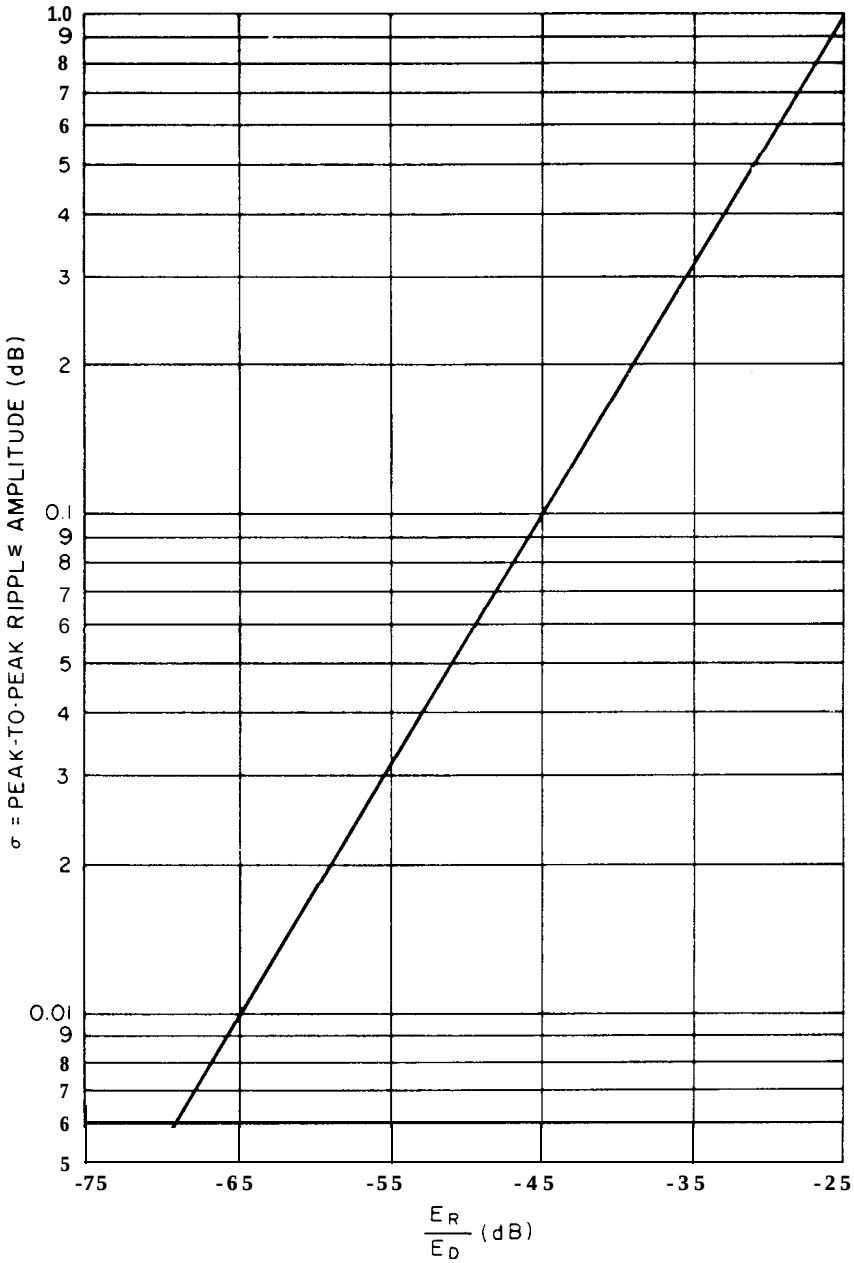

Fig 25
Amplitude of Spatial Interference Pattern Versus Ratio of Reflected-Signal to Direct-Signal Strengths for an Aperture-Probe Cut in the Plane of E_R and E_D

corrective measures shall be taken, that is, the source antenna shall be reoriented with respect to the positioner mounting surface or, perhaps, in the case of a reflector antenna its primary antenna may need repositioning. Then the alignment procedure is repeated until the beam of the source antenna is symmetric about the roll axis of its positioner and at the same time is properly aligned with respect to the test aperture. This entire procedure is repeated for the vertical plane.

Once the effect of reflections has been reduced to the point that the amplitude distribution over the test aperture is found to be satisfactory and the alignment of the source antenna has been achieved, it is desirable that the relative phase over the test aperture be measured. In the absence of reflections, the phase distribution over the test aperture is primarily a function of the spacing between source and test antennas. Therefore, for the elevated range, this measurement is one of precaution rather than necessity.

The one remaining characteristic of the incident field which may be measured is its polarization. If the field-probe antenna is equipped with a rotator as is the one depicted in Fig 23, then polarization patterns can be measured at various positions in the test aperture (see 11.2.2). It should be pointed out that the alignment of the source antenna shall be completed before this measurement can be made.

6.4 Incident-Field Measurements Near the Range Axis on a Ground-Reflection Range. Unlike the elevated range, the ground-reflection range is designed to utilize the reflection from the range surface in order to produce a broad interference pattern in the elevation plane. The source antenna shall be positioned so that the broadest maximum of this pattern is centered upon the test aperture. This is accomplished by first locating the source antenna at the position Predicted under the assumption that the reflection coefficient of the range surface is equal to minus one, that is, $h_t = \frac{\lambda R}{4h_r}$. Then field-probe measurements are made along the intersection of the elevation plane and the test aperture. The source-antenna height is adjusted until the field in the vertical direction is symmetrical about the center of the test aperture. This should be done for both polarizations since the optimum height for each polarization can be different. The orientation of the source antenna in the elevation plane usually does not have to be corrected in the case of ground-reflection ranges since a small change in the source-antenna-beam pointing direction in elevation has little effect on the desired interference pattern produced at the test aperture. In the horizontal plane, alignment can be accomplished by use of the same procedure as outlined for the elevated range.

In addition the test aperture should be probed and, as in the case of the elevated range, sources of extraneous reflections should be located. If necessary the reflecting objects should be removed, or absorbing baffles and reflecting screens used, to minimize the reflected energy reaching the test aperture.

For polarization measurements it is necessary to orient the field probe so that the linearly polarized probe antenna is pointing toward the phase center of the array formed by the source antenna and its image (refer to Fig 8). As previously pointed out, this is not at the range surface but rather at an approximate height given by

$$h_t' \approx \frac{1 - |\Gamma|}{1 + |\Gamma|} h_t$$

where $|\Gamma|$ is the magnitude of the reflection coefficient of the range surface. $|\Gamma|$ can be taken to be simply the amplitude ratio of the specularly reflected wave from the range surface to the direct path wave as taken from Fig 25. Once this orientation has been achieved, then polarization patterns at various positions in the test aperture can be made.

If the ground-reflection range is to be used for circular polarization, then it is highly desirable that the polarization of the source antenna be adjustable so that precision adjustments in the polarization of the incident field can be made. By varying the relative ampli-

tude and phase of the vertical and horizontal field components of the source antenna, it is possible to compensate for the effects of unequal reflection coefficients exhibited by the range surface for the two field components. By transmitting the proper elliptical polarization, the axial ratio of the incident field can be adjusted to less than 0.1 dB at any given position in the test aperture. It should be pointed out that the characteristics of the range surface may change as a function of time and frequency of operation.

6.5 Wide-Angle Incident-Field Measurements

6.5.1 ***General.*** The two most commonly used techniques for the evaluation of wide-angle fields are the antenna-pattern-comparison method and the longitudinal-field-probe method. These methods can be used on either the elevated range of the ground-reflection range.

6.5.2 ***Antenna-Pattern-Comparison Method.*** The ***antenna-pattern-comparison method*** is based upon the premise that in the absence of any reflected or extraneous signals the measured azimuthal antenna patterns of a test antenna will be unchanged with small changes in the test antenna's position with respect to the source antenna. If, on the other hand, antenna patterns are measured for several different positions of the test antenna and the patterns exhibit changes from position to position, then this indicates the presence of reflected or extraneous signals.

To illustrate the effect that reflected waves may have on the measured pattern of a directive antenna, consider the situation depicted in Fig 26. A reflected wave is incident from a direction θ degrees from the test antenna's beam axis. Usually the level of wide-angle reflected waves is at least 30 dB below the level of the direct wave. When the test antenna is oriented so that its major lobe is pointing toward the source antenna, the reflected wave is received on a side lobe. The effect upon the measured level of the major lobe is negligible. However, if the antenna is rotated such that the major lobe is pointing toward the direction of the incoming reflected wave and a side lobe is pointing toward the source antenna, then the apparent level of the side lobe can deviate significantly from that obtained in the absence of the reflected wave. The actual deviation depends upon the relative amplitudes and phases of the direct and reflected waves. Thus if the azimuthal pattern of the test antenna is measured at several positions along the range axis, variations will occur in the resulting patterns because of the change in the relative path lengths of the two waves.

The antenna-pattern-comparison method then consists of recording the azimuthal patterns of a test antenna for enough different positions along the range axis so that the maximum excursions of the side lobe levels are obtained. It is convenient to record all the patterns on a single chart from which the apparent direction of the incoming wave and its relative level can be determined. An example of such a measurement is shown in Fig 27. Note that there is a variation of approximately 12 dB in the patterns at an azimuth angle of 120°. If the direct and major reflected waves were both received on the side lobe, this would mean that the reflected wave is 4.5 dB below the level of the direct wave. However, the reflected wave was received on the main beam and the direct wave on the side lobe. Since the variation occurred approximately 30 dB below the peak of the main beam, the reflected wave is at least -34.5 dB relative to the level of the direct wave. The graph shown in Fig 28 is useful in the determination of the reflected signal levels from measured data. Of course it takes many measurements to ensure that the greatest variation is obtained; indeed, it is possible to miss the worst case conditions.

Another useful antenna-pattern-comparison measurement can be made by measuring two azimuthal patterns about the same center of rotation with the test antenna rotated 180° about its beam axis between cuts. Also for convenience, the direction of travel of the abscissa on the chart recorder can be reversed and the synchros appropriately adjusted so that, in the absence of reflected or extraneous signals, the recorded pattern should be identical with that of the first cut. If there are reflections, the patterns will not be identical unless the reflections are perfectly symmetrical about

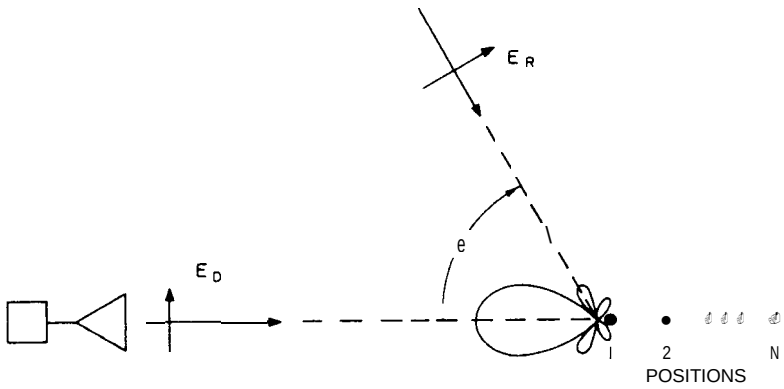

(a)

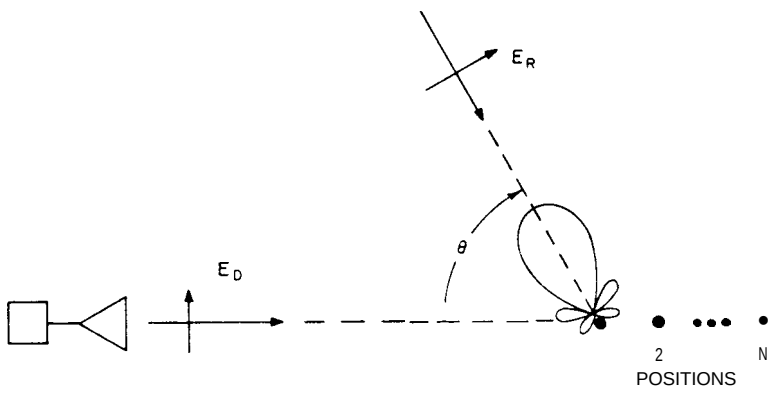

(b)

Fig 26
Illustration of how the Side-Lobe Level of the Test Antenna Is Affected During Antenna-Pattern-Comparison Measurement
(a) Test **Antenna Pointing Toward Source.**
(b) Side Lobe Pointing Toward Source

the range axis. From these data one can deduce the apparent direction from which the reflected signal is incident upon the test antenna.

On some ranges, particularly where model towers are used, it might be desirable to make the antenna-pattern comparison by taking identical conical cuts at symmetric azimuth-Pointing directions with respect to the range axis. For example, the azimuth positioner can be rotated to an angle of θ degrees, and the conical cut can be made by rotating the head of the model tower. Then the azimuth positioner can be rotated to $-\theta$ degrees. It will be necessary to also rotate the test antenna 180° about the head axis to achieve the same starting point. After appropriately resetting the synchros, the pattern is repeated and a comparison is made.

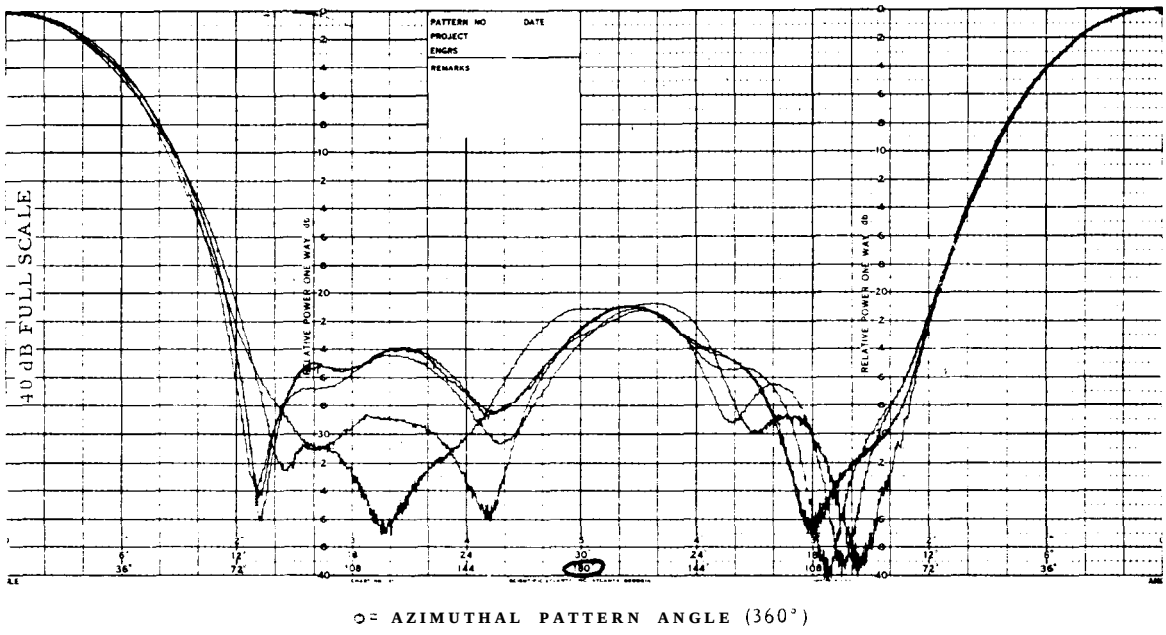

Fig 27
Azimuthal Pattern Comparisons (360" Cuts) for Incremental Longitudinal Displacements of the Center of Rotation

6.5.3 ***Longitudinal-Field-Probe Methods.*** An alternate method of determining the level and direction of reflected waves is by use of the ***longitudinal-field-probe method.*** Unlike the field probe previously described, which was pointed in a direction transverse to its path of travel, the longitudinal field probe is oriented with its beam axis along its direction of travel. The length of travel of the probe antenna should be great enough to detect maximum and minimum points of the interference pattern formed by the direct and reflected waves. The approximate longitudinal distance P_{ℓ} between the points of constructive interference between the direct and reflected waves is given by

$$P_{\ell} = \frac{\lambda}{2 \sin^2(\theta/2)}$$

where θ is the angle between the direction to the source antenna and the direction from which the reflected wave is approaching [1, pp 14.63–14.66]. Thus by measuring the period of the amplitude variation of the received signal, the approximate direction to the source of the reflected signal can be determined for one reflected wave.

The level of the reflected signal relative to the direct wave can be approximately determined from the peak-to-peak variation in the measured data. The radiation pattern of the probe antenna shall be taken into account when the data are analyzed. To obtain a more complete determination of reflected or extraneous signals it is usually necessary to make longitudinal probe measurements along several different azimuthal directions.

6.6 Evaluation of **Anechoic** Chambers. Anechoic chambers are designed in such a manner that the uniformity of the illuminating field

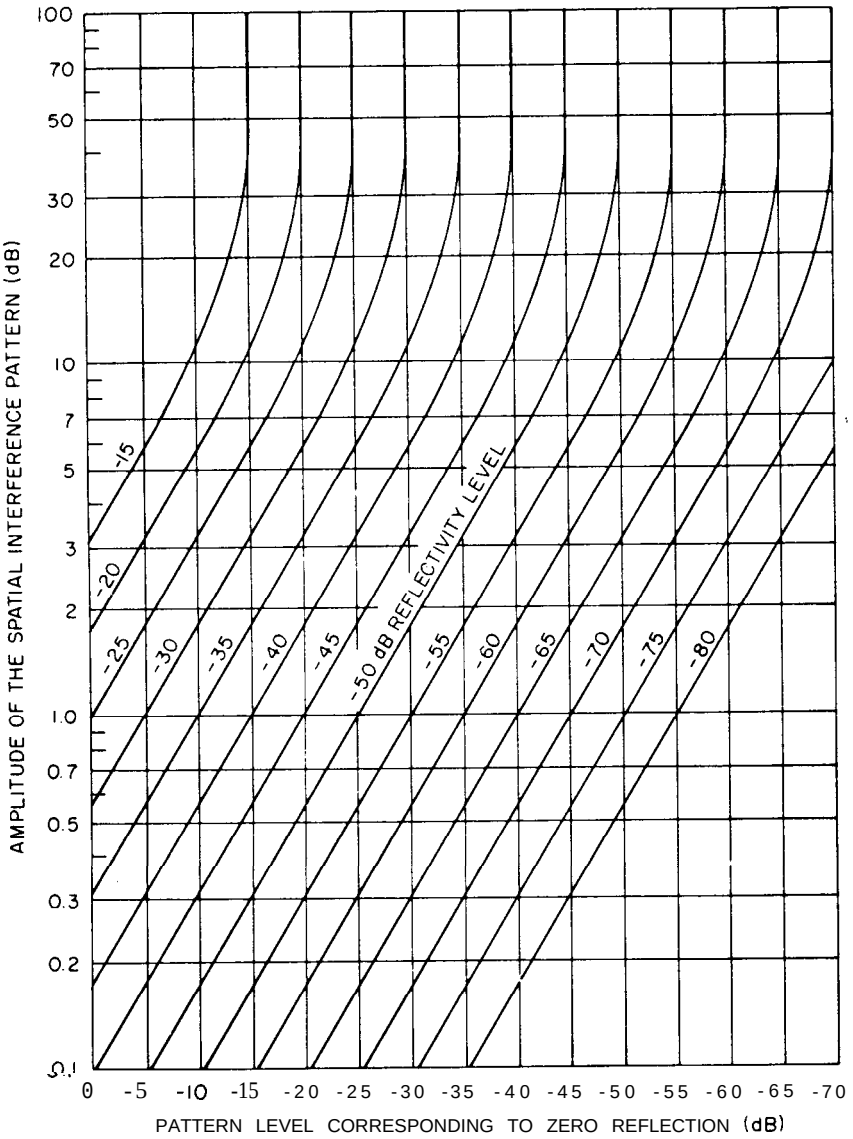

NOTE: The curves plotted as straight lines below the 5.7 dB ordinate value are actually very slightly concave upward. All curves are correct as plotted above the 5.7 dB ordinate value.

Fig 28
Amplitude of Spatial Interference Pattern for a Given Reflectivity Level and Antenna-Pattern Level

over a given region within the chamber meets certain specifications. This region is usually referred to as the quiet zone and is the region in which the test antenna is to be placed. The actual size of the quiet zone may, for example, be specified in terms of the direct wave from the source antenna, that is, by specifying the amplitude and phase variations of the direct wave from the center of the quiet zone to the edge of the zone. Then the "quietness" of the zone is dependent upon the magnitudes of the reflections from the walls, floor, and ceiling

of the chamber. There is no standardized figure of merit for anechoic chambers. What is done is to establish the ratio of an "equivalent" reflected wave, that is, the aggregate effect of all reflected waves incident upon the probe antenna used to test the chamber, to the direct wave. This means that the directivity of the probe antenna will certainly affect the results obtained [21].

When an anechoic chamber is to be used for antenna-pattern measurements, usually the chamber is evaluated by means of the *free-space voltage-standing-wave-ratio (VSWR) method* [21],[22]. This method is similar in principle to the field-probe method previously described, except that instead of fixing the orientation of the probe antenna normal to the direction of motion, it is made adjustable as shown in Fig 29. This allows for a more directive antenna to be chosen for the probe. Usually a standard-gain antenna is used for this purpose. For a given orientation the probe antenna is moved continuously along a transverse line, although other directions of travel may be chosen. The linear motion of the antenna is coupled to the recorder so that the interference pattern may be recorded. The graph of Fig 28 can be used to determine the ratio of the reflected to the direct wave, provided the component of the direct wave received is larger than that of the reflected wave [21]. This entire procedure is repeated for various orientations of the probe antenna. The orientation for which the maximum ratio is obtained represents the direction from which the equivalent reflected wave approaches. Measurements should be made over several transverse directions, including one horizontal and one vertical. Also all measurements should be made with both vertical and horizontal polarization.

The wide-angle incident field, including the reflected signal from the rear of a chamber, can be determined from a longitudinal probe (see 6.5). For this measurement the probe carriage is oriented parallel to the axis of the chamber, thus providing the longitudinal travel for the probe. Again, free-space VSWR measurements are made as a function of the angle of orientation of the probe antenna with respect to its direction of travel. In this manner the entire rear portion of the chamber, including the critical points such as corners can be evaluated.

As previously mentioned, the results of the measurements depend upon the radiation pattern of the probe antenna. One way to avoid this effect is by the use of an isotropic probe antenna. For example, the probe can be a tridipole antenna consisting of three mutually orthogonal dipoles which are designed in such a manner that the antenna pattern is essentially isotropic. Such antennas have been designed which respond equally. well (within ± 1 dB) to signals arriving from any direction and with arbitrary polarizations. Of course great care shall be exercised in the design of the carriage used to position the probe in order to avoid the introduction of additional reflections in the chamber. The advantage of this type of probe is that complete reflectivity information can be obtained with only three orthogonal scans per frequency required. In general this system yields higher reflectivity levels than that obtained with a directional antenna since the equivalent reflected wave is composed of all the reflected waves from all surfaces.

This technique is most useful when the antennas to be tested in the chamber are quasi-isotropic. If on the other hand the test antennas are moderately or highly directive, reflections from the rear of the chamber will be suppressed. For these cases the use of a directive probe for the free-space VSWR measurement may be more appropriate.

The antenna-pattern-comparison method has been used for evaluating anechoic chambers. This method is not recommended as the primary technique for evaluating a chamber since it is difficult to determine the maximum reflectivity levels [21].

7. Special Measurement Techniques

7.1 Modeling Techniques. Scale-modeling techniques are often used when the measurement of an antenna in its operational environment is impractical. This situation frequently exists for antennas located on large supporting

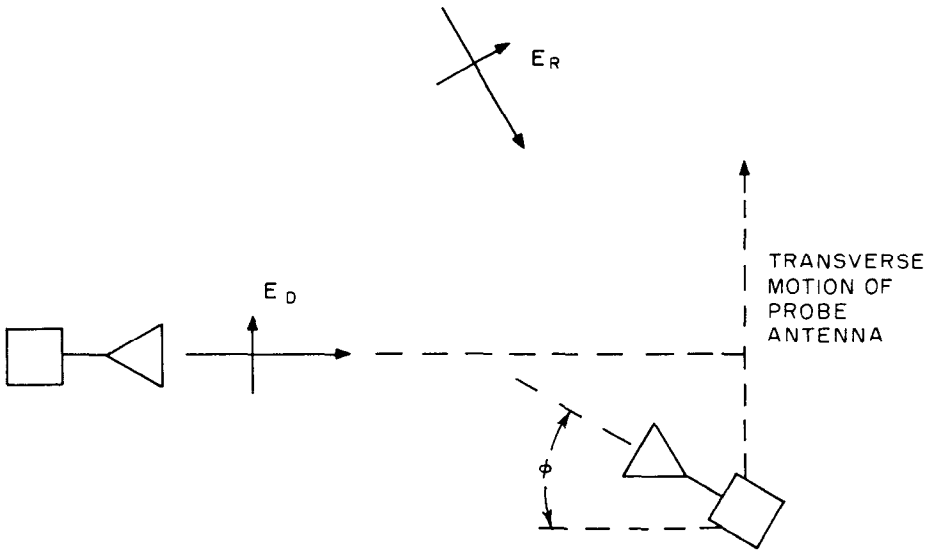

Fig 29
Geometry for Free-Space VSWR Method

structures, such as ships, aircraft, and large man-made satellites, which influence the properties of the antenna. In moving systems or changing environments, instability of the supporting vehicle or surrounding medium may compel an unreasonable amount of experimental data, which require statistical treatment. Another major situation, for which modeling is often used, is in development work requiring successive modifications which are costly due to the large size or, occasionally, the very small size of the final antenna system. Thus the main motives for modeling are to obtain greater experimental control over the measurements, or to obtain an economic advantage in the measurement program.

Generally the model is reduced in size from the full-scale antenna; but whether reduced or increased, the requirements [23]–[25] for exact simulation by the model are as follows:

(1) Linear dimensions of the model shall be $1/n$ times those of the full-scale antenna.

(2)' Operating frequency and conductivity of the materials used in the model shall be n times those of the full-scale antenna.

(3) Permittivity and permeability of the materials used in the model shall have the same values at the scaled frequency as at the original frequency.

In the preceding, n is an arbitrary number (generally, but not necessarily, greater than unity) which determines the scale of the model. Also in the preceding, the imaginary parts of the complex permittivity and complex permeability are included in the expression for conductivity [26]. More general forms of scaling, which permit additional parameters to be changed, are occasionally desired; these are described in the literature [27].

In a practical model it is usually not feasible to exactly satisfy the full set of requirements in the preceding list. However, for antennas that are not highly resonant the error will usually be small if good conductors such as copper or aluminum are used to simulate good conductors, and if low-loss dielectric materials of identical electric permittivity and magnetic permeability are used to simulate low-loss dielectrics. The principal problem is presented by poor conductors or lossy dielectrics. In such cases it is not always possible to obtain materials that satisfy the scale-modeling requirements.

In constructing a scale model, not only does the antenna need to be simulated, but also

those portions of the surrounding structures and environment which have an appreciable effect on the properties of the antenna. In many cases it is difficult to construct simulated surroundings due to the complexity of the electromagnetic environment. For example, when the antenna interacts with the earth, it has often proven to be impractical to accurately scale the highly variable and sometimes unknown properties of the soil. In such cases simplified models are employed. Good judgment is required in determining the extent to which one simulates the antenna's surroundings.

It is usually necessary to devise a means by which the scale model of the antenna alone can be tested independent of its environment to determine if it has the same electrical characteristics as the full scale antenna. One way of accomplishing this check is to build asimplified environment, such as a flat circular ground plane, to test the salient characteristics (for instance, radiation patterns) for the full-scale antenna. The simplified environment and antenna are then scaled.

If the results obtained using the scaled model of the antenna sufficiently duplicate those of the full scale antenna then the scaled model can be used in the scale model of the antenna environment.

NOTE: Usually a choke is required along the edge of the modelled circular ground plane to prevent currents from being excited on the rear side of the plate.

In the case of an input-impedance and pattern measurement using a scale model, all nearby antennas shall be included in the model and terminated in the appropriate impedances. Since the other antennas may operate at frequencies different from that of the modeled antenna, the impedances at the operating frequencies shall be scaled correctly. To obtain this information, the matching section may be terminated in a network equivalent [28] to the impedance measured on the scale model.

Special measurements on antennas which are electrically small, as is common at low frequencies, can often be made by quasistatic methods using electrostatic cages [29]. Here the charge induced by a known field strength is measured, allowing an equivalent area to be determined.

While the radiation pattern is usually the antenna characteristic of most concern in model measurements, other antenna properties of interest can also be reliably reproduced. If the exact scaling procedure described is followed throughout the antenna system, all fields are reproduced exactly in shape, both externally and within the feed line. Thus power gain, directivity, radiation efficiency, input impedance, mutual impedance, boresight error, and in general all properties dependent only on field ratios are preserved. If the modified scaling procedure is followed, efficiency and hence power gain will not be reproduced, but the remaining properties will be reproduced accurately enough for most purposes, providing that the antenna does not have extremes of current, charge concentration or mismatch. Certain antenna characteristics, such as the power level for high-voltage breakdown (see Section 18) and the noise temperature, (see 12.43) cannot be scaled because of the frequency-dependent nature of the mechanisms involved.

In the measurement of radiation patterns the feed cable may perturb the measured quantities appreciably. In that event the scale-model antenna may transmit from a battery-operated transmitter, or, alternately, the scale-model antenna may contain a receiver from which the demodulated signal can be removed by means of high-resistance wire leads which minimize the disturbance of the radio-frequency field [30]. Another approach is to use a semiconductor laser and transmit the signal via an optical fiber. The support for the model should receive particular attention if the pattern null structure is to be accurately determined.

In addition to the special problems of scale-model measurements referred to in this section, there are general procedures and precautions to be employed during any of the measurements. These procedures are essentially the same as those described in Section 8.

7.2 Antenna-Focusing Technique. For some test situations it is difficult or impractical to measure antenna characteristics using far-field-range techniques. A technique that can be used to measure the far-field antenna pattern at reduced ranges is that of focusing the

test antenna at the range at which the measurement will be made [16],[31]. This approach is limited to those test antennas which are provided with a means of changing their focus from infinity to a finite distance. This can usually be accomplished with phased arrays and reflector-type antennas. Considerable work has been done with paraboloidal reflector antennas, since they are the most common of the large antennas. The geometry for the use of ray optics in establishing the focusing of a parabola is shown in Fig 30. When the feed antenna is located at point *F*, the antenna is focused at infinity. By moving the feed to position *F'*, the rays are brought into a quasi-focus at *F"*. It is not a true focus since the reflector shape is paraboloidal rather than ellipsoidal, which is required for two finite foci.

The required distance ϵ that the feed shall be moved can be determined by ray tracing and is expressed approximately as

$$\epsilon \cong \frac{1}{R}\left[f^2 + \left(\frac{D}{4}\right)^2\right]$$

where *R* is the distance *OF"*, *f* is the distance *OF* and ϵ is the distance *FF'* as shown in Fig 30. Once the feed is moved to point *F'*, the antenna's radiation pattern is measured at a range *R*. After testing the feed is returned to its original position at point *F*. For ranges as short as $D^2/8\lambda$ the measurement will yield a fairly accurate description of the main lobe of the far-field pattern of the antenna focused at infinity; however, the side lobe description will be in error. An improvement can be made by making a fine adjustment of the feed about point *F'*. One approach is to adjust the position of the feed for a maximum depth of the first null. This yields a better description of the main lobe. However, if the power gain is measured on the focused antenna at range *R*, it will be low by several tenths of a decibel as compared to a far-field measurement. Another approach is to adjust the feed for the maximum power gain in the direction of the peak of the main lobe of the focused test antenna as measured at a range *R*. This will yield a slight improvement in the measurement of power gain over that which would be obtained using the maximum depth of the first null criterion. Despite these shortcomings this method has been found to be very useful.

7.3 Near-Field Probing with Mathematical Transformation. Another near-field technique for the determination of antenna characteristics is that of *near-field probing with mathematical transformation*. In this technique the complex (phase and amplitude) vector field is sampled over a well-defined surface. The measured data are computer processed to obtain an angular spectrum of plane, cylindrical, or spherical waves appropriate to the measurement surface employed. The angular spectrum is then corrected for the directive and polarization effects of the measuring probe, and far-field parameters such as power gain, relative pattern, and polari-

Fig 30
Geometry for Geometric Optics Approach to Focusing

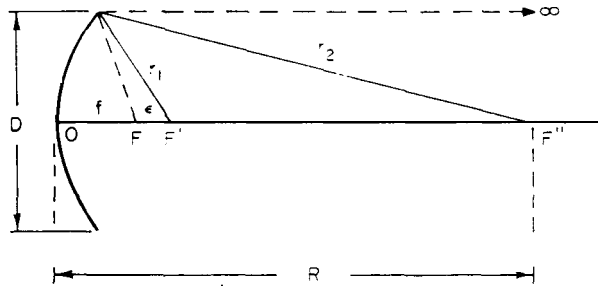

zation are calculated from the corrected spectrum. In the general theoretical formulation the field of the test antenna is represented by a superposition of basis fields [32], which are solutions to Maxwell's equations on the surface being used. These would be plane waves expressed in terms of complex exponentials for a planar surface, cylindrical waves expressed in terms of Bessel functions and complex exponentials for a cylindrical surface, and spherical waves expressed in terms of associated Legendre functions and spherical Bessel functions for a spherical measurement surface. The expression for the response function of the probe in terms of the same basis fields is obtained by fitting its complex vector-receiving pattern with the corresponding basis functions. The output voltage of the probe as it moves over the surface may now be expressed in terms of the probe response which is known, the basis fields of the test antenna, and the effect of the orientation and motion of the probe.

These ideas, as well as the concepts associated with measurement techniques and computations, can best be understood by referring to the example of measurements on a planar surface. Much of the work in near-field measurements has been done for planar measurements [32]–[35], and the concepts associated with cylindrical or spherical surfaces can be viewed as an extension of this more familiar case. For the case of the planar surface, the far-field response of the probe is denoted by s_{01} (K), where K is the x-y part of the wave vector k, $K = k_x e_x + k_y e_y$. $s_{01}(K)$ is a complex vector function, and its value for each value of K gives the response of the antenna to a plane wave incident from that direction. The magnitude of each component of $s_{01}(K)$ is identical with the far-field patterns of the probe, and $s_{01}(K)$ may therefore be determined from a conventional pattern measurement where phase as well as amplitude are measured. If P denotes the x-y position of the probe in the plane $z = d$, $t_{10}(K)$ the transmitting characteristic of the test antenna to be determined, and $\gamma = \pm k_z$, then the complex signal at the output of the probe is given by

$$V(P) = a_0 \iint [s_{01}(K) \cdot t_{10}(K) e^{i\gamma d}] e^{iK \cdot P} \, dk_x \, dk,$$

NOTE: In this section the time dependence is $e^{-i\omega t}$ (see 10.1).

The factors $e^{i\gamma d}$ and $e^{iK \cdot P}$ are the result of the motion of the probe, which in this case can be expressed quite simply as compared to the cases of cylindrical and spherical motions. The equation for $V(P)$ may be inverted to obtain one equation for the two components of $t_{10}(K)$ given by

$$s_{01}(K) \cdot t_{10}(K) = \frac{e^{-i\gamma d}}{4\pi^2 a_0} \iint V(P) e^{-iK \cdot P} \, dx \, dy$$

A required second equation is obtained by repeating the measurement with a second "independent" probe, which may be obtained by rotating a linearly polarized probe about its axis by 90°. From the two equations both components of $t_{10}(K)$ may be determined as well as the far-field parameters. For instance, the power gain is given by

$$G(K) = \frac{4\pi(\gamma/k)^2 |t_{10}(K)|^2}{1 - |\Gamma_t|^2}$$

where Γ_t is the antenna reflection coefficient.

The essential components of a measurement system are shown schematically in Fig 31. The scanner is a large mechanical structure which resembles an x-y recorder. It supports the probe and moves it over the plane to perform the measurements. The scanner shall be precisely made so that the probe maintains a planar motion ($\delta z \leq \lambda/100$) and the x–y position of the probe is accurately known. Data shall be measured at equally spaced points in both the x and the y directions over an area somewhat larger than the area of the antenna. The size of the area essentially determines the maximum angle to which accurate far-field data can be calculated through the relationship

$$\theta_m \simeq \tan^{-1} \frac{L_x - a_x}{2d}$$

where a_x and L_x are, respectively, the antenna dimension and scan length in the x direction.

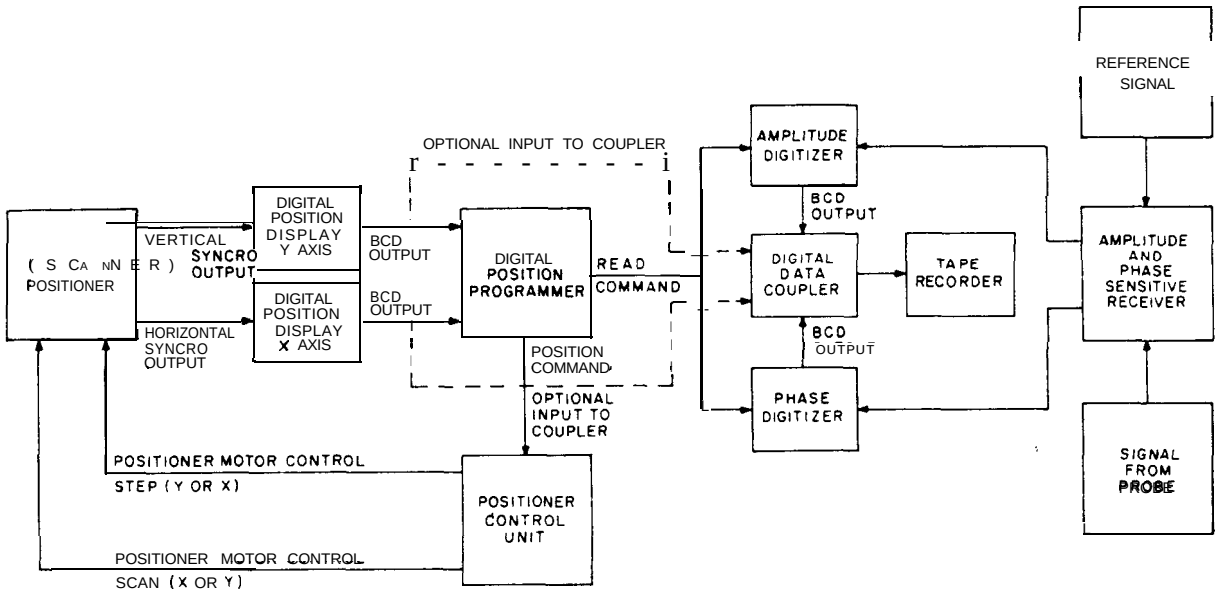

Fig 31
Block Diagram of Automatic Position and Measurement System

In general the spacing between data points should be slightly less than h/2. For broad-beam antennas the spacing may have to be as small as h/4, while for highly directive antennas it may increase to approximately 1 wavelength. Tests should be performed [36] on the actual antenna-probe pair to determine the optimum spacing and scan area as well as to verify that multiple reflections are small enough to be neglected.

The major computation is the integration required to evaluate $s_{01}(K) \cdot t_{01}(K)$, which is a two-dimensional Fourier transform of complex data. The fast Fourier transform is used to accomplish this integration with great efficiency [37].

Planar near-field techniques have been used for a variety of antennas at frequencies from about 1 GHz to 65 GHz. The lower frequency limit is due primarily to the effectiveness of absorbing material and the beamwidths of antennas, while the upper limit is due to the accuracy of positioners. In general the planar technique works very well for directive antennas, and the errors are largest for angles close to $\pm 90^\circ$ from the normal to the measurement plane. If there is significant energy at these wide angles, a prohibitively large scan area may be required. It is for such cases that the cylindrical or spherical scan surfaces are more attractive.

For the cylindrical scan surface [38] the theory and computations are somewhat more involved than for the planar case. The major computations can still be performed using the fast Fourier transform, and compensation for the directive effects of the measuring probe is still included. A cylindrical scan surface may be obtained by a onedimensional motion of the probe plus a rotation of the test antenna on an azimuth positioner. This reduces the complexity of the scanner, but will increase the amount of microwave absorber required.

When a spherical scan surface is used, the mathematics become much more involved [39]-[41], and while the fast Fourier transform can still be used for a large part of the computations, there still remains a sizable effort to obtain far-field parameters from measured data. A complete probe correction

can only be obtained for certain ideal or simple probes. In principle this scan surface is best suited to broad-beam antennas, and a "self-scan" is possible by mounting the test antenna on a two-axis positioner and leaving the probe fixed. This is especially attractive for large antennas already mounted on a positioner, since the scan surface could be generated without additional hardware.

7.4 Swept-Frequency Technique. When the antenna patterns of very broad-band antennas, such as the log-periodic types, are measured at discrete frequencies over their operating bands, it is possible to miss significant variations in their amplitude patterns [42]. These variations are typically frequency dependent and narrow band. They are often referred to as "anomalies" in the pattern. Usually it is possible to optimize the design of these antennas in such a way that the "anomalies" are removed [43],[44].

It is necessary to employ the swept-frequency technique in order to determine the frequencies at which the "anomalies" occur. Principal plane cuts are usually all that are required, and for linear polarization these would be in the ***E*** plane and the ***H*** plane of the test antenna. For the measurement one of the angular space coordinates of the test antenna is fixed, while the other is varied incrementally over the angular range of interest. For each angular increment the amplitude of the received signal is recorded continuously as the frequency of operation is swept over the operating band of the test antenna. All the curves are recorded on the same chart so that a family of curves is obtained. If the gain and amplitude patterns of the test antenna were ideal, that is, invariant under a change in frequency, then the measured family of curves should consist of approximately parallel straight lines with a -6 dB per octave slope on a log-frequency scale, as predicted from the Friis transmission formula. To obtain such a result, the antenna range with its instrumentation would also have to be ideal.

If the measurements are made on a good free-space range for which an optimum broad-band source antenna and a receiving system with an approximately flat frequency response are chosen, then good results can be obtained. The curves shown in Fig 32 are typical results.

Frequency-dependent reflections and an insufficiently flat frequency response of the instrumentation are the principal sources of error. If the response of the instrumentation is known, then corrections to the data may be accomplished. There is an alternate approach that may be employed. This method is basically a swept-frequency gain-transfer measurement. A single swept-frequency measurement is made using a reference antenna, and the data are stored. Then all data taken on the antenna under test are electronically compared to the response of the reference antenna. It is the difference between the response of the reference antenna and that of the test antenna that is recorded. This can be accomplished by the use of a data normalizer or by use of an on-line minicomputer. The relative amplitude pattern of the test antenna can be obtained for any given frequency in the band by plotting the relative levels for each increment of angle as a function of angle.

The reference antenna should have an amplitude pattern similar to the antenna under test, so that the response to reflections on the range is about the same for the reference antenna as for the test antenna. In this way the effect of reflections tends to be removed. Obviously, as the test antenna is rotated away from boresight, the error due to reflections increases. Note that it is possible to use the test antenna itself as the reference antenna. This results in the first curve being a straight line.

If the measurements are made in a tapered anechoic chamber, it is necessary to ensure that the source antenna is sufficiently close to the apex of the chamber so that deep nulls do not appear in the illumination field (see 4.5.4). It is advisable that the swept-frequency technique be used to check the position of the source antenna.

The swept-frequency technique is particularly well suited to the measurement of cross polarization in the far field of an antenna [45]–[46].

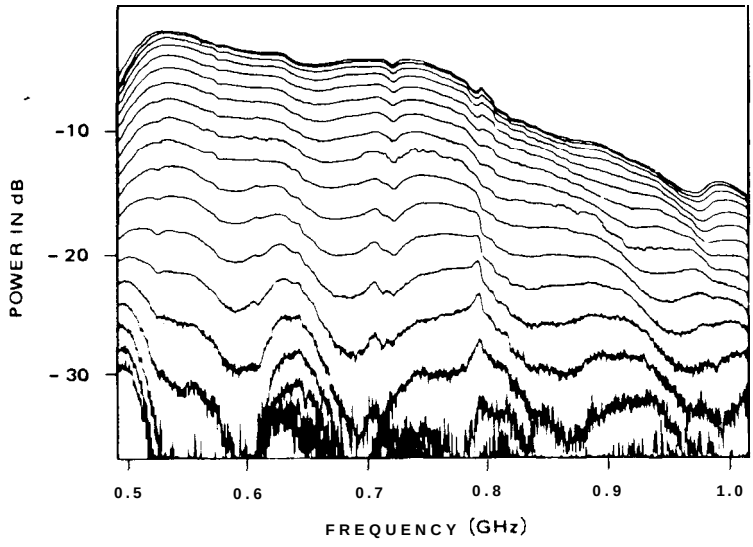

Fig 32
Amplitude Pattern of a Broad-Band Antenna Taken as a Function of Frequency with Angular Coordinate Taken in 5" Steps. Top of Line Is Broadside Case.

The reason for this is that cross polarization often is generated in mechanically complicated support structures in which a variety of electrical resonances can exist, thus producing scattered radiation the amplitude of which varies rapidly with frequency. It should be noted that the relevant frequency range need not be great if the antenna structure is large in wavelengths.

Power-gain measurements can also be performed as a function of frequency [47]. Such methods are discussed in 12.2.2 and 12.3.1.

7.5 **Indirect Measurements of Antenna Characteristics. The** performance of a reflector antenna is principally determined by the mechanical accuracy achieved in its construction. It is, therefore, possible to measure the actual surface of a reflector and, from that information, to compute the electrical performance of the antenna. Moreover, such a technique can be used as a diagnostic tool for the adjustment of the reflector surface to within acceptable tolerance bounds. In general a measurement accuracy of at least one twentieth of the shortest wavelength of operation is desirable.

For some applications analytical photogrammetric triangulation [48] can be used to measure the surface of reflector antennas. This method utilizes two or more long-focal-length cameras that take overlapping photographs of the surface to be measured. The surface is uniformally covered with self-adhesive photographic targets the images appearing on the photographic record as shown in Fig 33. A least-square triangulation process is used in which two-dimensional measurements of the images of the targets are processed simultaneously to generate a unique set of three-dimensional coordinates for each discrete target. Accuracies of the order of one part in 20 000 to 100 000 of the diameter of the reflector, depending upon the extent of the measurement procedure, are attainable.

For large reflector antennas operating at millimeter wavelengths the photogrammetric technique may not be sufficiently accurate to adequately predict the antenna's performance characteristics. Another method that can be used is that of precise range measurements. As an example of the accuracy demanded of such range measurements, a 65 meter antenna designed to operate at a wavelength of 3.5 mm

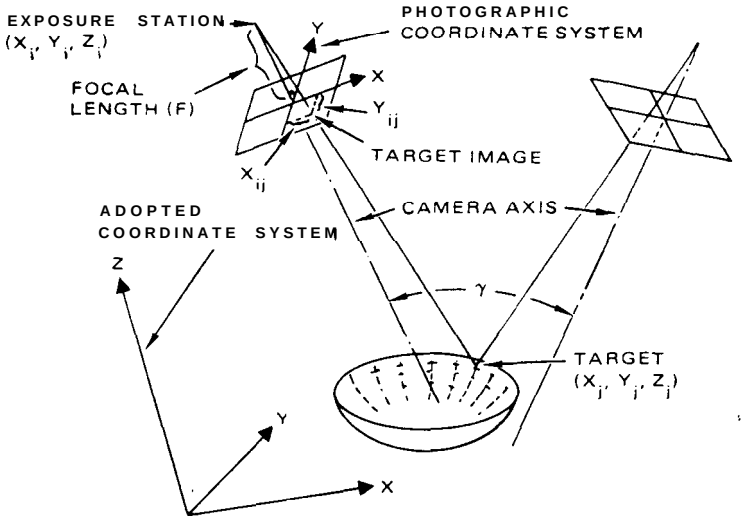

Fig 33
Schematic Illustration of Analytical **Photogrammetric** Triangulation

[49] requires over 3000 points on the surface to be set to an accuracy of ± 0.1 mm. This accuracy may be achieved by range measurements from two fixed points, such as the focus and vertex of the parabolic reflector. These range measurements, over distances from a few meters up to about 60 meters, shall be made rapidly, preferably using an automated system. A modulated laser beam can be used for this purpose [50]. The surface of the reflector is covered with targets (small optical corner cubes) in a manner similar to that shown in Fig 33. The laser beam is directed to the targets by means of programmable mirrors. The entire measurement procedure can be controlled by a small digital computer. The phase of the returned signal is measured with respect to a reference. The phase shift is proportional to the total distance traversed. If the distance and modulation frequency are such that the phase is shifted more than one cycle, an ambiguity will occur. This can be resolved by a crude knowledge of the distance or by using a dual-frequency system. An accuracy of ± 0.08 mm at ranges up to 60 meters has been achieved using this technique [50]. This technique has been successfully used on very large reflectors [51].

For high-precision reflector surfaces it is possible to measure very accurately the curvature of the surface at a point by use of a device that contacts the surface at three points and has a precise depth transducer at its center (located over the point to be measured). The method can be illustrated by reference to Fig 34. The curvature ***K*** of the curve S is given by

$$K = \frac{d\theta_P}{dS}$$

where θ_P is the angle that the tangent at point P makes with the x axis, and S is a length of arc. The angle θ_P can be obtained by integration, that is,

$$\theta_P = \int_0^{S_P} K \, dS$$

Since sin θ_P is the derivative of the y coordinate with respect to the arc S, then

$$\mathbf{Yn} = \int_0^n \sin \theta_n \, dS$$

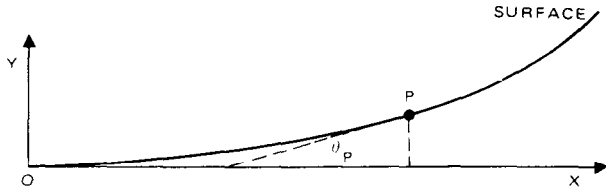

Fig 34
Geometry Used to Relate the Coordinates of a Point on the Surface of a Reflector to the Measured Curvature

Thus performing the two integrations one can obtain the coordinates of each point along the curve.

By making the three contact points wheels, the device can be rolled along various radii of the reflector, continuously sampling the curvature. An accuracy of 0.05 mm has been achieved by use of this method [52].

After the antenna has been set as accurately as possible, it may deform as it moves into position or *as* the ambient temperature changes. A knowledge of these deformations permits pointing corrections to be made and may also suggest ways of improving the performance of the antenna. Various instruments have been constructed for measuring these deformations [53]–[55].

8. Antenna-Range Operation

It is highly desirable that a set of standard operating procedures be developed for an antenna range. These procedures should be documented in an operations manual. The contents of the manual will be determined to a large degree by the mission of the range. Certainly a range developed for a single function *requires* much less documentation than does a multifunction range. The manual should be complete enough so that new personnel can operate the range with a minimum of assistance.

The manual might include but not be limited to the following

(1) *General information.* General information concerning the methods for antenna testing, description of the range, coordinate systems, and lists of references including appropriate customer specifications and professional standards should be contained in this section.

(2) *Range-ecalua tıon techniques.* Standard procedures for the evaluation of the antenna range should be developed and documented (see Section 6). Included in the documentation might be a general description of the recommended methods, the instrumentation required, detailed procedures, sample data, and methods of data interpretation. Sometimes this material is contained in a separate document and is simply referenced in the operations manual for the range. An important part of the evaluation of the range, which should be included in the manual, is the alignment of the axes of the positioner and the boresighting of the source antenna as discussed in 6.2-6.4.

If the data indicate excessive reflections, then suggestions for the corrective action to be taken should be given. For elevation ranges the adjustment of the position and height of diffraction fences might be required, or if a single reflecting object is located, then it should be removed, or steps taken to redirect the reflected energy away from the test antenna.

(3) *Standard measurement setups.* For each type of measurement that is repeatedly made on the range a standard measurement setup should be specified. For example, in the case of antenna-pattern measurements, the documentation should include a procedure for the selection of the positioner, transmitter, source antenna, receiver, recorder, and data-processing

equipment. In addition it should provide a means of determining the required spacing between source and test antennas and their heights. If scale models are used, there should be a procedure for the selection of the scale factor and construction technique (see 7.1). When vehicles, buildings, or other structures on which the antenna is mounted are to be modeled, it is necessary to decide the extent of the modeling. For example, if a VHF antenna is located near the cockpit of an aircraft, the interior of the cockpit may have to be modeled quite accurately; whereas, if the antenna were mounted on the tail section of the aircraft, the cockpit area probably would not have to be modeled so accurately.

If other antennas are located on the structure, they must also be included in the model and appropriately electrically terminated, a fact that should be included in the manual, as well as the method of mounting the model on the positioner. The method of feeding the model antenna should also be discussed.

(4) *Standard operating procedures.* A step-by-step procedure for equipment operation should be provided including warm-up times and any calibration of components that is required. The following considerations should be discussed. The stability of the equipment ought to be checked prior to making any measurements. Repeatability of measurements is most important. For example, if it is relative amplitude measurements that are to be made and a polar recorder is employed, then a θ-cut and an ϕ-cut should be recorded and for each case allowed to retrace four or five times. Each retrace should fall exactly on top of the previous patterns. If they do not, corrective action should be taken.

If the antenna under test is known to have a symmetrical pattern, then its symmetry should be tested at the outset. This can be accomplished by recording a pattern about the plane of symmetry. Again corrective action can be taken if the resulting pattern so indicates.

A cursory check of the pattern range using the antenna-pattern-comparison method (see 6.5) should be included in the procedure. For the case of a production range which has high usage, a set of two patterns may be all that-is required. For example, if a model tower is used, a 90” conical pattern recorded on the right side of the tower should be identical to one taken on the left side.

The operating procedure should indicate what constitutes a complete set of data. For example, when conical cuts are made for antenna-pattern measurements, what will be the maximum number of increments of θ to be taken? Perhaps both a complete set and a partial set will be defined.

There shouid be a continuous check of the equipment and range performance during the recording of a complete set of data. It is good practice to monitor the transmitted signal during the measurement of a pattern set.

It is also good practice for a set of crossover patterns to accompany each set of conical patterns. These are obtained for a set of conical patterns by recording an extra set of θ cuts with ϕ = 0” and ϕ = 90” as reference patterns. For each conical pattern (ϕ cuts) there will be two crossover points on each of the reference patterns. As each conical cut is recorded, the appropriate crossover points are marked with a dot or a small X on the reference patterns. These points should fall on the reference patterns. If they deviate from the reference pattern by a specified amount, corrective action should be taken.

If the range is equipped with an automatic integrator, positioner programmer, or any data-processing equipment, then the appropriate calibration procedures should be detailed as well as the operating instructions.

A method of identification of patterns is essential to the operation of an antenna range and should be described in the operation manual. The conditions of the measurement should be written on each pattern. Usually for each set of patterns a cover sheet is prepared which contains the general information and a sketch of the antenna under test along with a code that designates the particular pattern set. For this case only the polarization, code number, and cut designation will be required on the individual patterns. Sometimes it is desirable to make a rubber stamp to indicate what information is required. and perhaps to indicate the orientation of the test antenna.

Any special conditions should be noted either on the patterns or on the cover sheet. In an automated system this can be accomplished in the software by requiring the operator to input the required information.

9. On-Site Measurements of Amplitude Patterns

The measurement of the complete two-dimensional radiation patterns of a full-scale antenna located on its ultimate site may be laborious and an expensive task. It is necessary to make such measurements when the antenna radiation is significantly affected by the site on which the antenna is located or when its construction and/or assembly are practical only if carried out at the site. Furthermore, on-site measurements of an antenna may have the additional usefulness as a conclusive demonstration that the performance of the antenna is as desired and that it interacts with its environment in a predicted manner.

A wide variety of techniques have been employed for the on-site measurements of the amplitude patterns of an antenna. The procedures outlined in the following discussion are commonly used and illustrate some of the problems involved. It should be emphasized, however, that each on-site antenna measurement has special considerations and techniques that are not necessarily discussed here.

Fig 35 indicates the essential parts of the typical measurement system. A distant source is carried by a vehicle, which is maneuvered through the space surrounding the test antenna to produce a source of an essentially plane wave incident on the antenna from all directions of interest. The direction to the source, with respect to a reference direction at the antenna, is obtained from a tracking device. This information provides the angular data to a recording device. The amplitude of the signal received by the antenna provides the amplitude data to the recording device. These data may then be processed to present the antenna patterns in the desired form.

Airborne vehicles, such as conventional airplanes. helicopters. blimps, and free and captive balloons, have been employed to carry the source. The source should be in the far-field region of the antenna system being measured. If this is not possible to achieve with airborne vehicles, man-made earth-orbiting satellites [56], the sun [57], and radio stars [58], have been used.

If the attitude of the source antenna relative to the antenna under test changes, a change in the received signal is likely to occur. To minimize this possibility, the source antenna should be oriented so that the peak of its beam is in the direction of the antenna being measured, and the useful portion of the source pattern should be as uniform as possible. In addition, when the source antenna cannot change the direction of its beam, the course flown by the aircraft should be chosen to minimize changes in attitude. A favorable course for this purpose lies along a circle centered on the antenna being measured and contained in a plane perpendicular to a vertical axis through the antenna. It is equally important that the design and placement of the source antenna include the effects of its environment. These environmental effects are greatly dependent on the relative size of the aircraft and the operating wavelength. The source antennas may be separated into two classes according to this distinction.

In the lower frequency class (HF and VHF) the selection of a source antenna may depend on polarization. For horizontal polarization a sleeve-dipole antenna trailed behind the aircraft has proved satisfactory. This antenna is fabricated from a length of standard coaxial cable by removal of the shielding braid for a distance of a quarter wavelength, and it can be supported in a horizontal position by a miniature parachute. For vertical polarization useful results have been obtained with a monopole where the aircraft serves as the “ground.” Since its radiation pattern has a null in the vertical direction, measurements made with the source antenna near the antenna’s zenith should take the inherent pattern variations into account. For techniques where the polarization has to be changed during the course of the measurement, rotatable ferrite-loaded dipoles, which can be mounted on the side of the aircraft,

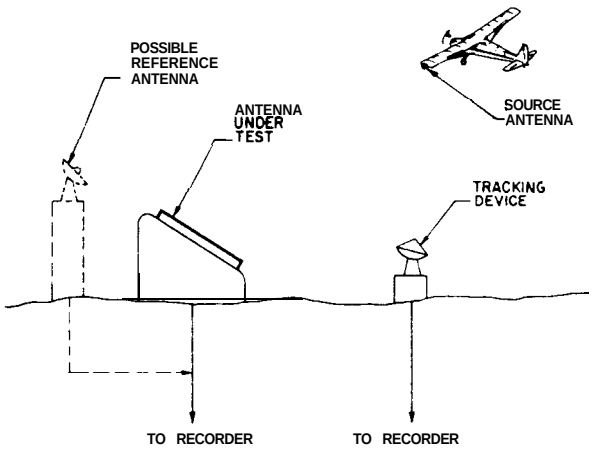

Fig 35
System for On-Site Measurements of Amplitude Patterns

have been found useful [59]. Careful calibration is needed due to the asymmetry of the aircraft structure with respect to the antenna.

In the higher frequency class (microwave region) wing-tip antennas have been successfully utilized. This placement minimizes excitation of the airplane structure and permits a source radiation pattern that is reasonably close to the pattern of the isolated source antenna.

As indicated in Fig 35, a tracking device is required to establish the relative direction to the source. In particular, the direction of the aircraft with respect to the tracker is measured. The direction of the aircraft relative to the antenna under test shall then be determined by taking into account the parallax error introduced because of the known separation between the antenna under test and the tracker. In addition to the source direction, it may be necessary for the tracking system to determine the range to the source. This information may be needed either to compute the parallax correction, or to correct for the change in the incident power flux density caused when the aircraft does not fly in a perfect circle about the antenna under measurement.

Two types of tracking instruments are in common use, optical and radar trackers. An important distinction between the two is that the ordinary optical tracker furnishes only the direction of the source, while radar furnishes direction and range. A laser tracker would furnish range also. When an optical system is employed, the range of the source can be calculated from the aircraft attitude measured by an instrument in the aircraft and transmitted to the test site.

The system described in the preceding discussion may be adequate for measuring the on-site amplitude patterns of an antenna. However, there are occasions when this system is not sufficiently accurate, because the amplitude or polarization of the wave radiated by the source toward the antenna under test is insufficiently stable. This variability is particularly likely at microwave frequencies. In these cases a reference antenna (Fig 35) may be placed close to the antenna under test to measure the apparent variation in the strength of the source. These data can be used to normalize the signal received by the antenna under test and hence remove the apparent variations in the source signal. In addition to the shape of the amplitude pattern, the reference antenna also may be used in a measurement of power gain, as discussed in 12.3. Finally the reference antenna can sometimes be designed to determine the polarization of a set of source antennas, as discussed in 11.2. This feature, in turn, may permit the polarization of the antenna under test to be determined. It should be recognized, however, that unless the reference antenna

system is carefully designed, it may introduce errors as great as those it is intended to cancel. For example, its received signal may vary because of site reflections in addition to source variations.

At microwave frequencies it is desirable to make the response of the reference antenna substantially independent of the ground and surrounding structures. Such independence requires the use of a reference antenna having a narrow beam and low minor lobes and may also require treatment of the ground and other structures near the reference antenna, which may be satisfied by slaving the reference antenna to the tracking device. At frequencies well below the microwave range, the pattern of the reference antenna may be so broad that ground reflections produce significant variations in the received reference signal. If the pattern of the reference antenna system can be accurately determined, then it is still possible to employ its output as a means for correcting variations in the wave radiated by the source during measurement of the patterns of the antenna under test. However, at the lower frequencies such as HF it is customary to use the reference antenna only during the measurement of power gain at one angle, as described in 12.3.3. Regardless of the frequency being employed, the reference antenna system should be designed and located so that it has a negligible effect on the patterns of the antenna under test.

The process of pattern measurement and recording may involve either a point-by-point or a continuous method; the latter is preferable. Commercially available continuously recording equipment can often be adapted to introduce automatically the various corrections that are needed in both the signal and the angle inputs. The data may also be stored on magnetic tape and processed by computer. The antenna patterns can be presented in different forms as discussed in Section 5. The most comprehensive form is that of the contour plot.

10. Phase

10.1 General. The radiation pattern of an antenna is completely described by the magnitude and phase of the radiated field components in two particular orthogonal polarizations. Most commonly only the magnitude of a specified component of the field is measured, namely, that for which the antenna is designed. However, the phase of this component may also be of importance. Furthermore, for a complete description of the field, the magnitude and phase of the cross-polarized component shall also be measured. The variation of the phase of the far field provides necessary information for focused reflectors and beams, tracking antennas, and phase interferometers. The variation of the phase and magnitude of the near field may be necessary to permit an accurate prediction of the far field patterns (see 7.3) or in other cases to interpret the characteristics of an antenna.

A single-frequency field component of radian frequency ω can be represented as a scalar function of time by

$$\mathcal{E}(t) = E_0 \cos(\omega t + \psi) = \mathrm{Re}\,(E_0 e^{j\psi} e^{j\omega t})$$

where ψ is a real number and E_0 is a positive real number.

NOTE: There are two generally accepted conventions in the writing of the complex time factor, $e^{j\omega t}$ and $e^{-i\omega t}$. For a positively traveling wave the phase factor will be e^{-jkx} when $e^{j\omega t}$ is used. The factor $e^{j\omega t}$ is used in this standard except in 7.3. To change any formula replace -i by +j.

The phase at time t of $\mathcal{E}$ (t) is the angle of the complex number $E_0 e^{j(\psi + \omega t)}$, or

$$\text{phase } \mathcal{E}\text{ (t)} = \psi + \omega t$$

If the phase of $\mathcal{E}$ is used without specifying the time, it is implied that $t = 0$, and

$$\text{phase } \mathcal{E} = \psi$$

If the field $\mathcal{E}$ propagates along the x axis with a velocity $v = \omega/k$, where k is the wave number, then

$$\mathcal{E}(t, x) = E_0 \cos(\omega t - kx + \psi)$$

At point x, as a function of t, $\mathcal{E}$ is represented by the curve $\mathcal{E}(t, 0)$ shifted in the positive di-

reaction by x/v (see Fig 36). This is considered as a phase delay, lag, or retardation. The phase is decreased by amount kx in the propagation from 0 to x.

In contrast to the scalar case, when dealing with a vector field it is important to realize that, while there is a "natural" or canonical way of defining the phase of a linearly polarized field vector, this is not true for elliptically or circularly polarized field vectors. For example, in the linearly polarized case it is natural to express the field $\mathcal{E}$ (t) as the product of a scalar function $\mathcal{E}$ (t) and a unit real vector u which indicates the direction of polarization. The phase of $\mathcal{E}$ (t) is the phase angle of $E_0 e^{j\psi}$. If the polarization is not linear, this is no longer possible. A complex vector $\hat{u}$ of magnitude 1 ($\hat{u}^* \cdot \hat{u} = 1$) can be used, but it is not uniquely defined by the polarization alone: the vector $\hat{u}$ can be replaced by $\hat{u}' = \hat{u} e^{j\alpha}$, which represents the same polarization, but the phase relative to $\hat{u}'$ differs from that relative to $\hat{u}$ by α. This concept will be expanded in the next section.

10.2 Phase Patterns. A specified component of the far field produced by an antenna can be expressed in the form

$$E_u (r, \theta, \phi) = E (\theta, \phi) e^{j\psi(\theta,\phi)} \frac{e^{-jkr}}{r} \hat{u}$$

where E and ψ represent the (θ,ϕ) dependence of the magnitude and phase, respectively, of the specified component, and (r, θ,ϕ) are spherical coordinates of the observation point. The vector $\hat{u}$ is a vector of magnitude unity (unitary vector), which indicates the polarization of the specified component. For a linearly polarized component the vector $\hat{u}$ is taken as real; for instance, it may be the unit vector u_θ (or u_ϕ) in the direction of increasing θ (or ϕ). Then the phase ψ is defined unambiguously. However, for an elliptically or circularly polarized component the vector $\hat{u}$ is complex, as previously stated, and is not uniquely defined by its polarization and the normalizing condition. Multiplication by $e^{j\alpha}$ preserves these conditions. This changes ψ accordingly. Therefore a definite convention shall be used to specify $\hat{u}$ and, when discussing a pattern, this convention shall be specified for every direction (θ, ϕ) of interest.

10.3 Antenna Phase Center. For many applications it is desirable to assign to the antenna a specific reference point, the phase center, from which radiation may be said to emanate.

Fig 36
Phase Shift of Single-Frequency Field Propagating **in the x Direction. The Phase** of $\mathcal{E}(t,x)$ **Lags the Phase of** $\mathcal{E}(t,0)$ **by** kx

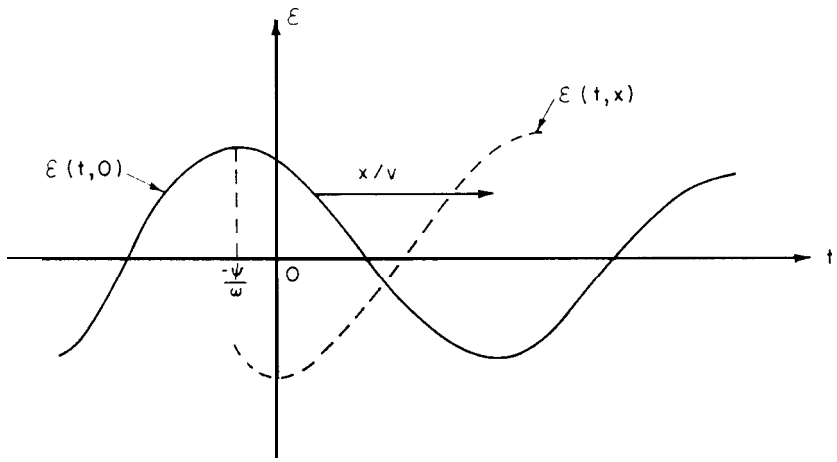

Knowledge of the location of this reference point is highly desirable and sometimes a prerequisite to the successful design of antennas such as phased arrays and primary feeds for reflectors. In addition, the design of tracking and homing systems on aerospace vehicles and of rendezvous radar systems may require the precise determination of the phase characteristics and phase reference point of the elements of these systems.

If there exists an origin of coordinates such that, for any given frequency, the function ψ in the preceding equation is independent of θ and ϕ, this origin will be the center of spherical wave fronts or equiphase surfaces. It is the reference point or the phase center of that component of the radiated field, and the pattern is described for the specified polarization by the single real function $P(\theta, \phi)$. This occurs for linear antennas and arrays that have odd or even crossing symmetry, that is, such that the current satisfies the condition [60]

$$I(-x) = \pm I^*(x)$$

For most antennas a "true" phase center, valid for all directions does not exist. However, one may sometimes find a reference point such that ψ becomes constant over a range of directions of interest, for instance, over a portion of the main beam of the antenna. This point has also been called a phase center, or an *apparent phase center* [60]. It is particularly important to determine such a point for the primary feed of a reflector since it allows one to use geometrical optics to properly place the feed with respect to the reflector and to compute the radiation pattern.

Some antennas, such as the conical log-spiral, have a natural axis of symmetry. It is convenient to take this axis as the polar axis of the system of spherical coordinates. The phase pattern may then be separated into the product

$$\psi(\theta, \phi) = \Theta(\theta)\, \Phi(\phi)$$

For a particular choice of the origin 0 on the axis it may happen that, at least over some range of interest, the phase ψ is independent of θ and reduces to $\Phi(\phi)$. This point 0 can be considered as a phase center for the θ coordinate. It can be found by the same methods as the ordinary phase center by observing a cut of the phase pattern for a constant value of ψ (see 10.4).

The theoretical calculation of the apparent phase center is usually laborious and limited to those antennas for which the complete expression for the far field is known [61]–[64]. In doing so, the most straightforward approach is to calculate the radius of curvature of this equiphase surface at the point of interest. The rays from the phase reference point to the observation point form a pencil of lines as one of the spherical coordinates, say θ, varies. The evolute of the far-field equiphase contour is traced by the envelope curve of the rays. The evolute is the locus of the phase reference points for varying 6. As θ and ϕ are both allowed to vary, the evolute of the equiphase surface generates a warped surface upon which the phase reference points or apparent phase centers lie. There are in general two principal phase centers on each normal.

For many applications it becomes necessary to determine or check, by experimental methods, the location of the phase centers of the antennas under study or construction. The experimental determination of a phase center can be done by finding an equiphase surface in the far field. If this surface is a sphere, its center is the phase center. If it is not, one can sometimes approximate the equiphase surface by a sphere over a limited range of directions and thus obtain the corresponding apparent phase center. There are methods that depend only upon amplitude measurements of the far field [63]. However, the use of amplitude patterns to derive phase information is severely limited by the realizable recording accuracy and not normally suited for the determination of small phase changes.

10.4 Phase Measurements

10.4.1 General. The radiation pattern of an antenna is completely described by the magnitude and phase of the radiated field components in two particular orthogonal polarizations. In this section emphasis is given to the aspect of the measurement of the phase patterns. It is

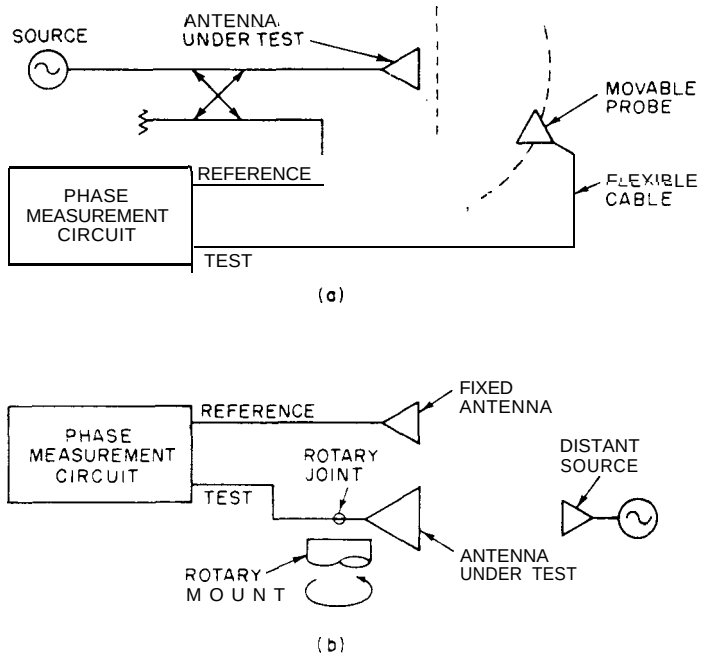

Fig 37
Arrangements for Measuring Phase Patterns
(a) Near-Field, or Short-Distance, Pattern Phase.
(b) Far-Field Pattern Phase

understood that in an actual measurement both phase and amplitude would be recorded simultaneously.

Since phase is a relative quantity, a reference signal shall be provided at all times for comparison.

NOTE: Because of the periodic nature of angles, phase is only defined up to multiples of 2π rad.

For measurements made at short distances the antenna under test may be used as the transmitting antenna and a simple receiving antenna or probe may be used to sample the radiated field [65], as shown in Fig 37(a). A reference signal may be coupled out from the transmission line leading to the test antenna and compared with the received signal in a suitable circuit. For measurements at distances too great to permit direct comparison between the sampled signal and this type of reference signal, the arrangement of Fig 37(b) may be used. The signal from a distant source is received simultaneously by the antenna under test and by a fixed reference antenna. To measure a phase pattern the antenna under test is rotated in the usual manner as for measuring radiation patterns. The arrangement of Fig 38 can be used for the measurement of the relative phase between two ports of amultiportantenna as a function of the angle around the antenna.

The ‘most comprehensive information about the phase characteristics of an antenna can be gained by recording the complete phase patterns, preferably with an automatic system. From these phase patterns contours of constant phase and the phase center or reference point can be determined (see Section 5).

A consideration of the typical characteristics of the phase pattern of antennas with a well-defined phase center is useful in the interpretation of patterns from an antenna with unknown characteristics [60]. Let us assume that a

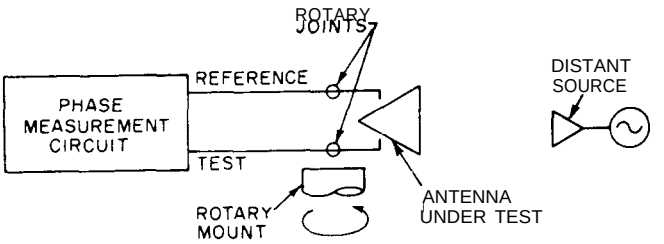

Fig 38
Phase Measurement Between Two Ports of a Multiport Antenna

given antenna has a phase center on the axis of the structure and that the antenna is positioned in a r,θ,ϕ coordinate system with $\theta = 0$" as the antenna axis. If a phase pattern is recorded for this antenna about some origin, or center of rotation, which coincides with the phase center, this pattern over the main beam will, by definition, be a constant. If the amplitude pattern has side lobes, there will be a 180° phase reversal at each null, and the phase pattern will exhibit an abrupt transition. If a phase pattern is recorded as this antenna is rotated about some origin along the axis of the structure, but displaced a distance r' from the phase center, the phase of the field of the antenna will be modified by a cosinusoidal function of θ. When r' is very small compared to the distance to the point of observation, and the pattern is normalized to the phase of the signal received when the phase center is at position *A* in Fig 39(a), the resultant phase pattern for an antenna with only one radiated beam will be given by

$$\Psi \approx kr'(1 - \cos\theta)$$

Normalization to the phase of the signal received when the phase center is at position *B* in Fig 39(b) will produce the image of the first pattern.

In theory the position of the phase center can be calculated from one such phase pattern. If a change in phase Ψ is measured as the antenna is rotated from $\theta = 0$" to $\theta = \theta_1$, the phase is displaced from the center of rotation by the distance

$$r' = \frac{\lambda}{2\pi}\left(\frac{\Psi}{1 - \cos\theta_1}\right)$$

In practice it may be necessary, because of both pattern and experimental anomalies, to record several patterns as the antenna is repositioned along its axis to bracket the curve for $r' = 0$.

If the apparent phase center is displaced from the axis of the antenna by *d*, as indicated in Fig 39(c) and (d), the phase change with rotation will be

$$\Psi \approx kr''\left[1 - \cos\left(\theta + \arctan\frac{d}{r'}\right)\right]$$

where $(r'')^2 = (r')^2 + d^2$. If the minimum detectable phase change, that is, the resolution of the phase-detection system, is 0.5" and a phase comparison is made over a range of $\theta = \pm$ 10" from the axis of the antenna, the indeterminacy in the position of the measured phase center may be as great as 0.1 wavelength. In practice this uncertainty can be minimized by recording over a greater range of θ if there is an apparent phase center over this greater range, and/or by recording a second value for r'_{min} when the phase center approaches the center of rotation from the opposite direction. In the ideal case the geometry is such that the two values of r'_{min} should indicate a bracket of the apparent phase center.

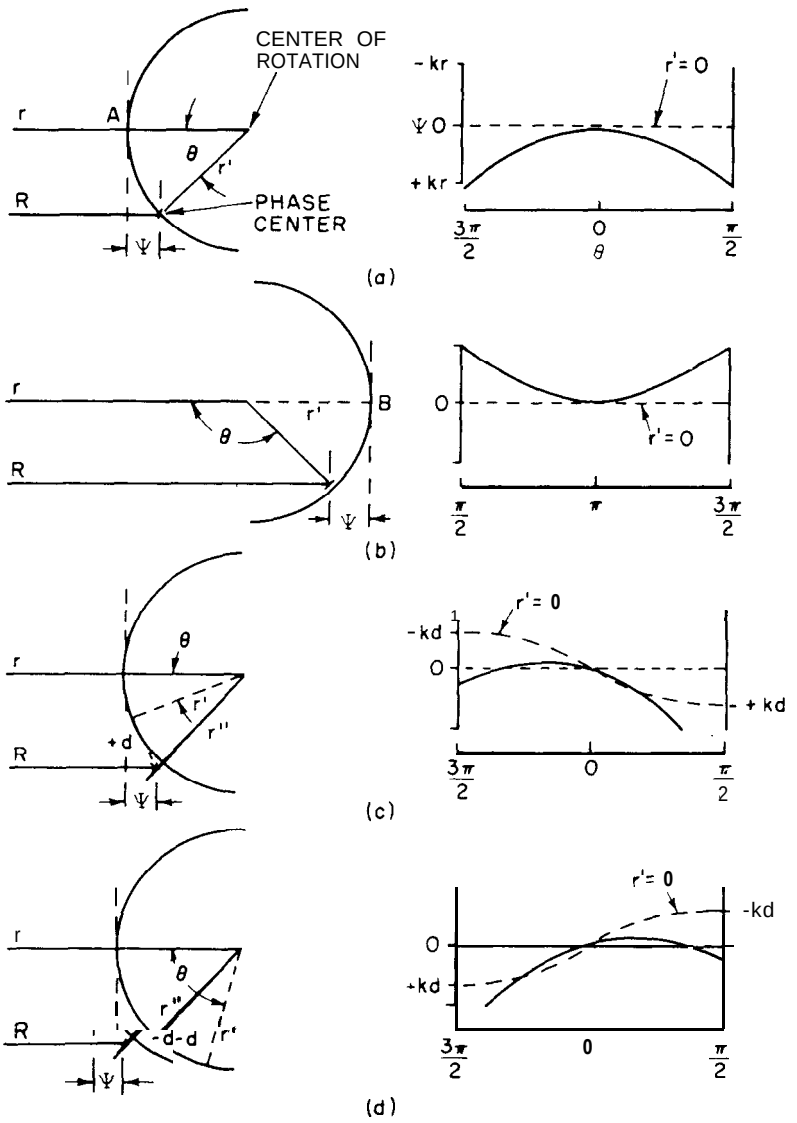

Fig 39
Geometry and Phase Change as a Displaced Source Is Rotated about a Given Origin

To make these measurements, the antenna under test is placed in the far field of a source of the desired polarization, on a positioner that is capable of precise rotation about a point and of precise translation along the axis of the antenna. To correct for and evaluate a transverse displacement of the phase center from the axis, and to correct for minor mechanical tolerances in the positioner, it is highly desirable to also be able to precisely translate the antenna in a path that is orthogonal to its axis.

10.4.2 ***Instrumentation.*** When considered from the viewpoint of measurement system error and instrumentation complexity, few antenna-system measurements have been more difficult or time consuming than those involving the measurement of phase of the radiated field.

However, recent advances in phase-measurement instrumentation, for example, the introduction of radio-frequency vector voltmeters, computer-controlled and manual radio-frequency network analyzers, and phase and amplitude receivers, have greatly reduced the magnitude of the measurement problem. If it is necessary, or for some reason desirable, that a phase-measurement system be assembled, there are, in the literature, papers concerned with the analysis and classification of most of the measurement systems that have been proposed and used [19],[66] (see Section 5).

10.4.3 *Sources* **of** *Error.* Whether a commercial phase-measuring instrument or an assembled system is used, considerable attention shall be paid to the numerous sources of error. A major **source** of *error* in the measurement of phase is due to the interaction of reflected waves from components which are not matched to the waveguide or transmission line in use [67]. In addition to possible phase errors introduced by nonideal components, multiple reflections between the components alter the relative magnitude and phase of the traveling waves on these lines. The relative phase and magnitude of these wavefronts may coincide with those that would be present in the matched case, but more likely will lie somewhere between extreme limits set by the mismatch. For two cascaded discontinuities, with reflection coefficients small with respect to unity, the maximum possible phase mismatch error is approximately

$$\arcsin |\Gamma_1| |\Gamma_2|$$

where Γ_1 and Γ_2 are the reflection coefficients of the two discontinuities when viewed from a common point between them. For example, the relative phase between the fields at any two points on a transmission line connecting two connected instruments or components with reflection coefficients such that they would cause voltage-standing-wave ratios of only 1.3:1 and 1.5:1, respectively, could vary by as much as ± 1.49" from that on a reflectionless line.

The only way to reduce this possible error is to reduce the magnitude of the mismatch of these sources. This can be done with well-matched attenuators or pads. However, such an improvement is limited by the cascaded discontinuities due to the irreducible mismatch of the transmission-line connectors. Lapped waveguide flanges and precision connectors should be used where possible. It is particularly convenient to use signal-flow-graph techniques for error analyses of these measurement systems [68],[69].

Measurement systems which involve the propagation of energy from the source to the phase-measurement receiver through two paths impose strict requirements on the frequency stability of the source. If these paths are not exactly equal in electrical length, a shift in the frequency of operation from f_1 to f_2 will cause a shift in the measured phase difference $\Delta\Psi$ between the signals on two paths of approximately

$$\Delta\Psi = 360 \left| \frac{\ell_1 - \ell_2}{\lambda_1} - \frac{\ell_1 - \ell_2}{\lambda_2} \right|$$

degrees, where Q, and ℓ_2 are the lengths of the two paths, and λ_1 and λ_2 are the guide wavelengths at f_1 and f_2. If these paths involve combinations of waveguides or transmission lines and free space, the electrical lengths of the paths shall be calculated accordingly.

As an example, for measurements made at 1000 MHz, with a difference in a free-space path length of 1 meter between two channels, a change in frequency of 1 MHz (that is, 0.1 percent) will cause a phase change between the two channels of 1.2". If this change in frequency occurs during a measurement, the change in phase appears as an error in the measurement. To minimize such errors, the two path lengths should be kept equal in electrical length by adding an additional transmission line to the shorter channel. This latter requirement is, of course, a necessity for swept-frequency measurements.

In many phase measurements, such as in the measurement of fields around an antenna, it becomes necessary to move a receiving probe in space. This movement involves a bending or flexing of the coaxial cable leading to the

probe, or where waveguides are used the rotation of several rotary joints may be required. Most rotary joints change, to some degree, the phase of the output' signal with rotation. At microwave frequencies it is not difficult to change the electrical length of a short section of coaxial cable by a degree or more when it is bent or flexed. A change in temperature will cause similar errors. This change in electrical length will appear as an error in the measurement of the change in phase of the fields as a function of space. This phase shift is difficult to eliminate although there are cables which are designed to minimize it. Alternately it can sometimes be minimized by first selecting a section of cable that exhibits little change with the necessary flexing. A difference can sometimes also be noted between different pieces of the same cable. The cable should be long enough so that sharp bends are not necessary and the movement of any one section of the cable is held to a minimum. A dissipative or lossy cable sometimes may show less phase shift with flexing than the low-loss cables. In waveguide systems there is little that can be done to eliminate this error except to calibrate the phase shift of the movable arms and rotary joints as a function of position in space if such a calibration is required.

These examples should indicate to the experimenter that accurate measurements require careful attention to the details of the system, and assumed accuracies of say 5° or less shall be viewed with caution unless all factors have been taken into account. One factor that is sometimes overlooked is the signal-to-noise ratio in the system. A high signal-to-noise ratio is necessary to prevent the noise from contributing to errors in the phase measurements.

11. Polarization

11.1 General. Polarization is a property of single-frequency electromagnetic radiation describing the shape and orientation of the locus of the extremity of the field vectors as a function of time [1, 3.1–3.4],[70].

NOTE: Some of the methods of analysis used for single-frequency fields can be extended to partially polarized fields [71],[72]. Random fields or random antennas will not be considered here.

In common practice, when only plane waves or locally plane waves are considered, it is sufficient to specify the polarization of the electric field vector *E*. In a plane wave with a known direction of propagation the magnetic field vector *H* is simply related to the *E* field. It can be deduced by a 90" rotation about the propagation vector, followed by multiplication by the intrinsic admittance Y_0 of the medium,

$$Y_0 = \sqrt{\frac{\epsilon}{\mu}}$$

where ϵ is the permittivity and μ is the permeability of the medium. In vacuum $Y_0 \approx 1/377 = 2.66 \times 10^{-3}\,\Omega^{-1}$.

The far field radiated by an antenna is generally observed in a small region where it can be considered as a plane wave propagating away from the antenna in the radial direction. The electric field is in a plane perpendicular to that direction. The locus of its extremity, is, in general, an ellipse that may degenerate into a segment of a straight line or into a circle. Correspondingly, the polarization is called elliptical, linear, or circular.

The sense of rotation of the extremity of *E* describing a circle or an ellipse in the plane of polarization (perpendicular to the direction of propagation) is called the sense of polarization, or handedness. This sense is called right handed (left handed) if the direction of rotation is clockwise (counterclockwise) for an observer looking in the direction of propagation (see Fig 40). Alternative conventions are discouraged as they could be a source of confusion. If, instead of considering the field vector at a point as a function of time, one considers the vector at a given instant of time, as a function of distance along the direction of propagation, one might be lead to incorrect designations.

Elliptical polarization is characterized by the axial ratio of the polarization ellipse, the sense of rotation, and the spatial orientation of the ellipse with respect to a reference direction in

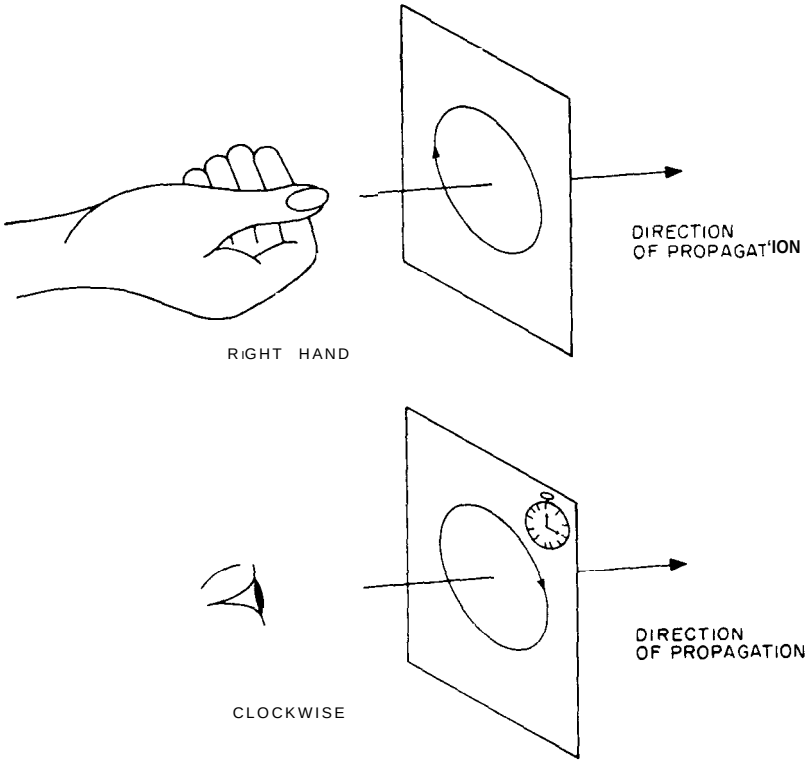

Fig 40
Illustration of the Sense of Rotation

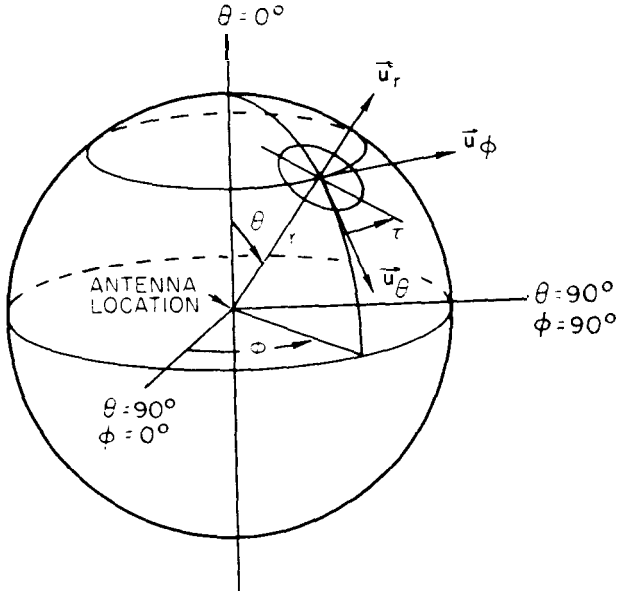

Fig 41
Polarization Ellipse in Relation to Antenna Coordinate System

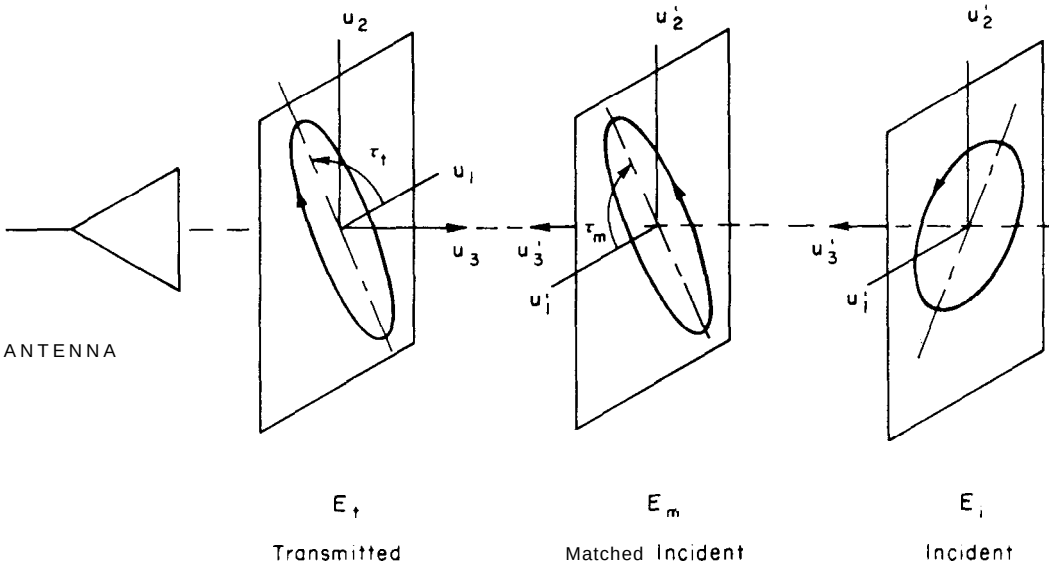

Fig 42
Relation Between Polarization Properties of an Antenna when Transmitting and Receiving
E_t — Far-Field Electric Vector of Antenna; E_m — Electric vector of Incident Wave which Is Polarization Matched to Antenna; E_i — Electric Vector of Arbitrarily Polarized Incident Wave

the plane containing the ellipse. The angle between the reference direction and the major axis of the ellipse is called the *tilt angle.*

For a plane wave, the tilt angle is measured clockwise from the reference direction when looking in the direction of propagation [73,475–477]. The horizontal axis is usually chosen as the reference direction. This convention shall be employed throughout this standard.

E_t electric field vector of far field, radiated by the antenna in that direction. Since an antenna usually has a spherical coordinate system associated with it (see 3.1), its polarization in a direction (θ, ϕ) can be illustrated with respect to the coordinate system, as shown in Fig 41. Although the reference direction for establishing the orientation of the polarization ellipse is arbitrary, it is common practice to take the u_θ axis as the reference direction [2].

When an antenna receives a plane wave coming from a given direction, the response (open-circuit voltage, short-circuit current, or available power) is maximum, for a given intensity of the incident plane wave, when the polarization E_m has the same axial ratio, the same sense of polarization, and the same spatial orientation of the major axis as that of the antenna for that direction (see Fig 42). Because the sense of polarization is relative to the direction of propagation, and E_t and E_m, the senses appear to be different when looked at from a single point of view. Also, in antenna-pattern-measurement situations it is

order to be consistent with the definition of antenna polarization, the local coordinate system associated with each of the waves is oriented so that one of the coordinates is in the direction of propagation. As a result the tilt angles for the two polarization ellipses, which are measured according to a right-hand rule, are different. As shown in Fig 4.2 if τ_t is the tilt angle for the ellipse described by E_t, then the one described by E_m will be

$$\tau_m = 180^\circ - \tau_t$$

It should be noted that τ_m may also be expressed as $-\tau_t$ plus any integral multiple of 180° since all these angles correspond to the same orientation of the major axis of the polarization ellipse. The polarization of the incident wave, which yields the maximum response at the antenna terminals, as described above, is called the *receiving polarization* of the antenna.

If the incident plane wave has a polarization that is different from the receiving polarization of the antenna, then a polarization loss occurs due to this mismatch. The *polarization efficiency p* is used to account for polarization mismatch [70, pp 544–549],[74].

NOTE: This factor is also called polarization mismatch factor [75], and polarization receiving factor (ANSI/ IEEE Std 100-1977, Dictionary of Electrical and Electronics Terms).

It is defined as the ratio of the power actually received by the antenna divided by the power that would be received if a wave from the same direction, with the same intensity and polarization matched, were incident on the antenna.

The Poincare sphere [70, pp 540–544] is a useful graphical aid for the visualization of polarization effects since the polarization efficiency is uniquely determined by the separation of two points on the sphere which describe the polarizations of the incident wave and the receiving antenna, respectively.

The construction of the Poincare sphere is a consequence of the fact that any wave can be resolved into two orthogonal components (they may be two orthogonal linear, elliptical, or circularly polarized components). The total power in the wave can then be represented as the sum of the powers contained in the orthogonal components:

$$Y_0 E_t^2 = Y_0 E_A^2 + Y_0 E_B^2$$

where E_t represents the effective value of the magnitude of the electric field vector of the given wave, and E_A and E_B *are* those of the two orthogonal components. By dividing the equation by the total power $Y_0 E_t^2$ one obtains

$$\overline{E}_A^2 + \overline{E}_B^2 = 1$$

where $\overline{E}_A^2$ and $\overline{E}_B^2$ represent the fractions of power in their respective polarizations. This latter equation leads to the construction shown in Fig 43. It is evident in Fig 43 that the position of W along the arc AWB indicates the division of power in the wave W between the two orthogonal polarizations *A* and B.

For example, if *W* represents the incident plane wave and *A* the antenna's receiving polarization, then the angular separation 2ζ between *A* and W determines the division of power density in the wave between the receiving polarization and the orthogonal polarization. The polarization efficiency *p* is given by

$$p = \overline{E}_A^2 = \cos^2 \zeta$$

Note that $p = 1$ when *A* and *W* are coincident and 0 when *A* and *W* are diametrically opposite. For the former case the wave is said to be co-polarized with respect to the antenna's receiv*ing* polarization and for the latter case they are cross-polarized. Fig 44 depicts the relative spatial orientation of the polarization ellipses of two cross-polarized fields. Note that for elliptically polarized fields a rotation of 90° about the direction of propagation alone does not produce a cross-polarized field. The rotation shall be accompanied by a change of the sense of polarization.

The Poincare sphere is generated by rotating the semicircle AWB about the *A-B* axis with the angular measure around the equator of the resulting sphere being the relative phase

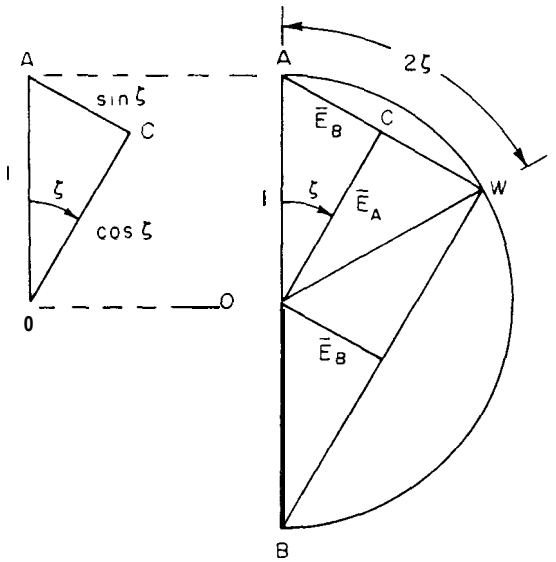

Fig 43
Illustration of the Division of Power Between Two Orthogonal Elliptical Polarizations A and *B*

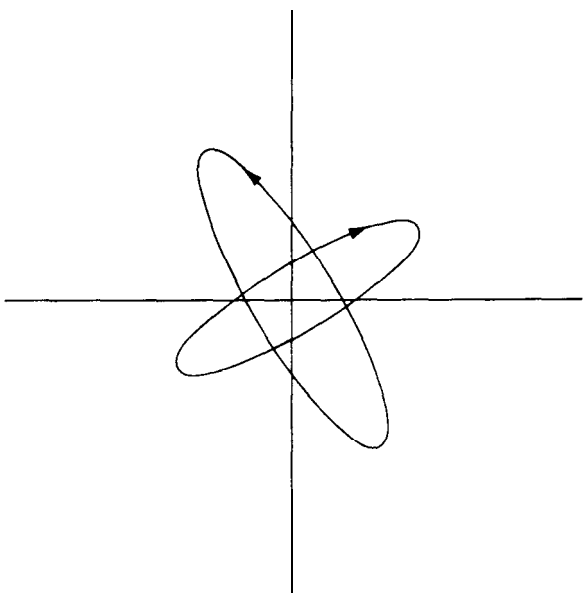

Fig 44
Cross-Polarized Field Vectors

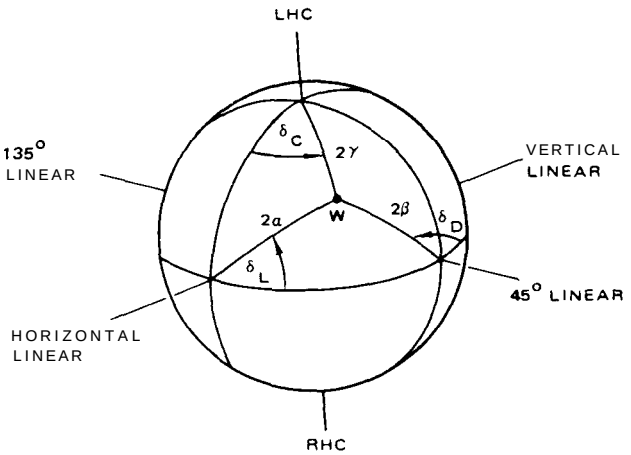

Fig 45
Poincard Sphere Representation of the Polarization of a Plane Wave W

between the two orthogonal polarizations *A* and *B (see* Fig 45). In Fig 45 the angle 2ζ of Fig 43, which was defined for arbitrary elliptical components *A* and *B,* is assigned the symbols $2\alpha, 2\beta$, and 2γ as the polarizations A and *B* become

$$2\alpha \begin{cases} \overline{E}_H & \text{(horizontal linear)} \\ \overline{E}_V & \text{(vertical linear)} \end{cases}$$

$$2\beta \begin{cases} \overline{E}_{45} & (45^\circ \text{ linear}) \\ \overline{E}_{135} & (135^\circ \text{ linear}) \end{cases}$$

$$2\gamma \begin{cases} \overline{E}_L & \text{(left-hand circular (LHC))} \\ \overline{E}_R & \text{(right-hand circular (RHC))} \end{cases}$$

There is a one-to-one correspondence between all possible polarizations and points on the Poincare sphere (see Fig 46).

The *complex polarization ratios* are *given* by

$$\hat{\rho}_L = \rho_L e^{j\delta_L}$$

$$\hat{\rho}_D = \rho_D e^{j\delta_D}$$

$$\hat{\rho}_C = \rho_C e^{j\delta_C}$$

where

$$\rho_L = \tan\alpha = \overline{E}_V/\overline{E}_H$$

$$\rho_D = \tan\beta = \overline{E}_{135}/\overline{E}_{45}$$

$$\rho_C = \tan\gamma = \overline{E}_R/\overline{E}_L$$

and where δ_L, δ_D, and δ_C are the relative phases between the corresponding orthogonal components. The relative phase δ_C of the circularly polarized components is defined by the angle of the instantaneous electric vector of the right-hand circular component with respect to the horizontal direction at the instant that the electric vector of the left-hand circular component is in the horizontal direc-

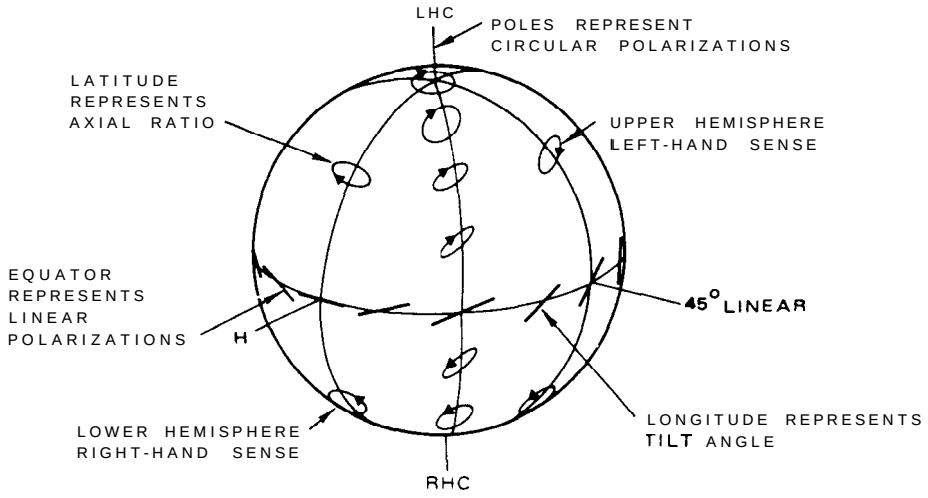

Fig 46
Representation of Polarization on the Poincaré Sphere

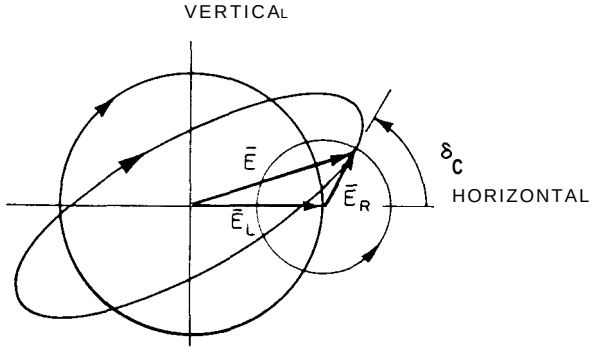

Fig 47
Definition of Phase Reference for Orthogonal Circular Components

tion, as shown in Fig 47. Hence the two circularly polarized components are in phase when the electric field vectors in these two waves are in the same horizontal direction at the same time. The circular polarization ratio ρ_C is of particular interest since the axial ratio r of the polarization ellipse may be expressed as

$$r = \frac{\rho_C + 1}{\rho_C - 1}$$

Note that the sign of the denominator gives the sense of polarization with r positive for the right-hand sense and negative for the left-hand sense. Also, the tilt angle τ is given by

$$\tau = \delta_C/2$$

If the points corresponding to the receiving polarization of the antenna A, and the polarization of the incident wave W are located on the Poincaré sphere, then the polarization

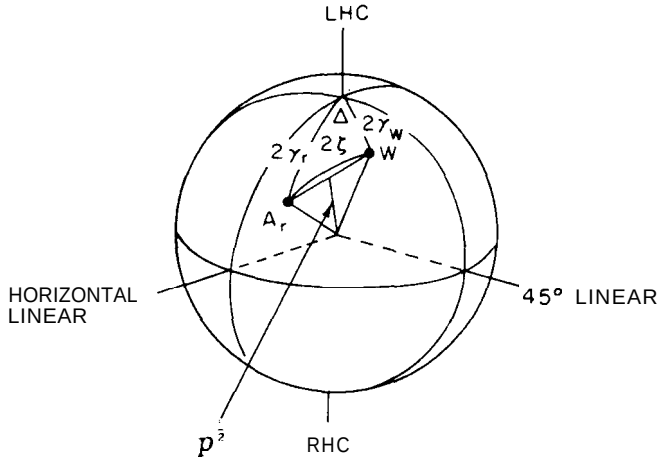

Fig 48
Polarizations of Incident Wave W and Receiving Antenna A_r, Plotted on the Poincark Sphere

efficiency can be determined by use of the expression

$$p = \cos^2 \zeta$$

where 2ζ is the angular separation between A_r and W

p can be obtained with the use of the polarization ratios. For example, it can be shown that

$$p = \frac{1 + \rho_W^2 \rho_r^2 + 2\rho_W \rho_r \cos A}{(1 + \rho_W^2)(1 + \rho_r^2)}$$

where ρ_W and ρ_r can be any of the three polarization ratios ρ_L, ρ_D, or ρ_C, with A being the corresponding difference in phase angles $[(\delta_L)_W - (\delta_L)_r]$, $[(\delta_D)_W - (\delta_D)_r]$, or $[(\delta_C)_W - (\delta_C)_r]$. When the circular polarization ratio ρ_C is chosen, the angle A is twice the spatial angle between the tilt angles of the polarization ellipses of the two polarizations. This equation for p can also be written as

$$p = \frac{|1 + \hat{\rho}_W \hat{\rho}_r^*|^2}{(1 + \rho_W^2)(1 + \rho_r^2)}$$

where $\hat{\rho}_W$ and $\hat{\rho}_r$ are the complex polarization ratios. This form is interesting because it is similar to the equation for mismatch loss in lossless transmission lines with the source and load reflection coefficients being analogous to ρ_W and ρ_r, respectively (see 12.5).

The polarization efficiency can also be written in terms of the axial ratios for the two polarizations by the use of the relationship between the circular polarization ratio ρ_C and the axial ratio :

$$p = \frac{(1 + r_W^2)(1 + r_r^2) + 4 r_W r_r + (1 - r_W^2)(1 - r_r^2) \cos \Delta}{2(1 + r_W^2)(1 + r_r^2)}$$

In this formula the axial ratios are taken as positive for right-hand polarization and negative for left-hand polarization. The angle A is the difference between the relative phases $(\delta_C)_{W,r}$ for the two polarizations W and A_r.

The Poincaré Sphere and the polarization box [1, PP 3.1–3g.7], which is a graphical representation of the Stokes parameters, provide a convenient means of converting from one set of polarization parameters to another. The polarization box is shown in Fig 49 which also indicates its relationship to the Poincaré sphere. It can be shown that the sides and the side

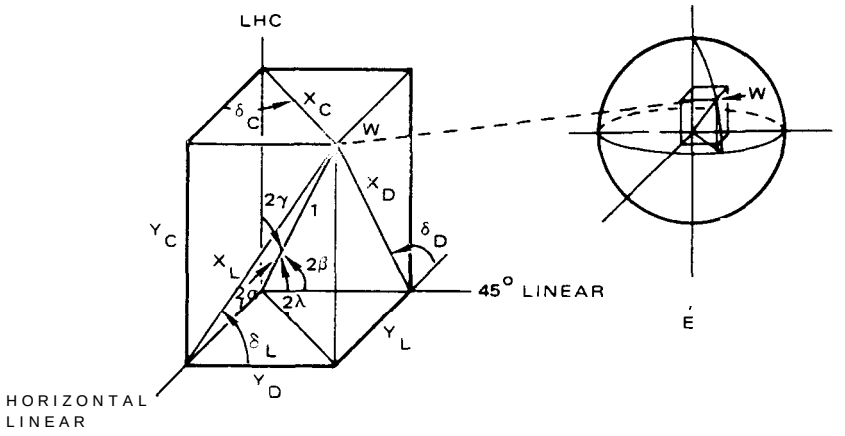

Fig 49
Polarization Box and Its Relation to the Poincare Sphere

diagonals are given by

Sides	Side Diagonals
$Y_L = \cos 2\alpha$	$X_L = \sin 2\alpha$
$Y_D = \cos 2\beta$	$X_D = \sin 2\beta$
$Y_C = \cos 2\gamma$	$X_C = \sin 2\gamma$

As an example of the use of the polarization box in converting between polarization parameters, let ρ_L and δ_L be known from measurements, and let it be required to find ρ_C, δ_C, γ, and the tilt angle τ. The solution is as follows. From the polarization box it can be seen that

$$Y_C = X_L \sin \delta_L$$

so that

$$\cos 2\gamma = \sin 2\alpha \sin \delta_L$$

From the definition of ρ_L one can compute α:

$$\alpha = \tan^{-1} \rho_L$$

Thus γ can be determined, from which ρ_C can be calculated by the use of

$$\rho_C = \tan \gamma$$

and

$$\delta_C = \cos^{-1} \left[\frac{Y_L}{X_C}\right] = \cos^{-1} \left[\frac{\cos 2\alpha}{\sin 2\gamma}\right]$$

The ambiguity in defining δ_C from its cosine alone is removed by inspection of the polarization box. Finally, once ρ_C and δ_C are known, the axial ratio r and the tilt angle τ can be obtained by use of

$$r = \frac{\rho_C + 1}{\rho_C - 1}, \qquad \tau = \delta_C/2$$

For some applications it is advantageous to express the polarization of a field in the form of a unitary vector. A wave W, for example, can be expressed in terms of two orthogonal elliptical polarizations as

$$W = \begin{bmatrix} \overline{E}_A \\ \overline{E}_B e^{j\delta_E} \end{bmatrix} = \begin{bmatrix} \cos \zeta \\ \sin \zeta e^{j\delta_E} \end{bmatrix}$$

where $\overline{E}_A, \overline{E}_B$, and ζ are defined in Fig 43, and δ_E is the relative phase between $\overline{E}_A$ and $\overline{E}_B$. A and B can become (H, V), [45],[135], or (L, R), in which case ζ and δ_E become (a, δ_L), (β, δ_D), or (γ, δ_C), respectively.

To illustrate the use of polarization vectors, let the incident wave W and the antenna receiving polarization A, be expressed in terms of the circular polarization components, that is,

$$W = \begin{bmatrix} \cos\gamma_W \\ \sin\gamma_W e^{j(\delta_C)_W} \end{bmatrix}$$

$$A_r = \begin{bmatrix} \cos\gamma_r \\ \sin\gamma_r e^{j(\delta_C)_r} \end{bmatrix}$$

The normalized voltage response $\overline{V}$ of the antenna to the wave is proportional to the inner product of A_r and W which can be expressed as

$$\overline{V} = (A_r, W) = A_r^{\dagger} W$$

where the superscript † denotes the complex conjugate of the transpose. (Note that V is a phasor.) The matrix operation yields

$$\overline{V} = \cos\gamma_r \cos\gamma_W + \sin\gamma_r \sin\gamma_W e^{j\Delta}$$

where

$$\Delta = (\delta_C)_W - (\delta_C)_r = 2(\tau_W - \tau_r)$$

The polarization efficiency is then given by

$$p = \overline{V}\overline{V}^* = |\overline{V}|^2$$

The determination of the polarization efficiency by the vector method is a formalization of the process of resolving the power density of the incoming wave and the effective aperture of the antenna each into two components corresponding to two orthogonal polarizations such that each component of the wave is polarization matched to the corresponding components of the antenna's effective aperture. It should be noted that partial responses due to the pairs of polarization-matched components do not, in general, add to give a maximum value of $\overline{V}$. The condition for a polarization match is that $\gamma_r = \gamma_W$ and $\Delta = 0$, in which case

$$p = |\overline{V}|^2 = (\cos^2\gamma + \sin^2\gamma)^2 = 1$$

11.2 Polarization Measurements

11.2.1 General. The radiation pattern of an antenna designed for a specific polarization is usually described in terms of the field components for that polarization. It is only a partial description, since a cross-polarized component may be present. A complete description of the radiation pattern requires the measurement of polarization as a function of direction. In particular, away from the direction of the peak value of the main beam, the polarization may be quite different from the design value and, even over the main beam, its variation may be of importance.

The various techniques used to measure the polarization of antennas may be broadly classified into three categories:

(1) those that yield partial information about the antenna's polarization properties

(2) those that yield complete polarization information, but require comparison with a polarization standard

(3) those that yield complete polarization information, but require no standard or *a priori* knowledge of the polarizations of the antennas used in the measurement

The methods of category (2) are termed transfer or comparison methods, and those of category (3) are referred to as absolute methods. The method one selects depends upon the type of test antenna, the required accuracy, the amount of polarization data required, the time available for the measurements, and the permissible cost.

The following methods may be employed to measure polarization [1, pp 10.1–10.38]:

(1) polarization-pattern method
(2) rotating-source method
(3) multiple-amplitude-component method
(4) phase-amplitude method

To completely characterize the polarization

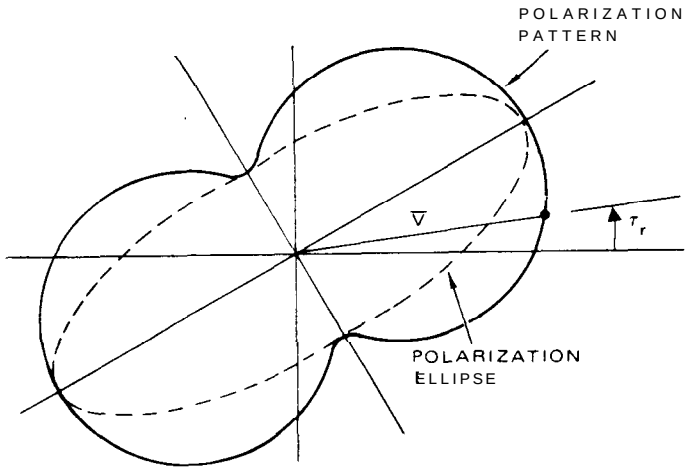

Fig 50
Polarization Pattern of a Wave

of an antenna, it is necessary to determine the polarization ellipse (axial ratio and tilt angle) and the sense of rotation of the electric field vector of the wave radiated by the antenna. The polarization state of the wave can be represented as a unique point on the Poincaré sphere (see 11.1). Some methods of polarization measurement yield insufficient information to completely characterize the state of the wave, hence a unique point on the Poincaré sphere is not determined. For example, when the axial ratio and tilt angle are measured, but the sense of rotation is not determined, there will be an ambiguity between conjugate points in the upper and lower hemispheres of the Poincaré sphere. This information may be adequate when the sense of polarization is otherwise known or when the polarization is nearly linear so that the two conjugate points lie close to the equator.

It should be noted that some of the methods discussed hereafter require sequential measurements; one or more antennas are rotated for a second measurement. These methods pose a problem with regard to system stability, since any change in frequency or gain in the system will introduce errors in the measurement. This is particularly severe when it is necessary to calibrate an antenna over a large field of view, as is the case in the near-field-probing method (see 7.3). For these methods an extremely stable signal source is required. Frequency synthesizers and phase-lock techniques may be employed to achieve the required frequency stability. Those methods of polarization measurement where the measurements are made simultaneously do not require such a high degree of stability.

11.2.2 ***Measurement of the Polarization Pattern.*** The ***polarization-pattern method*** may be employed to determine the tilt angle and the magnitude of the axial ratio, but it does not determine the sense of polarization. For this measurement the antenna under test can be used in either the receive or the transmit mode. If it is used in the transmit mode, the method consists of the measurement of the relative voltage response $|\overline{V}|$ of a dipole, or other linearly polarized probe antenna, as it is rotated in a plane normal to the direction of the incident field. The magnitude $|\overline{V}|$ will be unity whenever the system is polarization matched.

The magnitude $|\overline{V}|$, when plotted as a function of the tilt angle τ_r of the receiving polarization of the linearly polarized probe antenna, is called a ***polarization pattern (see*** Fig 50). The polarization pattern is tangent with the

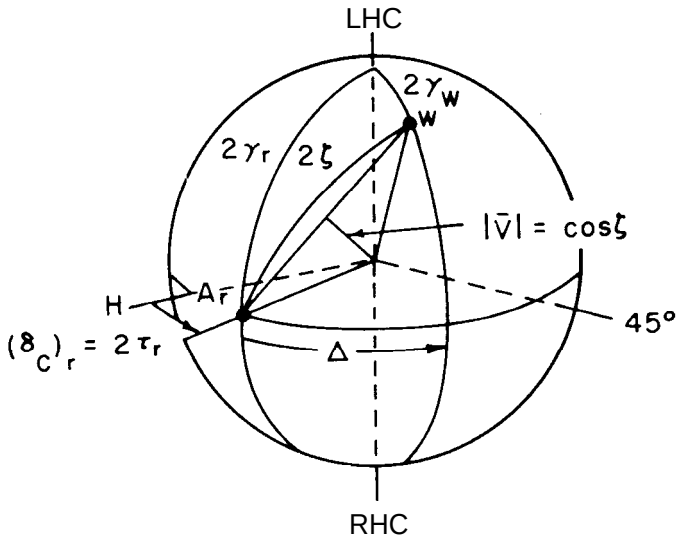

Fig 51
Poincare Sphere Representation of the
Polarization-Pattern Method. $\Delta = (\delta_C)_W - (\delta_C)_r$

polarization ellipse of the field at the ends of the major and minor axes. Hence the magnitude of the axial ratio and the tilt angle of the incident wave are determined.

The method can be illustrated by the use of the Poincaré sphere. For this example assume that the polarization of the incident wave W is located on the sphere, as shown in Fig 51. The receiving polarization A_r of the rotating linearly polarized probe antenna is always located along the equator of the sphere. The square root of the relative response $|\bar{V}|$ is equal to the cosine of one half of the angular separation of W and A_r, as shown in Fig 51. As the tilt angle of A_r is rotated, its position on the sphere moves along the equator so that the magnitude of $|\bar{V}|$ varies. When it is plotted as a function of the tilt angle τ_r the polarization pattern is obtained. It should be noted that the same polarization pattern would be obtained if W were located in the conjugate point W' on the lower hemisphere. The sense of polarization shall be measured in order to resolve the ambiguity.

The polarization pattern can also be obtained from the polarization vector formulation (see 11.1) since

$$\bar{V} = \cos\gamma_r \cos\gamma_W + \sin\gamma_r \sin\gamma_W e^{j\Delta}$$

where

$$\Delta = (\delta_C)_W - (\delta_C)_r = 2(\tau_W - \tau_r)$$

This is illustrated by the phasor diagram in Fig 52. As τ_r varies, the magnitude of $|\bar{V}|$ varies accordingly, and when plotted as a function of τ_r the polarization pattern results.

Fig 52
Generation of the Polarization **Pattern Using the Polarization Matrix Result.**
$\Delta = (\delta_C)_W - (\delta_C)_r$

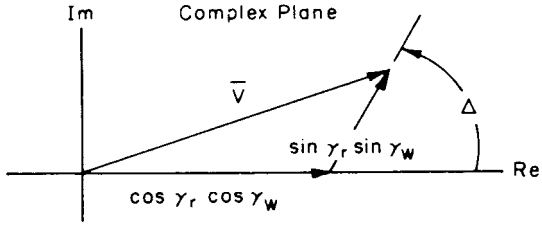

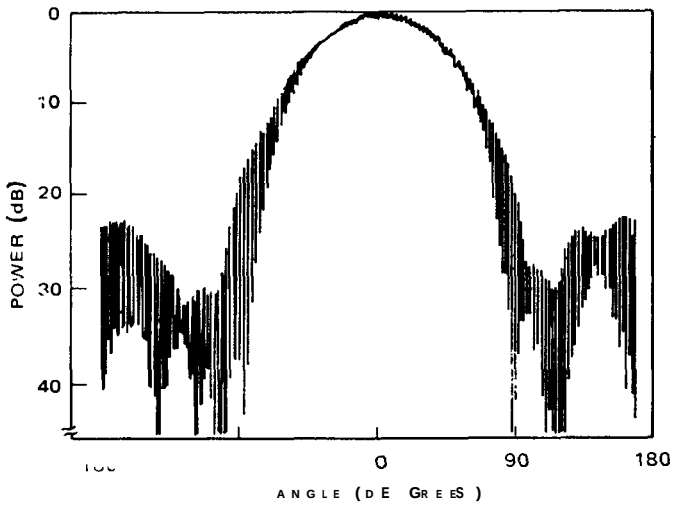

Fig 53
Continuously Scanned Polarization Pattern as a Function of Angle θ

The polarization efficiency (see 11.1) for the system is equal to $|V|^2$ so that it can be obtained directly from the polarization pattern. This is a useful result if the test antenna is to be used in a system with a linearly polarized antenna whose spatial orientation is known. A disadvantage of the polarization-pattern method is that the probe antenna shall be rotated 360° while the antenna under test is fixed so that it is not convenient to obtain polarization information as a function of direction.

11.2.3 ***Rotating-Source Method.*** The axial ratio (and not the sense of polarization or the tilt angle) can be determined as a function of direction by using the ***rotating-source method.*** The method consists of continuously rotating a linearly polarized source antenna as the direction of observation of the test antenna is changed. This method is of greatest value for testing nearly circularly polarized antennas. The rotating source antenna causes the tilt angle τ_W of the incident field to rotate at the same rate. The rate of rotation $\dot{\tau}_W$ shall be very much greater than that of $\dot{\theta}$ or $\dot{\phi}$ as θ or ϕ cuts are made and recorded. Care shall be taken to ensure that the time response of the recording system can adequately follow the excursions in τ_W. An extension of this technique to a spiral cut pattern (see 3.2), where τ_W, θ and ϕ are all varying and $\dot{\tau}_W >> \dot{\phi} >> \dot{\theta}$, permits recording on one pattern of the axial ratio for essentially all directions from the antenna [76].

A pattern of an eliptically polarized antenna obtained by the rotating source method is shown in Fig 53. If the amplitude variations are plotted in decibels, the axial ratio, also in decibels, for any direction in space that is recorded on the pattern is the width of the envelope of the excursions. This particular antenna is essentially circularly polarized on axis ($\theta = 0°$) and elliptically polarized in the direction of the maxima of the minor lobes. This sense of polarization is not available from this pattern.

11.2.4 ***Multiple - Amplitude - Componenr Method.*** The ***multiple-amplitude-component method can*** be used to determine the polarization completely without the measurement of phase. It has been shown that the polarization of a wave can be determined from the magnitudes of the responses of four antennas having different, but known, polarizations [70, pp 540–544],[77],[78]. The most convenient choices of polarization for the sampling antenna are horizontal or vertical linear, 45" or 135" linear, and right-hand or left-hand circular, and in addition, any fourth component from this set of six components. These sampling antennas shall have known gains, and the instrumentation

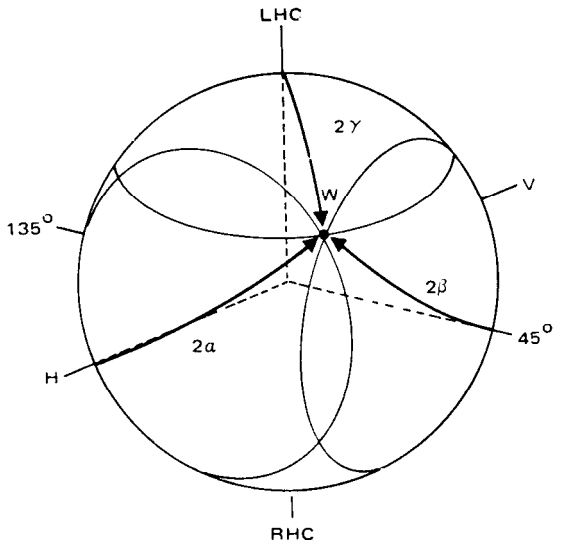

Fig 54
Multiple-Amplitude-Component Method of Polarization Measurement

shall be suitably calibrated to compensate for gain differences. From these data the polarization of the wave, and hence that of the test antenna, can be completely determined. Graphical construction or a solution of a system of linear equations may be used to find the Stokes parameters.

Usually it is more convenient to measure the magnitudes of the polarization ratios. Hence all six components are used [77]. This method is illustrated by use of the Poincaré sphere as shown in Fig 54. The linear, diagonal linear, and circular polarization ratios (ρ_L, ρ_D, and ρ_C, respectively) are measured. From these data 2 α, 2β, and 2 γ, the angles that define the loci of all possible polarizations on the Poincaré sphere and correspond to the polarization ratios ρ_L, ρ_D, and ρ_C, respectively, are determined. The common intersection of the three loci determines the polarization of the wave.

The axial ratio *r* and the sense of polarization are determined from ρ_C since

$$r = \frac{\rho_C + 1}{\rho_C - 1}$$

If *r* is positive the sense is right handed, and if *r* is negative the sense is left handed. The phase angle of the complex circular polarization ratio can be computed by the use of

$$\delta_C = \tan^{-1} \frac{Y_D}{Y_L}$$

where from the polarization box (see 11.1)

$$Y_D = \frac{(1 - \rho_D^2)}{(1 + \rho_D^2)}$$

and

$$Y_L = \frac{(1 - \rho_L^2)}{(1 + \rho_L^2)}$$

Since the tilt angle is one half of Fc, the polarization is completely determined.

A modified version of the multiple-amplitude-component method, which involves measure-

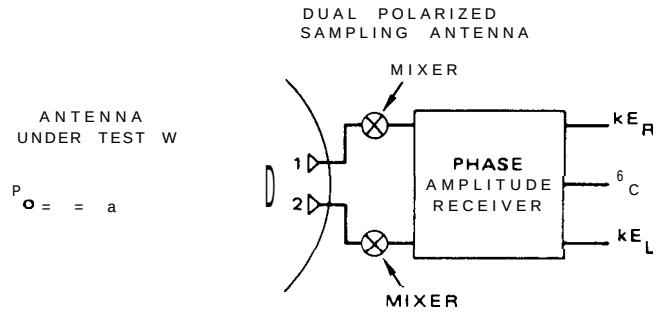

Fig 55
Instrumentation of the Phase-Amplitude Method of Polarization Measurement

ments with a single linearly polarized antenna, may be employed to determine the axial ratio and tilt angle over the entire radiation pattern of the test antenna, provided that the sense is not required. The pattern of the test antenna is measured with the source antenna oriented at 0" (horiztonal), 45°, 90" (vertical), and 135". From these data the polarization ratios ρ_L and ρ_D are determined. With these results δ_C can be computed. The value obtained can be used to determine the tilt angle. The axial ratio is given by

$$r = -\cot \lambda$$

where

$$\lambda = \frac{1}{2} \cos^{-1} (Y_L^2 + Y_D^2)^{1/2}$$

This last result can be obtained from the polarization box (see 11.1). For highly accurate results the linearly polarized antenna should be a polarization standard.

11.2.5 *Phase-Amplitude Method.* In the *phase-amplitude method* all the data required for complete polarization determination can be measured simultaneously, permitting the complete polarization and radiation patterns of an antenna to be measured with a single run through a complete set of pattern cuts. The instrumentation required is illustrated in Fig 55. A dual-polarized receiving antenna is used to sample the field of the antenna under test which is, in this case, used as a transmitting antenna. The outputs of the receiver will be the magnitudes of the responses for each of the polarizations of the sampling antenna and their relative phases. If the two polarizations are orthogonal, the complex polarization ratio can be obtained. The polarizations of the sampling antenna shall be known, and the gains of the two antenna-receiver channels shall be made identical.

In general it is not economically feasible to design a dual-polarized sampling antenna with known pure polarizations. For antenna ranges that employ automated instrument&ion with a computer, it is not necessary to use antennas the polarizations of which are precisely linear or circular, as the case may be, since the measured data can be adjusted by computation, provided that the actual polarizations of the sampling antenna are known. For example, suppose that the measurement requires a sampling antenna with orthogonal circular polarizations, but the sampling antenna has polarizations which are almost, but not quite, circular. The polarizations of the sampling antenna can be measured by use of the modified multiple-amplitude-component method, provided the senses of polarization are known. These data can be entered into the computer. The computer software can be designed to automatically compensate for the characteristics of the sampling antenna.

If the antenna range is not automated and no computer is available, an alternate approach would be the use of a *polarization adjustment network*, external to the sampling antenna, to

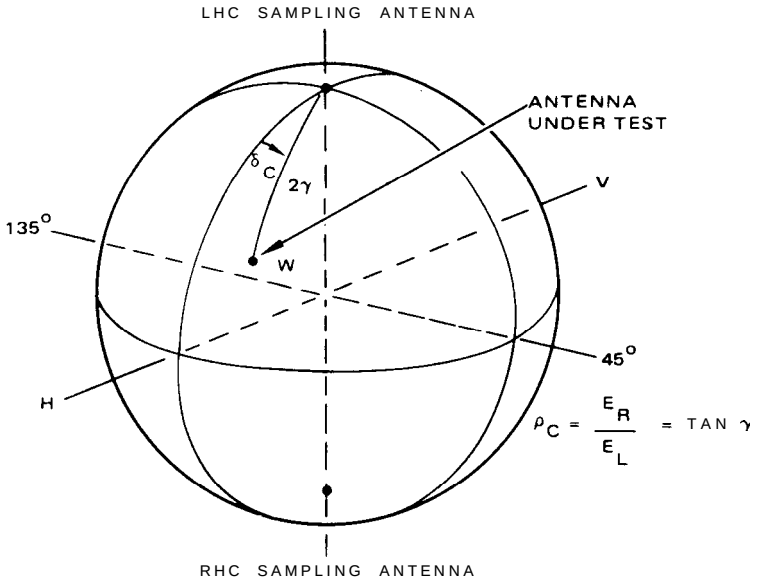

Fig 56
Phase-Amplitude Measurements with Circularly Polarized Antennas

provide the desired polarizations [1, pp 10.1% 10.231. A typical sampling antenna might consist of two orthogonal linear antennas; they may be feeds for a single reflector, for example. The antennas are connected to the inputs of a phase-amplitude receiver (see 5.4). The polarization adjustment network, in its simplest form, consists of an attenuator and a phase shifter inserted in each channel. These networks can be designed to operate at radio frequency and can be inserted between the sampling antenna and the receiver's mixer. Alternately, the network can be designed to be operated at an intermediate frequency. Thus the same network can be used for any frequency covered by the receiver. If the measurement system is capable of recording digital data, and a computer is available, a digital polarization adjustment network may be employed.

If it is desired that right- and left-handed circular polarizations be used, adjustment of the network can be made by employing the polarization-pattern method. A nominally linear reference antenna can be used. Usually the accuracy of adjustment to circular polarization is limited by range reflections, misalignments, and so on. When precise measurements are required, a polarization standard is needed for the adjustment of the gains of the two channels. If a linearly polarized standard is used, the output signals from the two channels are adjusted to be equal. The phase angle δ_C is set equal to zero for horizontal polarization. The system can be checked by rotating the standard through 360°. The output levels should remain constant, whereas the phase angle δ_C should always be twice the value of the rotational angle of the standard, measured with respect to the horizontal.

The measurement of the polarization of the test antenna using circularly polarized sampling antennas is illustrated by use of the Poincare sphere in Fig 56. The complex circular polarization ratio

$$\hat{\rho}_C = \rho_C e^{j\delta_C} = \left[\frac{E_R}{E_L}\right] e^{j\delta_C}$$

and

$$\gamma = \tan^{-1} \rho_C$$

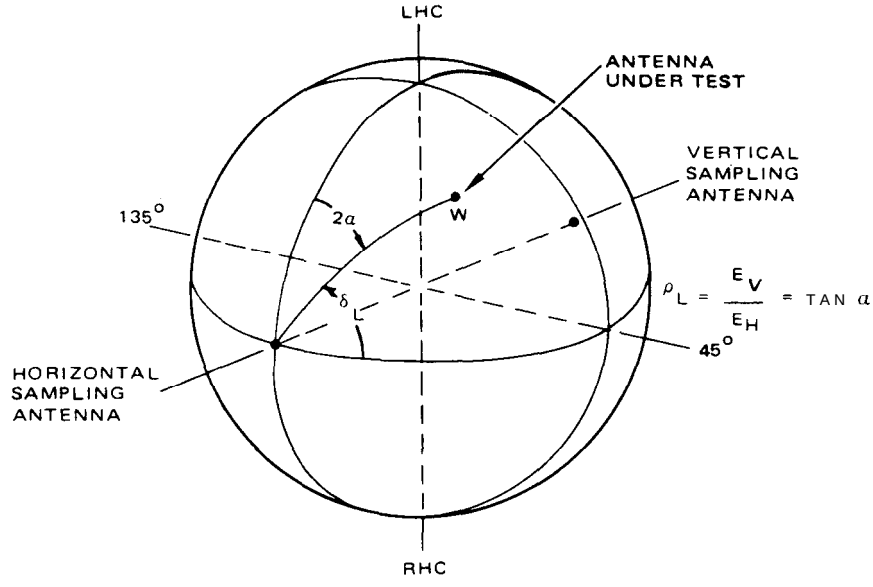

Fig 57
Phase-Amplitude Measurements with Linearly Polarized Sampling Antennas

are obtained from the measurement, and hence the polarization of the wave radiated by the test antenna is uniquely determined.

When orthogonal linear polarizations are used, a polarization standard, usually linear, is required to adjust the polarizations of the sampling antennas and the gains of the two channels. If a linearly polarized standard is employed, the polarizations of the two sampling antennas are first adjusted for optimum nulls for the cases where the orientation of the standard should be cross polarized for each sampling antenna. The outputs of the two channels are then adjusted to be equal with the standard oriented to 45" or 135" with respect to the horizontal. The phase δ_L should be set to zero with the polarization standard rotated to 45" and should remain at zero or 180° as the standard is rotated through 360°. The sense of polarization can be checked using any elliptically polarized antenna with a known sense of polarization, such as a helical antenna. The phase angle δ_L should be positive and less than 180" for left-hand elliptical polarization. It should be negative and with a magnitude less than 180° for right-hand elliptical polarization.

When the field of the test antenna is sampled, the measured result is

$$\hat{\rho}_L = \rho_L e^{j\delta_L}$$

This can be converted to the complex circular polarization ratio by use of the relation

$$\hat{\rho}_C = \rho_C e^{j\delta_C} = \frac{1 + j\hat{\rho}_L}{1 - j\hat{\rho}_L}$$

from which the axial ratio and tilt angle may be found (see 11.1). The method is illustrated by use of the Poincare sphere in Fig 57.

For many applications adequate accuracy can be obtained if care is taken in the fabrication of a linearly polarized antenna which is to be used as a standard without proof of its polarization. Where precision is required, the standard shall be calibrated by an absolute method. The three-antenna method can be employed for this purpose [79],[80]. The only restrictions placed on the antennas for this method are that at least two of them not be circularly polarized and that the polarization be such that sufficient signal levels are maintained. The method is

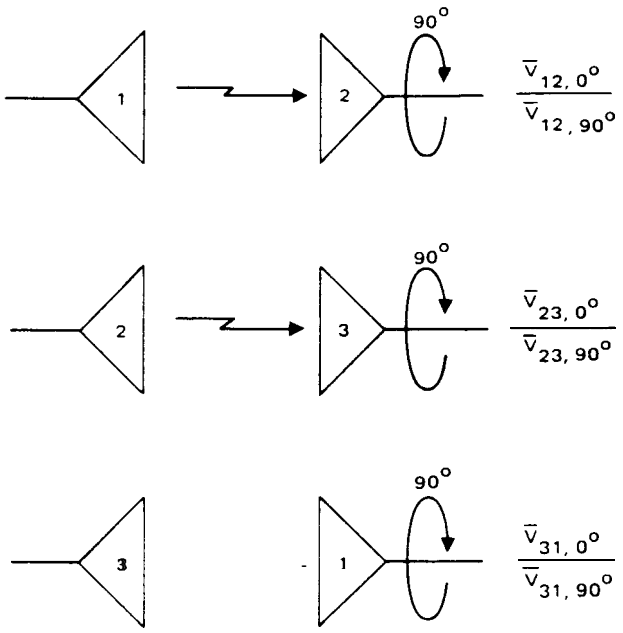

Fig 58
Three-Antenna Absolute Method of Polarization Measurement
$V_{12,0}$ -- Relative Response at Antenna 2 with Its Orientation at 0" ;
$V_{12,90}$ — Relative Response with Its Orientation at 90" ; etc

illustrated in Fig 58. The response is measured twice for each combination of two antennas. The receiving antenna in each case is rotated through 90° for the second measurement. The ratio of the two responses (the antenna at 0° and at 90") is formed. The result yields three complex equations:

$$\frac{\overline{V}_{12,0}}{\overline{V}_{12,90}} = j\left[\frac{1 - \hat{\rho}_{C1}\,\hat{\rho}_{C2}}{1 + \hat{\rho}_{C1}\,\hat{\rho}_{C2}}\right]$$

$$\frac{\overline{V}_{23,0}}{\overline{V}_{23,90}} = j\left[\frac{1 - \hat{\rho}_{C2}\,\hat{\rho}_{C3}}{1 + \hat{\rho}_{C2}\,\hat{\rho}_{C3}}\right]$$

$$\frac{\overline{V}_{31,0}}{\overline{V}_{31,90}} = j\left[\frac{1 - \hat{\rho}_{C3}\,\hat{\rho}_{C1}}{1 + \hat{\rho}_{C3}\,\hat{\rho}_{C1}}\right]$$

where

$\hat{\rho}_{C1}, \hat{\rho}_{C2}$ and $\hat{\rho}_{C3}$ are the complex circular polarization ratios corresponding to the antennas' polarizations. These equations can be solved simultaneously, and the complex polarization ratios for each antenna can be determined. Thus all three antennas can be calibrated with this procedure; for a modified approach see [153].

12. Measurement of Power Gain and Directivity

12.1 General. The power gain of an antenna, in a specified direction, is 4π times the ratio of the power radiated per unit solid angle in that direction to the net power accepted by the antenna from its generator. This quantity is an inherent property of the antenna and does not involve system losses arising from a mismatch of impedance or polarization. To determine the power transfer in a complete system, the antenna input impedance (see 16.1) and the antenna polarization (see 11.2) shall be measured and taken into account.

The directivity of an antenna in a specified direction is 4π times the ratio of the power radiated per unit solid angle in that direction to the total power radiated by the antenna. This term differs from power gain because it does not include antenna dissipation losses.

The ratio of power gain to directivity in the same direction is the radiation efficiency of the antenna (see Section 13).

The power gain (or directivity) of an antenna is usually measured in the direction of its maximum value, and that value is called the peak power gain (peak directivity). Knowledge of the radiation pattern (see Section 3) permits the determination of the gain in any other direction. Of particular importance, when considering pencil-beam antennas, is the determination of side lobe levels. Most often the side lobe levels are referenced to the peak gain of the antenna. Another way to express the side lobe levels is relative to the gain of a lossless isotropic radiator. In both cases the levels are expressed in decibels. Since it is not uncommon for the magnitudes of these two results to be approximately the same for a given side lobe, confusion can arise if the gain reference is not properly specified.

The techniques that are employed for the determination of the power gain of an antenna are dependent upon its frequency of operation. Above 1 GHz, for example, free-space antenna ranges (see Section 4) are commonly available for gain measurements. For these frequencies microwave techniques can be employed since waveguide devices, including electromagnetic horns, are readily available.

For frequencies between 0.1 and 1 GHz, ground-reflection ranges are usually required because free-space conditions are difficult to simulate. Because of the longer wavelengths, microwave techniques become less practical at these frequencies. Antennas operating in this frequency range are often mounted on structures, such as aircraft, which affect their characteristics. For these cases, scale-modeling techniques may be employed (see 7.1). Since it is impractical to scale the finite conductivities and loss factors of the materials of which the antenna and aircraft are constructed, power-gain measurements cannot be performed using the scale model. However, the directivity can be measured. If the efficiency of the full-scale antenna can be established by other means, then the power gain can be determined since the directivity of a properly scaled model antenna and of the corresponding full-scale antenna are the same. It is good practice to verify the results by requiring the aircraft, with the full-scale antenna mounted, to fly a prescribed path relative to a suitable ground station. The system performance, using the full-scale test antenna, can be measured and compared to that predicted from the scale-model measurements.

As the frequency is decreased below 0.1 GHz, the effect of the ground upon the antenna's characteristics becomes increasingly pronounced, making power-gain measurements very difficult. Directive antennas at these lower frequencies are physically large and must be measured in *situ (see* 12.3.3). Often it is satisfactory to calculate the antenna gain and estimate the effect of the ground. Again, scale models can be employed. However, because of the strong effect of the ground on the characteristics of the antenna, the electrical properties of the ground shall also be scaled.

For frequencies below about 1 MHz the antenna power gain is not usually measured, but rather it is the field strength of the ground wave radiated by the antenna which is measured (see Section 17).

For those frequencies for which power-gain measurements are practical, there are two general categories into which the various methods can be placed: ***absolute-gain measurements*** and ***gain-transfer measurements.***

For an absolute-gain measurement no a ***priori*** knowledge of the gains of any of the antennas used in the measurement is requried. This method is usually employed for the calibration of gain-standard antennas and is rarely used in any laboratory except one that specializes in the calibration of standards.

The gain-transfer method, which is also referred to as the ***gain-comparison method,*** is the most commonly employed method for power-gain measurements. This method requires the use of a gain standard to which the gain of the test antenna is compared.

The directivity of a test antenna is obtained by integrating the measured far-field radiation patterns of the antenna over a closed spherical surface. If the antenna losses can be determined by other means, then the power gain of the antenna can be determined from the directivity measurement [81].

12.2 Gain Standards

12.2.1 ***Types of Gain Standards.*** Antennas which are to be used for gain standards should have the following characteristics:

(1) The gain of the antenna shall be accurately known.

(2) The antenna shall have a high degree of dimensional stability.

(3) The antenna's polarization should be linear or, for some applications, circular. If circular polarization is required, two antennas are needed, one right-hand circular and the other left-hand circular. Whether the antenna is linearly or circularly polarized, a high degree of polarization purity is necessary.

Although any antenna meeting these criteria may be used as a gain standard, the two universally accepted antenna types are the dipole and the pyramidal horn. The gains of these antennas can be fairly accurately calculated, and because of their mechanical simplicity they can be manufactured with a high degree of reproducibility.

A thin dipole antenna, properly driven, has a gain of approximately 2.15 dB when its length is adjusted to half-wavelength resonance. (The calibration consists of the adjustment of the dipole length to obtain resonance.) These antennas are commercially available covering frequencies from 77 MHz to 1 GHz.

Pyramidal-horn antennas are commercially available for frequencies from 0.35 to 90 GHz with nominal power gains from about 14 to 25 dB. The calibration curves accompanying them are usually based upon data published by the United States Naval Research Laboratory [82]. These calibration curves have a smooth characteristic, whereas the gain when measured as a function of frequency exhibits an undulating characteristic that is believed to be due to multiple reflections between the horn aperture and the transition between the waveguide and the horn [13],[83]. The computed calibration is considered accurate to ± 0.25 dB for frequencies above 2.6 GHz and to ± 0.50 dB below 2.6 GHz. If a higher degree of accuracy is required, the antenna shall be calibrated by an appropriate standards laboratory.

Both the dipole and the pyramidal-horn antennas are nominally linearly polarized. The dipole antenna by itself has a very high degree of polarization purity. However, because of its broad pattern its characteristics can be greatly affected by its environment and especially by the transmission line used to feed it. For this reason it is difficult to place limits of uncertainty on its polarization. Pyramidal-horn antennas, having directional patterns, are less affected by their environment when used for gain measurements. However, they are likely to be slightly elliptically polarized on axis, with axial ratios between 40 dB and approaching infinity.

It is sometimes necessary to design a gain standard with special properties. For example, the dipole antenna has an omnidirectional pattern in its principal *H* plane, and therefore its pattern can be greatly altered by the measurement environment. Because of this it is sometimes necessary to design a directional antenna such as a dipole array with a reflector, a comer reflector antenna or a log-periodic antenna which is then calibrated for use as a

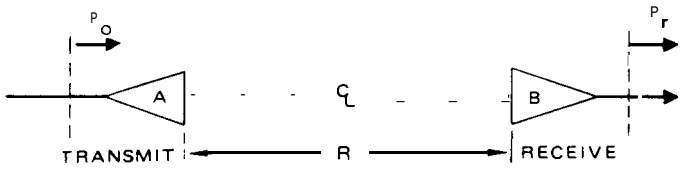

Fig 59
Two-Antenna System Illustrating the Friis Transmission Formula

gain standard. The corrugated conical horn antenna is often used as a gain standard, particularly for the measurement of the gain of antennas operating at millimeter wavelengths [151].

Absolute-gain measurements are usually recommended for the calibration of gain standards. It should be emphasized that if a high degree of accuracy is required, the antenna should be calibrated by a standards laboratory specializing in the calibration of gain standards.

12.2.2 ***Calibration of Gain Standards on a Free-Space Antenna Range.*** Absolute-gain measurements are based upon the Friis transmission formula, which states that for a two-antenna system as shown in Fig 59, the power received at a matched load connected to the receiving antenna is given by

$$P_r = P_0 G_A G_B \left(\frac{\lambda}{4\pi R}\right)^2$$

where P_r is the power received, P_0 is the power accepted by the transmitting antenna, G_A is the power gain of the transmitting antenna, and G_B is the power gain of the receiving antenna [1, pp. 8.2–8.8]. This form of the transmission formula implicitly assumes that the antennas are polarization matched for their prescribed orientations and that the separation between the antennas is such that far-field conditions prevail.

The Friis transmission formula can be written in logarithmic form, from which the sum of the gains, in decibels, of the two antennas can be written as

$$(G_A)_{dB} + (G_B)_{dB} = 20 \log \left(\frac{4\pi R}{\lambda}\right) - 10 \log \left(\frac{P_0}{P_r}\right)$$

If the two antennas are identical, it follows that their gains are equal so that

$$(G_A)_{dB} = (G_B)_{dB} = \frac{1}{2}\left[20 \log \left(\frac{4\pi R}{\lambda}\right) - 10 \log \left(\frac{P_0}{P_r}\right)\right]$$

The procedure in determining the power gain of the antennas is to measure ***R,*** λ, and 10 log P_0/P_r and then compute $(G_A)_{dB}$. Since two identical antennas are required, this method is referred to as the ***two-antenna methbd.*** If antennas A and B are not identical, a third antenna is required to determine the gains.

For the ***three-antenna method*** three sets of measurements are performed using all combinations of three antennas. The result is a set of three simultaneous equations of the form

$$(G_A)_{dB} + (G_B)_{dB} = 20 \log \left(\frac{4\pi R}{\lambda}\right) - 10 \log \left(\frac{P_0}{P_r}\right)_{AB}$$

$$(G_A)_{dB} + (G_C)_{dB} = 20 \log \left(\frac{4\pi R}{\lambda}\right) - 10 \log \left(\frac{P_0}{P_r}\right)_{AC}$$

$$(G_B)_{dB} + (G_C)_{dB} = 20 \log \left(\frac{4\pi R}{\lambda}\right) - 10 \log \left(\frac{P_0}{P_r}\right)_{BC}$$

From these equations all three gains can be determined.

The block diagram of Fig 60 is typical of the instrumentation required for the measurement of gain using the two-antenna or three-antenna methods. The instrumentation shall be highly stable with the source producing a single sinusoidal frequency. With reference to Fig 60 the procedure is to first calibrate the coupling

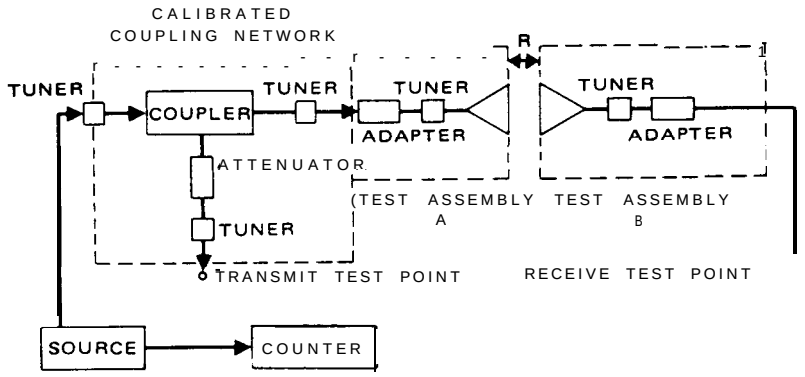

Fig 60
Typical Instrumentation for Two-Antenna and Three-Antenna Methods of Power-Gain Measurement

network between the **source and** the transmitting antenna so that the power measured at the transmit test point can be accurately related to the power into antenna A. Then all components of the system are impedance matched using tuners. The two antennas are separated so that far-field conditions prevail and boresighted so that they are properly aligned and oriented.

The attenuator of the coupling network is adjusted so that the power level at the transmit test point is the same as that at the receive test point. From the calibration of the coupling network the relative power level P_0/P_r can be determined.

If the gains of broad-band antennas are to be measured, it may be necessary to use the swept-frequency technique (see 7.4). Both the two-antenna and the three-antenna methods can be employed [1, pp 8.20–8.24]. **A** block diagram of a typical instrumentation setup is shown in Fig 61. It should be noted that it is not possible to match all the components over a band of frequencies. Therefore the impedances or reflection coefficients of all components shall be measured. The swept-frequency technique should be used for those measurements.

12.2.3 ***Calibration of Gain Standards on a Ground-Reflection Antenna Range.*** For frequencies below about 1 GHz, antennas which might be chosen for use as gain standards will necessarily have moderately broad beams. For these antennas, ground-reflection ranges are often used if accurate gain measurements are required. With some restrictions and modifications, the two- or three-antenna method of gain measurement can be used on a ground-reflection range [84].

The method, as described hereafter, is limited to linearly polarized antennas that couple only to the electric field. To be used with loop antennas, the equations would have to be modified. Since the reflective properties of the earth are different for vertical and horizontal polarizations, elliptically or circularly polarized antennas are excluded. It is recommended that the antennas be oriented for horizontal polarization because of the rapid variation of the earth's reflection coefficient as a function of the angle of incidence when vertical polarization is employed. Such a phenomenon is not present for horizontal polarization.

The criteria for ground-reflection ranges, outlined in 4.4, should be satisfied. The geometry of the ground-reflection range for gain measurements is shown in Fig 62. It is desirable that the range length R_0 be such that $R_0 >> 2h_r$, where h_r is the height of the receiving antenna. When the height of the transmitting antenna is adjusted so that the field at the receiving antenna is at the first maximum closest to the ground, then the gain

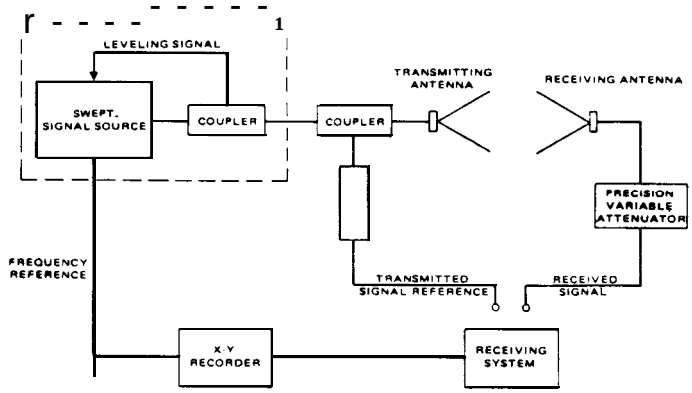

Fig 61
Typical Instrumentation for Swept-Frequency Two-Antenna and Three-Antenna Methods of Power-Gain Measurement

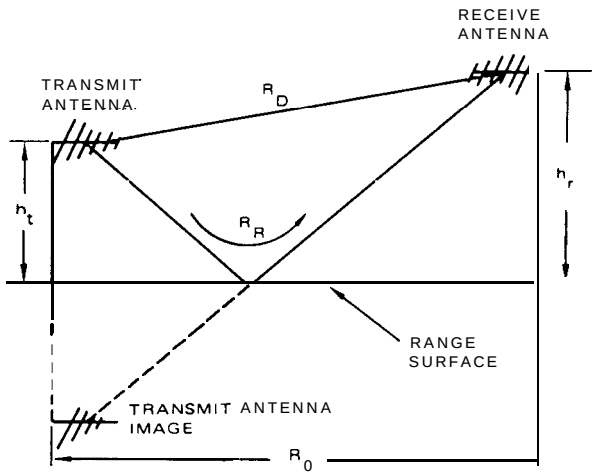

Fig 62
Ground-Reflection-Range Geometry

sum equation for the two-antenna or the three-antenna method can be modified to read

$$(G_A)_{dB} + (G_B)_{dB} = 20 \log \left(\frac{4\pi R_D}{\lambda}\right) - 10 \log \left(\frac{P_0}{P_r}\right) - 20 \log \left[(D_A D_B)^{\frac{1}{2}} + \frac{r R_d}{R_R}\right]$$

where D_A and D_B *are* the directivities along R_D relative to the peak directivities of antennas A and B, respectively. The factor *r* is to be determined. It is a function of the electrical and geometrical properties of the antenna range, the radiation patterns of the antennas, and the frequency of operation. D_A and D_B are obtained from amplitude patterns of the two antennas which should be measured prior to performing the gain measurement. The quantities R_D, R_R, λ, and the ratio P_0/P_r are quantities that are measured directly. Once *r* is determined, the gain sum can be evaluated.

To obtain *r* the preceding measurement is repeated, but this time with the height of the transmitting antenna adjusted to a position such that the field at the receiving antenna is a minimum. To distinguish the quantities measured with this geometry from those of the previous one, let all the quantities associated with the latter geometry be represented by the same letters, except with primes. With this notation the equation for *r can* be written as

$$r = \left(\frac{R_R R'_R}{R_D R'_D}\right) \left[\frac{\left[(P_r/P'_r)(D'_A D'_B)\right]^{\frac{1}{2}} R_D - \left(D_A D_B\right)^{\frac{1}{2}} R'_D}{\left(P_r/P'_r\right)^{\frac{1}{2}} R_R + R'_R}\right]$$

where R_R, R_D, and P_r *are* obtained with the transmitting antenna adjusted for a maximum signal at the receiving antenna, and R'_R, R'_D, and P'_r are obtained with the antenna adjusted for a minimum signal at the receiving antenna. The relative directivities D_A, D'_A, D_B, and D'_B are obtained from the amplitude patterns of the two antennas.

The instrumentation for this measurement is essentially the same as that for the free-space range measurement (see Fig 60). Accuracies of ± 0.3 dB are attainable with this method.

12.2.4 ***Calibration of Gain Standards on an Extrapolation Antenna Range.*** Multipath and proximity effects are always present for measurements made on antenna ranges (see 4.2 and 12.5). The extrapolation technique [79] includes provisions for rigorously evaluating and correcting for errors due to these effects. The received signal is measured as a function of the spacing between the transmitting and the receiving antennas. The multipath effect is manifested by a cyclic characteristic on the curve obtained by plotting the received signal as a function of spacing.

The cyclic variation in the received signal due to the effect of multipath can be averaged out mathematically or by adjusting the time constant of the instrumentation so that it cannot track the cyclic variations but rather allows the average value to be recorded. By fitting a curve to the averaged data, the signal level can be extrapolated to that which would be measured in the far field. The method of curve fitting is described in detail in [79]. In this manner both the proximity and the multipath interference effects are removed. From this result the power gain can be computed.

The extrapolation technique, when combined with the ***generalized three-antenna measurement technique*** [32],[33],[79], is capable of yielding not only the power gains but also the polarizations of the three antennas (see 11.2). There is the restriction that none of the three antennas be nominally circularly polarized. If one of the antennas is circularly polarized, then only that antenna's characteristics may be completely determined. If two or more of the antennas are nominally circularly polarized, the method fails.

The extrapolation range shall have a precision movable tower which allows boresight between the transmitting and the receiving antennas to be maintained as it is moved over the length of the range. Measurements may be conducted at distances less than $2D^2/\lambda$, where *D* is the maximum dimension of the antennas under test.

The tower heights should be at least 15 percent of the maximum separation between antennas. This places a practical limitation on the gains of antennas that may be tested since the required maximum spacing between towers increases as the gains of the test antennas are increased. Since the tower heights must also be proportionally increased, it becomes increasingly difficult and expensive to construct a movable tower that maintains boresight over the required length of the range. Antennas with gains of about 40 dB represent a practical upper limit [85].

This technique is capable of yielding measured gains with uncertainties as low as ±0.05 dB and with more routine measurements to ±0.08 dB [152].

12.3 Gain-Transfer Measurements

12.3.1 ***Measurement of Linearly Polarized Antennas.*** The gain-transfer method is one in which the unknown power gain of a test antenna is measured by comparing it to that of a gain-standard antenna [1, pp 8.15–8.18]. The measurements can be performed on either a free-space or a ground-reflection range. (It can also be performed with a test antenna the power gain of which has to be measured ***in situ*** as discussed in 12.3.3 and 12.4.)

Ideally the test antenna is illuminated by a plane wave which is polarization matched to it, and the received power is measured into a matched load. The test antenna is replaced by a gain standard, leaving all other conditions the same. The received power into its matched load is again measured. From the Friis transmission formula it can be shown that the power gain $(G_T)_{dB}$ Of the test antenna, in decibels, is given by

$$(G_T)_{dB} = (G_S)_{dB} + 10 \log P_T/P_S$$

where $(G_S)_{dB}$ is the power gain of the gain-standard antenna, P_T is the power received with the test antenna, and P_S is that power received with the gain- standard antenna.

One method of achieving this exchange between test and gain-standard antennas is to mount the two antennas back to back on either side of the axis of an azimuth positioner. With this configuration the antennas can be switched by a 180“ rotation of the positioner. Care shall be taken to position the antennas so that they will be in the same location when switched. Usually absorbing material is required immediately behind the gain standard to reduce reflections in its vicinity which might perturb the illuminating field.

Swept-frequency gain-transfer measurements can be performed for testing broad-band antennas [1, pp 8.23–8.24]. The procedure is essentially the same as that for the swept-frequency absolute-gain measurement (see 12.2.2), except that the measurement is repeated with the test antenna and the gain standard. The reflection coefficients of all the components shall be measured as a function of frequency so that corrections can be made to the measured power gain.

12.3.2 ***Measurement of Circularly and Elliptically Polarized Antennas.*** For the special case of circularly polarized test antennas it is possible to design and calibrate orthogonal circularly polarized gain-standard antennas. This is particularly useful when production runs of power-gain measurements are required. In general, however, the power gains of circularly and elliptically polarized test antennas are measured with the use of linearly polarized gain standards. This is valid because the total power of the wave radiated by an antenna can be separated into two orthogonal linearly polarized components (see 11.1). Thus partial power-gain measurements can be performed using two orthogonal linearly polarized gain standards from which the total power gain of the test antenna can be determined. A single linearly polarized gain standard can be employed and rotated 90” to achieve the two orthogonal polarizations.

A power-gain-transfer measurement as outlined in 12.3.1 is performed with the gain standard oriented for vertical polarization. The measurement is then repeated with the gain-standard and source antennas oriented for horizontal polarization. From these partial power-gain measurements the total power gain $(G_T)_{dB}$, of the test antenna, in decibels, can

be computed by use of the equation

$$(G_T)_{dB} = 10 \log (G_{TV} + G_{TH})$$

where G_{TV} and G_{TH} are the partial power gains with respect to vertical linear polarization and horizontal linear polarization, respectively. These measurements can be performed on either a free-space or a ground-reflection range.

12.3.3 ***Measurement in the High-Frequency Range (3-30 MHz).*** At frequencies between about 3 and 30 MHz medium- and long-distance propagation of electromagnetic waves depends chiefly upon sky waves reflected from the ionosphere. For paths of 2000 to 4000 km the antenna pattern and power gain at elevation angles between 5 and 30" above the horizon are of primary importance. Antenna-pattern and power-gain measurements shall be made at full scale and *in situ* as discussed in Section 9 [59].

The measurements require the use of an aircraft with a suitable transmitting atenna mounted on it, which flies at fixed altitudes along circular paths centered upon the test antenna. To measure the pattern, the amplitude of the received signal along with the azimuthal angles and elevation angle to the aircraft are recorded. The power gain is measured by comparing the power received by the test antenna to that received by a gain-standard antenna located near the test antenna.

A horizontally polarized dipole antenna may be used as a gain standard, At these frequencies the pattern and power gain of a dipole antenna are greatly affected by the ground. For the gain measurement the dipole height is adjusted so **that its** main lobe is pointing in the same direction as that of the test antenna (between 5 and 30° from the horizon). The power gain $(G_S)_{dB}$ of **the** dipole antenna, in decibels, as a function of height and elevation angle can be computed from the following equation:

$$(G_S)_{dB} = 2.15 + 10 \log \left[\frac{R_{11}}{R_{11} + \mathrm{Re}(R_H(90°)Z_m)} \left| e^{jkH \sin \Psi} + R_H(\Psi)\, e^{-jkH \sin \Psi} \right|^2 \right]$$

where Re means the real part of, R_{11} is the real part of the self-impedance of the dipole in free space, Z_m is the mutual impedance between the dipole and its image in a perfect conductor, k is the free-space wave number, ***His*** the height of the dipole above ground, Ψ is the elevation angle of the first lobe of the vertical radiation pattern of the dipole, and $R_H(\Psi)$ and $R_H(90°)$ ***are*** the complex reflection coefficients of the imperfect ground for horizontal polarization at angles Ψ and 90°, respectively, measured from the horizontal (the complement of the angle of incidence). With the use of this equation, contour plots of the, power gain of the dipole as a function of height above ground and elevation angle can be constructed [86].

It is not practical to employ vertically polarized gain-standard antennas for this purpose [87], since the power gain of such antennas at low elevation angles is low, and varies drastically with the moisture content of the ground. Thus if the test antenna is vertically polarized, it is necessary to compare its cross-polarized partial gain (partial gain with respect to horizontal polarization) to a horizontally polarized gain standard for the gain-transfer measurement. From this result the partial gain with respect to vertical polarization, which is the quantity desired, can be determined.

This can be accomplished by rotating the transmitting antenna on the aircraft in such a way that the transmitted signal is alternately vertically and horizontally polarized. It is usually necessary to calibrate the rotating antenna since its gain will vary as it is rotated. The signal is received by the test antenna and the gain standard. A comparison between the maximum power received by the gain standard and the minimum signal received by the test antenna yields the partial gain of the test antenna with respect to horizontal polarization. A comparison of the maximum and minimum powers received by the test antenna then yields the partial gain with respect to vertical polarization which is the gain sought.

The accuracy of this technique depends upon how well the characteristics of the ground are

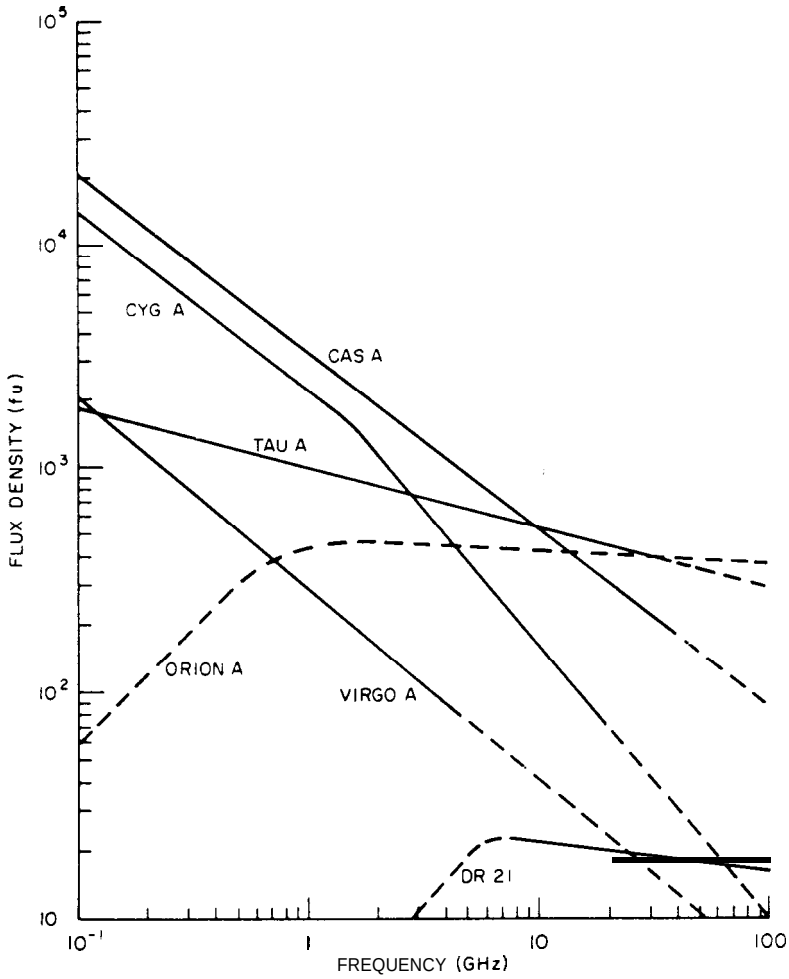

Fig 63
Flux-Density Spectra of Several Radio Stars (from [92])

known and upon the terrain of the antenna site. If the site is flat and unobstructed and the ground constants are accurately known, the uncertainty in the measured gain can be ± 0.5 dB or better. In general, however, uncertainties of ± 1 dB can be conservatively expected.

12.4 Measurement of the Power Gain of Electrically Large Antennas

12.4.1 General. The measurement of the power gain of electrically large antennas is generally impractical and in some cases even impossible to perform on an antenna test range due to the fact that the antenna-range length, required to satisfy the far-field criterion, may be several tens of kilometers. In addition, large steerable antennas usually experience gravity-induced structural deviations as the antenna is moved. This necessitates the measurement of gain as a function of the antenna's elevation pointing angle. These problems can be largely overcome by the use of extraterrestrial radio sources or satellite-borne beacons [58, pp 10–15], [85], [88]–[90].

The locations and radiation flux densities of certain extraterrestrial radio sources are ac-

Table 1
Information about Several Radio Sources [92]

Radio Star	Type	Position: Right Ascension *hours*	Position: Declination degrees	Size: Right Ascension hours	Size: Declination degrees	Visibility: North Latitude degrees	Visibility: South Latitude degrees	Spectral Index
Cas A	SR	23.4	58.6	3.43	x 4	90	11	- 0.787
Tau A	SR	5.5	22.0		x 4	90	48	- 0,263
Orion A	EN	5.5	- 5.4	3.5	x 3.5	65	75	0
Cyg A	RG	20.0	40.6	1.6	x 1	90	29	- 1.205
Virgo A	RG	12.5	12.7	1	x 1.8	73	57	- 0.853
DR 21	EN	20.6	42.2		< 0.3	90	28	1.75, - 0.13

*SR ≡ supernova remnant; EN ≡ emission nebula; RG ≡ radio galaxy.

curately known so that they may be used for power-gain measurements. Furthermore these sources cover a broad frequency spectrum. Their flux densities vary with frequency, but they have been accurately measured over the 100 to 10 000 MHz range [91].

Man-made beacons aboard satellites have the advantage of being coherent sources, and a sufficient signal-to-noise ratio can usually be obtained to test moderate gain antennas. The disadvantages are that the beacon is usually limited to a single frequency, and for accurate measurements a geostationary satellite shall be used. Thus the measurement is limited to a single pointing direction. If the incident flux densities from satellites are not accurately known, the gain-transfer method of gain measurement shall be employed for these sources.

12.4.2 Use of ***Extraterrestrial Radio Sources for Power-Gain Measurements.*** The flux-density spectra of several radio stars are given in Fig 63. The location, size, spectral index α, and type of phenomenon believed responsible for the radio star are given in Table 1. Also given is the visibility of the source. Visibility refers to that interval of terrestrial latitudes from which the source's apparent daily path through the sky rises to at least 20° above the horizon. This 20" minimum assumes that the source can be seen by an antenna for at least one hour and is sufficiently far above the horizon to be discernible above the atmospheric and ground noise [92].

Cassiopeia A, Cygnus A, and Taurus A are the strongest resources of relatively small angular size. Their flux densities have been accurately measured over a frequency range of 30 MHz to 16 GHz[93]. These are the most useful sources for antenna-gain measurements. It, should be noted, however, that Cassiopeia A has an annual decrease in flux density of 0.9 ± 0.1 percent, Cygnus A has a curvature in its spectrum, and Taurus A shows a significant degree of linear polarization [89]. These effects have been thoroughly studied and documented. Because of their small angular size, they may be treated as discrete or point sources, provided the test antenna's beamwidth is greater than 10 minutes.

The tabulated flux densities for celestial radio sources are usually given at discrete frequencies, which may be different from the frequency at which the antenna's gain is to be measured. The relation between power flux density S and radio frequency f can be expressed as $S \propto f^{\alpha}$, where α is the spectral index. Thus one can use the known flux density at the frequency that is nearest to the test frequency to compute the required flux density. If f_k is the frequency at which the flux density for a given source is known, and f the frequency at which the gain is to be measured, then

$$S(f) = \left(\frac{f}{f_k}\right)^{\alpha} S(f_k)$$

The noise power radiated by a radio star is in general randomly polarized. Thus the polarization efficiency of the wave and antenna system is ½, and the power received when the antenna is pointing at the radio star is given by

$$P_R = \frac{SA_e}{2} \equiv \frac{S\lambda^2 G_T}{8\pi} \quad [W/Hz]$$

$$= kT_a$$

where A_e is the effective area, G_T is the antenna gain, λ is the wavelength, k is Boltzmann's constant, S is the power flux density, and T_a is the effective noise temperature of the radio star referred to the antenna terminals. (It is the measured antenna temperature due to the source above that due to sky background.) From this the gain of the antenna can be written as

$$G_T = \frac{8\pi k T_a}{S\lambda^2}$$

The equation is valid for a point-source radio star radiating through a lossless atmosphere. Since this condition is not normally satisfied, correction factors shall be inserted in the equation, that is, the gain can be written as

$$G_T = \frac{8\pi k T_a}{S\lambda^2} K_1 K_2$$

where K_1 corrects for atmospheric attenuation and K_2 for the effect of the angular extent of the source.

The factor K_1 can be obtained from the approximate expression

$$K_1(\theta_z) = (a_o \ell_o + \rho_{aw} \ell_w) \sec \theta_z \ [dB]$$

where θ_z is the zenith angle at which the antenna is pointing, ℓ_o (4 km) and ℓ_w (2 km) are characteristic heights for the atmospheric oxygen and water vapor, respectively, and a, and ρ_{aw} are the frequency-dependent attenuation coefficients for molecular oxygen and water vapor, respectively. The values of a, and ρ_{aw} are available at some frequencies [94]. However, it may be more accurate to measure this effect than to calculate it [95].

The correction factor K_2 is approximately unity when the angular diameter of the source is less than about one fifth the antenna half-power beamwidth. If the source is larger than one fifth the antenna half-power beamwidth, K_2 can be computed from the equation

$$K_2 = \frac{\iint_{\Omega_s} B(\Omega)\, d\Omega}{\iint_{\Omega_s} B(\Omega) F_n(\Omega)\, d\Omega}$$

where $B(\Omega)$ is the brightness distribution of the radio source, $F_n(\Omega)$ is the normalized power pattern of the antenna, and Ω_s is the solid angle subtended by the source. Curves of the correction factor K_2 versus the ratio of source diameter to antenna half-power beamwidth have been developed for several representative antenna power patterns [90].

An examination of the equation for antenna gain reveals that the gain measurement with the use of celestial sources is basically a noise-power or noise-temperature measurement. This type of measurement requires the use of a radiometer. The accuracy of the measurement is strongly dependent upon the accuracy of the instrumentation used.

A simplified block diagram of the instrumentation is shown in Fig 64. The measurement of the antenna noise temperature due to the source is accomplished by comparing the change in output ΔP_S of the radiometer, which results from pointing tine antenna at the source from a region in the vicinity of it, to the change in output ΔP_K due to a known temperature change of a load connected in place of the antenna. If ΔT_K is the known change in temperature of the load, then the antenna temperature T_a is given by

$$T_a = \Delta T_K \frac{\Delta P_S}{\Delta P_K}$$

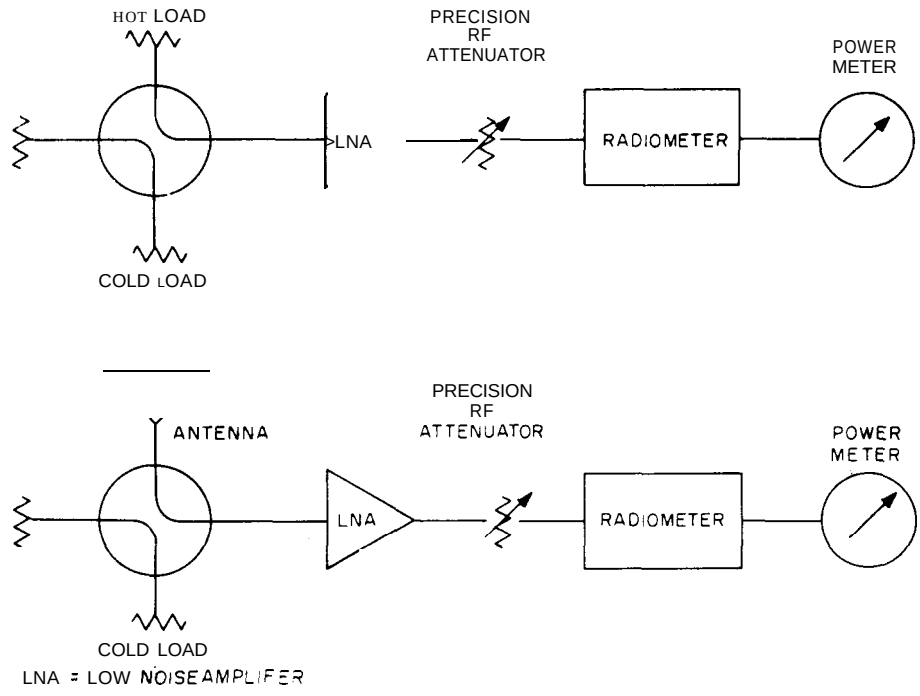

Fig 64
Typical Instrumentation for the Measurement of Antenna Power Gain and Temperature Using a Radio-Star Method

This result assumes that the radiometer is linear with respect to power.

To move the antenna from the sky to the source, it is convenient to use the diurnal rotation of the earth. The measurement is made by locking the antenna in a position ahead of the source and letting the earth's diurnal rotation move the source through the antenna's electrical axis [58, pp 137–156]. The advantage of this procedure is that the background emission received by the antenna's side and back lobes remains unchanged during the measurement.

The change in load temperature ΔT_K is obtained by switching from the calibrated cold load to the calibrated hot load. ΔP_S and ΔP_K can be measured with the use of the precision radio-frequency attenuator shown in Fig 64. For example, ΔP_K can be determined by first connecting the cold load and adjusting the output to a convenient reference level. The hot load is then substituted for the cold load. The radio-frequency attenuator is adjusted to restore the output to the original reference level. The change in attenuator setting gives ΔP_K in decibels.

Once the antenna noise temperature due to the source is measured, the gain can be computed.

In addition to the correction factors K_1, which is due to the atmospheric absorption, and K_2, which is due to the relative angular size of the source with respect to the antenna bearnwidth, there are additional factors which should be considered if highly accurate measurements are required [96]. The most significant ones are:

(1) K_3, *the antenna pointing factor.* If the main beam of the antenna does not pass through the center of the source, the measurement will be in error. This factor includes the error in alignment of the antenna's axes.

(2) K_4, *the polarization factor (polarization*

efficiency). If the source has a linearly polarized component, then the assumption that the polarization efficiency is one half is in error. To determine this factor the polarization of the source and the antenna shall be measured.

(3) K_5, the ***system response factor.*** This is due to the instabilities of the instrumentation and to the radiometer time constant which may result in a time delay of the recorded power levels and therefore reduced amplitudes [58, pp 144–146].

NOTE : See [96] for additional atmospheric effects.

If these factors are included, the gain of the test antenna can be written as

$$G_T = \frac{8\pi k T_a}{S\lambda^2} K_1 K_2 K_3 K_4 K_5$$

12.4.3 ***Measurement of Absolute Antenna Noise Temperature and Figure of Merit*** G/T. In order to determine the absolute antenna noise temperature it is first necessary to measure the effective noise temperature of the receiver. This is accomplished by the Y-factor technique which requires the use of calibrated hot and cold reference loads (see Fig. 64). The effective noise temperature of the receiver T_R is given by [97].

$$T_R = \frac{T_H - Y_1 T_C}{y_1 - 1}$$

where T_H and T_C are the temperatures of the hot and cold loads, respectively, and Y_1 is the ratio of the noise power received with the hot load connected $(T_H + T_R)$ to the noise power received with the cold load connected $(T_C + T_R)$.

Once Y, is determined, the hot load is replaced by the test antenna. Its absolute noise temperature T is given by

$$T = Y_2 T_C + T_R (Y_2 - 1)$$

where Y_2 is the ratio of the noise power received with the antenna connected to that with the calibrated cold load connected.

The measurement of Y, and Y_2 can be accomplished by means of the precision radio-frequency attenuator shown in Fig 64 in the same manner as outlined for the determination of ΔP_K and ΔP_S (see 12.4.2).

Generally it is the figure of merit of the antenna-receiver system that is sought. The system figure of merit is defined as the antenna gain G divided by the system noise temperature T referred to the antenna output terminals. The system noise temperature T is the sum of the antenna noise temperature and the effective input noise temperature of the receiver [92]. The system ***G/T can*** be measured with a radio-star method [97], that is

$$G/T = \frac{8\pi k (Y - 1)}{S\lambda^2} K_1 K_2$$

where Y is the ratio of the noise power available when the antenna is directed toward the radio star to that available when the antenna is pointed toward the background sky at the same elevation angle, K_1 is the correction factor for atmospheric attenuation, and K_2 is the correction factor for the relative angular size of the source with respect to the antenna's beamwidth. For high accuracy the additional correction factors discussed in 12.4.2 apply here also.

A typical procedure for the measurement is as follows. The antenna is pointed toward the radio star (either automatic or manual tracking is required). A peak response establishes a reference level. The antenna tracking is stopped and, as the radio star drifts away, the antenna points toward the background sky. The radio-frequency attenuator is adjusted to restore the original reference level. The change in attenuator setting is taken as the Y factor in decibels.

12.4.4 ***Measurement of the Power Gain of Electrically Large Antennas Using the Gain-Transfer Method. As*** discussed in 12.2 there is a practical limitation on the maximum gain of a gain-standard antenna imposed by the available techniques for accurate calibration. At microwave frequencies the maximum gain is about 30 dB. This gain is marginal for use with even the strongest celestial ***sources.*** Therefore

the gain-transfer method in general is not recommended when celestial sources are to be employed. It is adequate if man-made beacons on satellites are employed. Highly accurate measurements can be performed for this case [85].

The procedure is basically the same as the one used on an antenna test range. Usually the gain standard is mounted on the large antenna and oriented so that the beam axes of the two antennas are parallel. In some cases the gain standard is permanentally installed for a continued system check.

The polarization mismatch between the wave radiated from the satellite and the test and gain-standard antennas can be a significant source of error. To correct for this effect, the polarizations of the wave and the antennas shall be measured. From these results the polarization efficiencies for the wave-test antenna and the wave-standard gain antenna systems can be computed (see 11.1). Other sources of error include errors in tracking the satellite, instabilities in the transmitting and receiving systems, and receiver nonlinearity [85].

12.5 Errors in Power-Gain Measurements

12.5.1 *General.* This section deals with the estimation of the uncertainties that are encountered when power-gain measurements of antennas are performed. The term "uncertainty" is used here to mean the overall error of the test parameters, that is, the sum of the systematic errors and the random errors, as distinguished from the various component errors.

Many of the sources of error associated with specific techniques are discussed in the sections describing those techniques. There are sources of error, however, that most methods of power-gain measurement have in common. These will be discussed in this section.

12.5.2 Sources of ***Error.*** Ideally the conditions required for power-gain measurements can be catagorized as follows [83]:

(1) *Antenna* ***range.*** Free-space conditions, uniform plane-wave field at the receiving antenna

(2) ***Antennas.*** Reciprocal, impedance matched, aligned and properly boresighted, in addition the antennas shall be suitably polarization matched (see 11.1)

(3) ***Equipment operation.*** Components, ideal and impedance matched, single sinusoidal frequency, single waveguide mode, stable generator and receiver, adequate sensitivity and dynamic range

It is the deviations from these ideal conditions that produce uncertainties in the measurement of power gain.

In general, deviations from the conditions listed in catagory (1) are the ones for which it is the most difficult to establish corrections. Those conditions imply an infinite separation between the transmitting and the receiving antennas, and an absence of multipath interference, extraneous scattering of energy into the receiving antenna, and reradiative mutual coupling (see 4.2). Multipath interference, extraneous scattering, and reradiative mutual coupling are always present. Their effects and the methods of suppressing them are discussed in detail in 4.2.

The free-space conditions listed imply that the transmitting medium is reciprocal, lossless, linear, and isotropic. These conditions usually can be considered to prevail for antenna ranges. (This is not true for the case of measurements employing radio stars or satellite beacons as sources or for measurements on antenna ranges at millimeter wavelengths.)

A finite spacing between transmitting and receiving antennas cannot be avoided. The error produced by finite spacing is of a systematic type which results in a measured value of gain lower than the actual far-field gain. This negative-valued systematic error decreases asymptotically with increasing separation between antennas. In order to estimate the magnitude of the correction factor, it is convenient to think of the error as being caused by two effects. One is due to the fact that the gain of the test antenna does indeed vary with distance due to the near-field components still present, even though the spacing may be greater than $2D^2/\lambda$, where D is the maximum dimension of the test antenna and λ is the

wavelength. At $2D^2/\lambda$, for a typical antenna, this correction factor is about 0.05 dB, and it will decrease with increased spacing. The second effect is that of a nonuniform illumination of the test antenna due to the relative sizes of the transmitting and receiving antennas and their separation. A technique for estimating the effect of nonuniform illumination is presented in 4.2. For typical transmitting and receiving antennas, for which the amplitude taper across the aperture is about 0.25 dB at a spacing of $2D^2/\lambda$, an error of about 0.1 dB can be expected. This results in a total error of 0.15 dB for a $2D^2/\lambda$ spacing. It should be noted that a reduction in amplitude taper of the illuminating field can only be achieved either by increasing the spacing between the two antennas or by choosing a transmitting antenna with a broader beam. In either case there is a danger of increasing multipath interference. The effects of finite spacing between antennas has been studied extensively for the special case of electromagnetic horns [13], [82], [98]–[101].

Impedance and polarization mismatches can be important sources of error in gain measurements. Corrections for these errors can be made if measurements of the appropriate impedances and polarizations of the antennas can be performed.

Impedance mismatches involve not just the antennas but also the generator and receiver (load). To illustrate this point, recall that the power P_0 which appears in the Friis transmission formula is the power accepted by the transmitting antenna. Usually one measures the available power from the generator P_A by conjugately matching a power meter to the generator through a length of transmission line. Alternately one can simply match the power meter to the transmission line and measure what one might refer to as the line-matched power P_M. The values P_A and P_M are equal only for the case where the generator is matched to the transmission line. If the generator has a reflection coefficient Γ_G looking into its output from an arbitrary reference plane on the transmission line and the transmitting antenna has a reflection coefficient Γ_T measured at the same reference plane, then the power accepted by the antenna is given by either

$$P_0 = P_A M_1$$

or

$$P_0 = P_M M_1'$$

where

$$M_1 = \frac{(1-|\Gamma_G|^2)(1-|\Gamma_T|^2)}{|1-\Gamma_G\Gamma_T|^2}$$

$$M_1' = \frac{1-|\Gamma_T|^2}{|1-\Gamma_G\Gamma_T|^2}$$

The form that is used is dependent upon which power was measured. If there is any significant loss between the reference plane and the antenna, that loss shall be taken into account. Likewise, if the test antenna has an input reflection coefficient of Γ_R and its load has a reflection coefficient of Γ_L, then the power into the load is further reduced by a factor M_2, where

$$M_2 = \frac{(1-|\Gamma_R|^2)(1-|\Gamma_L|^2)}{|1-\Gamma_R\Gamma_L|^2}$$

M_1 and M_2 can be evaluated by measuring Γ_G, Γ_T, Γ_R, and Γ_L. Often the load and generators are matched using tuners. In this case M_1 and M_2 reduce to

$$M_1 = (1-|\Gamma_T|^2)$$

$$M_2 = (1-|\Gamma_R|^2)$$

These corrections can be made in the absolute gain method (see 12.2) and in the gain-transfer method.

The equation for the measured gain of the test antenna $(G_T)_{dB}$, using the gain-transfer method, can be written to include these effects as

$$(G_T)_{dB} = (G_S)_{dB} + 10 \log \left[\frac{P_T}{P_S}\right] + 10 \log \frac{(M_2)_T}{(M_2)_S}$$

where $(G_S)_{dB}$ is the gain of the standard in decibels, P_T/P_S is the ratio of the power received with the test antenna and the standard antenna, $(M_2)_T$ is the correction factor M_2 with the test antenna connected to the load, and $(M_2)_S$ is the correction factor M_2 with the standard connected to the load.

For absolute-gain measurements the corrections can be made in the same manner. However, by treating the measurement as an insertion-loss measurement, the correction factors for impedance mismatches are included automatically [83]. The procedure, in this case, is to connect the generator directly to the load and measure the absorbed power P_L^i. The antennas are then inserted at the proper spacing. By using a precision attenuator, the power level at the load is adjusted to restore the original level. The ratio of the power P_L^f delivered with the antennas inserted to the power P_L^i delivered when the load is connected directly to the generator is obtained by noting the change in the settings of the precision attenuator. The product of the gains of the receiving and transmitting antennas is given by

$$G_T G_R = \left(\frac{4\pi R}{\lambda}\right)^2 \left(\frac{P_L^f}{P_L^i}\right) M$$

where

$$M = \frac{|1 - \Gamma_R \Gamma_L|^2 \, |1 - \Gamma_G \Gamma_T|^2}{(1 - |\Gamma_R|^2)(1 - |\Gamma_T|^2)|1 - \Gamma_G \Gamma_L|^2}$$

If the transmitting and receiving antennas are not polarization matched, then the Friis transmission formula, as given in 12.2, shall be multiplied by the polarization efficiency p (see 11.1). Thus there is an apparent error in the measured gain unless the factor p is known and the measured gain is corrected. The effect of polarization mismatch can be illustrated with the following examples. First consider the case where the gain of a circularly polarized test antenna is measured using the method of partial gains (see 12.3.2). Suppose that the test antenna is purely circularly polarized, and that the gain standard is purely linearly polarized, but that the transmitting antenna has a finite axial ratio. Then Table 2 indicates the errors one might expect due to the finite axial ratio of the transmitting antenna.

Table 2
Errors in the Measured *Gain* **of a Purely Circularly Polarized Antenna Due to a Finite Axial Ratio of the Transmitting Antenna**

Transmitting Antenna Axial Ratio (dB)	Measurement Error [dB]	
	Same Sense	Opposite Sense
20	+0.828	-0.915
25	+0.475	-0.503
30	+0.270	-0.279
35	+0.153	-0.156
40	+0.086	-0.109
45	+0.049	-0.049
50	+0.027	-0.028

Next consider the case of the measurement of a linearly polarized antenna with an axial ratio of 25 dB using an ideal gain standard (linearly polarized) and a transmitting antenna having a finite axial ratio. The errors expected for several different axial ratios are given in Table 3.

Table 3
Errors in the Measured Gain of a Linearly Polarized Antenna Due to a Finite Axial Ratio of the Transmitting Antenna*

Transmitting Antenna Axial Ratio (dB)	Measurement Error [dB]	
	Same Sense	Opposite Sense
20	-0.035	+0.063
25	-0.014	+0.041
30	-0.002	+0.003
35	+0.005	+0.022
40	+0.009	+0.019
45	+0.011	+0.016
50	+0.012	+0.015

*The test antenna has an axial ratio of 25 dB. The gain standard is purely linearly polarized.

For the preceding examples the errors due to polarization mismatch can be significant, especially when a linearly polarized gain standard is used to measure circularly polarized antennas by means of the partial-gain method. The effect is less severe when a nominally linearly polarized antenna is being measured. As a point of reference, a typical electromagnetic-horn gain standard is likely to have an axial ratio between 40 dB and approaching infinity. If corrections for these effects are to be made, the polarizations of all antennas used shall be measured. In an automated system with a minicomputer, the computations could be made a part of the computer software.

12.5.3 ***Estimation of Uncertainty in Gain Measurements.*** The determination of the gain of an antenna involves the measurement of a number of quantities which are used to compute the gain. For example, consider the insertion-loss method of absolute gain measurement discussed 12.5.1 The gain-product equation can be written as

$$G_T G_R = \left(\frac{4\pi Rf}{c}\right)^2 \alpha M$$

where f is the frequency in hertz, c is the free-space velocity of light, α is the measured power ratio, and M is the correction factor for impedance mismatch. To determine $G_T G_R$ one has to measure the length of the range R, the frequency f, the power ratio α, and the impedances, so that the correction factor M may be calculated. There will be random and systematic errors associated with each of these individual measurements. In addition to these quantities, which appear explicitly in the gain equation, there are other factors that affect the accuracy of the gain such as polarization mismatch, the effect of the amplitude taper of the incident field over the aperture of the receiving antenna, multipath effects due to range reflections, and system errors such as alignment of the antennas, equipment instabilities, and so on. One can account for these effects by multiplying the gain equation by correction factors corresponding to each of the preceding as follows:

$$G_T G_R = \left(\frac{4\pi Rf}{c}\right)^2 \alpha M K_1 K_2 K_3 K_4$$

For the case of nearly identical antennas (where $G_T = G_R$), the gain uncertainty of the antennas can be shown to be

$$\frac{\Delta G}{G} = \frac{\Delta R}{R} + \frac{\Delta f}{f} + \frac{1}{2}\left(\frac{\Delta\alpha}{\alpha} + \frac{\Delta M}{M} + \frac{\Delta K_1}{K_1} + \frac{\Delta K_2}{K_2} + \frac{\Delta K_3}{K_3} + \frac{\Delta K_4}{K_4}\right)$$

This result assumes that the individual uncertainties associated with each term are independent. Unfortunately the signs of the individual uncertainties are not known; however, the probability that all signs are the same is quite low. Thus the root-sum-square method of computation is usually used to determine the uncertainty, that is

$$\frac{\Delta G}{G} = \left[\left(\frac{\Delta R}{R}\right)^2 + \left(\frac{\Delta f}{f}\right)^2 + \left(\frac{\Delta\alpha}{2\alpha}\right)^2 + \left(\frac{\Delta M}{2M}\right)^2 + \left(\frac{\Delta K_1}{2K_1}\right)^2 + \left(\frac{\Delta K_2}{2K_2}\right)^2 + \left(\frac{\Delta K_3}{2K_3}\right)^2 + \left(\frac{\Delta K_4}{2K_4}\right)^2\right]^{1/2}$$

Often both the arithmetic sum and the root-sum-square values of uncertainty are reported.

The limits of the 99 percent confidence interval are often taken to be the limits of the uncertainity which, for a single measurement, corresponds to $\pm 3\sigma$, where σ is the standard deviation. The standard deviation for the gain measurement can be obtained from the standard deviations of the individual measurements, which make up the gain measurements, by the use of the root-sum-square computation [99].

12.6 Directivity Measurements. When the complete radiation pattern of an antenna is known

or is measurable, it may be used to determine the directivity of the antenna, The particular quality of the pattern that is employed is the radiation intensity $\Phi(\theta,\phi)$, which is the power radiated from the antenna per unit solid angle in a given direction. The peak directivity of an antenna is the maximum radiation intensity $\Phi_m(\theta',\phi')$, divided by the average radiation intensity. The latter quantity multiplied by 4π is the total power radiated. To compute the directivity D_m, the following relation may be employed :

$$D_m(\theta',\phi') = \frac{\Phi_m(\theta',\phi')}{P_t/4\pi} =$$

$$\frac{\Phi_m(\theta',\phi')}{(1/4\pi)\int_0^{\pi}\left[\int_0^{2\pi}\Phi(\theta,\phi)\,d\phi\right]\sin\theta\,d\theta}$$

P_t is the total power radiated by the test antenna, and the angles θ' and ϕ' give the direction for which the radiation indensity is a maximum.

Since the radiation intensity $\Phi(\theta,\phi)$ can be contained in any two orthogonal polarizations, it is convenient to write the expression for directivity as

$$D_m(\theta',\phi') = \frac{\Phi_{m1}(\theta',\phi')}{(1/4\pi)(P_{t1}+P_{t2})} + \frac{\Phi_{m2}(\theta',\phi')}{(1/4\pi)(P_{t1}+P_{t2})} = D_1(\theta',\phi') + D_2(\theta',\phi')$$

where the subscripts indicate the two orthogonal polarizations. $D_1(\theta',\phi')$ and $D_2(\theta',\phi')$ are called partial directivities. Note that the total power radiated in both polarizations is required in order to determine either $D_1(\theta',\phi')$ or $D_2(\theta',\phi')$. Usually the orthogonal polarizations employed are θ and ϕ linear or right and left circular.

When the antenna under test has been designed to be essentially linearly polarized, then θ and ϕ linear polarizations are most often used. For this case it is desirable that the test antenna be oriented such that the design polarization corresponds with either the θ or the ϕ polarization. If, for example, the antenna is designed to have θ polarization, the ϕ polarization is referred to as the cross polarization. $D_\theta(\theta',\phi')$ and $D_\phi(\theta',\phi')$ are the *partial directivities with respect to θ and ϕ polarization,* respectively. Often it is the partial directivity with respect to the design polarization that is sought. Note that if right and left circular polarizations were employed, the directivity could be obtained, but the partial directivity with respect to the design polarization would not be obtained.

For test antennas that have been designed to be essentially circularly polarized, it may be desirable to use right and left circular polarizations. In this case, if the maximum coupling is obtained with the use of, say, right circular polarization, then left circular is the cross polarization. Note that if θ and ϕ linear polarizations were employed, the partial directivity with respect to the design polarization would not be obtained.

For either of the preceding cases the manner in which the test antenna is used operationally will usually dictate which orthogonal polarizations should be used. For example, if a circular polarized test antenna is to be used operationally to receive a known linearly polarized signal, then appropriate orthogonal linear polarizations may be desirable. Additionally, practical considerations may dictate which approach will be taken. For example, it is usually more difficult to produce a circularly polarized field than a linearly polarized one with sufficient purity to make accurate measurements.

For conciseness in the following discussion, the equation for directivity will be treated as though all the radiated power were contained in a single polarization and that polarization is used for the measurement, that is, the cross polarization is taken to be zero, the discussion applies equally well to both partial directivities.

The radiation intensity may be measured by sampling the field over a sphere centered on the test antenna (see Section 3). This can be accomplished by making conical cuts, successive ϕ cuts through the pattern at increments of θ, or by great-circle cuts, successive θ cuts at increments of ϕ. For either case, the number of increments required is determined by the complexity of the antenna's pattern structure. In general the number of increments increases as the pattern becomes less uniform. Also, an antenna with a narrow major lobe is likely to have a large number of narrow minor lobes which must be included in the measurement and subsequent integration. Generally it is practical to determine directivity accurately only for those antennas having antenna patterns that are not highly directive.

A normalized value of the radiation intensity is usually recorded instead of the absolute value. Typically the normalization is with respect to the maximum value, and the peak directivity may be expressed as

$$D_m(\theta',\phi') = \frac{1}{(1/4\pi)\int_0^{\pi}\left[\int_0^{2\pi}\overline{\Phi}(\theta,\phi)\,d\phi\right]\sin\theta\,d\theta}$$

where

$$\overline{\Phi}(\theta,\phi) = \Phi(\theta,\phi)/\Phi_m(\theta',\phi')$$

If ϕ cuts are employed, then the θ interval from 0 to π rad is divided into M equal spherical sectors, and the expression for directivity becomes

$$D_m(\theta',\phi') = \frac{4M}{\sum_{i=1}^{M}\left[\int_0^{2\pi}\overline{\Phi}(\theta_i,\phi)\,d\phi\right]\sin\theta_i}$$

where $\theta_i = i\pi/M$ rad.

If the normalized radiation intensity is recorded in rectangular coordinates, then each of the integrals within the brackets is equal to the area under the curve, and a planimeter, for example, can be used to evaluate them. When polar coordinates are used, it is necessary to record voltage rather than power because the area of a differential wedge in polar coordinates is given by $\frac{1}{2}V^2\,d\theta$, where V is the voltage recorded at the angle ϕ. Since the radiation intensity is proportional to V^2, the area in the polar curve will be proportional to the integral within the brackets.

If θ cuts are employed, the ϕ interval from 0 to 2π is divided into N equal increments, and the expression for peak directivity can be written as

$$D_m(\theta',\phi') = \frac{2N}{\sum_{j=1}^{N}\int_0^{\pi}\overline{\Phi}(\theta,\phi_j)\sin\theta\,d\theta}$$

Note that $\overline{\Phi}(\theta,\phi_j)$ shall be multiplied by sin θ during the process of integration. If it is necessary to use graphical integration, then a special sine graph paper can be used.

The directivity can be evaluated numerically by use of a digital computer. The patterns can be recorded digitally and can be entered into a digital computer at a later time. If an on-line computer is available, real-time computation can be made. As discussed in 5.7, an on-line computer offers the possibility of automated measurements.

13. Determination of Radiation Efficiency

The radiation efficiency of an antenna is the ratio of the total power radiated by the antenna to the net power accepted by the antenna at its terminals during the radiation process. The difference between these two powers is the power that is dissipated within the antenna. Radiation efficiency is an inherent property of an antenna, and is not dependent on system factors such as those due to impedance or polarization mismatch.

A fundamental method for determining radiation efficiency relies on the measurements described in 12.2 and 12.3. As noted in 12.1, radiation efficiency is equal to the ratio of the

power gain in any specified direction to the directivity in that same direction. It is usually convenient to take the direction of maximum radiation for this determination of radiation efficiency. Thus

$$\text{radiation efficiency} = \frac{\text{peak gain}}{\text{peak directivity}}$$

In measuring peak gain and directivity, all the precautions mentioned in 12.2, and 12.6 shall be carefully observed. Even when this is done, the results are not very accurate for low-loss highly-directive antennas because of the difficulty in calculating directivity from the measured patterns with sufficient accuracy.

Another method may be available when the antenna is electrically small and simple. In this case an equivalent series circuit can frequently be found in which the real part of the input impedance, that is, the antenna resistance, is equal to the sum of the radiation resistance and a loss resistance [102].

The radiation resistance accounts for all radiated power, and the loss resistance accounts for all dissipation within the antenna. For antennas such as dipoles and loops, where the theoretical pattern can be integrated, the radiation resistance is best found by calculation from the dimensions [73, pp 136, 143-148, 166-169],[103 section 11]. The antenna resistance is obtained from measurements of input impedance (see 16.1). The radiation efficiency is then

$$\text{radiation efficiency} = \frac{\text{radiation resistance}}{\text{antenna resistance}}$$

This method is valid only if the antenna can be accurately represented as a series circuit. When the dissipation cannot be represented by a resistance in series with the radiation resistance, as in the case of an antenna coated with lossy dielectric or an antenna over a lossy ground, the method should not be used. Furthermore, the calculated radiation resistance and the measured antenna resistance shall be referred to the same set of antenna terminals. It should also be noted that the input impedance of this type of antenna may present a large mismatch to the connecting transmission line, and a matching network having appreciable dissipation might be used. Such a loss is not usually included within the meaning of radiation efficiency, although it is clear that the loss would be important to the system as a whole.

14. Special Measurements for Angle-Tracking Antennas

14.1 General. In directive antennas the direction of the beam or the tracking axis often has to be determined precisely on the basis of an electrical indication from the antenna system. Such a direction is called the electrical boresight. This electrical boresight is determined with respect to a reference direction, called the reference boresight. The latter is either a specified stationary direction or a direction derived from a measurable parameter, such as an optical axis or a mechanical axis of symmetry, or a prior electrical indication. The angular deviation of the electrical boresight of an antenna from its reference boresight is called the boresight error and is a measured quantity. On the basis of such measurement, the electrical boresight of the antenna system is aligned with the axis of symmetry or the axis about which the antenna rotates, and the boresight error is minimized.

The beam direction of an antenna with a single major lobe is usually determined by noting the direction of maximum response or the direction halfway between equal responses either side of the peak. The precision of such determination is usually on the order of one tenth the half-power beamwidth.

Greater precision of direction is demanded of tracking antennas that employ two or more overlapping beams or lobes as indicated in Fig 65(a). These lobes are compared to indicate a direction through equality of amplitude or phase. When the comparison is done sequentially, it is termed sequential lobing, and typically amplitudes are compared. Two examples of this class are conical scanning

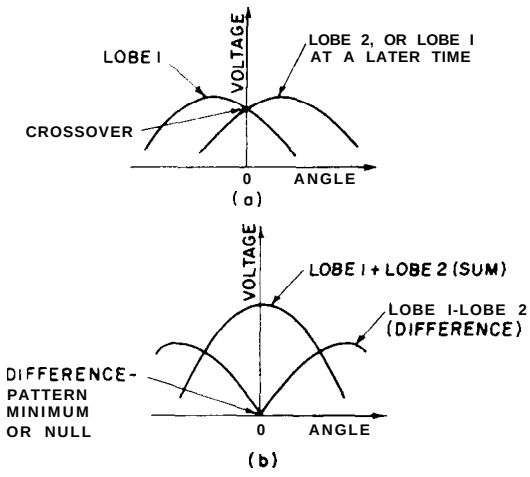

Fig 65
Signals Received by Tracking Antenna Versus Angle of Target.
(a) Lobe Patterns, Monopulse, or Conical Scanning.
(b) Monopulse Sum and Difference Patterns

[104] and lobe switching. When the comparison is done simultaneously, it is called simultaneous lobing or monopulse. In this case either amplitude or phase may be compared [105]. The electrical boresight with such antennas can be determined with a precision on the order of one hundredth of the beamwidth, depending upon the available signal-to-noise ratio.

14.2 Conical Scanning Angle Tracking. Conical scanning antennas use a single beam, the peak traversing a nearly circular path, so that the beam axis describes a cone. Fig. 65(a) represents a cross section through the pattern showing two extreme positions of the beam on opposite sides of its circular path.

During the scan cycle the radio-frequency voltage received or transmitted by the antenna is amplitude modulated because the signal varies with the beam position when the target is not on the crossover axis, which is determined by equal voltages for the two lobes as in Fig 65(a). The amplitude modulation envelope is a complex signal in which the lowest observed frequency, or fundamental, is the scan frequency [106]. The percent modulation of the radio-frequency voltage by the fundamental is of importance in tracking systems. Harmonics of the fundamental scan rate arise from the inherent nonlinearity of the scanning process. At crossover the harmonics ideally go to zero as does. the fundamental. In practice, however, antenna pattern imperfections, such as unequal *E* - and H-plane beamwidths, leave a residual harmonic signal.

The fundamental and higher harmonic modulations are often measured as a function of target error, which is the target displacement from the boresight direction. The null of the fundamental modulation (or error signal) defines the electrical boresight. The slope and linearity of the error signal with respect to target error, as well as the angular range over which the error signal maintains unique polarity are important to the tracking system design. The uniqueness of polarity determines the extent of the angular region over which the antenna system can acquire a target. The harmonic content of the modulation envelope is important to the demodulator design.

These modulation properties may be measured by a system which employs one-way transmission as in a normal pattern measurement, but which utilizes the square-law characteristic of a bolometer to simulate the two-way transmission of normal radar angle track-

ing. The equipment required consists of a microwave transmitter, a bolometer detector and mount, an amplifier, and a wave analyzer. The transmitter, located in the far field and oriented to simulate the target position, may be a square-wave-modulated klystron or a pulsed magnetron which is amplitude modulated at a suitable repetition rate. The antenna under test is terminated with the bolometer mount from which the detected signal is fed to the amplifier. For the measurement of the fundamental modulation, the bolometer-amplifier combination shall have an essentially flat response for the frequencies that lie between the repetition rate plus or minus the conical scan frequency. The fundamental of the amplified signal and the first-order sidebands, which are at the repetition rate plus or minus the scan frequency, are compared using a wave analyzer to determine the percent modulation which is defined as

$$\% \text{ modulation} = \frac{\text{lower sideband amplitude} + \text{upper sideband amplitude}}{\text{amplitude at repetition rate}} \times 100\%$$

The upper and lower sidebands are theoretically equal. In practice, however, they may be slightly different due to the measurement errors and are averaged in the preceding equation.

Before the system measurements are attempted, a check for linearity shall be made. This can be done by inserting a radio-frequency attenuator ahead of the bolometer, and noting the relative output voltage displayed on the wave analyzer for a given change in attenuation. Over a range of at least 20 dB of input level, the output voltage variation in decibels shall be double the change in the radio-frequency attenuation.

Because the angle sensitivity of the two-way fundamental modulation is not easily measured, it may be determined, to a good approximation at least in the region of crossover (where the harmonic content of the modulation wave form is not large), by the following relation:

$$\frac{\% \text{ modulation}}{\text{degree}} = \frac{2 \log_{10}}{5} \times \frac{\sqrt{3D}}{\beta} \times 100\% = \frac{1.6\sqrt{D}}{\beta} \times 100\%$$

where D is the crossover depth in decibels, β is the 3 dB beamwidth in degrees, and % modulation is two-way percent fundamental modulation.

The angle sensitivity can also be expressed in terms of a dB difference curve which is the algebraic difference between two azimuth patterns at the extreme scan positions as shown in Fig 65(a), with the data being measured in decibels.

$$\text{dB difference} \cong (20 \log_{10} e) \times \left(\frac{\% \text{ modulation}}{100\%}\right) = 8.686 \times \left(\frac{\% \text{ modulation}}{100\%}\right)$$

14.3 Monopulse Angle Tracking. Measurements of monopulse tracking antennas are made at the sum and difference ports. The difference-signal pattern minimum defines the electrical boresight (see Fig 65(b)). There are additional errors contributed by the interaction between the antenna and the associated circuits in the tracking loop. These can be determined from additional measurements and from a graphical computation [107]. The angle-sensitivity information usually desired is the slope of the lobe-signal patterns at crossover or the asymptotic slope of the difference-signal patterns. During measurement these slopes should be referred to a reference level of signal voltage, such as a signal from an isotropic radiator or some other appropriate reference [109], to permit an evaluation of the antenna design and the system signal-to-noise ratio.

14.4 Electrical Boresight Measurements. The test equipment for determining the electrical boresight of an antenna comprises the antenna under test, the associated circuits for performing the appropriate signal processing to obtain an error signal, a distant source, a precise means for orienting the antenna direction

(or moving the source), and a highly accurate optical or mechanical indication of antenna direction (or source location). The antenna (or source) is oriented for minimum output at the appropriate error-signal port of the circuit. This antenna direction (or source location) is then noted under the particular condition of frequency, environment, or other test variable. The direction may be compared with a reference direction to determine a component of boresight error. If the antenna system output cannot be noted continuously as a function of source angle, the minimum point may be interpolated. Since the absolute direction of the electrical boresight during a test is often of less interest than its variation with the system parameters, the chief requirement of the antenna direction-indicating mechanism may be one of high precision over a very small angular range. A telescope rigidly fixed to the antenna mount may be used to sight a calibrated optical target at the distant source, or a dial indicator on a long-radius arm may be used. A camera or laser may be similarly employed to measure dynamic errors between electrical and mechanical axes when tracking a moving target,

15. Measurement of the Electrical Properties of Radomes

15.1 General. For many applications operational antennas have to be protected from the effects of the environment. These protecting structures, called radomes, are generally designed to be nearly transparent to the electromagnetic radiation and occasionally to affect radiation in some desired way. Most radomes consist of dielectric materials, although some contain significant amounts of conducting materials. Metallic space frames have been utilized to increase the strength of large radomes, and perforated metallic layers have been developed for both flat and curved radomes. Radomes may take the shape of hollow shells or flat sheets. The hollow shells, in the form of blunt curved radomes, are frequently used with shipborne antennas and occasionally on aircraft. Pointed shapes such as ogives are used on the nose of aircraft and missiles. Flat sheets cover the radiating elements of electronically scanned arrays and also contribute to the antenna impedance match.

This section describes the measurement of the effect or perturbations introduced by the radomes on the performance of the antennas they enclose. For realistic tests to be performed, ancillary parts such as pitot tubes and lightning rods found on some radomes should be included. Multiple scattering between multiple antennas in one radome can be appreciable, thus all antennas shall be present and appropriately terminated during the tests. Because the effects of the radome on the antenna occur in the near field, the evaluation of the radome shall be performed in the presence of the antenna's auxiliary structures as well as of the actual antenna.

Radome testing is an extension of antenna testing because the tests are performed on antennas with and without the radome. The apparatus and tests are more extensive, especially when a mechanically or an electronically scanned antenna is involved.

In the following discussion the quantities that define the significant electrical parameters of the radome are delineated, and the apparatus and the procedures to be used are described.

The coordinate systems used for radome testing are usually the same as those described in 3.1. Two sets of coordinates are used, one is fixed to the antenna to describe the pattern, and a second set is fixed to the radome to describe antenna orientation. Special coordinates are sometimes used for airborne guidance systems.

15.2 Significant Antenna-Radome Parameters. The performance of a radome is characterized by the *power transmittance,* the *power reflectance,* the squint angle, the boresight error, and the radiation patterns in the presence of the radomes.

The power transmittance IS the ratio of the power density in a given direction emerging from the radome with an internal radiating source to the power density radiated by the source without the radome. Power trans-

mittance is usually measured in the direction of the peak of the main lobe. Alternately it may be specified in terms of the crossover level for a conical-scan antenna, or the null direction for a monopulse system. The positions and orientations of both antenna and radome shall be specified in measurements of power transmittance.

The power reflectance is the ratio of the power density that is internally reflected from the radome to that incident on the radome from the internal radiating source. It indicates the contribution of the radome to the antenna mismatch.

The squint angle (beam shift) is the angular displacement of the main lobe of the sum channel patterns from a reference beam direction. The squint angle often is treated as a vector quantity with two components that are usually resolved into the directions of the coordinates specifying the antenna-radome orientation.

Boresight error describes the angular displacement from the zero error direction in a tracking system which uses an antenna system that generates a conical scanning, lobing, or monopulse difference pattern. The boresight error can be considered to be a vector with two components resolved into the directions of the coordinate system that specifies antenna-radome orientations.

The antenna patterns in the presence of the radome change most significantly in the side-lobe regions. The side lobe levels may be expressed in terms of peak or mean levels, depending on the application. For all the quantities discussed, polarization shall be specified and taken into account in the measurements.

In performing radome measurements, all the relevant quantities shall be measured for a sufficiently wide range of coverage to allow the significant effects of the radome to be obtained. For example, antenna patterns should be measured over the full hemisphere to locate wide-angle side lobes caused by reflections from the radome. Similarly, patterns should be recorded for wide ranges of antenna position. However, the scope of all tests, including data reduction and evaluation, shall be carefully planned because of the costs involved. Thus to reduce the total number of variables, antenna patterns are measured with the radome and enclosed antenna in a fixed relative orientation, while both are rotated as a unit. Measurements are then repeated for several relative orientations of the antenna radome. Specialized automated equipment and computerization are available that gather and reduce the data efficiently.

15.3 Apparatus. The apparatus to be used and the procedures to be employed are outlined for the quantities enumerated in the preceding paragraphs. In many instances the degrees of freedom of the antenna with respect to the radome and exterior region are complex; fixtures shall be adequate to duplicate the angular relationships in the actual system. The fixtures are devices that hold and position the antenna to simulate actual system operation. The fixture shall also duplicate the sequence of axis rotations to be found in the actual system [109]. The fixtures themselves shall not add extraneous reflections. A check can be made by taking successive measurements with the antenna (without the radome) displaced in steps of fractions of a wavelength so that reflections add and subtract. Thus the magnitude of the standing wave will show up in the several quantities to be measured. Side-lobe levels are especially sensitive to the antenna motion. Particular attention shall be paid to the overall implementation of the measurements to minimize spurious range reflections and to illuminate the test antenna and radome with a plane wave. The far field is defined in terms of the maximum dimension of the overall structure, including the radome and the nearby portions of the vehicle to which it may be attached. To check for reflections within the radome, measurements can be repeated with successive quarter-wave shifts of the antenna relative to the radome in the direction of the antenna axis. These displacements reveal reflections that can affect the measured values of trans-

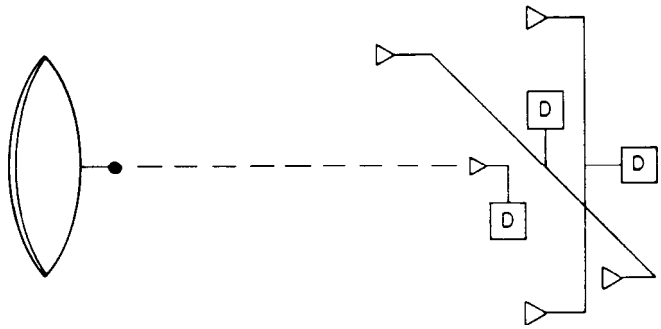

Fig 66
Orthogonal Arrays for Beam-Shift Measurement
(D-detector, other components omitted)

mittance, reflectance, and side-lobe levels. Precautions shall also be employed in the design of the transmitting and receiving systems to assure sufficient amplitude and frequency stability, particularly in measurements that involve phase.

Power transmittance and beam-shift, or radome boresight error, measurements can be performed simultaneously. For these tests the radome is pivoted about the enclosed test antenna, which remains stationary except possibly for small displacements that permit measurement of the radome boresight error.

Two techniques are used for automatic measurements of radome boresight errors. In the first technique an external antenna (called a null seeker) is automatically positioned to track the direction of the null as the radome is pivoted. In the second technique, called the closed-loop test, the antenna being tested is moved to maintain a null as the radome is pivoted.

For boresight measurements with antennas that have a null tracking system, the usual practice is to operate the test antenna in reception, because many systems operate only in the receiving mode. The boresight error can be obtained by rotating the test antenna to preserve the antenna null that exists without the radome. Alternately the external antenna can be laterally displaced to maintain the null of the test antenna. Precision in angular measurements is greater for the latter case because the displacement is the product of the range between transmit and receive and the boresight error. For large antennas that require long ranges, the necessary displacement may be so large that moving the external antenna is impractical. With either technique, the angular deviations are obtained from the error voltages generated by the servo mechanism of the system. Different measurement setups are required with the two techniques.

For boresight measurements of antennas without tracking nulls, the test antenna is used in transmission. Reception is obtained by using two orthogonally oriented pairs of antennas as shown in Fig. 66. The plane containing each pair is perpendicular to the electrical boresight. Each pair is interconnected so that the amplitude or the phase of the received signals may be compared. A balanced output from each pair is initially established without the radome. In some cases the test antenna is fixed, and the receiving antennas are laterally displaced to preserve the balanced output while the radome is pivoted. In other cases the receiving antennas are fixed and error voltages are derived from the test antenna. Alternately, the test antenna can be displaced to preserve the balanced condition with the fixed receiving antennas.

Power transmittance measurements are made with additional apparatus. When the beam shift is measured, a fifth antenna is used. It is located

at the intersection of the two base lines that connect the beam-tracking antennas (see Fig 66). Received power is measured while the radome is pivoted and the beam is tracked. The received power is compared with the value that is received when the radome is removed. When the boresight error is measured with the radome-enclosed test antenna in the receiving mode, the power is measured at a port of the enclosed antenna. For monopulse antennas, power is extracted from the sum port. For conical-scan antennas, a directional coupler samples the power ahead of the detector that is used to define the boresight error.

Reflectance is measured when the enclosed antenna is in the transmitting mode. The radome is pivoted and the enclosed antenna is stationary.

Very large radomes and the antennas they enclose can only be measured when they are located in their operational environments. Preliminary tests may be performed using parts of the radome in the form of flat sheets. The same quantities are measured and then extrapolated to the complete structure. The measurements for large radomes involve the extension of techniques used for the in situ measurements discussed in Section 9. The environment in which the antenna and radome must operate shall be taken into account. These environmental conditions include rain, snow, wind etc. The effects of rain are discussed separately in the next subsection.

15.4 Testing of Wet Radomes. A weathered radome, especially one covered with dirt or one that absorbs water, will show appreciable changes in use. Rain or sea spray can cover a radome with a thin layer of water that can produce significant effects. The water reduces transmittance and causes reflections that can increase side-lobe levels. In communication links the noise temperature can also be increased.

The effects of water can be tested by spraying the radome during the previously described tests of transmittance, patterns, and so on. However, testing with water present is complicated because accurate measurements of water thickness and distribution are difficult. Capacitance measurements can be utilized to determine the thickness in controlled measurements, but the sensors can perturb the propagation. In addition, because of surface roughness, water can accumulate locally so that the contour of the radome should be checked. The significance of test results should be assessed in terms of the amount of. water than can accumulate when the radome is being used in its operational environment, for example, rainfall rates should be measured. If salt water is of interest, the salinity of the water used in the tests shall be determined.

16. Measurement of Impedances

16.1 Input-impedance Measurements. The input impedance of an antenna at the specified terminal pair (or port) affects the interaction between the antenna and its associated circuits. Antenna impedance can be an important factor in the consideration of power transfer, noise, and stability of active circuit components. Frequently it is the antenna impedance that limits the useful bandwidth of the antenna.

The optimum impedance relationship between an antenna and its associated circuits is determined by the application. In some receiving situations, in the interest of a minimum noise figure, the antenna impedance should be lower than the matched impedance. In some transmitting situations, in order to attain maximum power efficiency, a mismatch in the opposite direction may be required. However, in many applications a matched condition is the ideal. By this is meant a conjugate match between the antenna and the circuits; maximum power transfer is attained in this case. When a conjugate match does not exist, some of the available power is lost, as follows:

$$\frac{P_{\text{lost}}}{P_{\text{available}}} = \left| \frac{Z_{\text{ant}} - Z^*_{\text{cct}}}{Z_{\text{ant}} + Z_{\text{cct}}} \right|^2$$

where Z_{ant} is the input impedance of the antenna, Z_{cct} is the input impedance of the circuits at the antenna terminals, and Z^*_{cct} is the complex conjugate of the circuit imped-

ance. This expression may be useful during the measurement of power gain with a mismatched system, as mentioned in 12.5.

Most antennas are connected to the electronic networks via a transmission line, and the desired degree of match or mismatch could be adjusted at either end of the line. In practice, however, it is usually advantageous to perform the matching as near to the antenna terminals as possible. This minimizes the line losses and the voltage peaks on the line, and generally maximizes the useful bandwidth of the system. Imperfect matching of the antenna to the transmission line creates a reflected wave in the line; the reflected power relative to the incident power is:

$$\frac{P_{\text{refl}}}{P_{\text{inc}}} = \left| \frac{Z_{\text{ant}} - Z_0}{Z_{\text{ant}} + Z_0} \right|^2$$

where Z_0 is the characteristic impedance of the line. This ratio is related to the voltage reflection coefficient Γ and to the voltage-standing-wave ratio (VSWR) by the standard transmission-line relationships

$$\frac{P_{\text{refl}}}{P_{\text{inc}}} = |\Gamma|^2 = \left| \frac{\text{VSWR} - 1}{\text{VSWR} + 1} \right|^2$$

If the transmission line has a characteristic impedance that is purely real, and if the electronic networks are perfectly matched to the transmission line, this ratio yields the loss of available power caused by the reflection at the antenna terminals; if not, this loss shall be determined using methods given in ANSI/IEEE Std 148-1959 (Reaff 1971), Measurement of Waveguides and Components. (See also 12.5.)

Measurement of the input impedance is made at a single port of the antenna. For the usual problems and procedures related to this measurement, reference should be made to ANSI/IEEE Std 148-1959 (Reaff 1971). There is, however, a particular problem inherent in radiating structures, since the input impedance is modified by the environment of the antenna. For this reason the antenna shall be placed in a simulation of its operating environment before the measurement is made. Usually this requirement is easily approximated for narrow-beam antennas that can be pointed away from reflecting obstacles, but it may be more difficult for omnidirectional antennas where much of the surrounding structure affects the input impedance.

The measurement of impedance, or equivalently, of the complex reflection coefficent, can be performed using impedance bridges or slotted lines at frequencies where these techniques are applicable [110],[111],[154]. The increasing availability of broad-band, swept-frequency network analyzer systems that measure impedance or the entire network scattering matrix has made measurements of this type the choice for many applications. These instruments are commercially available at frequencies up to and through the microwave spectrum and are suited for computer-controlled data collection, storage, and display, as well as for analog display using X-Y recorders and optical display units. At microwave frequencies the units feature automatic swept-frequency display of complex reflection and transmission coefficients with various overlay charts to relate the reflection coefficient locus to impedance coordinates. Two such coordinate systems are in common use. One involves the resistive and reactive components of the impedance [112], while the other involves the magnitude and phase of the impedance [113]. The impedance so determined is in a form which is normalized to that of the reference transmission line. This is usually the convenient form at microwave frequencies where transmission lines are common.

16.2 Mutual-Impedance Measurement. In an array antenna, there is usually an interaction between the array elements which significantly affects the behavior of the antenna, and it is often necessary to determine the effect of this interaction. An important measure of the interaction is the mutual impedance between the elements of the array antenna.

The mutual impedance between any two ele-

ments is defined by the equation

$$Z_{mn} = \frac{V_m}{I_n}$$

where I_n in the current at the reference point of the driven element n, and V_m is the voltage produced at the reference point in element m, when all the elements except the driven element are open-circuited at their reference points.

The mutual coupling between two elements can also be described in terms of the incident, reflected, and coupled waves measured in the transmission lines connected to each element. This description of coupling utilizes the cross-coupling coefficient of a scattering matrix:

$$S_{mn} = \frac{b_m}{a_n}$$

where a, is the incident wave at a reference point in the transmission line of the driven element n, and b_m is the received wave in the transmission line of element m, when all other array elements are terminated in matched loads.

These measures of mutual impedance or coupling depend upon the type of elements, their size and spacing in terms of a wavelength, and the geometrical arrangement of the elements and their environment. In general the magnitude and the phase angle of the mutual impedance or coupling decreases with increased spacing.

The reference terminals (or ports) at which the currents and voltages are determined may be selected for greatest convenience, but in any case they shall be specified. In tower radiators, which are the elements of a broadcast array antenna, the reference terminals are customarily taken at the base of the towers, even though the towers may be of unequal heights, and the effect of the base insulators is often subtracted from the measured values. In dipole arrays, such as those used at high frequency and very high frequency, the reference terminals are generally taken to be at the current maximum of the radiating portion of the elements. In such cases the current distributions themselves are sometimes measured using loop probes [114] mounted within slits in the dipole or along the dipole surface. In microwave arrays the reference points are often taken to be at the ports where the waveguides connect to the elements or at the array face for waveguide elements. For cases in which the element feed transmission lines are of uncertain or unequal lengths, it is convenient to use symmetric probe techniques to assure a consistent measurement of the reference plane [114],[115].

An impedance or scattering matrix can be made up of a set of mutual, impedance values Z_{mn} or a set of scattering coefficients S_{mn} for a given antenna array. These matrices include the self-impedances Z_{mm} or the complex reflection coefficients S_{mm}. These two types of matrices are interrelated and can be converted from one to the other by means of a matrix transformation [116]. The self-impedance or reflection coefficient terms are properties of each element individually excited in its array environment for specific loading conditions, and differ from the active impedance or reflection coefficient that exists when the entire array is excited. The quantities measured at the terminals under the latter condition are influenced by mutually coupled contributions throughout the array [117]. The active *impedance,* or *active reflection coefficient,* is defined as the input impedance or reflection coefficient of an element with all other elements excited as in actual array operation.

In general the active input impedances or reflection coefficients will change if the excitation is changed, because the changed relative phases or amplitudes of excitation produce different resultant terminal voltages. Such changes occur, for example, when the pattern of an array of broadcast towers is being adjusted, or when the major lobe of a large planar array is being scanned. If either the impedance or the scattering matrix is known, the active impedance or reflection coefficient of all elements in an array can be evaluated under all scan conditions [118],[119] . For microwave arrays the scattering matrix is more convenient to use for measurement and analysis. A par-

tially filled scattering matrix consisting of only the outward coupling coefficients about a given excited element provides an efficient means to determine the active array performance from a specified set of array incident-wave excitations by indexing it over the full array [120]. This procedure eliminates the need to invert very large impedance matrices as well as the need to determine the complete scattering matrix.

The mutual impedance between two elements of an array is sometimes determined by a calculation [117],[121],[155]. Such a calculation is usually practical only when all the elements of the array have some simple, idealized configuration. This situation occurs if the form of the current distribution or aperture distribution is not significantly affected by the environment in which the element is located.

The direct determination of the mutual impedance from voltage and current measurements is most commonly made on antenna arrays in the medium-frequency range. A common example is a broadcast antenna array consisting of several electrically-small tower elements. A knowledge of the mutual impedance in such arrays is necessary to determine the branching and coupling circuit requirements which will provide the proper current amplitude and phase relations in the array elements to produce the desired directional characteristics. Frequently such antenna arrays employ tower elements of different heights in irregular geometric arrangements with unequal current amplitudes and irregular phase relationships in order to produce a radiation pattern that best fits the desired coverage and projected directions. In an antenna array containing only a few radiating elements, the nonrepetitive relative position of each element in the array may result in a substantially different mutual impedance between different pairs of elements.

At much lower frequencies, antenna arrays are not generally used. When they are, however, the currents and voltages which establish the mutual impedances are directly measurable as at medium frequencies. In the higher radio-frequency region, where currents and voltages are not readily measurable, the mutual impedances between elements of an array may be derived from measurements of the input impedances of the elements at their reference points under appropriate conditions. Two or more terminating conditions for the coupled elements are required, such as short and open circuits at the terminals, the latter permits measurement of the self-impedances of the elements. Such measurement procedures are based on an exact analogy between the current and voltage relations between the terminals in a system of radiating elements and the corresponding current and voltage relations in a circuit network. An impedance bridge, admittance meter or vector voltmeter is often used for such measurements, and a specific method is described in the literature [122].

In UHF and microwave antenna arrays consisting of a large number of identical regularly-spaced radiating elements, the mutual impedance between all pairs of elements having the same relative position tends to approximate a constant value, except near the edges of the array [118],[123]. In such cases measurements are sometimes made on a limited-size array having an element design and arrangement like that of the full-size array. By measuring the mutual impedance or coupling between elements near the center of the limited array, a partial impedance or scattering matrix can be determined which has values that approximate the corresponding ones in the full-size array. However, care shall be taken in interpreting the results in terms of various related aspects of array performance such as the active impedance as a function of electronic beam scanning, or the gain and shape of the element pattern. The omission of the effect of the missing elements on the limited array may correspond to significant errors in the aformentioned quantities when they are used for the full-size array.

Alternative techniques that overcome this limitation have been described [124],[125] for the measurement of the active impedance of an element in a large array of identical, regularly spaced elements. The effect of elements in an infinite array is simulated by the use of waveguide techniques. These techniques are based upon image theory and yield results for a limited number of discrete beam positions.

1’7. Ground-Wave Measurements

The measurements described in Sections 3, 7, and 9-12 presumed that the performance of the antenna is desired in the far-field region. However, some antenna systems deliver their useful power to regions were the simplifying far-field relationships do not apply. An important class of such antennas are ground-based vertically polarized antennas which operate at frequencies that are low, which rely on the ground as an essential means for wave propagation, and which radiate their useful power to receiving antennas located on or near the ground. In this case the ground can be considered a significant part of the antenna itself, and cannot be in the far-field region.

The useful component of radiation for such antennas is usually represented by the ground wave (see IEEE Std 211-1977, Standard Definitions of Terms for Radio Wave Propagation). This is a wave associated with currents that flow in the ground, which is an imperfect conductor. Power is absorbed by the ground, and the ground wave ordinarily decays at a more rapid rate than would a wave in free space. The concepts of power gain, directivity, radiation resistance, and radiation efficiency are not directly applicable in this situation; although arbitrary assumptions regarding the extent of the antenna system are sometimes made. This permits a limited use of these terms. Furthermore the electrical properties of the imperfectly conducting ground and the type of terrain may vary over the useful coverage area surrounding the antenna, so that irregularities in the ground-wave field strength are likely to exist.

A complete measurement of the ground-wave radiation by an antenna involves the measurement of the field strength at every significant point on the ground within the useful coverage area (see IEEE Std 291-1969, Standards Report on Measuring Field Strength in Radio Wave Propagation). The power supplied to the antenna during these measurements shall also be determined. A pattern may then be plotted showing the field strength throughout the coverage area for the specified value of antenna power. Such a pattern is often plotted in terms of contours of equal field strength [103, Section 10],[126].

When certain conditions exist, a relatively small number of measurements can be used, in conjunction with well-known propagation formulas and published curves [127]–[130], to estimate the field strengths at various other points throughout the coverage area. For antennas operating below approximately 5 MHz the useful component of the ground wave is usually the surface wave because the space-wave component cancels out near the ground [103, Section 10],[131]. If the electrical properties of the ground are reasonably constant along lines radially outward from the antenna, the surface-wave field strength can approximate simple functions of distance on each line. These simple functions usually apply for distances from the antenna greater than 1 wavelength and greater than five times the vertical height of the antenna, and for distances less than $8 \times 10^{6}(f)^{-1/3}$ meters (where f is the frequency in hertz), beyond which the curvature of the earth begins to have a significant effect.

Four theoretical curves of relative field strength versus relative distance are shown in Fig 67 for this ideal situation. Each curve represents a different set of electrical properties of the ground. In addition, the relative distance p is a function of the ground properties, so that each curve requires a translation in the scale of relative distance. By making about 10 or 20 measurements of field strength for evenly spaced intervals along a radial line within the range of distances mentioned, and by plotting these on the same logarithmic scales as those of Fig 67, a curve may be chosen and located horizontally and vertically so that it represents the best fit to the measured data. This process is repeated for each radial line. By interpolation and extrapolation the field strength may now be estimated at any point within the described range [132]. If more detailed theoretical curves are desired, they may be found in both graphical [133] and tabular form in the literature [128] (see also IEEE Std 291-1969). The electrical properties of the ground may be

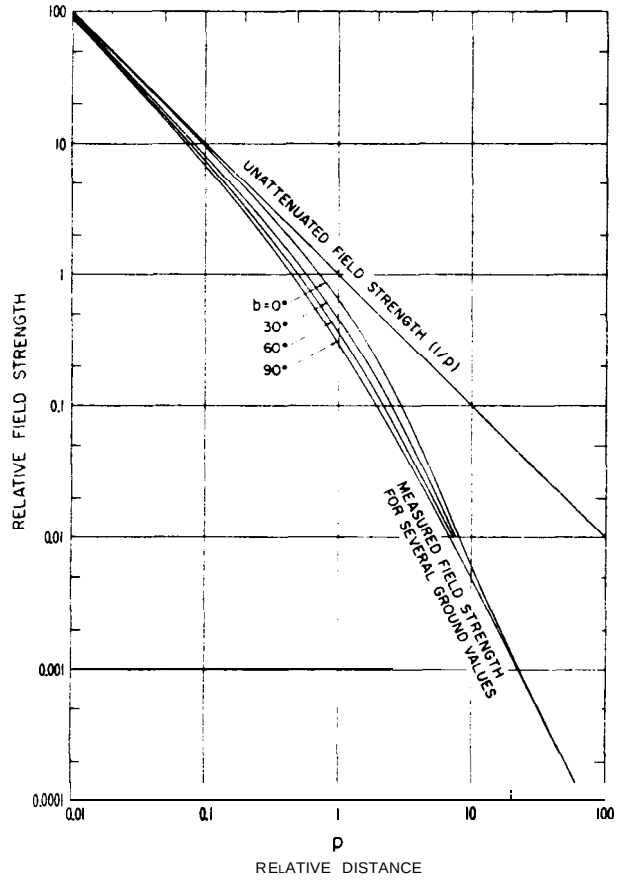

Fig 67
Decay of Surface-Wave Component of the Ground Wave for a Plane Earth

determined from the quantities b and p in Fig 67 and from relationships presented in the literature [127],[128]. This is necessary in order to determine that the best fit to the measured data as established in the preceding, represents a reasonable value.

It is often desired to estimate the field strength at distances beyond the range where it approximates a simple function of distance, and a helpful factor for this purpose is the unattenuated surface-wave field-strength pattern at a standard distance from the antenna. This is a hypothetical pattern that may be obtained from the measurements and the curve-fitting procedure described. For each radial set the line marked "unattenuated field strength" in Fig 67 is extended until it intersects the standard distance (such as 1 kilometer or 1 mile), and the value of field strength is read off. The resulting pattern of unattenuated field strength versus azimuth angle for the standard distance may be used, in conjunction with well-known propagation formulas and published curves [127]–[130], to estimate the field strengths at greater distances, where effects such as the curvature of the earth become important.

For antennas operating above about 5 MHz the space-wave component of the ground wave cannot usually be neglected, and the contour of the ground is a significant factor. However, a hypothetical unattenuated pattern at a

standard distance is still a helpful concept in estimating field strengths over a coverage area. In this case the unattenuated field strength may be determined by a comparison method in which the antenna being tested is compared with a standard antenna. The comparison method requires that the antenna under test be removable. This is generally possible in the frequency range above 5 MHz where antennas are usually not extremely large. The standard antenna may consist of either a vertical loop or a vertical dipole for which the vertical electric field E_S expected over a perfectly conducting ground plane can be calculated when the antenna current is specified. This value is just twice the free-space value of the vertical field strength. The method is valid only if the vertical-plane patterns of the antenna under test and of the standard antenna are such that the relative effect of the ground-reflected component of the space wave is the same in either case. First the signal voltage V_X received in a vertically polarized pickup antenna placed at some standard distance from the antenna under test is measured. This distance should be greater than 1 wavelength and greater than ten times the largest dimension of the test antenna. Then the antenna under test is removed and the standard antenna is placed in the same effective location with due consideration given to the probable difference in current distributions of the two antennas. The signal voltage V_S received in the pickup is now measured for a current in the standard antenna equal to that assumed in the field-strength calculation. The unattenuated field strength E_X of the test antenna at the standard distance is then determined from the following relation:

$$E_X = \frac{V_X}{V_S} E_S$$

To determine the complete unattenuated ground-wave field-strength pattern in the horizontal plane, this procedure is repeated in a number of directions from the antenna under test.

In addition to its use in estimating field strengths, the unattenuated ground-wave field-strength pattern is helpful as an indication of the quality of the antenna design. With the unattenuated pattern some of the variable effects of the ground are removed, particularly those at distances far from the antenna. An example of this is the determination of equivalent radiated power for ground-wave transmission (see IEEE Std 291-1969).

It is sometimes desired to determine the vertical-plane pattern of a ground-based vertically polarized antenna. This pattern is of interest, for example, when the "skywave" radiation characteristics are important [103, Section 10] (see also IEEE Std 211-1977). Although the pattern in the far-field region of the antenna-ground system may be desired for the prediction of skywave characteristics, practical limitations may rule out the far-field measurements described in Section 9. In particular, at low elevation angles and low frequencies, there may be a special problem in the measurements because of the presence of ground-wave components in the total radiation field of the antenna. In this case the shape of the vertical-plane pattern can depend very markedly on the distanceat which the pattern is measured [127],[134]. However, it is sometimes possible to estimate the far-field vertical-plane pattern from a series of near-field measurements by subtracting out, with appropriate relative phase, the surface-wave and the space-wave components of the ground wave.

18. Power-Handling Measurements

Antennas are often tested to determine their ability to handle the power generated by their associated transmitters. These tests may be concerned primarily with limitations imposed by metallic or dielectric heating at high average power levels, or with limitations imposed by the arcing, voltage breakdown, or corona discharge associated with high electric fields at high peak-power levels.

In cases wnere the antenna is subject to low atmospheric pressures it is necessary to simulate the high-altitude conditions by means of a bell jar or some other suitable chamber in

order to achieve satisfactory peak-power-handling measurements [135],[136], since extrapolation from tests conducted at sea level is not reliable. At very low pressues the breakdown power level decreases with increasing pressure, reaches a minimum at a pressure that depends on the wavelength (the glow discharge region), and then increases with pressure at high pressures. The use of a radioactive material to create a continuous supply of free electrons in the atmosphere in the near vicinity of the antenna under test is a useful means of providing reliability and consistency in the breakdown tests, and does not lower the absolute breakdown threshold. At satellite altitudes, multipacting [137] may cause problems and shall be considered as a possible breakdown mechanism in any antenna power-handling tests. Multipacting is an antenna resonance phenomenon occurring under high vacuum conditions. When the travel time of electrons from one antenna electrode to another is comparable to the inverse of the operating frequency, a buildup in electron density may take place. This is due to surface ionization caused by electron bombardment.

Because of the great variety of antenna configurations and environmental conditions, no attempt will be made to provide a specific procedure for conducting power-handling measurements. For accurate results it is important to ensure that the source of power for the measurements has the same characteristics as the actual transmitter with which the antenna is to be used, that is, the modulation, pulse shape. pulse width, pulse rate, and so on should be the same and should not change with the applied power level during the test. Temperature rise may be measured by means of thermocouples or temperacure-sensitive paints applied to critical surfaces. Care should be taken that these added components are not themselves heated by the radio-frequency power. Depending on the type, breakdown may be detected by visual observation, audible indication, change in signal picked up by a transmission-monitor antenna, or change in a reflected-wave-monitor signal as the applied power level is increased. It is sometimes important, as in the case of glow discharge, to determine the power level at which breakdown ceases once it has been initiated. Sharp comers, dirt, metal particles, and corrosion are often major offenders in lowering the breakdown power level.

In the case of antennas carried on reentry vehicles, it is necessary to determine the power-handling capability in the presence of the ionized air enveloping the reentry vehicle [138]. As the power transmitted from the antenna is increased, a level is reached where the power absorbed by the ionized gas is sufficient to heat the gas and increase the electron density. The critical plasma density is the most important parameter in determining breakdown in such cases. It is defined as that electron density where the natural oscillation frequency of the ionized gas is equal to the frequency at which the antenna is being driven. When the natural oscillation frequency of the ionized gas is much lower than the frequency applied to the antenna, the plasma is termed undercritical or underdense. If the initial plasma density is greatly undercritical, the effect of the unperturbed gas upon the antenna field may be neglected. Breakdown is then usually defined as that input power at which the perturbed ionized gas has become overcritical (overdense) and a precipitous drop in the transmitted power beyond the plasma takes place. If the initial plasma density is close to or overcritical, the definition of breakdown is more complex. The unperturbed ionized gas may have a strong effect on the antenna field and, in general, may not be neglected. One commondefinitionof breakdown for this case is that input power level above which an increase in power no longer results in a significant increase in the power transmitted beyond the plasma.

In order to measure the power-handling capability of a missile antenna in the laboratory it is necessary to model the plasma conditions. The breakdown power level may depend critically upon a number of plasma parameters along with the magnitude and spatial variation of electron density. A number of techniques are available to produce plasmas in the laboratory suitable for antenna-breakdown measure-

ments [139],[140]. When testing an antenna, it is desirable to measure not only the breakdown power level, but also the changes in input impedance, radiation pattern, power gain, and distortion of the transmitted signal for power levels below, at, and above the breakdown level.

Analytical and numerical techniques [141], have been developed to predict the power-handling capabilities of missile antennas. The breakdown power levels predicted by these techniques are in good agreement with flight-test results. If it should be impossible to model particular reentry conditions in the laboratory, these prediction techniques may prove sufficient in providing data for antenna designs.

Whenever measurements are performed in which high average power levels exist, it is essential that proper safety devices and procedures be employed for the protection of the personnel in the vicinity (see Section 19).

19. Electromagnetic Radiation Hazards

19.1 General. Individuals involved in the generation of electromagnetic signals and in the testing of antennas shall consider carefully the potential hazard of exposure of humans to excessive electromagnetic radiation. The spectrum of nonionizing radiation covers the frequency range up to the ultraviolet-light region. The nonionizing radiation is the radiant energy that interacts with body tissue causing heating because the body is a lossy dielectric.

NOTE: The biological effects of nuclear radiation (ionizing radiation) can be largely attributed to ionization and electronic excitation which causes destruction of various molecules.

This section presents brief comments pertinent to health and safety precautions, which apply primarily to radiant energy in the radio-frequency region. The purpose is to alert those engaged in testing antennas, microwave components, and so on, to potential radio-frequency radiation hazards. In addition to radiation damage, bums may be incurred when contact is established by arcing between the body and exposed components of a system operating at high RF power levels.

The interaction of radio waves and the human body involves very complex processes that are not completely understood. Considerable research has been conducted, and indeed is being conducted, by researchers in many different countries. (For example, there are several hundred references listed in four publications [142]–[145].) Safe exposure limits are set as a result of an analysis of all the data generated by such research. As a consequence, one can expect that standards for exposure limits will possibly change as new knowledge is acquired.

In the United States the organizations which are the principal proponents and sponsors of work leading to the setting of standards are the Bureau of Radiological Health of the US Public Health Service, the National Science Foundation, the American National Standards Institute (ANSI Committee C-95), and the IEEE Committee on Man and Radiation (COMAR). Similar organizations exist in other countries.

The injurious effects on human beings are believed to be principally due to the heating of tissues at various depths of penetration. Such heating can be especially detrimental to sensitive organs, such as the eyes, testicles, the kidneys, and the liver. Excessive exposure can also cause skin bums, but at RF the energy usually penetrates below the surface of the skin causing either deep-skin bums or damage to internal organs. It should be noted that the body or parts of the body exhibit resonances. In fact, the whole body is resonant in the VHF range of frequencies. The exact frequency depends upon the size and shape of the body.

The principal factors which affect the amount of RF energy absorbed by the human body are the frequency, polarization and power flux density of the incident wave, the exposure time, and the electrical properties of the body.

The ability of the body to tolerate heat stress due to absorbed RF energy without deleterious effects depends upon a number of factors. These include the environmental temperature and humidity, the amount of heat already generated in or absorbed by the body, and the state of health of the person being exposed. Because of the variability of conditions under which personnel must work, the safety limits must be

Table 4
Electromagnetic Radiation Safety Limits

Country	Regulating Body	Safety Limit	Exposure Time
US	American National Standards Institute †	10 mW/cm² (averaged over any 6 minutes)	6 minutes
u s	Air Force [146]††		
	RF >10 MHz	50 mW/cm²	over 6 minutes
		300 mW-min/cm²	under 6 minutes
	RF ≤ 10 MHz	10 mW/cm²	over 6 minutes
		60 mW-min/cm²	under 6 minutes
USSR	State Committee on Standards*	0.01 mW/cm²	over 24 hours**
		0.1 mW/cm²	up to 2 hours
		1.0 mW/cm²	20 minutes

†All exposures limited to Mean Squared Electric Field Strength of 40 000 V²/m², Mean Squared Magnetic Field Strength of 0.25 A²/m² and an Energy Density of 1 mW-h/cm²
††All exposures limited to a Peak Electric Field Strength of 100 kV/m
*For frequencies between 0.01-0.03 GHz the RMS Electric Field Strength is limited to 20 V/m; for frequencies between 0.03-0.05 GHz, 10 V/m, 0.3 A/m; for frequencies between 0.05-0.3 GHz, 5 V/m all for an exposure duration of one working day
**Continuous exposure.

considered to be upper limit guide numbers for a normal or moderate environment. If, for example, the temperature and humidity are high in the area where personnel are exposed to RF. radiation, it is appropriate to include a safety factor, thereby reducing the guide numbers recommended in the applicable standard. Also, it should be noted that individuals with circulatory difficulties are especially vulnerable to adverse affects, due to heat stress.

19.2 Safe Radiation Limits. Uniform radiation limits have not been established worldwide. For instance, there is a wide discrepancy between the United States and the USSR in the establishment of maximum allowable limits for the radiation exposure of human beings. ANSI C95.1-1974, American National Standard Safety Level of Electromagnetic Radiation Respect to Personnel, includes limitations on the E and H fields as well as the power density. It recommends a radiation protection guide of 10 mW/cm², averaged over any possible 0.1 hour period for frequencies from 10 MHz to 100 GHz. In the USSR's Occupational *Safety Standard,* GOST 12.1.006-76, the safety limits are given in step-function levels of milliwatts per square centimeter for different exposure times and frequencies between 0.3 GHz and 300 GHz. For frequencies between 0.01 GHz and 0.3 GHz, the limits are on the electric and magnetic field strengths [156]. Table 4 summarizes the safety limits of the two countries. Other countries have similar standards which shall be adhered to by engineers and scientists [157] practicing within their boundaries.

The safety limits presented in Table 4 are based upon plane wave or locally plane wave propagation. This means that they apply unambiguously only for the far field of an antenna [147]. In the absence of reflecting obstacles, the far field power flux densities can often be calculated. In the near field, however, such calculations are too inaccurate and measurements are required [148],[149]. For the near field case where reactive fields are significant, the concept of power flux density is invalid [147]. One can, however, measure the magnitude of either the electric or magnetic fields or the squares of these quantities, which are proportional to the energy density of the electric or magnetic fields respectively [150]. These results are sometimes used to obtain the *power*

flux density of an equivalent plane wave in order to reconcile the results with a standard.

19.3 Measurement and Instrumentation. In the United States the appropriate standard on measurements is ANSI C95.3-1973, Techniques and Instrumentation for the Measurement of Potentially Hazardous Electromagnetic Radiation at Microwave Frequencies (also see [150] and [158]). Most often in antenna measurements it is the near field of an antenna that is of concern. For this case an 'isotropic' probe is required to sample the field. These probes usually consist of three mutually perpendicular, and very short, dipoles. The induced currents on the dipoles are detected by diodes, bolometers or thermocouples; the three detected signals are combined and amplified. The output of the instrument is calibrated so that the magnitude of the electric field or its square can be presented on a meter or other type of indicator. Some instruments are calibrated in terms of an equivalent power flux density as discussed in 19.2. Such instruments are commercially available.

The measurement must be performed with care since the probe and its associated 'instrumentation can distort the field being measured to the degree that erroneous results are obtained. In addition the presence of the person performing the measurement can also disturb the field being measured. Measurements made remotely are to be preferred.

It is good laboratory practice to experimentally survey any region where potentially hazardous fields may exist and appropriately post those areas where the measured field strengths exceed prescribed limits. This is to alert all personnel to the possible hazard. Also, the range operations manual [see Section 8] should contain warnings to personnel of any potential hazardous situations that may commonly occur.

20. Environmental Factors

An antenna can be considered adequately tested only when the tests have included the environmental conditions under which the antenna will operate. Many of these environmental factors are of a specialized nature, and it is impractical to include all the appropriate effects in this test procedure. Instead a few cases will be briefly mentioned as pertinent examples.

One category of environmental factors may be defined as those directly affecting the material properties or structure of an antenna and, thus, indirectly affecting the electrical characteristics. Mechanical loading of the antenna structure by wind and ice is a common, but nevertheless important, effect to be considered in the testing of many antennas. Vibration and shock tests are often made to assure that an antenna that is subject to severe accelerations will maintain its structural integrity, and to determine whether dynamic deformations are within allowable electrical limits. Antennas in exposed locations are often provided with lightning protection and anti-icing devices; the effect of such devices on the electrical characteristics must be evaluated.

Various natural or man-made environments may impose special requirements. For example, shipborne antennas may have to withstand water-wave impact and salt-water corrosion. Antennas on hypersonic vehicles shall withstand very high temperatures and pressures, and antennas designed for satellite or space-probe application shall withstand intense ionizing radiation, hard vacuum, and extreme temperatures. Ground-based antennas that are intended to operate in the vicinity of a nuclear blast should maintain their essential properties in the wake of seismic waves, atmospheric shock waves, thermal radiation, ionizing radiation, blast-product erosion, and radioactive debris.

Certain antenna applications necessitate unusual attention to tests that involve quite ordinary aspects of the physical environment. For instance, rapid-scan antennas employing ferrite components are especially sensitive to changes in ambient temperature. Antennas in which intermodulation distortion has to be minimized may have difficulty with nonlinear corrosion films. In the case of precision tracking antennas, a boresight error can be caused merely by deflections resulting from nonuni-

form heating of the antenna by the sun. Large antennas rotated in the elevation plane may also undergo significant deflections because of the change in the effect of the gravitational force on the antenna.

The other category of environmental factors may be defined as those directly affecting the electrical properties of the antenna. In some cases this electrical environment is permanent and is included in the design as an integral part of the antenna. Familiar examples of this situation are the presence of the ground for ground-based antennas, the superstructure for shipbome antennas, and the vehicle for airborne or space antennas. Techniques for testing in these circumstances have been developed and are widely used. They are described in 7.1 and Section 9. Another example is the noise environment of an antenna, including galactic radiation, thermal atmospheric radiation, atmospheric and man-made static, and thermal earth radiation. A less familiar but more extreme example of permanent electrical environment occurs with low-frequency antennas designed to operate underground or beneath the surface of the sea.

In many cases the electrical environment of an antenna is transient, and causes problems of a more elusive nature. Moisture, when combined with impurities, can create conducting paths that are troublesome, especially in regions of high electric field. Even pure water, if it exists in a continuous film, may affect the performance of a microwave antenna because of its high dielectric constant. Ice or snow are also factors that can directly affect the characteristics of an antenna. In the case of antennas for missile application, ionized gases may exist in the exhaust or may be generated by high vehicle velocity through the atmosphere; these gases are also a part of the electrical environment. Finally, certain antennas may be susceptible to precipitation static, which is a series of noise pulses created when charged particles such as raindrops discharge on the antenna.

There is a particular type of antenna environment that deserves special mention, namely, the radome. A radome is a structure that is often used to enclose an antenna to protect it from the physical environment. However, in so doing it introduces an electrical environment the effects of which should not be overlooked. Radome testing is described in Section 15.

21. Bibliography

[1] HOLLIS, J. S., LYON, T. J., and CLAYTON, L., Jr, Eds. Microwave Antenna Measurements. Atlanta, GA. Scientific-Atlanta, 1970.

[2] Standard Coordinate System and Data Formats for Antenna Patterns, Electronic Trajectory Measurements Working Group, Inter-Range Instrumentation Group, Range Commanders Council, United States National Ranges, IRIG Document AD 637 189, May 1966.

[3] CUMMING, W. A. Radiation Measurements at Radio Frequencies: A Survey of Current Techniques, *Proceedings of the IRE*, vol 47, May 1959, pp 705-735.

[4] CUTLER, C. C., KING, A. P., and KOCK, W. E. Microwave Antenna Measurements, *Proceedings of the IRE.* vo135, Dec 1947, pp 1462-1471.

[5] PIPPARD, A. B., BURRELL, 0. J., and CROMI, E. E. The Influence ,of Re-Radiation on Measurements of the Power Gain of an Aerial, *Journal of the Institution of Electrical Engineers.* vol 93, pt III A, 1946, pp 720-722.

[6] KING, H. E., SHIMABUKURO, F. I.. and WONG, J. L. Characteristics of a Tapered Anechoic Chamber, *IEEE Transactions on Antennas and Propagation* (Communications), vol AP-15. May 1967, pp 488–490.

[7] BACHMAN, C. G., KING, H. E., and HANSEN, R. C. Techniques for Measurement of Reduced Radar Cross Sections, pt 1, *Microwave Journal.* vol 6, Feb 1963, pp 61-67.

[8] MOELLER, A. W. The Effect of Ground Reflections on Antenna Test Range Measurements, *Microwave Journal, vol 9,* Mar 1966, pp 47–54.

[9] ARNOLD, P. W. The "Slant" Antenna Range, *IEEE Transactions on Antennas and Propagation* (Communications), vol AP-14, Sept 1966, pp 658-659.

[10] COHEN, A., and MALTESE, A. W. The Lincoln Laboratory Antenna Test Range, *Microwave Journal*, vol *4*, Apr 1961, pp 57-65.

[11] JORDAN, E. C., and BALMAIN, K. G. Electromagnetic Waves and Radiating Systems, Englewood Cliffs, NJ, Prentice-Hall, 1968, 2nd ed.

[12] REED, H. R., and RUSSELL, C. M. Ultra High Frequency Propagation, Cambridge, MA, Boston Technical Publishers, 1966, 2nd ed.

[13] JULL, E. V., and DELOLI, E. P. An Accurate Absolute Gain Calibration of an Antenna for Radio Astronomy, *IEEE Transactions on Antennas and Propagation*, vol AP-12, July 1964, pp 439-447.

[14] Minimum Standards for Land-Mobile Communication Antennas. Part 1 -Base or Fixed Station Antennas, Engineering Department, Electronic Industries Association, Washington, DC, Dec 1966.

[15] JOHNSON, R. C., ECKER, H. A., and MOORE, R. A. Compact Range Techniques and Measurements, *IEEE Transactions on Antennas and Propagation*, vol AP-17, Sept 1969, pp 563-576.

[16] JOHNSON, R. C., ECKER, H. A., and HOLLIS, J. S. Determination of Far-Field Antenna Patterns from Near-Field Measurements, *Proceedings of the IEEE*, vol 61, Dec 1973, pp 1668-1694.

[17] EMERSON, W. H. Electromagnetic Wave Absorbers and Anechoic Chambers Through the Years, *IEEE Transactions on Antennas and Propagation, vol AP-21*, July 1973, pp 484-490.

[18] *POUND*, R. V. Electronic Frequency Stabilization of Microwave Oscillators, *Review of Scientific Instruments*, vol 17, Nov 1966, pp 490-505.

[19] DYSON, J. D. The Measurement of Phase at UHF and Microwave Frequencies, *IEEE Transactions on Microwave Theory and Techniques*, vol MTT-14, Sept 1966, pp 410-413.

[20] LOMBARDI, A. J., and POLGAR, M.S., Jr. Wide Band Antenna Facility, *Electrical Communication*, vol 49, no 1, 1974, pp 94-98.

[21] APPEL-HANSEN, J. Reflectivity Level of Radio Anechoic Chambers, *IEEE Transactions on Antennas and Propagation, vol AP-21*, July 1973, pp 490-498.

[22] BUCKLEY, E. F. Outline of Evaluation Procedures for Microwave Anechoic Chambers, *Microwave Journal*, vol *6*, Aug 1963, pp 69-75.

[23] SINCLAIR, G., JORDAN, E. C., and VAUGHAN, E. W. Measurement of Aircraft-Antenna Patterns Using Models, *proceedings of the IRE*, vol *35*, Dec 1947, pp 1451-1462.

[24] STRATTON, J. A. Electromagnetic Theory, New York, McGraw-Hill, 1941, pp 488-490.

[25] KING, R. W. Electromagnetic Engineering, vol 1, New York, McGraw-Hill, 1945, pp 316-320.

[26] MARCUVITZ, N. Waveguide Handbook, M.I.T. Radiation Laboratory Series, vol 10, New York, McGraw-Hill, 1951, pp 18-23.

[27] SINCLAIR, G. Theory of Models of Electromagnetic Systems, *Proceedings of the IRE*, vol *36*, *Nov* 1948. pp 1364–1370.

[28] FANO, R. M. Theoretical Limitations on the Broadband Matching of Arbitrary Impedances, *Journal of the Franklin Institute*, vol 249, 1950, pp 57-154.

[29] BOLLJXHN, J. T., and REESE, R. F. Electrically Small Antennas and the Low-Frequency Aircraft Problem, *IRE Transactions on Antennas and Fropagation*, vol AP–1, Oct 1953, pp 46-54.

[30] GREENE, F. M. NBS Field-Strength Standards and Measurements (30 Hz to 1000 MHz), *Proceedings of the IEEE*, vol 55, June 1967, pp 970-981.

[31] CHENG, D. K., and MOSELEY, S. T. On-Axis Defocus Characteristics of the

Paraboloidal Reflector, *IRE Transactions on Antennas and Propagation* (Communications), vol AP-3,Oct 1955, pp 214-216.

[32] KERNS, D. M., and DXYHOFF, E. S. Theory of Diffraction in Microwave Interferometers, *Journal of Research of National Bureau of Standards,* vol 64B, Jan/Mar 1960, pp l-13.

[33] KERNS, D. M. Correction of Near-Field Antenna Measurements Made with an Arbitrary but Known Measuring Antenna, *Electronics Letters,*

[34] WACK-

Antenna Measurements, vol 6,

[35] JOY, E. B., and PARIS, D. T. Spatial Sampling and Filtering in Near-Field Measurements, *IEEE Transactions on Antennas and Propagation,* vol AP-20, May 1972, pp 253-261.

[36] NEWELL, A. C., and CRAWFORD, M. L. Planar Near-Field Measurements on High Performance Array Antennas, *National Bureau of Standards,* Boulder, CO, Rep NBSIR 74-380, 1974.

[37] Special Issue on Fast Fourier Transform, *IEEE Transactions on Audio and Electroacoustics*, vol AU-17, June 1969, pp 65-172.

[38] LEACH, W. M., Jr, and PARIS, D. T. Probe Compensated Near-Field Measurements on a Cylinder, *IEEE Transactions on Antennas and Propagation,* vol XP-21, July 1973, pp 435-445.

[39] JENSEN, F. Electromagnetic Near-Field Far-Field Correlations, Ph.D. dissertation. Technical University of Denmark, Lyngby, July 1970.

[40] LUDWIG, A. C. Near-Field Far-Field Transformations Using Spherical-Wave Expansions, *IEEE Transactions on Antennas and Propagation,* vol AP-19, Mar 1971, pp 214-220.

[41] WACKER, P. F., Non-Planar Near-Field Measurements: Spherical Scanning, *National Bureau of Standards,* Boulder. CO, Rep NBSIR 75-809, 1975.

[42] BANTIN, C. C., and BALMAIN, K. G. Study of Compressed Log-Periodic Dipole Antennas, *IEEE Transactions on Antennas and Propagation,* vol AP-18, Mar 1970, pp 195-203.

[43] BALMAIN, K. G., BANTIN, C. C., OAKES, C. R., and DAVID, L. Optimization of Log-Periodic Dipole Antennas, *IEEE Transactions on Antennas and Propagation* (Communications), vol AP-19, Mar 1971, pp 286-288.

[44] OAKES, C. R., and BALMAIN, K. G. Optimization of the Loop-Coupled Log-Periodic Antenna, *IEEE Transactions on Antennas and Propagation,* vol AP-21, Mar 1973, pp 148-153.

[45] GRUNER, R. W., and ENGLISH, W. J. Antenna Design Studies for a U.S. Domestic Satellite, *COMSTAT Technical Reuiew,* vol *4,* no *2,* Fall 1974, pp 413-447.

[46] KREUTEL, R. W., DIFONZO, D. F., ENGLISH, W. J., and GRUNER, R. W. Antenna Technology_ for Frequency Reuse Satellite Communications, *Proceedings of the IEEE,* vol 65, Mar 1977, pp 370-378.

[47] FITZGERRELL, R. G. Swept-Frequency Antenna Gain Measurements, *IEEE Transactions on Antennas and Propagation,* vol AP-14, Mar 1966, pp 173-178.

[48] KENEFICK, J. F. Ultra-Precise Analytics, *Photogrammetric Engineering,* vol *37, Nov* 1971, pp 1167-1187.

[49] FINDLAY, J. W., and VON HOEMER, S. A 65-Meter Telescope for Millimeter Wavelengths, National Radio Astronomy Observatory, Charlottesville, VA, 1972.

[50] PAYNE, J. M. An Optical Distance Measuring Instrument, *Review of Scientific Instruments,* vol *44, Mar* 1973, pp 304-306.

[51] LALONDE, M. The Upgraded Arecibo Observatory, *Science,* vol 186, Oct 1974, pp 213-218.

[52] PAYNE, J. M., HOLLIS, J. M., and FINLEY, J. W. New Method of Measuring the Shape of Precise Antenna Reflectors, *Review of Scientific Instruments;* vol 47, Jan 1976, pp 50-55.

[53] FINDLAY, J. W., and PAYNE, J. M. An Instrument for Measuring Deformations in Large Structures, *IEEE Transactions on Instrumentation and Measurement,* vol IM-23, Sept 1974, pp 221-226.

[54] BALE, F. V., GOURLAY, J. A., and MEADOWS, R. W. Measuring the Shape of Large Reflectors by a Simple Radio Method, *Electronics Letters,* vol 2, July 1966, pp 252-253.

[55] CLARK, G. A., and SLATER, R. H. Experimental Laser System for Monitoring Deformations in Large Radio Reflectors, *Proceedings of the Institution of Electrical Engineers,* vol 118, Nov 1971, pp 1562-1568.

[56] BRUECKMANN, H. Antenna Pattern Measurement by Satellite, *IEEE Transactions on Antennas and Propagation,* vol AP-11, Mar 1963, pp 143-147.

[57] KENNEDY, J. T., and ROSSON, J. W. The Use of Solar Radio Emission for the Measurement of Radar Angle Errors, *Bell System Technical Journal,* vol 41, Nov 1962, pp 1799-1812.

[58] KUZ'MIN, A. D., and SALOMONOVICH, A.E. *Radio-Astronomical Methods of Antenna Measurement, New* York, Academic Press, 1966.

[59] FITZGERRELL, R. G. Gain Measurements of Vertically Polarized Antennas over Imperfect Ground, *IEEE Transactions on Antennas and Propagation,* vol AP-15, Mar 1967, pp 211-216.

[60] DYSON, J. D. Determination of the Phase Center and Phase Patterns of Antennas, in Radio Antennas for Aircraft and Aerospace Vehicles, BLACKBAND, W. T., Ed, AGARD Conference Proceedings, no 15, Slough, England, Technivision Services, 1967.

[61] HU, Y. *Y.* A Method of Determining Phase Centers and Its Application to Electromagnetic Horns, *Journal of the Franklin Institute,* vol 271, Jan 1961, pp 31-39.

[62] BAUER, K. The Phase Centers of Aperture Radiators, *Archiv der Elek trichen Übertragung*, vol 9, 1955, p 541.

[63] CARTER, D. Phase Centers of Microwave Antennas, *IRE Transactions on Antennas and Propagation,* vol AP-4, Oct 1956, pp 597-600.

[64] NAGELBERG, E. R. Fresnel Region Phase Centers of Circular Aperture Antennas, *IEEE Transactions on Antennas and Propagation* (Communications), vol AP-13, May 1965, pp 479-480.

[65] DYSON, J. D. The Measurement of Near Fields of Antennas and Scatterers, *IEEE Transactions on Antennas and Propagation,* vol AP-21, July 1973, pp 446-460.

[66] ELLERBRACH, D. A. UHF and Microwave Phase-Shift Measurements, Pro*ceedings of the IEEE,* vol *55,* June 1967, pp 960-969.

[67] SCHAFER, G. E. Mismatch Errors in Microwave Phase Shift Measurements, *IRE Transactions on Microwave Theory and Techniques,* vol MTT-8, Nov 1960, pp 617-622.

[68] HUNTON, J. K. Analysis of Microwave Measurement Techniques by Means of Signal Flow Graphs, *IRE Transactions on Microwave Theory and Techniques,* vol MTT-8, Mar 1960, pp 206-212.

[69] LEED, D. Use of Flow Graphs to Evaluate Mistermination Errors in Loss and Phase Measurements, *IRE Transactions on Microwave Theory and Techniques* (Correspondence), vol MTT-9, Sept 1961, p 454.

[70] BOOKER, H. G., RUMSEY, V. H., DESCHAMPS, G. A., KALES, M. I., and BOHNERT, J. I. Techniques for Handling Elliptically Polarized Waves with Special Reference to Antennas, *Proceedings of the IRE,* vol 39, May 1951, pp 533-552.

[71] DESCHAMPS, G. A., and MAST, P. E. Poincare Sphere Representation of Partially Polarized Fields, *IEEE Transactions on Antennas and Propagation,* vol AP-21, July 1975, pp 474-478.

[72] COHEN, M. H. Radio Astronomy Polarization Measurements, *Proceedings of the IRE,* vol 46, Jan 1958, pp 172–183.

[73] KRAUS, J. D. Antennas, New York, McGraw-Hill, 1950.

[74] BECKMANN, P. The Depolarization of Electromagnetic Waves, Boulder, CO, Golem Press, 1968, pp 183-187.

[75] TAI, C. T. On the Definition of the Effective Aperture of Antennas, *IRE Transactions on Antennas and Propaga tion* (Communications), vol AP-9, Mar 1961, pp 224-225.

[76] DYSON, J. D. An Approach to a Fully Isotropic Wide-Band Source of Radiation, Abstracts of the 20th Annual USAF Symposium on Antenna Research and Development, Sponsored by the AF Avionics Labratory. Monticello, IL, Oct 1970.

[77] CLAYTON, L. Jr., and HOLLIS, J. S. Antenna Polarization Analysis by Amplitude Measurement of Multiple Components, *Microwave Journal,* vol *8,* Jan 1965, pp 35-41.

[78] KNITTEL, G. H. The Polarization Sphere as a Graphical Aid in Determining the Polarization of an Antenna by Amplitude Measurements Only, *IEEE Transactions on Antennas and Propagation, vol AP-15,* Mar 1967, pp 217-221.

[79] NEWELL, A. C., BAIRD, R. C., and WACKER, P. F. Accurate Measurement of Antenna Gain and Polarization at Reduced Distances by an Extrapolation Technique, *IEEE Transactions on Antennas and Propagation,* vol AP–21, July 1973, pp 418-431.

[80] JOY, E. G., and PARIS, D. T. A Practical Method for Measuring the Complex Polarization Ratio of Arbitrary Antennas. *IEEE Transactions on Antennas and Propagation,* vol AP-21, July 1973, pp 432-435.

[81] LUDWIG, A. Gain Computations from Pattern Integration, *IEEE Transactions on Antennas and Propagation* (Communications), vol AP-15, Mar 1967, pp 309–311.

[82] SLAYTON, W. T. Design and Calibration of Microwave Antenna Gain Standards, Naval Research Laboratory, Washington, DC, Rept 4433, Nov 1954.

[83] BOWMAN, R. R. Field Strength Above 1 GHz: Measurement Procedures for Standard Antennas, *Proceedings of the IEEE,* vol *55,* June 1967, pp 981–990.

[84] HEMMING, L. H., and HEATON, R. A. Antenna Gain Calibration on a Ground Reflection Range, *IEEE Transactions on Antennas and Propagation,* vol AP–21, July 1973, pp 532-538.

[85] KANDA, M. Accuracy Considerations in the Measurement of the Power Gain of a Large Microwave Antenna, *IEEE Transactions on Antennas and Propagation* (Succinct Papers), vol. AP-23, May 1975, pp. 407-411.

[86] FITZGERRELL, R. G. The Gain of a Horizontal Half-Wave Dipole over Ground, *IEEE Transactions on Antennas and Propagation* (Communications), vol AP-15, July 1967, pp 569-571.

[87] FITZGERRELL, R. G. Limitations on Vertically Polarized Ground-Based Antennas as Gain Standards, *IEEE Transactions on Antennas and Propagation* (Communications), vol AP-23, Mar 1975, pp 284-286.

[88] SMITH, P. G. Measurement of the Complete Far-Field Pattern of Large Antennas by Radio-Star Sources, *IEEE Transactions on Antennas and Propagation*, vol AP-14, Jan 1966, pp 6-16.

[89] BAARS, J. W. M. The Measurement of Large Antennas with Cosmic Radio Sources, *IEEE Transactions on Antennas and Propagation,* vol AP-21, July 1973, pp 461-474.

[90] GUIDICE, D. A., and CXSTELLI, J. P. The Use of Extraterrestrial Radio Sources in the Measurement of Antenna Parameters, *IEEE Transactions on Aerospace and Electronic Systems,* vol AES-7, Mar 1971, pp 226-234.

[91] BXARS, J. W. M., MEZGER, P. G., and WENDKER, H. The Spectra of the Strongest Nonthermal Radio Sources in the Centimeter Wavelength Region, *Astrophysical Journal,* vol 142, 1965, pp 122-134.

[92] WAIT, D. F., DAYWITT, W.C., KANDA, M., and MILLER, C. K. S. A Study of the Measurement of *G/T* Using Cassiopeia A, National Bureau of Standards, Boulder, CO, Rep NBSIR 74-382, June 1974.

[93] BAARS, J. W. M., and HARTSUIJKER, A. P. The Decrease of Flux Density of Cassiopeia A and the Absolute Spectra of Cassiopeia A, Cygnus A and Taurus A, *Astronomy and Astrophysics,* vol 17, 1972, p 172.

[94] Influence of the Non-Ionized Regions of the Atmosphere on the Propagation of Waves, CCIR Plenary Assembly Rep 234–1, 1966.

[95] DICKE, R. H., BERINGER, R., KYHL, R., and VANE, A. B. Atmospheric Absorption Measurements with a Microwave Radiometer, *Physical Review,* vol 70, Sept 1 and 15, 1946, pp 340-348.

[96] KANDA, M. Study of Errors in Absolute Flux Density Measurements of Cassiopeia A, National Bureau of Standards, Boulder, CO, Rep NBIR 75-822, Oct 1975.

[97] KREUTEL, R. W., Jr, and PACHOLDER, A. 0. The Measurement of Gain and Noise Temperature of a Satellite Communications Earth Station, *Microwave Journal,* vol 12, Oct 1969, pp 61-66.

[98] JAKES, W. C., Jr, Gain of Electromagnetic Horns, *Proceedings of the IRE.* vol 39, Feb 1951, pp 160-162.

[99] WRIXON, G. T., and WELCH, W. J. Gain Measurements of Standard Electromagnetic Horns in the K and K_a Bands, *IEEE Transactions on Antennas and Propagation,* vol AP-20, Mar 1972, pp 136-142.

[100] CHU, T. S., and SEMPLAK, R. A. Gain of Electromagnetic Horns, *Bell System Technical Journal,* vol 44, June/Aug 1965, pp 527-537.

[101] BEATTY, R. W. Discussion of Errors in Gain Measurements of Standard Electromagnetic Horns, National Bureau of Standards, Boulder, CO, Tech Note 351.

[102] NEWMAN, E. H., BOHLEY, P., and WALTER, C. H. Two Methods for the Measurement of Antenna Efficiency, *IEEE Transactions on Antennas and Propagation,* vol *AP-23,* July 1975. pp 457-461.

[103] TERMAN, F. E. Radio Engineers' Handbook, New York, McGraw-Hill, 1943.

[104] CADY, W. M., KARELITZ, M. G., and TURNER, L. A. Radar Scanners and Radomes, M.I.T. Radiation Laboratory ser., vol 26, New York, McGraw-Hill, 1948, pp 7, 62, 66.

[105] RHODES, D. R. Introduction to Monopulse, New York, McGraw-Hill, 1959.

[106] POVEJSIL, D. J., RAVEN, R. S., and WATERMAN, P. Airborne Radar, Princeton, NJ, Van Nostrand, 1961, p 520.

[107] REDLIEN, H. W. The Monopulse Difference Chart, IEEE International Convention Record, pt I, Antennas and Propagation, 1963, pp 129-131.

[108] KINSEY, R. R. Monopulse Difference Slope and Gain Standards, *IRE Transactions on Antennas and Propagation* (Communications), vol AP-10, May 1962, pp 343-344.

[109] LYON, T. J. in Radome Engineering Handbook, WALTON, J. D., Jr, Ed., New York, Marcel Dekker, 1970, p 145.

[110] TERMAN, F. E., and PETTIT, J. M. Electronic Measurements, New York, McGraw-Hill, 1952, chap 3

[111] MONTGOMERY, C. G. Techniques of Microwave Measurements, M .I.T. Radiation Laboratory ser., vol 11, New York, McGraw-Hill, 1947, chap 8.

[112] SMITH, P. H. An Improved Transmission Line Calculator, *Electronics,* vol 17, Jan 1944, pp 130–138, 318.

[113] CARTER, P. S. Charts for Transmission-Line Measurements and Computations, *RCA Review,* vol 3, Jan 1939, pp 355-368.

[114] KING, R. W. P., MACK, R. B., and SANDLER, S. S. Arrays of Cylindrical Dipoles, New York, Cambridge University Press, 1968, chap 8.

[115] MAILLOUX, R. J., and LARUSSA, F. A Microwave Phase Bridge Technique for Measuring the Mutual Coupling of Identical Coupled Antennas, *IEEE Transactions on Microwave Theory and Techniques* (Correspondence), vol MTT-6, Feb 1968, pp 129-130.

[116] MONTGOMERY, C. G., DICKE, R. H., and PURCELL, E. M. Principles of Microwave Circuits, M.I.T. Radiation Laboratory ser, vol 8, New York. McGraw-Hill, 1948, p 140.

[117] OLINER, A. A., and MALECH, R. G. Mutual Coupling in Infinite Scanning Arrays, in Microwave Scanning Antennas, vol 2, HANSEN, R. C., Ed., Academic Press, 1966, chaps 2, 3, 4.

[118] CARTER, P. S., Jr. Mutual Impedance Effects in Large Beam Scanning Arrays, *IRE Transactions on Antennas and Propagation,* vol AP-8, May 1960, pp 276-285.

[119] KURTZ, L. A., ELLIOTT, R. S., WEHN, S., and FLOCK, W. L. Mutual-Coupling Effects in Scanning Dipole Arrays, *IRE Transactions on Antennas and Propagation,* vol AP-9, Sept 1961, pp 433-443.

[120] ALLEN, C. C. Mutual Coupling Effects in Phased Array Antennas, Abstracts of the 13th Annual USAF Symposium on Antenna Research and Development, University of Illinois, Urbana, Oct 15, 1963, DDC #AD–421483.

[121] CARTER, P. S. Circuit Relations in Radiating Systems and Applications to Antenna Problems, *Proceedings of the IRE,* vol 20, June 1932, pp 1004-1041.

[122] BROWN, G. H. Directional Antennas, *Proceedings of the IRE,* vol 25, Jan 1937, pp 78-145.

[123] ALLEN, J. L. Gain and Impedance Variation in Scanned Dipole Arrays, *IRE Transactions on Antennas and Propagation,* vol AP-10, Sept 1962, pp 566-572.

[124] HANNAN, P. W., MEIER, P. J., and BALFOUR, M. A. Simulation of Phased Array Antenna Impedance in Waveguide, *IEEE Transactions on Antennas and Propagation* (Communications), vol AP-11, Nov 1963, pp 715-716.

[125] GUSTINCIC, J. J. The Determination of Active Array Impedance with Multi-element Waveguide Simulators, *IEEE Transactions on Antennas and Propagation,* vol AP-20, Sept 1972, pp. 589-595.

[126] BURROWS, C. R., HUNT, L. E., and DECINO, A. Ultra-Short-Wave Propagation : Mobile Urban Transmission Characteristics, *Bell System Technical Journal,* vol 14, Apr 1935, pp 253-272.

[127] NORTON, K. A. The Propagation of Radio Waves over the Surface of the Earth and in the Upper Atmosphere, *Proceedings of the IRE,* vol *24,* Oct 1936, pp 1367-1385; vol 25, Sept 1937, pp 1203-1236.

[128] NORTON, K. A. The Calculation of Ground-Wave Propagation, *Proceedings of the IRE,* vol 29, Jan 1941, pp. 16-24. *Proceedings of the IRE,* vol 29, Dec 1941, pp 623-639.

[129] BURROWS, C. R. Radio Propagation over Plane Earth, Field Strength Curves, *Bell System Technical Journal,* vol 16, Jan 1937, pp 45-75: Oct 1937, pp 574-577.

[130] BURROWS, C. R., and GRAY, M. C. The Effect of the Earth's Curvature on Ground-Wave Propagation, *Proceedings of the IRE,* vol 29, Jan 1941, pp 16-24.

[131] JASIK, H. Antenna Engineering Handbook, New York, McGraw-Hill, 1961, pp 33.1-33.24.

[132] CUNNINGHAM, J. E. The Complete Broadcast Antenna Handbook-Design, Installation, Operation, and Maintenance, Blue Ridge Summit, PA, TAB Books, 1977.

[133] Federal Communications Commission Rules and Regulations, vol III, Sept 1961, sec 3.184; see also Dec 1963, sec 73.184.

[134] WAIT, J. R., and CONDA, A. M. Pattern of an Antenna on a Curved Lossy Surface, *IRE Transactions on Antennas and Propagation,* vol AP-6, Oct 1958, pp 348-359.

[135] MACDONALD, A. D. Microwave Breakdown in Gases, New York, Wiley, 1966.

[136] CHOWN, J. B., SCHARFMAN, W. E., and MORITA, T. Voltage Breakdown Characteristics of Microwave Antennas, *Proceedings of the IRE, vol 47,* Aug 1959, pp 1331-1337.

[137] WOO, R. Multipacting Discharges Between Coaxial Electrodes, *Journal of Applied Physics, vol 39,* Feb 1968, pp 528-533.

[138] TAYLOR, W. C., SCHARFMAN, W. E., and MORITA, T. Voltage Breakdown of Microwave Antennas, in *Advances in Microwaves,* vol 7, New York, Academic Press, 197 1.

[139] KUNKEL, W., Ed., Plasma Physics in Theory and Application, New York, McGraw-Hill, 1966, chap 10.

[140] VENUGOPALAN, M., Ed., Reactions under Plasma Conditions, New York, Wiley-Interscience, 1971, chaps 5, G.

[141] MAYHAN, J. T., FANTE, R. L., O'KEEFE, R., ELKIN, R., KLUGERMAN, J., and YOS, J. Comparison of Various Microwave Breakdown Prediction Models, *Journal of Applied Physics,* vol 42, Dec 1971, pp 5362-5369.

[142] Special Issue on Biological Effects of Microwaves, *IEEE Transactions on Microwave Theory and Techniques, vol* MTT-19, Feb 1971, pp 128–253.

[143] MICHAELSON, S. M. Human Exposure to Nonionizing Radiant Energy — Potential Hazards and Safety Standards, *Proceedings of the IEEE,* vol 60, Apr 1972, pp 389-421.

[144] TYLOR, P. E., Ed., Biologic Effects of Nonionizing Radiation, Annals of the New York Academy of Sciences, vol 247, Feb 1975.

[145] BARANSKI, S., and CZERSKI, P. Biological Effects of Microwaves, Stroudsburg, PA, Dowden, Hutchinson and Ross, 1976.

[146] U.S. Air Force, Radiofrequency Radiation Health Hazards Control, AF Regulation 161-42, Washington, DC, Nov 7, 1975.

[147] SCHWAN, H. P. Microwave Radiation: Biophysical Considerations and Standards Criteria, *IEEE Transactions on Biomedical Engineering, vol* BME-19, July 1972, pp 304-312.

[148] Instrumentation for Environmental Monitoring Radiation, Environmental Instrument Group, Lawrence Berkeley Lab., University of California, May 1, 1972.

[149] An Evaluation of Selected Satellite Communication Systems as Sources of Environmental Microwave Radiation, EPA–520/2. -74-008.

[150] WACKER, P. F., and BOWMAN, R.R. Quantifying Hazardous Electromagnetic Fields: Scientific Basis and Practical Considerations, *IEEE Transactions on Microwave Theory and Techniques,* vol MTT-19, Feb 1971, pp 178-187.

[151] CHU, T. S. and LEGG, W. E. Gain of Corrugated Conical Horns, International Symposium Digest, IEEE Antennas and Propagation Society, pp 427-430.

[152] KUMMER, W. H. and GILLESPIE, E. S. Antenna Measurements, 1978, Proceedings of the IEEE, vol 66, April 1978, pp 483-507.

[153] NEWELL, A. C., Improved Polarization Measurements Using a Modified Three Antenna Technique, IEEE AB-S International Symposium, pp 337-340, 1975.

[154] BEATTY, R. W., Microwave Impedance Measurements and Standards, National Bureau of Standards, Monograph 82, August 1965.

[155] HARRINGTON, R. F., Field Computation by Moment Methods, New York, McGraw Hill, 1968.

[156] Occupational Safety Standards, Electromagnetic Fields of Radiofrequency, General Safety Requirements, GOST 12.1.006-76, State Committee on Standards of the Council of Ministers of the USSR, Moscow, Jan 22, 1976.

[157] STUCHLY, M. A., and REPACHOLI, M. H., Microwave and Radiofrequency Protection Standards, *Transac tions of the In terna tional Microwave Power Institute,* vol 8, Microwave Bioeffects and Radiation Safety, 1978, pp 95-101.

[158] BOWMAN, R. R., Quantifying Hazardous Microwave Fields, *Transactions of the International Microwave Power Institute,* vol 8, Microwave Bioeffects and Radiation Safety, 1978, pp 113-128.

Appendixes

(These appendixes are not a part of IEEE Std 149-1979, Test Procedures for Antennas.)

Appendix A
Field Regions

A1. General

The distribution of field strength around an antenna is a function of the distance from the antenna. Three field regions are distinguished to express antenna patterns and field distributions in zones surrounding the antenna. In close proximity to the antenna the field strength may include, in addition to the radiating field, a significant reactive (nonradiating) field. The strength of the reactive-field components decays rapidly with the distance from the antenna (inversely as distance raised to powers greater than unity). That region of space immediately surrounding the antenna in which the reactive components predominate is known as the reactive near-field region. The size of this region varies for different antennas. For most antennas, however, the outer limit is on the order of a few wavelengths or less. For the particular case of an electrically small dipole, as indicated in Fig A1(a), the reactive field predominates out to a distance of approximately $\lambda/2\pi$, where the radiating and reactive fields are equal.

Beyond the reactive near-field region the radiating field predominates. The radiating region is divided into two subregions: the radiating near-field region and the far-field region. The former region exists for most electrically large antennas, but not for electrically small antennas. The latter region exists for all antennas.

In the radiating near-field region the relative angular distribution of the field (the usual radiation pattern) is dependent on the distance from the antenna. There are two reasons for this behavior.

(1) The relative phase relationship of field contributions from different elements of the antenna changes with distance

(2) The relative amplitudes of these field contributions also change with distance.

For an antenna focused at infinity, as indicated in Fig A1(b), the radiating near-field region is sometimes referred to as the Fresnel region in analogy to optical terminology.

In the far-field region the relative angular distribution of the field becomes essentially independent of distance. Correspondingly, the amplitude of the field is given, in the limit, by the reciprocal of the first power of distance. The reason for this behavior is that the relative phase and amplitude relationships between the field contributions from different elements of the antenna approach a fixed relationship. Although this situation is not attained precisely until the observation point is an infinite distance from the antenna, the relative angular distribution of the field at a comparatively short distance is often an adequate approximation of the field distribution at infinity. For an antenna focused at infinity, the far-field region is sometimes referred to as the Fraunhofer region in analogy to optical terminology.

For electrically large antennas of the broadside-aperture type, such as that shown in Fig A1(b), a commonly used criterion [A1], [A2] to define the distance in free space to the boundary between the radiating near-field and the far-field regions is

$$R = \frac{2D^2}{\lambda}$$

where D is the largest dimension of the aperture. The difference in path length between the center and the edges of the aperture to the point at the region boundary is X/16. At this boundary the antenna gain over most of the

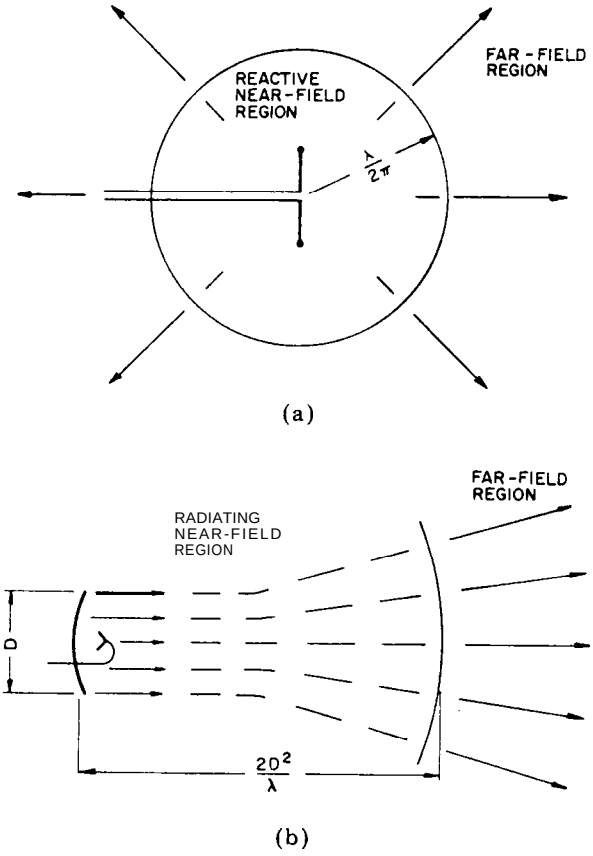

Fig Al
Field Regions for Two Antenna Types
(a) Electrically Small Dipole.
(b) Electrically Large Reflector

major lobe of the radiation pattern differs from that at infinity by a very small factor, the exact value depending on the shape of the aperture and the illumination taper. However, for directions corresponding to minor lobes and pattern minima the gain at the region boundary may differ from that at infinity by many decibels (see 4.2).

For most applications it is the radiation pattern in the far-field region that is important. It is, therefore, customary to make measurements in the far-field region. If the distances involved are prohibitively great, measurements in what would normally be the near-field region can be used and the pattern in the far-field region inferred (see 7.2 and 7.3).

For electrically large antennas other than conventional broadside-aperture types there is no recognized criterion defining the distance to the far-field inner boundary. However, the $2D^2/\lambda$ criterion, when D is taken as the largest linear dimension, will usually give a

distance that is within the far-field region. Special precautions should be observed when the antenna's environment plays a part in the formation of the radiation pattern. For such situations the distance to the inner boundary of the far-field region is determined by the dimension of the entire radiating structure. This structure may involve a large metallic supporting surface (for example, an aircraft fuselage) in a fixed installation (see Section 9).

Certain measurement situations do not permit separation of the useful space into simple near- and far-field regions. An important example of this class is that of a vertically polarized antenna operating over a ground of finite conductivity (see Section 17).

AZ. Bibliography

[A1] SILVER, S. Microwave Antenna Theory and Design, M.I.T. Radiation Laboratory ser, vol 12, New York, McGraw-Hill, 1949, sec 6.9.

[A2] HANSEN, R. C. Microwave Scanning Antennas, vol 1, New York, Academic Press, 1964, pp 30-46.

Appendix B
Reciprocity

B1. General

The reciprocity principle [B1]–[B3] is of fundamental importance in the determination of many antenna properties because, for a reciprocal antenna, these properties may be determined from measurements with the antenna in either the transmitting or the receiving mode. An antenna is said to be reciprocal if the constitutive parameters of the transmitting media through the antenna can be characterized by symmetric tensors. This generally means that there are no ferrite or plasma devices (with steady magnetic fields applied) within the antenna or in the transmission medium.

For such antennas the reciprocity principle can be used to produce relationships between their transmitting and receiving properties.

The reciprocity principle as applied to antennas can be divided into three areas:

(1) antenna pattern characteristics and measurements

(2) gain measurements

(3) polarization measurements

The polarization characteristics of a reciprocal antenna are discussed in 11.1.

If the antenna is not reciprocal, its transmitting and receiving properties are not simply related, and measurements shall be performed for the mode or modes in which it is designed to be used.

A modified reciprocity principle applies to the case of antennas containing magnetized ferrites, or to antennas in the presence of media such as ionized gases in static magnetic fields [B4]. The condition under which the modified reciprocity principle holds is that the static magnetic field shall be reversed when the transmitting and receiving roles are interchanged. When this condition is satisfied, all the antenna properties mentioned are preserved.

B2. Antenna Patterns

The pattern characteristics of an antenna under test, called the test antenna, are obtained by using the antenna in either of two ways. In the first way the test antenna is used in a receiving mode with the signal being transmitted by a source antenna. The signal is generated by a transmitter connected to the input of the source antenna. Amplitude and phase patterns are recorded at the output of a

receiving system connected to the terminals of the test antenna. The phase is referred to an arbitrary reference derived from the transmitting signal.

In the second way the transmitting source is connected to the test antenna, and the receiving system is connected to the source antenna. The antennas are not disturbed in the interchange of the transmitter and the receiving system. The amplitude and phase patterns measured by the receiving system will be the same in both cases. The phase reference shall remain unchanged, otherwise the phase pattern will be shifted by some constant value of phase.

NOTE: Strictly speaking, reciprocity applies to interchanges between current sources and open-circuit voltages or between voltage sources and short-circuit currents. These conditions can be satisfied by including the transmitter impedance as a part of the transmitting antenna and the load impedance as a part of the receiving antenna. However, when a physical source and a receiver are interchanged, their impedances shall move with them. Then unless these impedances are equal, the reciprocity condition is not satisfied. If these impedances are equal, reciprocity is satisfied for any separation between test and source antennas. However, if the antennas are separated sufficiently far so that multiple interactions are negligible, the amplitude patterns will be proportional and the phase patterns will differ only by a constant phase when the transmitter and the receiver are interchanged.

B3. Gain and Effective Area

Another antenna property which follows from the reciprocity principle is that the power gain G and the effective area A, of a reciprocal antenna are related by the equation [B3]

$$G = \frac{4\pi A_e}{\lambda^2} \qquad \text{(Eq 1)}$$

This latter property is often interpreted as: The power gain of a reciprocal antenna is the same when used for transmitting as it is when used for receiving. Strictly speaking, power gain is only defined for the transmit case. For the receive case the effective area is the appropriate quantity to be used.

B4. Expanded Reciprocity Relations [B5]

Applied to an antenna, the reciprocity principle implies that the far field radiated in a given direction and a given polarization, for a specified excitation, is proportional to the response of the antenna when a plane wave of opposite direction and of matched polarization is incident upon it.

NOTE: The incident plane wave is said to be polarization matched to the antenna if, in the same plane of polarization, their polarization ellipses have the same orientation, the same axial ratio, and the same sense of rotation. However, because of the usual convention in specifying the orientation of the ellipses, the tilt angles will be different (see 11.1).

The factor of proportionality depends on how the excitation and the response are expressed. Both shall be measured at the same point, or port, in the transmission line connected to the antenna. Furthermore, a reference point 0 shall be specified in the vicinity of the antenna to make-the phase of the incident plane wave and that of the radiated far-field unambiguous. A direction shall be specified by a wavevector $\boldsymbol{k}$ and an associated polarization by a unit vector $\hat{\boldsymbol{u}}$ perpendicular to $\boldsymbol{k}$ ($\hat{\boldsymbol{u}} \cdot \boldsymbol{k} = 0$, $|\hat{\boldsymbol{u}}| = 1$). In general $\hat{\boldsymbol{u}}$ is a complex vector.

If the excitation is by a source that is matched to the transmission line and produces a traveling wave of unit amplitude (that is, a wave that carries unit power and has zero phase at the antenna port), then the far-field in direction $\boldsymbol{k}$ and polarization $\hat{\boldsymbol{u}}$, referred to the origin 0, will have the form

$$E(r; \boldsymbol{k}, \hat{\boldsymbol{u}}) = \hat{\boldsymbol{u}}^* \cdot \boldsymbol{E}(\bar{k}r) = \sqrt{Z_0}\, A(\boldsymbol{k}, \hat{\boldsymbol{u}}) \frac{e^{-jkr}}{r} \qquad \text{(Eq 2)}$$

where $\bar{\boldsymbol{k}}$ is the unit vector in the direction of $\boldsymbol{k}$, r is the distance from 0 to the observation point $\bar{\boldsymbol{k}}r$, and Z_0 is the intrinsic impedance of space. Conversely, let a plane wave of wave-

vector $-k$ and electric field $\hat{u}^* \sqrt{Z_0}$ be incident upon the antenna. Note that $\hat{u}^*$ incident represents the polarization which is matched to the antenna's polarization $\hat{u}$ (see 11.1) and because of the factor $\sqrt{Z_0}$, this wave has unit intensity. Its Poynting vector is -k. This incident field produces, at the antenna port, a wave of amplitude a traveling toward the matched load. Reciprocity is expressed by the relation

$$a\ (-k,\ \hat{u}^*) = -j\lambda A\ (k,\ \hat{u}) \qquad \text{(Eq 3)}$$

valid for any k and $\hat{u}$ vectors. Equation 3 holds whether the transmission line is matched to the antenna or not.

If the antenna is excited by a unit current source of zero internal admittance, the far-field in direction k, polarization $\hat{u}$, at a distance r is expressed by

$$E\ (r;\ k,\ \hat{u}) = \hat{u}^* \cdot E\ (\bar{k}r) = -\sqrt{Z_0}\ \frac{jk}{4\pi}\ h\ (k\ \hat{u})\frac{e^{-jkr}}{r} \qquad \text{(Eq 4)}$$

where h is the effective length for direction vector $\bar{k}$ and polarization vector $\hat{u}$. In general h is a complex number. For an incident plane wave of wave vector $-k$ and electric field vector $\hat{u}^*$ at point 0, the open-circuit voltage V (also complex) is, according to reciprocity,

$$V\ (-k,\ \hat{u}^*) = h\ (k,\ \hat{u}) \qquad \text{(Eq 5)}$$

The electric far-field radiated in direction $\bar{k}$ can be expressed by the vector

$$E\ (\bar{k}r) = jk Z_0\ h\ (k)\frac{e^{-jkr}}{4\pi r} \qquad \text{(Eq 6)}$$

The complex vector h (effective current moment per unit current) indicates the polarization, has the dimensions of a length, and can be written as a product hU of a *real* effective length h and a unit magnitude vector U. This effect length, which is not to be confused with $h\ (k,\ u)$, is a function of vector k only. If an incident plane wave in direction $-k$ has an electric field vector U^* at reference point 0, the resulting open-circuit voltage is precisely h volts. It therefore is of zero phase. It is also larger in magnitude than the voltage that any other plane wave of unit intensity would produce. Reciprocity can therefore be expressed by saying that the scalar *real* effective length h (a function of direction $\bar{k}$) is the same when transmitting and when receiving. For transmitting, h is such that the current moment of magnitude $h|I|$ when the excitation current is I and for receiving a plane wave of matched polarization the open-circuit voltage is of magnitude $h|E|$ if E is the electric field. If the phase is important, one shall carefully specify the reference port and the reference point 0 and use the precise Eqs 3 or 5.

B5. Bibliography

[B1] JORDAN, E. C., and BALMAIN, K. G. Electromagnetic Waves and Radiating Systems, Englewood Cliffs, NJ, Prentice-Hall, 1968, chap 11.

[B2] COLLIN, R. E., and ZUCKER, F. J. Antenna Theory, pt 1, New York, McGraw-Hill, 1969, chap 4.

[B3] SESHADRI, S. R. Fundamentals of Transmission Lines and Electromagnetic Fields, Reading, MA, Addison-Wesley, 1971, chap 10.

[B4] HARRINGTON, R. F., and VILLENEUVE, A. T. Reciprocity Relationships for Gyrotropic Media, ***IRE Transactions on Microwave Theory and Techniques,*** vol MTT-6, July 1958, pp 308-310.

[B5] DESCHAMPS, G. E. I — Principe de Reciprocite en Electromagnetisme; II — Application du Principe de Reciprocite aux Antennes et aux Guides d'Ondes, Cethedec no. 8,4e trimestre 1966, pp 91–101.